Asset Health Index and Risk Assessment Models for High Voltage Gas-Insulated Switchgear Operating in Tropical Environment

Purnomoadi, Andreas

DOI
10.4233/uuid:d2a3bafb-f39d-49ba-a9c0-bb266a9f9ba5

Publication date
2020

Document Version
Final published version

Citation (APA)
Purnomoadi, A. (2020). *Asset Health Index and Risk Assessment Models for High Voltage Gas-Insulated Switchgear Operating in Tropical Environment*. [Dissertation (TU Delft), Delft University of Technology]. https://doi.org/10.4233/uuid:d2a3bafb-f39d-49ba-a9c0-bb266a9f9ba5

Andreas Putro Purnomoadi

Asset Health Index and Risk Assessment Models for High Voltage Gas-Insulated Switchgear Operating in Tropical Environment

Asset Health Index and Risk Assessment Models for High Voltage Gas-Insulated Switchgear Operating in Tropical Environment

Dissertation

for the purpose of obtaining the degree of doctor
at Delft University of Technology
by the authority of the Rector Magnificus prof. dr. ir. T.H.J.J. van der Hagen,
chair of the Board of Doctorates,
to be defended publicly on
Monday 13 January 2020 at 15:00 o'clock

by

Andreas Putro PURNOMOADI

Master of Science in Electrical Engineering
Delft University of Technology, the Netherlands
born in Yogyakarta, Indonesia

This dissertation has been approved by the promotors.

Composition of the doctoral committee:

Rector Magnificus,	chairperson
Prof. dr. J.J. Smit	Delft University of Technology, promotor
Dr. A. Rodrigo Mor	Delft University of Technology, copromotor

Independent members:

Prof. dr. R. Ross	Delft University of Technology
Prof. ir. P.T.M. Vaessen	Delft University of Technology
Prof. Dr. Ir. Suwarno, MT.	Bandung Institute of Technology, Indonesia
Prof. Dr. -Ing. S. Tenbohlen	University of Stuttgart, Germany
Dr. ir. A. Pharmatrisanti	PLN Research Institute, Indonesia

This research was technically supported and financially funded by PT. Perusahaan Listrik Negara (PLN), Jakarta, Indonesia.

ISBN 978-94-6384-098-9

An electronic version is available at http://repository.tudelft.nl

To My Parents, Ima, and Daya

Summary

Following deregulation in the energy sector during the 1990s, which was also triggered by the ageing of infrastructure and the increasing demands from regulators and customers, many network utilities adopted the Asset Management (AM) in the hope to earn more, have better credit ratings and gain from stock prices. In line with this fact, the emergence of the AM international standard, such as the ISO 55000 series in 2014, gained rapid acceptance among network utilities around the globe.

AM has its core in the asset decision-making process. This activity lies simultaneously at the strategic, tactical and operational level of AM, over the lifecycle of the asset. In such an environment, the asset managing department should not only focus on the reliability of the asset but also on balancing costs, risks and asset performance. Regarding maintenance, the money spent on every maintenance task should benefit the company's business values.

This thesis focuses on the development of decision-making tools for maintenance of high voltage AC (HVAC) gas-insulated switchgear (GIS) operating under tropical conditions. GIS has been chosen because of its critical role in the transmission network. Any GIS breakdown is usually expensive and requires an extensive outage. Moreover, under tropical conditions, this study observed GIS failure rates over twice the value reported by CIGRE's survey of 2007. The study was conducted in this research's case study termed the Java Bali (JABA) case study. The latter consists of 631 CB-bays of 150 kV and 500 kV GISs located in Java and Bali of Indonesia.

Today's AM decision-making tools for electrical power grids are generally based on Asset Health Index (AHI) and risk assessment (RA) models. These models assist the asset manager in answering the following questions:

1. What is the condition of each GIS in the network?
2. Which one is more likely to fail compared to the others?
3. Which one is more critical compared to the others in terms of making a possible impact on the company's business such that the mitigating action is prioritised?
4. What optimal action(s) is/are needed to be taken?

Developing the above-mentioned models requires sufficient knowledge of the characteristics of GIS operating under tropical conditions. To that purpose, both statistical analysis and forensic investigations in the JABA case study have been undertaken to find the critical condition indicators for the AHI model. The results are as follows:

1. The tropical conditions have influenced both directly and indirectly the performance of GIS. Corrosions at the exposed GIS parts were seen to have a common direct influence of tropical conditions. They can trigger leakages, secondary, and lead to driving mechanism subsystems' failures, which reduce the GIS' performance. The intensive and frequent lightning in tropical conditions is a so-called Failure Susceptibility Indicator (FSI), indicating that a failure mode is expected to initiate more likely than for the same GIS in other environments, especially if the surge arrester fails to protect. Moreover, the GISs outdoor and from the older generation are more susceptible to breakdown under tropical conditions.

2. A high amount of humidity was found in the non-CB enclosures of GIS from lower voltage class (i.e. Class 2 GIS with a voltage level of 150 kV). The origin of this humidity mainly comes from the desorption of moisture from the spacer or internal GIS surfaces during operation.
3. The critical failure modes in GIS operating under tropical conditions are as follows: dielectric insulation breakdown, loss of mechanical integrity in the primary conductor and failing to perform the requested operation due to driving mechanism failure.

Following this study's findings, laboratory tests in the HV Laboratory of TU Delft were conducted to investigate the influence of high humidity content on the spacer flashover in GIS. The results confirmed without condensation, humidity has no impact on the withstanding strength of the insulation system under AC, LI+/- and SI. Our model also showed that the breakdown voltage under LI+ due to condensation at the surface of a solid insulator is lower than that due to a 2 mm metallic particle attached on the identical solid insulator at 3000 ppmV.

We applied the findings from both field investigation and laboratory tests into our models in the following ways:

1. In the AHI model:
    a. Statistical and JABA lab case studies were performed to assess the system's vulnerabilities and normative levels, in particular, the humidity content in GIS the non-CB enclosure as long as the value was far from the possibility of condensation.
    b. The likelihood of failure is determined by so-called condition scale codes reflecting the deterioration of the subsystems.
    c. The failure susceptibility indicators (FSI) flag deviating circumstances, such as heavy environmental conditions, operation and maintenance records and the inherent/design factor of GIS. The FSI are just an expectation that is not based on evidence as in a condition indicator. Therefore, the FSI work as warning flags for the decision-maker.
2. In the RA model:
    a. Risk is defined as the likelihood of failure times the consequences. The result of the AHI defines the likelihood of failure in the RA model.
    b. On the other hand, the consequences consist of seven business values of a transmission utility from the JABA case study, namely, safety, extra fuel cost, energy not served, equipment cost, customer satisfaction, leadership and environment.

We have successfully implemented these models on a GIS example from the JABA case study. Evaluation of possible risk treatments was also done using multi-criteria analysis (MCA) to optimise three parameters: cost, time-to-finish treatment and residual risk.

In practice, transmission utilities face more complex situations with more types of equipment in the network. The methodology discussed in this thesis, however, can be the cornerstone for the development of decision-making tools for other assets at the tactical level of AM as well.

TABLE OF CONTENTS

SUMMARY i

CHAPTER 1 INTRODUCTION 1

1.1 GIS OPERATIONAL EXPERIENCES IN THE TROPICAL ENVIRONMENT 2

1.2 THE JABA CASE STUDY 3

1.3 AHI AND RA MODELS 7

1.4 OBJECTIVES OF THE RESEARCH 10

1.5 STRUCTURE OF THE BOOK 11

CHAPTER 2 GIS FAILURE EXPERIENCES IN THE TROPICAL ENVIRONMENT ... 13

2.1 GIS FAILURE STATISTICS IN THE JABA CASE STUDY 13

2.2 STATISTICAL LIFETIME ANALYSIS IN THE JABA CASE STUDY 17

2.2.1 Statistical lifetime analysis of all GISs in the case study 19

2.2.2 Statistical lifetime analysis of 150 kV and 500 kV GIS in the case study 20

2.2.3 Statistical lifetime analysis of indoor and outdoor GIS in the case study 21

2.2.4 Statistical lifetime analysis based on major failure modes in the case study 23

2.3 GIS INTERRUPTION STATISTICS IN THE JABA CASE STUDY 24

2.4 ORIGIN OF MOISTURE IN GIS IN THE JABA CASE STUDY 26

2.4.1 Humidity content in GIS from different manufacturers 26

2.4.2 Humidity content in the insulating gas of the leaking-enclosures 29

2.5 FORENSIC INVESTIGATION 30

2.5.1 Failures during normal operation 31

2.5.1.1 Case #1: Primary conductor failures 31

2.5.1.2 Case #2: Cable termination breakdown 32

2.5.1.3 Case #3: Spacer flashover in an earthing-switch compartment 33

2.5.1.4 Case #4: Sudden gas leaks from the Earthing Switch (ES) indicator 34

2.5.2 Failures in connection with switching operation 35

2.5.2.1 Case #5: Energy storage failure on Circuit Breaker (CB) 35

2.5.2.2 Case #6: Kinematic failure on Disconnector Switch (DS) 36

2.5.3 Failures in connection with transients from causes external to the GIS 37

2.5.3.1 Case #7: Spacer flashover on gas-insulated line (GIL) after a lightning stroke 37

2.5.3.2 Case #8: Joint conductor failure after a fault in the system 38

2.6 FAILURE MODE EFFECT AND CRITICALITY ANALYSIS (FMECA) 39
2.6.1 GIS Hierarchical Layers 40
2.6.2 Failure Modes of GIS Operating under Tropical Conditions 47
2.6.3 Failure Modes Effect Analysis 52
2.6.4 Failure Modes Criticality Analysis (FMECA) 52
2.6.4.1 Occurrence and Detection Criteria 53
2.6.4.2 Consequences Criteria 53
2.6.4.3 Result 56
2.7 CONCLUSION 58

CHAPTER 3 EXPERIMENTAL INVESTIGATION: SPACER FLASHOVER IN HUMID SF_6 UNDER DIFFERENT ELECTRICAL STRESSES 61

3.1 SPACER WITH HUMID SF_6 IN GIS 62
3.2 EXPERIMENT SETUP 63
3.2.1 Electrode configurations 63
3.2.1.1 Electric field distribution on the surface of a conical spacer in GIS 64
3.2.1.2 Homogeneous configuration 65
3.2.1.3 Quasi-homogeneous configuration 65
3.2.1.4 Inhomogeneous configuration with a particle attached on the sample 66
3.2.2 Material specification and dimension of the sample 66
3.2.3 Gas pressures in the test 67
3.2.4 Humidity manipulation in the test chamber 67
3.3 VOLTAGE GENERATION 68
3.3.1 AC voltage generation 69
3.3.2 LI and SI voltage generation 70
3.4 EXPERIMENTAL RESULTS 70
3.4.1 Flashover voltage in quasi-homogeneous configuration 71
3.4.2 Flashover voltage inhomogeneous configuration 75
3.4.3 Flashover voltage in the setup with a particle attached on the sample 78
3.5 ANALYSIS OF TEST RESULTS 81
3.5.1 Analysis-01: The influence of humidity on the flashover voltage 81
3.5.2 Analysis-02: The influence of gas pressure decrease on the flashover voltage in dry condition 84
3.5.3 Analysis-03: The effect of lightning polarity on the flashover voltage 86

3.5.4 Analysis-04: The influence of electric field distribution on the spacer flashover ...87
3.6 CONCLUSION 88

CHAPTER 4 ASSET HEALTH INDEX MODEL FOR GIS OPERATING UNDER TROPICAL CONDITIONS 89
4.1 GIS AHI MODEL 90
4.1.1 Methodology 91
4.1.2 Boundary of the GIS HI Model 94
4.2 SELECTING CONDITION INDICATORS 94
4.2.1 Aging and Deterioration in GIS 94
4.2.2 Methodology to capture condition indicators 97
4.3 GENERATING NORMS 101
4.3.1 Example of Norm Generation 110
4.4 HEALTH INDEX CODING 115
4.4.1 Condition Coding of Subsystems in GIS 115
4.4.1.1 Condition coding of primary conductor subsystem in GIS 116
4.4.1.2 Condition coding of the dielectric subsystem in GIS 119
4.4.1.3 Condition coding of driving mechanism subsystem in GIS 123
4.4.1.4 Condition coding of secondary subsystem in GIS 126
4.4.1.5 Condition coding of the construction and support subsystem 127
4.4.2 Condition coding of components in GIS 128
4.4.3 Condition coding of enclosures in GIS 129
4.4.4 Condition coding and indexing of bays in GIS 129
4.4.5 Condition indexing at the substation layer of GIS 130
4.5 FAILURE SUSCEPTIBILITY INDICATORS (FSI) 130
4.5.1 Sub FSI due to environmental indicators (Sub FSI_E) 132
4.5.1.1 Sub FSI due to pollutants (Sub FSI_{E1}) 132
4.5.1.2 Sub FSI due to lightning stroke (Sub FSI_{E2}) 133
4.5.2 Sub FSI due to operation and maintenance indicators (Sub FSI_{OM}) 133
4.5.2.1 Sub FSI due to voltage transients generated during interruption (Sub FSI_{OM1}) 133
4.5.2.2 Sub FSI related to service time of GIS (Sub FSI_{OM2}) 134
4.5.2.3 Sub FSI related to the maintenance history (Sub FSI_{OM3}) 134
4.5.3 Sub FSI due to inherent/ design indicators (Sub FSI_{ID}) 135
4.5.3.1 Sub FSI related to the O-ring design of GIS (Sub FSI_{ID1}) 135

4.5.3.2 Sub FSI due to availability of absorbent in GIS (Sub FSI_{ID2}) 136
4.5.3.3 Sub FSI related to GIS specific make/ manufacturer (Sub FSI_{ID3}) 136
4.5.4 Relating Failure Susceptibility Indicators with Failure Modes in GIS *136*
4.6 DEALING WITH DATA UNCERTAINTY 137
4.7 APPLYING AHI TO GIS EXAMPLE 139
4.7.1 Condition Indexing a GIS example *141*
4.7.1.1 Condition Coding of Circuit Breaker 141
4.7.1.2 Condition Coding for the other components in the other enclosures 146
4.7.1.3 Condition coding and condition indexing of bays 147
4.7.1.4 Condition indexing of GIS substation 148
4.7.2 Assessing Failure Susceptibility Indicators (FSIs) *148*
4.8 CONCLUSION 151

CHAPTER 5 RISK ASSESSMENT MODEL FOR GIS OPERATING UNDER TROPICAL CONDITIONS 153
5.1 RISK ASSESSMENT METHODOLOGY 153
5.2 ESTIMATING THE LIKELIHOOD OF FAILURE (LOF) 154
5.3 CLASSIFYING CONSEQUENCES 155
5.4 RISK ACCEPTANCE MATRIX 157
5.5 APPLYING THE RISK ASSESSMENT MODEL TO GIS EXAMPLE 157
5.5.1 Estimating the Likelihood of Failure (LoF) of GIS example *157*
5.5.2 Assessing consequences *158*
5.5.2.1 Consequence on Safety 158
5.5.2.2 Consequence on Extra Fuel Cost 158
5.5.2.3 Consequence on Energy Not Served (ENS) 158
5.5.2.4 Consequence on Equipment Cost 158
5.5.2.5 Consequence on Customer Satisfaction 158
5.5.2.6 Consequence on Leadership 159
5.5.2.7 Consequence on Environment 159
5.5.3 Summarizing the risk of GIS Example *159*
5.6 RISK COMPARISON AMONG GISS 160
5.7 CONCLUSION 161

CHAPTER 6 RISK TREATMENT 163
6.1 RISK TREATMENT METHOD 163
6.1.1 Step-1: Defining the problem or opportunity 164
6.1.2 Step-2: Developing cost and benefit parameters 164
6.1.3 Step-3: Determining the optimal solution 165
6.2 SENSITIVITY ANALYSIS 165
6.3 APPLYING RISK TREATMENT PROCEDURE TO GIS EXAMPLE 166
6.3.1 Step-1: Defining the Problem and Opportunity 166
6.3.2 Step-2: Developing Cost and Benefit Parameter 167
6.3.3 Step-3: Determining the Optimal Solution 168
6.3.4 Sensitivity Analysis 169
6.4 CONCLUSION 169

CHAPTER 7 CONCLUSIONS AND RECOMMENDATIONS 171
7.1 CONCLUSIONS 171
7.2 MULTIPLE RECOMMENDATIONS FOR FUTURE RESEARCH 174

REFERENCES 175
LIST OF ABBREVIATIONS AND SYMBOLS 179
DEFINITIONS 183

APPENDIX A LIST OF GIS AND MAJOR FAILURES IN THE JABA CASE STUDY 185
APPENDIX B STATISTICAL LIFETIME ANALYSIS 189
APPENDIX C RISK QUANTIFICATION FOR FMECA 193
APPENDIX D CURVES REGRESSIONS FROM THE LABORATORY TESTS 195
APPENDIX E DETERMINING CONDITION STATUS OF SURGE ARRESTER (SA) 203
APPENDIX F HEALTH INDEX OF GIS EXAMPLE 205
APPENDIX G TECHNICAL RECOMMENDATIONS 213

ACKNOWLEDGEMENTS 215
CURRICULUM VITAE 216
LIST OF PUBLICATIONS 217

Chapter 1 Introduction

Network utilities all over the world are now facing profound challenges in managing their assets. The liberalization of electricity markets drives the utilities to optimise between the asset's performance and costs while facing the ageing of their infrastructure [1]. In response, the way of managing the assets has been shifted from a focus on the "reliability" to that on the optimisation between the cost and the asset's performance through the lifecycle of the assets. This can be seen, for example, from the evolution of the maintenance strategy from "corrective-based" to "time-based", then "condition-based" and later to "reliability-centred" and "risk-based" strategies. The work on the asset is now being justified based on the asset's condition and importance in business. A growing number of network utilities have adopted AM according to the ISO 55000-series standard. This international standard is suitable for AM of large electrical infrastructures, as it offers benefits such as improved financial performance, managed risk and enhanced efficiency and effectiveness [2].

In AM, one of the most critical and challenging tasks is to elaborate on the risks involved in the prioritisation of AM options. In practice, the company has limited resources (including a budget, people and spares). Therefore, risk analysis could help to prioritise these resources. Different decision-making tools are needed to assist the asset manager in the following processes:

1. To assess the condition of the assets.
2. To estimate the remaining lifetime of the asset.
3. To quantify the risk if the asset fails, based on the company business values.

Today's AM decision-making tools for electrical power grids are generally based on Asset Health Index (AHI) and risk assessment (RA) models. The underlying methods are at focus in the present research in the case of HVAC Gas Insulated Switchgear (GIS) installations operating under tropical conditions. The case study termed "JABA" consists of 150 kV and 500 kV GISs located in Java and Bali two tropical islands of Indonesia. The GISs belong to Perusahaan Listrik Negara, PLN, The Indonesian Government's electricity company and are spread across 79 substations, with a total of 631 CB-bays.

This research focuses on the health of a GIS in the tropics because the JABA case study found failure rates over twice the value in a report by the CIGRE's survey in 2007 [3]. Having a model to assist the asset manager in prioritising maintenance based on the risk of failure will benefit the utilities facing a similar problem such as the one in the case study.

This thesis starts off at the component level, discussing the critical indicators and the Failure Susceptibility Indicator (FSI) of GIS operating under the tropical conditions through failure statistics and forensic investigations in the JABA case study. After this, the results from the laboratory tests in the HV laboratory in TU Delft are presented. The experiments focused on the influence of humid SF_6 on spacer flashover as it has been

found in many 150 kV GIS of the JABA case study. Moreover, humidity has also been suspected to be involved in breakdowns of the insulation system, especially the spacer.

In the first chapter, general information about a GIS' operational experiences in tropical conditions is presented in Section 1.1 followed by the explanation of the JABA case study in Section 1.2. Section 1.3 provides a brief discussion about the AHI and RA models. Following this, sections 1.4 and 1.5 give the objectives and novelty of the research and the structure of the thesis.

1.1 *GIS operational experiences in the tropical environment*

GIS has been reliable for more than 40 years. The technology has been improved significantly since its first introduction in the 1930s. The drawback of GIS, which is the use of the SF_6 gas, a high global warming potential gas, has been mitigated by the technology nowadays which makes possible to use less SF_6 and better sealant technology. Failure behaviours have also lessened in that the number of failures due to the design and manufacturing process have been reduced [4]. Now, failure is more likely to occur due to the in-service cause.

Figure 1.1 shows the improvement of GIS design from one manufacturer [5] where the current GIS technology employs only 25% of SF_6 volume and needs 85% less space in comparison to those of the first generation, without sacrificing reliability. The leakage rate in the newly GIS can be maintained to be below 0.5% of the volume/year for about 20 years of operation [5]. Apart from these improvements, researches are also coming up with ways to replace SF_6 with a more environment-friendly gas [6].

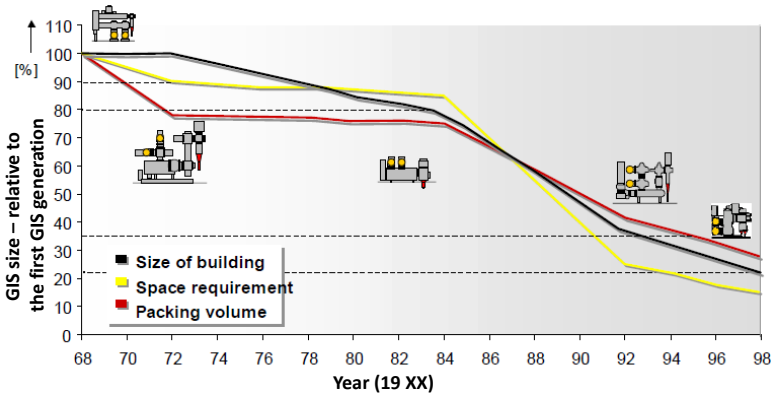

Figure 1.1 The improvement design of 145 kV GIS from a manufacturer as taken from [5]. The current technology employs only 25% of SF_6 gas in comparison to the first generation of GIS technology.

However, in the JABA case study, GIS failure rates were seen to be more than twice the value reported by the 3rd CIGRE survey in 2007. In particular, tropical parameters may both, directly and indirectly, be involved in the GIS' failures through the following processes:

1. The humid environment, the intense sunlight with the (relatively) constant warm temperature over the year, can quickly provide a thin film layer of electrolyte on the metallic surface as a basis for corrosion, especially in GIS with the outdoor installation. This corrosion is responsible for the leakages and the following failure in the driving mechanism subsystem.
2. The frequent lightning strikes with high amplitude in the tropics increases the likelihood of insulation breakdown, especially when the surge arrester fails to protect or when a defect exists in the insulation system.
3. The humid environment contributes to the high amount of absorbed and adsorbed moisture in the internal parts of GIS, mainly, when the erection and/or the maintenance were misconducted. The moisture desorbs during GIS operation, creating humid gas inside GIS. The humid gas is responsible for the creation of the corrosive by-products in GIS and the possibility to have condensation in GIS.

Leakages and corrosions are common minor failures in the JABA case study (see Figure 1.2). While the critical failure modes include as follows:

1. Insulation breakdown.
2. Primary conductor (including joints and main contacts) failure.
3. Driving mechanism failure.

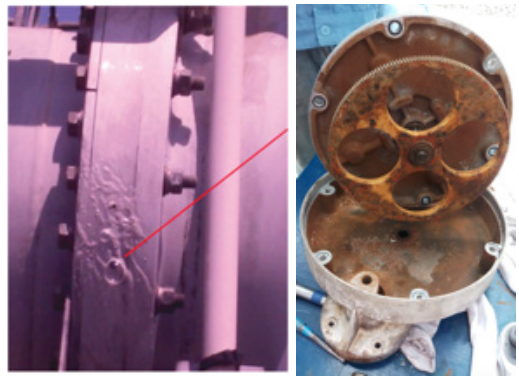

Figure 1.2 An example of leakage (left) and corrosion on the mechanical-gear of a disconnector (right) found in the JABA case study.

1.2 *The JABA Case Study*

The JABA case study has been chosen to study the performance of a GIS in the tropics. Through forensic investigations and statistical analysis, the characteristics of failures, which also cover the critical failure modes, of GIS operating under tropical conditions were drawn as the input for decision-making models.

The JABA case study consists of a GIS population with their service time spanning from 1 up to 30 years. The average service time is 21 years for 500 kV GIS and 17 years for 150 kV GIS. In total, there are 631 Circuit Breaker (CB) bays of 500 kV and 150 kV GIS. The total observed service times from 2005 to 2014 are 5177 CB-bay-years for 150 kV GIS and 730 CB-bay-years for 500 kV GIS. One CB-bay consists of a 3-phase GIS

assembly, including CB and its associated switches (disconnector switches and/or earthing switches), instrument transformers, interconnecting bus up to and including the line disconnecting switch (if applicable) and a section of the main bus (if applicable) [3]. The number of CB-bays with their operation years are presented in Figure 1.3. Most of the developments were made from 1990 to 2000. Figure 1.4 shows the locations marked with big red-dots (for 150 kV GIS) and blue-dots (for 500 kV GIS).

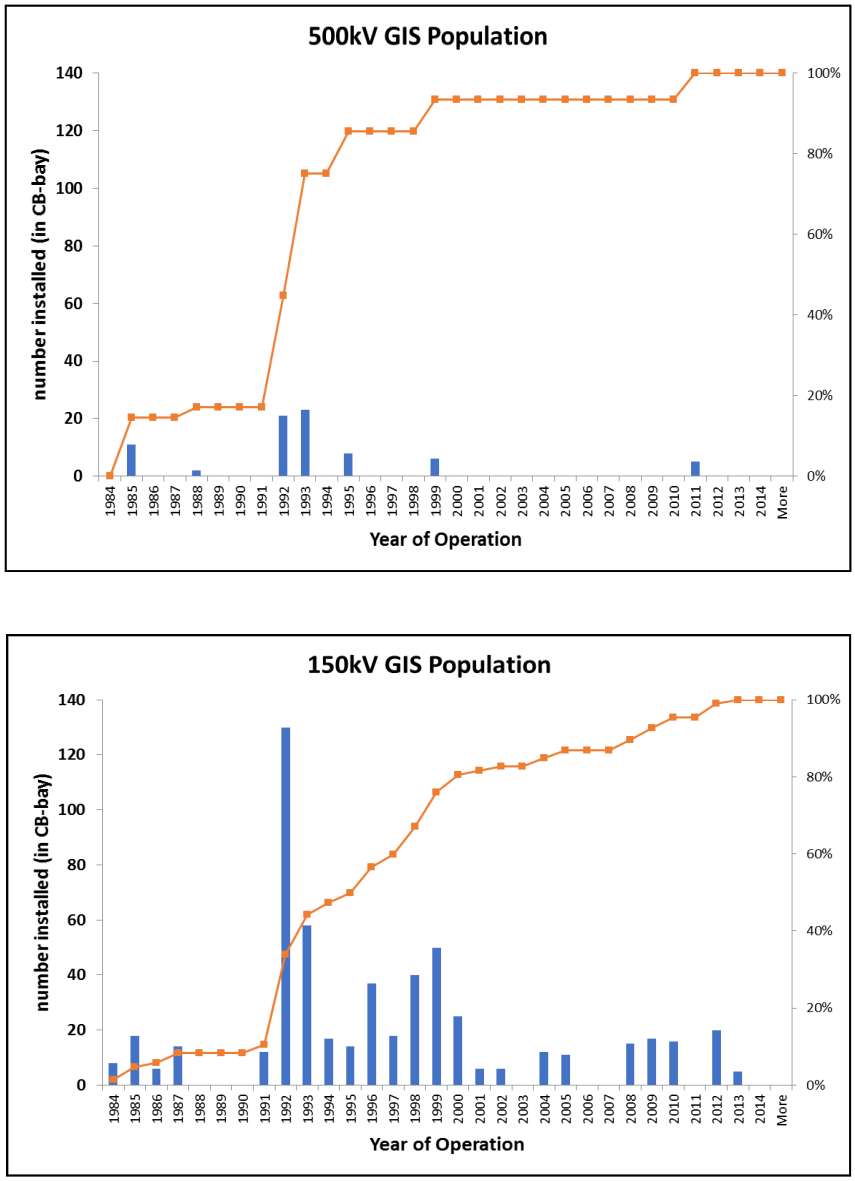

Figure 1.3 The total population of 500 kV GIS (top) and 150 kV GIS (bottom) of the JABA case study, including their years since in operation. The number is in CB-bay unit.

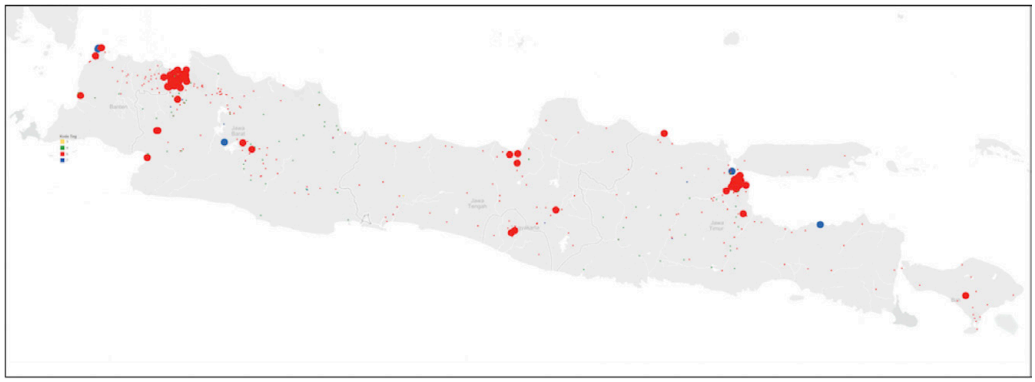

Figure 1.4 The locations of 500 kV and 150 kV GIS in the JABA case study. Most 150 kV GIS are located in big cities such as Jakarta and Surabaya, while the 500kV GIS is mostly installed at the substation of power plants.

The GIS population is heterogeneous, as indicated by the following:

1. There are 12 GIS brands, 70% of Europe's and 30% Asia's. GIS from Europe's brand can be manufactured in Asia.
2. The design is varying as follows:
   a. The circuit breaker could be installed vertically or horizontally (see Figure 1.5).
   b. In 150 kV GIS, the number of phase per enclosure can either be 1 or 3. All 500 kV GISs have 1 phase per enclosure configuration.
   c. The energy storage for CBs differs (in %-population): hydraulic system (41%), compressed spring system (34%) or a pneumatic system (25%). Almost all DS use the electric motor with a small fraction with the pneumatic system.
   d. The volume of the desiccants (absorbent materials) varies. There is one GIS type with no desiccants in all non-switching enclosures.
   e. The operational SF_6 density varies (see Table 3.2).
3. Other operational conditions are as follows:
   a. Most of 500 kV GISs are outdoor while the 150 kV mostly indoor.
   b. Nearly 100% of 150 kV GIS has a double-busbar configuration while 500 kV GIS one-and-a-half circuit-breaker scheme.
   c. GIS can terminate to an outdoor bushing connected to an overhead line or an underground cable.
   d. The production batch can be grouped into the 1980s, the 1990s and after 2000.

Figure 1.5 Two examples of 500 kV GIS of the JABA case study. Both GISs have a single phase per enclosure design. In the left figure, the outdoor GIS has a vertically designed CB, while in the right figure, the indoor 500 kV GIS has a horizontally designed CB. CB is shown by the enclosed red box.

The tropical parameters in the JABA case study

All GISs in the JABA case study were exposed to the tropical environment during their service time. In general, two parameters were used to identify the tropical conditions, i.e. the climate and the pollutants.

The tropical climate has the following characteristics [7–11]:

1. The average humidity per year is 80%.
2. The temperature is relatively warm over the year, with an average of 27°C.
3. The average annual rain precipitation is from 90 mm to 210 mm. The higher value occurs during the rainy season from October to March.
4. The lightning flash density is high with an average of 15 strikes /km^2 /year.

Meanwhile, the pollutants can be natural or pollutants caused by human activity. The natural pollutants, such as the salty aerosol and the salty film, can be found in abundance in the region close to the sea while in big cities, the industrial and the pollutants from vehicles like CO and SO_2 are prominent. Tables 1.1 and 1.2 present a comparison between the tropical and the subtropical parameters with the examples of Jakarta (Indonesia) and Amsterdam (the Netherlands).

Table 1.1 The climate parameters in Jakarta and Amsterdam [7-11]

Parameter	Jakarta	Amsterdam
Avg. Annual Relative Humidity (%)	80	83
Avg. Annual Temperature (°C)	27	May-Oct: 14 Nov-Apr: 4
Avg. Annual Rain Precipitation (mm)	Oct-Mar: 210 Apr-Sep: 90	60
Lightning flash density (strikes /km^2 /year)	15*	1
LI_{50} Positive/ Negative polarity (kA)*	28/ 17	19/ 23

**average value. An area with the lightning density above 95 strikes/km^2/year was found [11].*

***93% of the population is the negative lightning impulse [11].*

Table 1.2 The concentration of pollutants: PM_{10} (particles with size above 10μm), SO_2 (sulphur dioxide), CO (carbon monoxide), and NO_2 (nitrogen dioxide) in Jakarta and Amsterdam [12-13]

Parameter	Jakarta	Amsterdam
Avg. PM_{10} (μg/m^3)	59	27
Avg. SO_2 (μg/m^3)	32	0.8
Avg. CO (μg/m^3)	2947	406
Avg. NO_2 (μg/m^3)	17	39

The following interpretations were drawn from the tables:

1. The average relative humidity in Jakarta can be compared to the one in Amsterdam; however, the warmer temperature in Jakarta makes the air contain more moisture even though it is at the same level of relative humidity as in Amsterdam.
2. The higher rain precipitation in Jakarta makes the environment even more humid. The remaining water droplets from rain, plus the extended period of condensation during the night, can efficiently become an agent for corrosion. The high concentrations of pollutants in Jakarta accelerate the process of corrosion.

The fact that lightning is denser in Jakarta than in Amsterdam increases the susceptibility to a GIS insulation failure, notably when the surge arrester fails.

1.3 *AHI and RA Models*

In practice, an Asset Manager deals with tens to hundreds of GISs in the power network, consisting of hundreds to thousands of CB-bays. The asset manager needs to ensure all GISs are in good condition to avoid failure and the GIS can reach the expected lifetime.

On the other hand, GIS experiences electrical, mechanical, thermal and environmental stresses in daily service, which can initiate different failure modes. The GIS performance decreases with usage, and an asset manager must decide on a mitigating action before a failure occurs.

In AM, managing the asset's reliability is directly related to evaluating risk and performance, especially in the decision for maintenance, which is the most complex activity within the asset lifecycle [14]. In the case of GISs, the asset manager should answer the following questions:

1. What is the condition of each GIS in the network? Which one is more likely to fail compared to the others? Which part/component is more likely to fail?
2. When a failure is predicted, what is the possible mode to fail? What is the time to failure (TTF)? What action is advised to mitigate failure?
3. When several components or GISs from different locations exhibit a similarly poor condition, how should the action be prioritised? Which one has the biggest impact on the company's business if a failure occurs? What is the optimal solution (e.g. a decision with the most cost-effective way)?

Following the questions above, the Asset Health Index and RA models are the subject of research in this thesis, to enable better decision-making in future practice.

Typically to the methodology for AHI is that it merges all condition indicators into a single value to represent the health status of an asset [15–16]. It can also estimate the remaining lifetime of an asset or a likelihood of failure [17–18]. A condition indicator is an indicator that represents the condition of an item (i.e., component/sub-component or system/sub-system of an asset), which can be captured using inspection, measurement and examination. In practice, the condition indicators can be obtained from field inspection or site tests as part of regular maintenance and laboratory testing.

AHI categorises the asset health with increasing likelihood of failure, as illustrated in Figure 1.6. T1 is the point where the on-set of a failure mode occurs. The asset deteriorates from T1 to T2 and is continuous in T3, but the performance is still within an acceptable limit. When the deterioration continues, the condition drops into the red (critical) zone, where the likelihood of failure is high. T4 is the time before failure occurs, where the mitigating action needs to be taken.

Different health index models have been published for components in a power network, such as for power transformers, transmission lines and GISs [19-22]. The model is usually tailored among users who depend on specific needs and the available data. An AHI of a complete system usually consists of sub-HIs of the subsystems with weighting factors.

This thesis derives an AHI for GIS operating under tropical conditions. A GIS system consists of four layers, namely (in bottom-to-up indentures), components (including parts), enclosures, bays and substation. The health Index of GIS at the substation layer is determined by the sub HIs at the bay-layers and sub-sub HIs of the enclosures and the components.

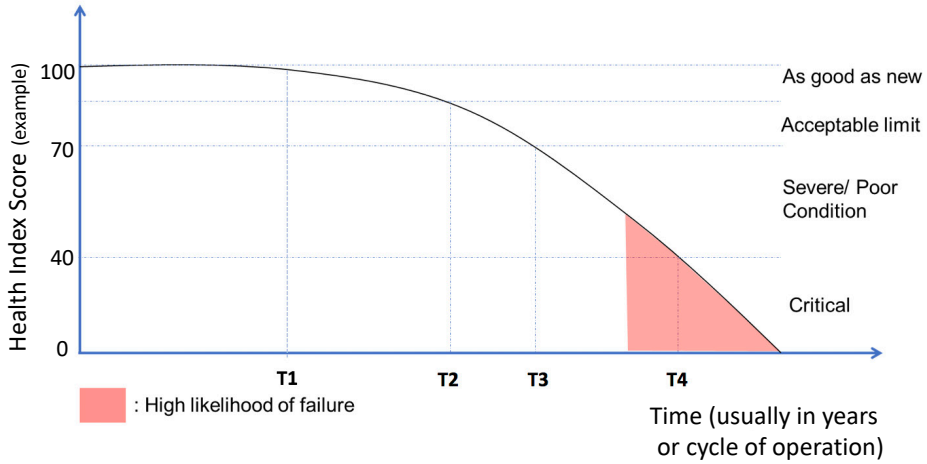

Figure 1.6 AHI as a function of time or cycle of operation. An asset will inevitably deteriorate. T1 is the point where the on-set of a failure mode occurs. The time between T1, T2 and T3 is seen when the asset deterioration is still within the acceptable limit while T4 presents the maximum time entering a critical zone where the asset has a high likelihood to fail.

GIS from different locations in a power network and from different makes may experience different deterioration factors and rates. Therefore, this study introduced the concept of FSI to indicate deviating circumstances exist that may accelerate the onset of failure modes more than usual [23]. The FSIs flag deviating circumstances, such as heavy environmental conditions, operation and maintenance records and inherent/design factor of GIS. The FSI is not a condition indicator or a failure mode but just an expectation that is not based on evidence. This study adopted the FSIs only as warning flags for the decision-maker. The FSIs have been defined based on the forensic investigation and statistical analysis from the JABA case study and includes GIS inherit indicators (e.g. design, makes), GIS operational indicators (e.g. service time, voltage transient intensity due to interruption, maintenance history and surge arrester conditions) and GIS environmental indicators (e.g. pollutant level). The combination of AHI and FSI gives a comprehensive result.

There is an urgency to prioritise the mitigating actions amongst GIS, especially if the resources are limited. Risk deals with uncertainty and is defined as the product of the likelihood of an event and consequences. In the proposed model, AHI defines the likelihood of failure while the consequences are determined based on the impact of failure on the business values of the company. A risk matrix from the JABA case study has been used as a practical reference in this thesis. There are six business values, namely safety, financial loss due to extra fuel cost, financial loss due to equipment cost, reliability, customer satisfaction, leaders reputation and environment. Each consequence has five severity levels that are qualitatively measured, from low up to catastrophic.

This thesis treats the RA at the bay and substation layers of GIS. The highest risk of the bays determines the risk of a GIS at the substation layer. As the output, the risk falls into one of the following categories: low, moderate, high, very high and catastrophic.

1.4 *Objectives of the Research*

The objectives of the research are as follows:

1. To investigate the factors that influence the performance of GISs operating under tropical conditions, which include the internal and external factors that increase the likelihood of failure of a GIS.
2. To investigate the condition indicators that constitute the health status of GIS. For the latter, an AHI model should be developed that is well-tuned with today's utility practice, which can categorise the actual health conditions of the components by identifying failure modes and by understanding their deteriorating effects and, finally, can generate an alarm when the expected time to failure falls short. The model has to be based on facts from practical failure experience in the so-called JABA case study and based on an experiment to validate such practical observations.
3. After knowing the health index of a GIS, another decision support tool is needed to assess the risk of failure among GIS. For this, an RA method should be proposed for prioritising the maintenance decisions. When several GIS locations have a risk above the acceptance level of the company, a method to mitigate the risk should be provided.

The novelty of this thesis:

1. This thesis makes an in-depth comparative investigation of the performances of GISs of the CIGRE survey of 2007 and the JABA Case Study. The influence of tropical conditions are assessed by performing the failure statistics and the statistical lifetime analysis, the critical failure modes based on the Failure Mode, Effects and Criticality Analysis (FMECA) and the humidity content in the CB and non-CB enclosures GIS.
2. Various AHI models for HV apparatuses have been provided in the works of research [4,16–22], but none of them has been developed for a GIS operating in a tropical environment. This thesis could fill the gap, where the norms to justify the health status of GIS have been developed based on the results from laboratory tests and field experiences in tropics.
3. This thesis introduces the FSI, non-conditional indicators to accelerate the initiation (onset) of a failure mode in GIS. These indicators are flags and excluded in the calculation of AHI but give additional information to decision-makers.

1.5 *Structure of the book*

This thesis contains 7 Chapters, with the following structure:

Chapter-1 presents the introduction of the thesis.

Chapter-2 presents the GIS' failure experiences in tropical conditions based on the observations in the JABA case study. The chapter's aims are listed below:

1. to explain the performance of GIS operating under tropical conditions through statistical analysis and forensic findings.
2. to explain failure modes of GIS operating under tropical conditions. The FMECA is used to determine the critical failure modes in the JABA case study.

Chapter-3 reports the laboratory tests in the HV Laboratory in TU Delft. The tests were aimed to investigate the influence of humid SF_6 on the spacer flashover found in many 150 kV GISs in the JABA case study. This chapter explains the test setup, including the procedure for humidity manipulation in the test. Three electric field distributions were simulated in the tests, homogeneous, quasi-homogeneous and with a particle-attached on the spacer. The electrical stresses under investigation are AC, lightning impulse (LI, + and -) and switching impulse (SI).

Chapter-4 discusses the AHI model for a GIS operating under tropical conditions. The input for the model are the condition indicators obtained from visual inspection and diagnostic tests and measurements. This chapter also provides the FSI of GIS operating in a tropical environment. The output of the model consists of an AH Index and a worksheet of different flags of FSIs that are colour-coded to indicate the level of each FSI. A solution to deal with data uncertainty is proposed in this chapter.

Chapter-5 discusses the RA model for GIS operating under tropical conditions. The AHI defines the likelihood of failure occurring in GIS while the consequences are determined based on the business values found in the JABA case study. In this thesis, RA will be demonstrated at the bay layer of GIS.

Chapter-6 provides a solution for risk remediation. The method consists of three steps: 1) defining the problem and opportunity, 2) developing cost and benefit parameters and 3) determining the optimal solution. An MCA is chosen to optimise the decision based on three indicators: cost, residual risk and time-to-execute the option.

Chapter-7 provides conclusions and recommendations.

Chapter 2 GIS Failure Experiences in the Tropical Environment

Substations with Gas Insulated Switchgear (GIS) does similar functions as a conventional air-insulated substation, apart from the power transformer. The GIS role is a node where the electricity is distributed within the transmission network. To that purpose, the GIS should be able to energize (and de-energize) the high voltage apparatus and to isolate a fault with the shortest possible time.

GIS technology has been known to have excellent reliability for more than 40 years. It is plausible because the live parts are placed inside enclosures that reduce the impact of environmental stresses. However, high failure rates, as found in the JABA Case Study, is contradicting to this fact. Therefore, an extensive investigation has been conducted in the JABA Case Study to find critical failure modes and whether the tropical parameters contribute to failures, as it will be presented in this chapter.

Section 2.1 to 2.3 present statistics from the JABA Case Study which include as follows: failure statistics, statistical lifetime analysis, and interruption statistics. Following to that, section 2.4 reports the analysis on the humidity content in GIS enclosures from the case study. The purpose of the analysis is to investigate the origin of moisture in GIS in the JABA Case Study. Section 2.5 gives forensic reports from 10 power failure investigations in the JABA Case Study. After that, section 2.6 explains the Failure Mode Effect and Criticality Analysis (FMECA) of the observed failures. Finally, the conclusion is provided in section 2.7.

2.1 *GIS failure statistics in the JABA Case Study*

The following statistical analysis is based on the data from the case study from 2005 to 2014 (detailed data are provided in Appendix A). The failure statistics will be presented with a comparison to the CIGRE's survey of 2007 [3].

Failure is defined as the inability of an asset to perform the required function(s) [24-25]. As a switchgear a GIS system has two main functions; firstly, it should be able to switch ON and OFF connected power apparatus and deliver the electrical energy; secondly, a GIS system should also be able to localize a fault in the shortest possible time. Any deviation or inability to perform these main functions is a failure.

The IEC in [24] classifies failures into major and the minor type based on the severity-level and the duration of the recovery process. The international failure statistical analysis in [3], and the other publication in [26] use the "major failure" as the basis of statistical calculation, and we are doing so in this thesis. The number is in per 100-CB-bay years.

A former GIS failure statistics had been published in [26] based on the data from 1997 to 2009, covering about a third region of the JABA Case Study. In the current study, 35 major failures have been recorded, of which 25 of failures occurred in 150 kV GIS, while the rest is in 500 kV GIS. Table 2.1 gives the comparison of failure rates in the case study and the CIGRE's survey of 2007.

Table 2.1 The comparison of GIS failure rates between the case study and the CIGRE's survey of 2007 (the number is given in per 100 CB-bay-years, 95% CI intervals are shown within the brackets)

	CIGRE [3]	Former Study [26]	Current Study
Class-2 (150kV)	0.24 (0.18 – 0.30)	0.93	0.48 (0.31 - 0.71)
Class-5 (500kV)	0.5 (0.29 – 0.82)	0.55	1.37 (0.66 – 2.52)

The result shows the following:

1. The failure rate in the CIGRE's survey is lower than in both surveys from the case study for GIS from both classes.
2. In the current survey, the failure rate is about twice the value of the CIGRE's survey for Class-2 GIS and close to triple for the Class-5 GIS.
3. Both surveys in case study result differently. The reason is due to differences in population and year observation. In the former report, the number of failures in Class-2 GIS is higher, while in Class-5 GIS is less.

Another analysis has been conducted on the distribution of the failed components involved in major failures of GIS. In CIGRE's report [3], the components are classified into four groups, namely: 1. Circuit Breaker (CB), 2. Disconnector/ Earthing Switches (DE), 3. General Instruments (GI), and 4) Instrument Transformer (IT). The general instruments consist of busbar and bus duct, all kind of terminations, surge arrester, and others. The absolute number of failures and their percentages of distribution from the JABA case study and the survey of CIGRE are given in table 2.2.

Table 2.2 The distribution of failed components in the JABA Case Study and the CIGRE's survey of 2007 [3]

		Class-2				Class-5			
		CIGRE [3]		Case Study		CIGRE [3]		Case Study	
		Abs.	%	Abs.	%	Abs.	%	Abs.	%
Major Component	CB	17	27%	4	16%	8	50%	4	40%
	DE	27	42%	6	24%	8	50%	4	40%
	GI-Busbar/Busduct	6	9%	5	20%	0	0%	0	0%
	GI-Terminations	4	6%	6	24%	0	0%	1	10%
	GI-Surge Arrester	0	0%	0	0%	0	0%	1	10%
	GI-Others	7	11%	2	8%	0	0%	0	0%
	IT	3	5%	2	8%	0	0%	0	0%

The distribution of failed components shows the following:

1. For the Class-2 GIS, the distribution of the failed components in the case study is different from the CIGRE's survey. In the case study the failed components are almost equally distributed among terminations, DE, bus bar and bus duct and CB; while in the CIGRE's survey, the highest failed component is DS, and then followed by CB.
2. For the Class-5 GIS, both surveys agree that the most failed components are CB and DE. In the case study, failures on the air bushing terminations and the surge arrester have also been observed.

Further statistical analysis on the distribution of the failure modes has also been investigated. CIGRE's survey classifies seven failure modes, as seen in table 2.3. The comparison for CIGRE's with the result from the JABA Case Study is provided in the table. The CIGRE report only provides the statistics of all voltage classes.

Table 2.3 The distribution of failure modes in the JABA Case Study and the CIGRE's survey of 2007 [3]

		CIGRE [3] (all voltage class)				Case Study (Class-2, 150 kV)				Case Study (Class-5, 500 kV)			
		Abs.		%		Abs.		%		Abs.		%	
1	Failing to perform requested operation	227		63%		4		16%		4		40%	
2	Loss of electrical connections integrity in primary conductor	1		0%		4		16%		0		0%	
3	Loss of electrical connections integrity in secondary (protection system)	2		1%		0		0%		0		0%	
4	Dielectric breakdown in normal service	67	81	19%	23%	8	12	32%	48%	2	3	20%	30%
5	Dielectric breakdown in connection with switching, and/or external transients.	14		4%		4		16%		1		10%	
6	Loss of mechanical integrity on enclosures, pressure gauge, including big SF_6 leakage	16		4%		3		12%		1		10%	
7	Other (including unknown)	31		9%		2		8%		2		20%	

According to the table, the distribution of failure modes is as follows:

1. In the survey of CIGRE, the "failing to perform the requested operation" is the highest counted failure mode found in GIS from all voltage classes. The number is followed by the dielectric breakdown which is mostly occurring under normal service condition.

2. In Class-2 GIS of the case study, the most dominant failure mode is the “dielectric breakdown” under normal service condition. The other failure modes, which are almost equally distributed are: the dielectric breakdown in connection with the switching operation, the failure to perform requested operation, the loss of electrical connections integrity in the primary conductor, and loss of mechanical integrity.
3. In Class-5 GIS of the case study, the highest failure mode is similar to the CIGRE’s survey, i.e., failing to perform a requested operation. The other significant failure modes are the dielectric breakdown and loss of mechanical integrity on the enclosure.

In addition, a statistical analysis has been conducted in the JABA Case Study to compare the failure rates of GISs based on as follows, 1. the GIS installation (indoor or outdoor), 2. the batch of production year 1980’s, 1990’s, or 2000’s, and 3. the number phases in one enclosure which is applicable only for the 150 kV GIS. The results are presented in Tables 2.4 to 2.6.

Table 2.4 GIS failure rates in JABA Case Study based on the GIS installation (indoor/ outdoor, the number is in per 100 CB-bay-years)

kV	**Indoor**	**Outdoor**	**Total**
150	0.36	3.48	0.48
500	0.87	1.60	1.37

Table 2.5 GIS failure rates in JABA Case Study as grouped by the production year (the number is in per 100 CB-bay-years)

kV	**Production Year**			**Total**
	1980’s	**1990’s**	**2000’s**	
150	1.09	0.51	0.1	0.48
500	1.54	1.38	0	1.37

Table 2.6 GIS failure rates of 150 kV GIS based on the number of phase in one enclosure (the number is in per 100 CB-bay-years)

kV	**1P**	**3P**	**Total**
150	0.37	0.57 0.44*	0.48

** without sample from one dominant location*

The failure rates from the tables above give the following interpretations:

1. The failure rate is higher for outdoor GIS. The reason is the outdoor GIS is exposed to higher environmental stress than the indoor GIS. The outdoor GIS is more prone to corrosion that can lead to further degradations.
2. The old generation GIS contributes to the higher failure rate, as seen in Table 2.5. Apart from aging, the other reasons might be addressed to the design improvement of the new GIS and the delay of the overhauls of some old GIS.

3. In 150 kV GIS, the failure rate is higher in GIS with the 3-phase per enclosure configuration. However, the number was dominated by a GIS from a single location (i.e., an outdoor GIS) with four failures during the observation period. The failure rate is down by 23% (i.e., from 0.57 to 0.44 /100 CB-bay-years) when the dominant GIS is removed. Now, the failure rate of GIS with a 1-phase design is only slightly lower than the 3-phase GIS. The 1-phase configuration offers better inter-phase insulation distance, but there are also more parts with this design which means the more possibility to have a failure.

4. As seen in Tables 2.4 and 2.5, the high failure rates in the JABA Case Study can be addressed by the high number of failures at the outdoor GIS and GIS from the generation of the 1980s and 1990s. On the other hand, failure rates of GIS from the installation after 2000 are lower than the value of CIGRE's as mentioned in Table 2.1.

2.2 *Statistical lifetime analysis in the JABA Case Study*

The statistical lifetime analysis gives the estimated lifetime of the GIS population based on the required reliability level. The reliability level is usually defined by the B-life factor as derived from the reliability curve. The B1-life, for example, defines that 1% of CB-bay in the population will fail after a period (in a year); this means, if the management wanted to achieve 99% of reliability, the mitigating action (e.g., maintenance) should be taken within the period of B1-life time.

Data in statistical lifetime analysis should have the following properties: 1. randomness, 2. independence, 3. homogeneity, and 4. pass the minimal number of data. The event of failures, which correspond to the time-to-failure, are assumed as continuous random variables that occur randomly in time, independently and homogeneously spread across space and time in the component population [27,29]. The methodology for the statistical lifetime analysis can be found in Appendix B.

The analysis in this section focuses on GIS major failures which require extensive repair works (e.g., requires long outage, high cost). Therefore, not all major failures, as reported in Table 2.3, are included in the analysis. Only failures related to the following modes:

1. Failing to perform the requested operation (8 major failures). In the JABA Case Study, this mode occurs due to driving mechanism failure (either CB or DE). Dismantling the driving mechanism requires an expert from the manufacturer and extensive outage time.

2. Loss of electrical connections integrity in the primary conductor (4 major failures). An example of this mode is reported in the section of forensic investigation, where a "tulip-contact" of the main conductor was separated as preceded by partial discharge. The repair work requires a major overhaul by opening the GIS compartment, extensive cleaning, and long outage time.

3. Dielectric breakdown, either during normal service or in connection with switching and/ or external transients (14 major failures).

Only 26 of 35 major failures were assigned to three failure modes above. Twenty cases occurred in 150 kV GIS (13 cases in indoor GIS and 7 cases in outdoor GIS), six cases

in 500 kV GIS (all outdoor GIS). Distribution of GIS failures (i.e. with three failure modes mentioned above, in percentage) and the service time at failure in years, are presented in Figure 2.1.

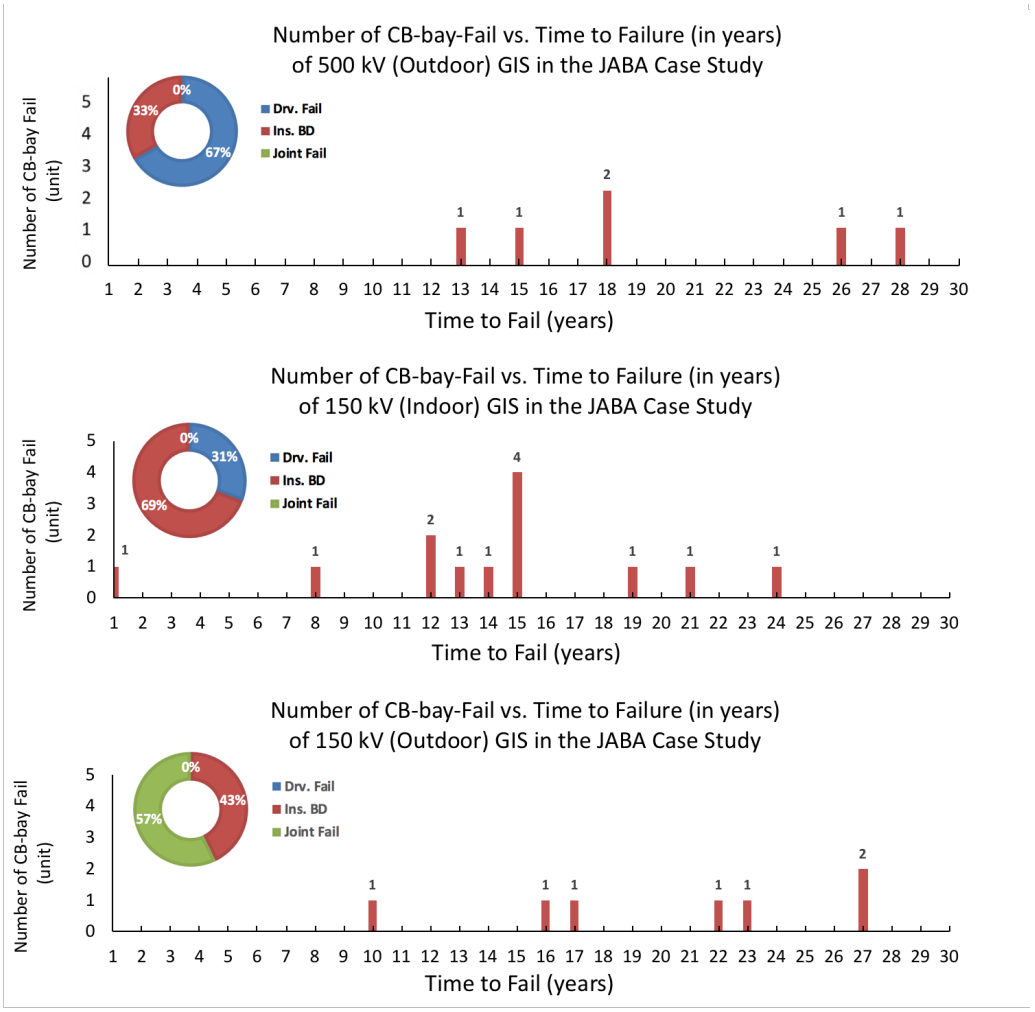

Figure 2.1 Number of major failures which requires extensive repair works and Time to Failure of 500 kV Outdoor GIS (top), 150 kV Indoor GIS (middle), and 150 kV Outdoor GIS (bottom).

As seen in the figure above, driving mechanism failure mode is dominating in 500 kV (outdoor GIS), while the primary conductor (including joints and main contacts) separation occurred only in 150 kV outdoor GIS. Dielectric breakdown is dominating in 150 kV indoor GIS.

Based on the available data from the JABA Case Study, we could perform:

1. Statistical lifetime analysis of all GISs in the JABA Case Study
2. Statistical lifetime analysis based on GIS voltage level.

3. Statistical lifetime analysis based on the GIS installation (i.e. indoor vs. outdoor installation).

Statistical lifetime analysis based on failure mode, regardless of GIS' voltage level.

2.2.1 Statistical lifetime analysis of all GISs in the case study

The inputs for the calculation are major failures and suspended lifetime data from all GIS in the population. The best-fitted distribution is the Normal distribution, which is indicating the failure mode is due to random causes [28], having a mean lifetime of 44 years with a standard deviation of 13.4 years. Figure 2.2 shows the derived reliability and failure or hazard rate together with the 90% confidence bounds.

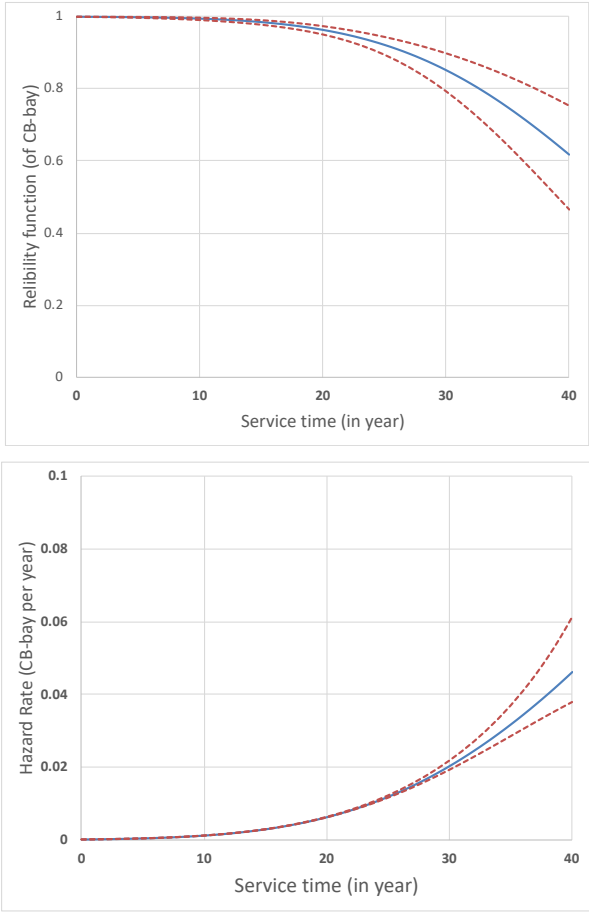

Figure 2.2 Fitted Normal distribution Reliability function for all GIS with 90% confidence bounds of Major Failures with three catastrophic failure modes (top). The accompanying hazard rate as a function of service time is also given with 90% confidence bounds (bottom).

As seen in the Figure 2.2, the hazard rate is below 0.0012 CB-bay per year up to 10 years of service time. The value then gradually increase after then, reaches 0.006 at 20 years, and 0.02 at 30 years of service time. The confidence bound is wider after 30 years.

2.2.2 Statistical lifetime analysis of 150 kV and 500 kV GIS in the case study

Another lifetime analysis has been conducted to compare the estimated lifetime between GIS 150 kV vs. 500 kV. The best-fitted distribution is the Normal distribution for 150 kV GIS subpopulation and Lognormal distribution for 500 kV GIS. The mean lifetime for 150 kV GIS is 46 years, while for 500 kV GIS is 48 years. The fitted reliability function, with 90% of confidence bounds, is given in Figure 2.3, together with the failure rate as a function of service time.

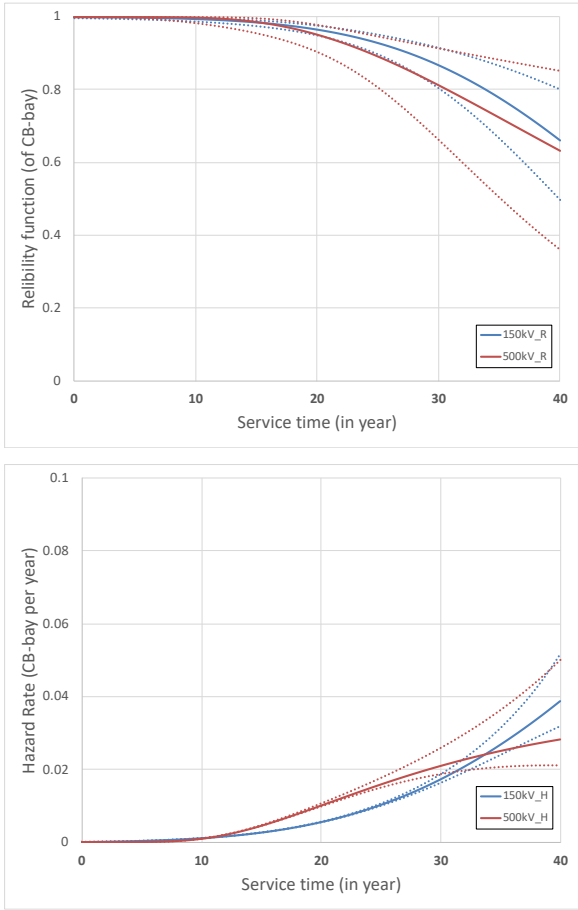

Figure 2.3 Fitted Normal (for 150 kV GIS) and Lognormal (for 500 kV GIS) distribution of reliability function with 90% confidence bounds (top). The failure rates of both sub-populations as a function of service time are also given with 90% confidence bounds (bottom).

The B-life is derived from the curves above. The B1, B5, and B10 of GIS in the case study have been summarized in Table 2.7. The values have been classified based on the GIS voltage level.

Table 2.7 The B-lives and the mean lifetime from the analysis of the total- and sub-populations of GIS based on the voltage level in the case study. The upper and lower values within 90% confidence bounds are given in parenthesis.

Case Study	Case Study			CIGRE* (years)
	All GIS (years)	GIS 150kV (years)	GIS 500kV (years)	
B1 life	13 (9-15)	13 (8-15)	14 (6-18)	
B5 life	22 (20-24)	22 (20-25)	20 (16-24)	
B10 life	27 (24-29)	27 (25-31)	24 (20-32)	
Mean life	44 (39-52)	46 (40-56)	48 (35-119)	42 (30-50)

** as taken from CIGRE Technical Brochure 176 [30], the value is the mean and range of asset life estimates for GIS with voltage level 110kV and above. GIS end of life covers various aspects including changes of rating requirement, maintenance costs, spares obsolescence, mechanical wear, safety, and environmental concern.*

It can be seen from the table, there is no significant difference among the B-lives and the mean lifetime of GIS sub populations based on the voltage level. Therefore, the GIS from both sub populations has comparable reliability.

In comparison with the value from the CIGRE document [30], the mean lifetime of GIS in the case study is higher (i.e., 2 to 6 years). However, the lifetime estimation reported in the CIGRE document was based not only from failures record, but also other factors, like the needs for capability-uprating, maintenance costs, spares obsolescence, mechanical wear, safety, and environmental concern.

2.2.3 Statistical lifetime analysis of indoor and outdoor GIS in the case study

In the following analysis, the performance of GIS installation, i.e., indoor vs. outdoor, is compared. There are three subpopulations in this analysis, namely: 150 kV indoor GIS, 150 kV, and 500 kV outdoor GIS. The best-fitted distribution is Normal distribution for 150 kV GIS, and Lognormal distribution for 500 kV Outdoor GIS. No failure related to the three catastrophic failure modes has been recorded on 500 kV Indoor GIS.

The mean lifetime of the indoor 150 kV GIS is 54 years, while for the outdoor 150 kV and 500 kV GIS, sequentially 33 and 44 years. The fitted distributions and the corresponding failure rates as a function of service time are given in Figure 2.4, with 90% confidence bounds.

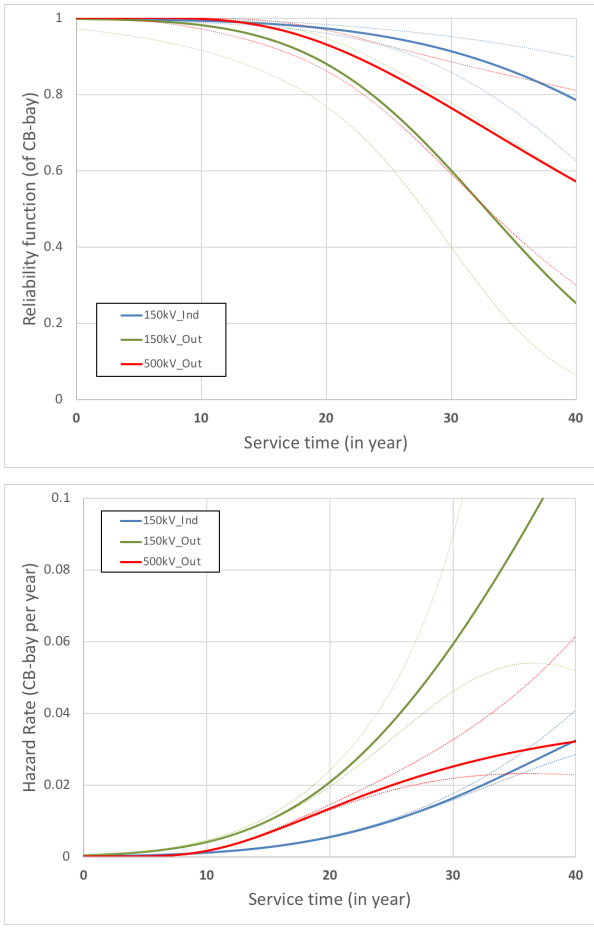

Figure 2.4 Fitted Normal (for 150 kV GIS indoor & outdoor) and Lognormal (for 500 kV GIS outdoor) distribution of Reliability function with 90% confidence bounds in the case study (top). The failure rate from each subpopulation is given with 90% confidence bounds (bottom).

As seen from the graphs, in general, the outdoor GISs from both 500 kV and 150 kV are having lower Reliability than the indoor GIS. The confidence bounds become wider at service time above 20 years, mainly for 150 kV – outdoor, and 500 kV- outdoor GIS, due to the low numbers of the sample. The B-lives and Mean life of all subpopulations are given in Table 2.8.

Table 2.8 The B-lives and mean lifetime from the analysis of the subpopulation GIS based on the installation (indoor/ outdoor). The upper and lower values within 90% confidence bounds are given in parenthesis

	Indoor GIS 150 kV (years)	**Outdoor GIS 150 kV (years)**	**Outdoor GIS 500 kV (years)**
B1 life	13 (8-17)	8 (0-14)	13 (6-16)
B5 life	25 (22-30)	15 (5-20)	18 (13-22)
B10 life	31 (27-40)	19 (12-23)	22 (18-28)
Mean life	54 (44-74)	33 (28-43)	44 (33-101)

The B-lives suggest that earlier action is necessary for outdoor GIS. The B5-life, for example, indicates that to reach the same reliability level as in indoor 150 kV GIS, ten years earlier action/ treatment on the outdoor GIS is considerable.

2.2.4 Statistical lifetime analysis based on major failure modes in the case study

The hazard rate of GIS population based on the three major failure modes have been investigated, and the result is presented in Figure 2.5. The fitted distributions are Normal distribution for the failure modes of “Failing to perform requested operation” and “Joint-conductor fail,” while the “Insulation Breakdown” is fitted into a Weibull distribution.

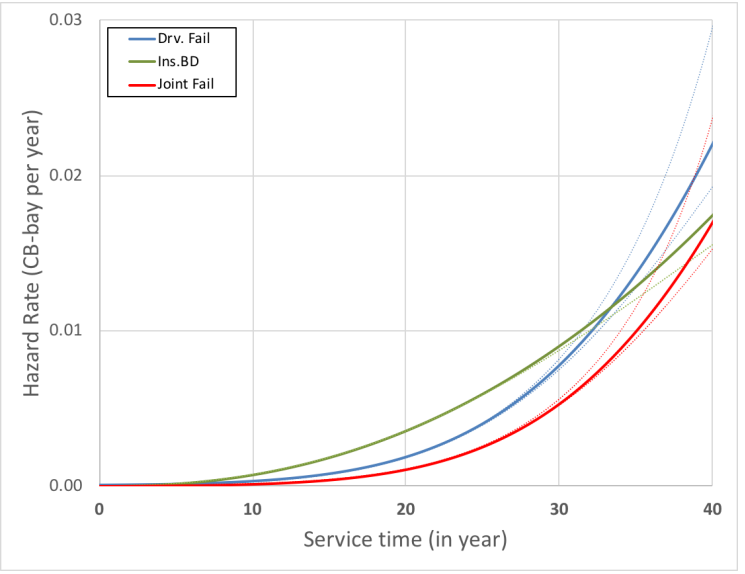

Figure 2.5 The hazard rate of three major failure modes of GIS in the JABA Case Study, i.e. failing to perform requested operation, insulation breakdown, and primary conductor fails.

As seen in the figure above, the hazard rate of the insulation breakdown starts earlier than the other failure modes. It is followed by the failure to perform the requested operation. The hazard rate of the insulation breakdown is the highest up to 34 years of service time.

2.3 *GIS interruption statistics in the JABA Case Study*

Circuit Breaker (CB) interruption in GIS generates switching and very fast transients that increase the susceptibility of insulation failure, mainly if a defect occurs. 16% of major failures in 150 kV GIS in the JABA Case Study have a connection with the switching operation. This section presents statistics of interruptions in the case study. We classify the interruption into three, namely:

1. Fault-interruption (i.e., interruption with fault current)
2. Load-interruption (i.e., interruption with only load current)
3. No-load interruption (i.e., without any current)

The fault-interruption exposes the highest energy discharge.

In this analysis, 2039 interruption-records have been collected from 10 years records in the JABA Case Study. The distribution is as follows:

1. 812 (40%) fault-interruptions.
2. 872 (43%) load-interruptions.
3. 355 (17%) no-load interruptions.

The numbers correspond to an average of 0.13 fault-interruption/ CB-bay/ year. In other words, every CB in one bay will experience a fault-interruption per 8 years. By adding the number from load-interruptions, the interval becomes a half (i.e., per 4 years). Table 2.9 gives the origin of interruptions.

According to Table 2.9, fault-interruptions are mostly (20%) triggered by a human-caused issue, like third-party works and human encroachment (disturbance) near the transmission line (including overhead line and underground cable). The second origin (19%) was faults from the Medium Voltage (MV) lines, in many cases, faulty setting between HV and MV caused the interruption at HV side. The third source (19%) is the lightning stroke on an overhead line connected to GIS. The number is closely similar to the second cause.

Lightning stroke is a typical fault in tropics. In average, 15 fault-interruptions per year in the JABA Case Study were triggered by the lightning. A spacer breakdown has been reported in one case.

System manoeuvre becomes the major reason for load- and no-load interruptions. This is due to a local condition in the JABA Case Study where, due to the insufficient network capacity (i.e., the N-1 capacity is not fulfilled), system manoeuvre frequently occur in several nodes of the transmission network.

Relay failure is the second largest reason for a load interruption. This kind of failure is usually hidden [3,37]. One of the reason was due to corrosion on the auxiliary relays and wirings, that might be affected by humid ambient in tropics.

Table 2.9 The distribution of various origins of interruptions in GIS in the case study

Fault-interruption			
Origins		Abs.	%
1	Human activities near the transmission line (e.g., third-party works, social encroachment)	162	20%
2	Distribution feeder (MV) faults	152	19%
3	Lightning stroke on an overhead line connected to a GIS bay-line	151	19%
4	Impact of fault in another substation	117	14%
5	Internal GIS failures (including sealing end breakdown, insulation breakdown, primary conductor failure)	65	8%
6	Failures on power transformers	47	6%
7	Transmission line's component failures (including insulator flashover, joint conductor fails)	46	6%
8	Other (including unknown)	72	9%
Load-interruption			
Origins		Abs.	%
1	System manoeuvre (including On load Shedding, Manual Load Shedding)	549	63%
2	Relay failures (including wiring-fault, auxiliary malfunction, faulty setting)	191	22%
3	Other (including unknown)	132	15%
No Load-interruption			
Origins		Abs.	%
1	System Manoeuvre (e.g., system recovery after a fault in the network)	328	92%
2	Other (including unknown)	27	8%

2.4 *Origin of moisture in GIS in the JABA Case Study*

The terms moisture and humidity have a different meaning. Moisture refers to the water molecules bonded on the surface (adsorbed-moisture) or in the structure of solids (absorbed-moisture) [31-33]. Meanwhile, humidity refers to the water molecules in vapor-form within a background gas [31-33]. It is worth to mention that the regular gas quality check measures the humidity, not the moisture.

The moisture infiltrates into the GIS by at least two mechanisms [31-33], the first is through the leaking points on the enclosure, and the second is due to the desorption of moisture from the spacer, the conductor and the internal surface of the enclosure. The IEEE Std. C37.122. 5 - 2013 [31] suggests that most of the moisture comes by the second mechanism.

This section reports the investigation on humidity content from various enclosures of GIS in the JABA Case Study. The objective is to find the origin of moisture in the insulating gas since 20% of the non-circuit breaker enclosures of 150 kV GIS in the JABA Case Study have humidity-content above the value recommended by IEEE and IEC standards [31,24].

For further analysis, two kinds of data were collected, i.e.:
1. Humidity content in GIS from different manufacturers.
2. Humidity content in leaking-enclosures.

2.4.1 Humidity content in GIS from different manufacturers

More than 3000 data of humidity-content have been collected from the JABA case study to investigate the amount of humidity inside different enclosures in GIS. The data were originated from GIS from 6 manufacturers, namely, A, B, C, D, E, and F. 150 kV GIS is represented by GIS from manufacturers A, B, C, and D (equals to 67% of population); while 500 kV GIS is represented by GIS from manufacturers A, E, and F (equals to 93% of population).

The Cumulative Distribution Functions (CDF) of the normal distribution of humidity content in the Circuit Breaker (CB) is given in Figure 2.6, while in the Non-CB enclosure in Figure 2.7. The curves show the distribution of various manufacturers. Every point in the graph represents the value of humidity (in ppmV), in a GIS enclosure with a service time of more than ten years. The data were taken during the noon with gas temperature within 30 to 33 °C.

Table 2.10 gives the recommended limits of humidity content from Manufacturer A, B, C, and IEC 62271-1 and CIGRE technical brochure [24,34]. The other manufacturers did not provide the data.

Table 2.10 Maximum recommendation for humidity limit from three GIS manufacturers, IEC and CIGRE technical brochure

Manufacturer	Voltage Class	Enclosure	Limit (in ppmV)
A	All	CB	350
	< 170 kV	Other than CB	840
	> 245 kV	Other than CB	610
B	170 kV	CB	150
	170 kV	Other than CB	500
C	170 kV	All	243
IEC [34]	At 5 bar (abs)		804
	At 7 bar (abs)		574
CIGRE [35]	Pressure < 8.5 bar (abs)		200

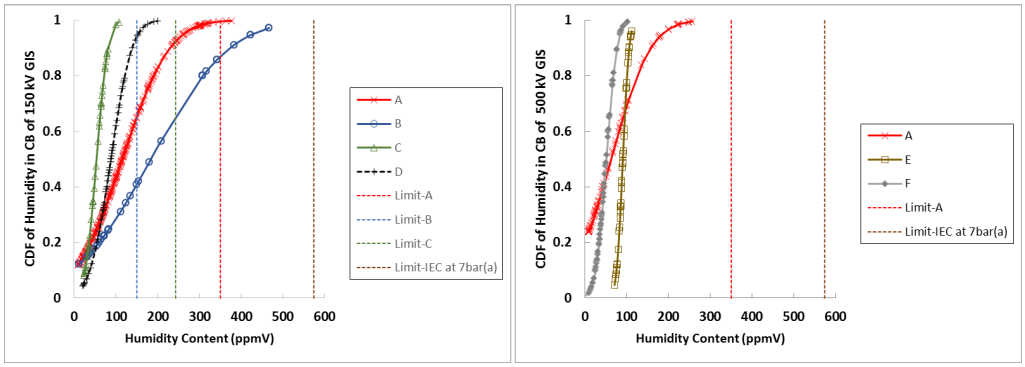

Figure 2.6 CDF of the normal distribution of humidity content in the CB enclosures of 150 kV (left) and 500 kV (right) GIS from the JABA case study. The humidity limits from manufacturers of A, B, C and from the IEC are given in the figure. The humidity value is in parts per million by volume (ppmV)

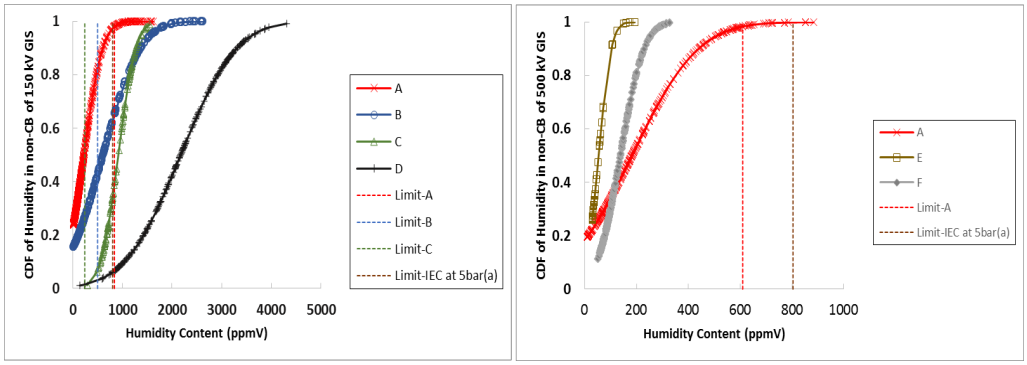

Figure 2.7 CDF of the normal distribution of humidity content in the non-CB enclosures of 150 kV (left) and 500 kV (right) GIS from the JABA case study. The humidity limits from manufacturers of A, B, C and from IEC are given in the figure. The humidity value is in parts per million by volume (ppmV)

The following interpretations are drawn from the table:

1. From Figure 2.6:
    a. Humidity content in CB enclosures of all voltage levels is below the maximum recommendation from the CIGRE at 7 bars gas pressure. All values are below 500 ppmV.
    b. In comparison with the recommended limits of humidity content for CB from its manufacturer:
        i. In 150 kV GIS:
            1. Only less than 5% of GISs from manufacturer A have humidity content beyond the limit.
            2. About 60% of GISs from manufacturer B have humidity content beyond the limit.
            3. All population of GISs from manufacturer C has the humidity below the limit.
        ii. In 500 kV GIS, only limit from manufacturer A was available. All GISs from manufacturer A humidity content below the recommended limit.
    c. In 150 kV GIS, the order of average humidity content in CB from the highest to the lowest based on the manufacturers is as follows B, A, D, C. While in 500 kV GIS, the order is as follows: A, E, F.

2. From Figure 2.7:
    a. In 500 kV GIS, all non-CB enclosures have humidity content below 1000 ppmV, meanwhile, in 150kV GIS, humidity content above 1000 ppmV was observed in many enclosures, except in GIS from manufacturer A.
    b. The humidity content in 150 kV GIS from manufacturer D is the highest. The reason is that the enclosure did not equip with desiccants.
    c. In comparison with the recommended limits of humidity content for non-CB enclosures from its manufacturer:
        i. In 150 kV GIS:
            1. Only less than 5% of GISs from manufacturer A have humidity content beyond the limit.
            2. About 50% of GISs from manufacturer B have humidity content beyond the limit.
            3. All GISs from manufacturer C have humidity content beyond the limit.
        ii. In 500 kV GIS, only less than 5% of the population of GIS from manufacturer A have the humidity beyond the limit.

3. From comparison with the limit from the IEC:
    In general, humidity content is below the limit from the IEC, particularly in CB enclosures. In non-CB enclosures, the recommended limit from IEC is above the humidity content in almost all 500 kV GIS. However, in 150 kV, higher humidity content from the IEC recommended limit has been observed, mostly in GIS from manufacturers B, C, and D.

4. By summarizing point 1 to 3:
    a. In general, humidity content in 500 kV GIS is lower than in 150 kV GIS. It is also true that the humidity content in the CB enclosure is lower than in the non-CB enclosure. The reason is that GIS at the higher voltage has a more significant dimension and higher SF_6 density (see Table 3.2). Moreover, the

CB is equipped with more desiccants that make the enclosure dryer than the others.

b. The amount of humidity is characteristic among different manufacturers and kinds of the active component inside the GIS enclosure. For example, the red-line in Figure 2.7 (left) shows that a small fraction of humidity content in the non-CB enclosures of GIS from the manufacturer A has value above 1000 ppmV. Observation from the field led to the conclusion that the high values come from the termination, where the layers of insulating-tapes contain much of the absorbed moisture. The same figure also shows a black-line with an enormous amount of humidity in GIS from manufacturer D, which does not use desiccants.

Conclusively, the amount of moisture in GIS depends on the following factors, 1. GIS design (like the volume of desiccants, the density of SF_6, type of material, dimension of enclosure and spacer), 2. GIS handling (including how to keep the parts dry during transportation, erection, and maintenance; duration of vacuuming after erection or after maintenance with opening the enclosure).

There is a possibility that humidity infiltrates from the ambient through leaking points on enclosures. The addition of humidity with this mechanism is reported in the following subsection.

2.4.2 Humidity content in the insulating gas of the leaking-enclosures

In the JABA Case Study, gas-leaking is the most dominant minor failure mode. In 2014, at least 20 cases were reported from 9 locations. Accidently, leakage rate over 7% of its original weight per year has been observed [26]. The leaking point is usually located at the corroded point in between enclosure junctions or at the piping to the gas pressure monitoring system.

Through the partial pressure difference, the moisture (in the form of vapor) from the ambient may diffuse into the GIS through the leaking points. The amount from this mechanism is much less in comparison with the humidity from the desorption of moisture from spacers [31-33].

This subsection gives a comparison of the humidity content between the leaking enclosure and the adjacent “sister-enclosure” that is known to be without a leak. The aim is to check whether the humidity content is higher in the leaking enclosure. If yes, then the additional moisture through diffuse mechanism could be significant for GIS operating under tropical conditions.

Observation has been conducted on 20 leaking enclosures, but only 6 data, from 4 manufacturers, are reported in this thesis. The leakage rate was recorded regularly as well as the amount of SF_6 topping up before any repair action. Depends on the system configuration, sometimes a shutdown for a repair action needs to be postponed for weeks or months, so that SF_6 topping-up, of few bars, in the leaking-enclosure is needed to maintain the withstand of the insulation system. Table 2.11 gives the result.

Table 2.11 Comparison of humidity contents between enclosures with & without a leak

Location #	In/Out	CB/ Non-CB	kV	Man.	Service Time* (years)	Leak rate per year of Volume (%)	Humidity in leaking enclosure (ppmV)	Humidity in sister enclosure (ppmV)	Δ hum. (%)
1	Outdoor	Non-CB	500	A	16	-8%	726	455	37%
	Outdoor	Non-CB	500	A	16	-5%	104	172	-65%
	Outdoor	Non-CB	500	A	16	-8%	75	100	-33%
2	Indoor	Non-CB	150	D	17	-12%	2442	2339	4%
3	Outdoor	CB	150	G	29	-13%	154	124	19%
4	Indoor	CB	500	H	3	-82%	N/A	N/A	N/A

**The service time when the leakage was firstly observed*

As seen in Table 2.11:

1. The humidity content is not always highest in the leaking enclosure.
2. In 5 cases, the leakage was first observed after 15 years. However, the first leakage at three years has been found in one case from Manufacturer H; unfortunately, no humidity content had been recorded for this GIS.
3. There is no tendency that the leakage rate is higher for outdoor GIS in comparison to the indoor. More samples are suggested for a more firm conclusion.

The results from this observation re-confirm that moisture in GIS is mostly not originating from a diffusion of external moisture through the leaking points. We also summarized four parameters that are increasing the possibility of leaking in GIS, namely: 1. Aging of seals or pipe works, 2. Sealing design, where, GIS with single O-ring is easier to leak than double-seals, 3. The quality of workmanship, and 4. The quality of the seal's material.

The IEEE [35] recommends a leakage rate of 0.5%/ year. A high leakage rate is not desirable since SF_6 is a substantial greenhouse gas with Global Warming Potential (GWP) of 23,500 times than CO_2. Quick repair work is suggested.

2.5 *Forensic investigation*

In this section, the forensic investigation of major failures in the JABA case study is presented. The aim is to investigate the failure modes and how the tropical parameters involve in failures of GIS. 10 out of 35 major failures will be presented in this section.

The failures are grouped into three, i.e.:

1. Failures during GIS normal operation.
2. Failures in connection with switching operation.
3. Failures in connection with voltage transients from causes external to GIS.

Each report consists of 1. event description, 2. forensic finding, 3. historical data, and 4. potential failure mode(s) including how tropical parameters may be involved.

2.5.1 Failures during normal operation

There are 6 failures from 4 locations in the JABA case study that occurred during the normal GIS Operation, namely:

1. Three cases of primary conductor failures.
2. Cable termination breakdown.
3. Spacer flashover in an earthing-switch compartment.
4. Sudden gas leaks from the Earthing Switch (ES) indicator.

2.5.1.1 Case #1: Primary conductor failures

Event description:

There are 3 cases of primary conductor separation in an outdoor 150 kV GIS with 3-phase per enclosure configuration. The rupture disc was blasting in each of the cases. In one case the failure occurred on a connection between voltage transformer (VT), while the other two were in disconnector switches.

Forensic finding:

The result was the melting of male and female of joint-conductor contacts, as shown in Figure 2.8 (a and b). The blasting of the rupture discs was indicating that a rapid energy discharge had occurred inside the GIS. Moreover, an arcing mark was found on the conductor during the investigation (see Figure 2.8, c). Excessive corrosions were found on many enclosures, including the affected one (see Figure 2.8, d).

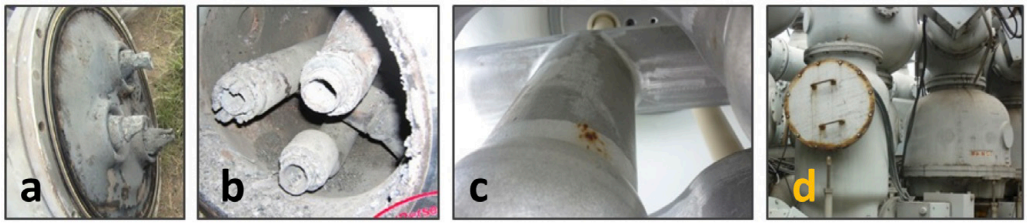

Figure 2.8 Forensic findings from Case #1: a, b) male and female contacts of the failed conductor-joints, c) an arcing mark found on the conductor inside the affected enclosure, and d) corrosions on many enclosures of the affected GIS.

Historical data:

The GIS substation is located in a polluted industrial area. The first failure occurred after a service time of 23 years, while the other two occurred at 27 years. The humidity content in all enclosures was high. The humidity values are over three times the recommendation of the manufacturer. Moreover, the humidity of above 3000 ppmV has been observed in several non-CB enclosures, which is more than six times the maximum recommendation.

Potential failure mode:

The possible failure mode is as follows:

1. Pollutants and acid rain accelerated the corrosion at the exposed parts of GIS. At a later stage, corrosion at the enclosure junction made the humidity to ingress into the seals. The oxidation at this point, made the seals degraded which enabled the gas leak.
2. The other significant amount of humidity might originate from the absorbed moisture in the spacers. The humidity is higher if desiccants are saturated.
3. Partial discharges (PD) probably occurred before the breakdown. The PD could be initiated from the normal vibration or corroded joint-conductor as well.
4. On the longer term, the contact deterioration is in progress resulting in resistive-heating, arcing, and local-melting of the joint. PD then grows, creating debris of free particles that may reduce the breakdown strength.
5. When both contacts finally separate, both inter-phase and phase-to-ground faults occurred. The arc current produced an adiabatic energy-release that resulted in a rapid pressure increase that blasted the rupture disc.

2.5.1.2 Case #2: Cable termination breakdown

Event description:

A breakdown in a termination made of XLPE cable of an indoor 150 kV GIS with the 3-phase per enclosure configuration has been reported. The termination of phase T was severely damaged by electrical breakdown – including its stress cone. The bursting of rupture disc has been observed.

Forensic finding:

One hole with the size of (length x width x depth) = 2x0.6x4.5 cm on the affected termination (phase T) has been found. Meanwhile, smaller holes, or a "crack," were also found on the other phases (see Figure 2.9).

Figure 2.9 Forensic findings from Case#2: Holes found after the breakdown on the cable termination of Phase T (a), Phase S (b), and Phase R (c); on a power transformer feeder bay.

Historical data:

The GIS substation is located in a urban area. The gas analysis before breakdown has shown that the humidity at the sealing end is higher than in the other enclosures, but still below 1000 ppmV.

From the fault recorder, we observed that six fault-interruptions occurred in the affected bay, two years before the breakdown. This number of faults is about twice that of other transformer-bays at the same location. The time to breakdown is 12 years.

Potential failure mode:

PD probably preceded arcing on the XLPE cable-termination. By taking into consideration that the breakdown already occurred at 12 years of service time, the following causes are possible:

1. An inherent defect, like a void inside the insulation of XLPE cable. This void possibly undetected during the site acceptance test.
2. Poor workmanship during installation, that possibly made the microcracks within the insulation of the cable.
3. The accelerated aging of the cable insulation due to the transients during the service lifetime [36].

Smaller holes are probably breakdown precursors in terminations of phase R and S. There is no influence of tropical parameters in Case #2.

2.5.1.3 Case #3: Spacer flashover in an earthing-switch compartment

Event description:

A loosen coupling rod at one vertically-assembled Earthing Switch of an indoor 150 kV GIS, made the contact-gap during the OPEN position, less than the required distance. Partial discharges (PD) then started to occur within the gap. PD and humid SF_6 produced solid by-products that accumulated on the surface of a solid spacer placed below the contacts. The surface flashover then occurred under the AC voltage followed by the bursting of the rupture disc.

Forensic finding:

Burn mark on the surface of the spacer below the ES-contacts had been observed, as seen in Figure 2.10. Besides that, solid decomposed by-products had also been found on the affected parts and the surface of the bottom enclosure.

Figure 2.10 A burn mark has been discovered on the surface of the conic spacer below the ES contacts. White powders, which is a solid decomposed SF_6 by-product, was found abundantly on the affected parts.

Historical data:

The GIS did not equip by desiccants except in the CB enclosure, so the humidity is high in every non-CB enclosure with humidity contents close to 3000 ppmV. Three weeks before breakdown, a thin metal fluoride layer was found on the surface of the bottom spacer. However, due to the system requirement, the GIS was put back on the operation. Gas reclamation was conducted at that time.

Potential failure mode:

The loosen coupling rod made the distance between the ES-contacts too short that started the partial discharge. The finding of the metal fluoride layer supported this statement. A further reaction between moisture and solid by-products on the spacer created a conductive path that lowered the flashover strength. Breakdown then occurred under AC voltage. The time to breakdown of this process turned out to be 12 years.

The influence of the tropical parameters might be indirectly by providing a humid environment. The GIS substation is located in high elevation with a relatively low temperature. Although the GIS is indoor, the humid air inside the building makes it still possible to accelerate the corrosion at the exposed parts of GIS, particularly on the mechanical coupling, gears, and in the driving mechanism subsystem. It is also possible that improper handling after opening the enclosure could give additional moisture into the GIS.

2.5.1.4 Case #4: Sudden gas leaks from the Earthing Switch (ES) indicator

Event description:

A sudden crack of an ES-position indicator in an indoor 500 kV GIS with the 1-phase per enclosure configuration, has triggered a sudden decrease of gas pressure in the compartment that leads into a load interruption of the GIS. The stage-2 of pressure relay tripped the Circuit Breaker (CB). There was no breakdown, but the outage represents an energy loss of 3334 MWh and a recovery process of hours.

Forensic finding:

The relay protection system was working correctly. The forensic investigation found a cracked part made of acrylic glass located inside a metallic encapsulation of the affected ES indicator (see Figure 2.11)

Historical data:

The time to failure is 18 years. The affected part was overlooked during the routine maintenance because the location is hidden inside the metallic encapsulation. No sign of excessive leaking before the breakdown.

Potential failure mode:

Hypothetically, the potential failure mode would be as follows:

1. The acrylic glass might be unsuitable to use under a constant warm temperature in tropics. On the longer term, a fraction of the material becomes aged and brittle that lead into the crack.
2. The acrylic glass might have an inherent defect that unexpectedly passed the quality control during the manufacturing process or due to a mounting error.

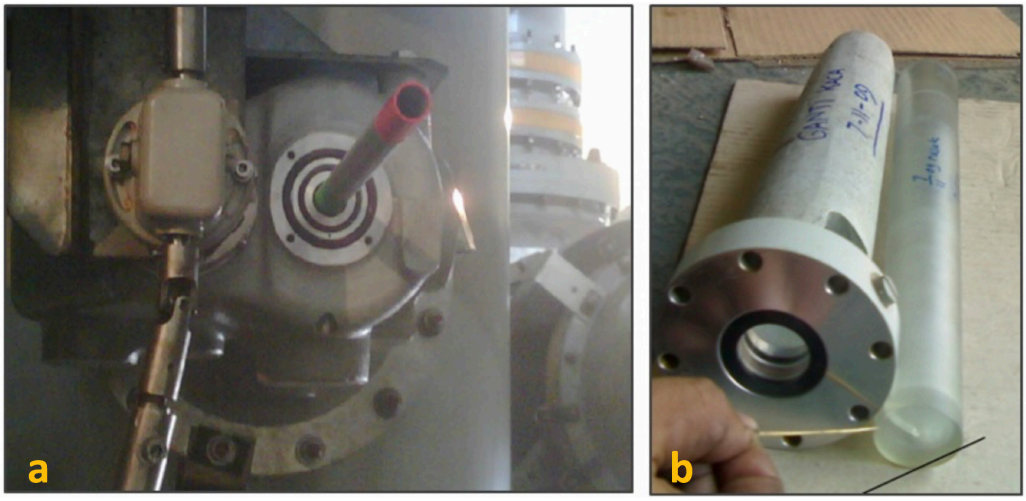

Figure 2.11 Failed ES indicator in Case #4: a) the complete ES indicator setup, b) the cracked acrylic glass.

2.5.2 Failures in connection with switching operation

There were two failures from 2 GIS locations occurred during a switching operation. The first failure was on a CB during a fault clearing, while the other was on a DS during a normal switching operation. The following paragraphs give the details.

2.5.2.1 Case #5: Energy storage failure on Circuit Breaker (CB)

Event description:

The failure was on a CB for a 150 kV transformer feeder in GIS with a 3-phase per enclosure configuration. The first failure originated from the inability of secondary (20kV) CB on the distribution feeder to clear a fault. The fault current of 15 kA was then passing through the power transformer and made the winding deformed and caused an insulation breakdown after 107 milliseconds. The transformer's differential relay then commanded the primary 150 kV CB (and also the secondary 20 kV CB) to trip, but, the 150 kV CB was failed to open in one phase. The CB contacts on the failed phase were melting and followed by the insulation breakdown.

Forensic finding:

The energy storage of the 150 kV CB comes from a compressed-spring. At the moment of failure, the secondary subsystem was successfully sending the tripping command to the CB, but, the spring on one phase failed to react. The investigation team after the failure found a melted-spring on phase S and also melted contacts (see Figure 2.12).

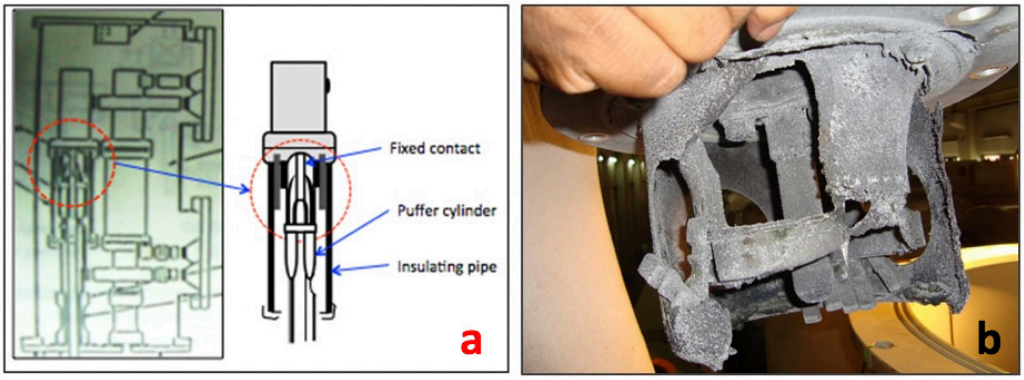

Figure 2.12 a) the diagram of the melted fixed contact in the failed CB in Case#5. b) Remaining fixed contact after the failure.

Historical data:

The GIS substation is located indoor. The relays function check 1.5 years before the breakdown, had proved that all relays were working correctly. The partial discharge measurement and the gas analysis three years before breakdown did not show any degradation or humid condition inside the GIS.

Potential failure mode:

The failure started on the energy storage system on one phase of the CB. The spring was stuck, so it failed to activate the CB as commanded by the relay system.

The faulty spring was probably due to fatigue of the spring holder. Fatigue could be due to the operational cycle of the driving mechanism. However, the cycle number was still below the limit accordingly to the CB classification [24]. The humid environment may accelerate fatigue. For instance, corrosion occurs in some parts due to which lubricating grease degraded faster before the next major inspection. The service time this failed CB is 19 years.

2.5.2.2 Case #6: Kinematic failure on Disconnector Switch (DS)

Event description:

A phase of a disconnector switch (DS) of an outdoor 500 kV GIS had been failed under the closing command, while the other two phases were successful. Although the switching was no-load, the generated very fast transient overvoltage (VFTO) is held responsible for the gas breakdown on the stress shield of the CB next to the failed DS contacts.

Forensic finding:

Besides white powder in the affected enclosure, the DS main contacts were found melted as seen in Figure 2.13 (a). A spark trace was found inside the CB (see Figure 2.13, b). The spark was starting from the stress shield of the CB, placed next to the failed DS contacts, to the ground. In this case, the rupture disc was still intact.

Historical data:

The GIS location is close to the sea, where plenty of pollutants like the salty aerosol are around. Former gas analysis on the affected CB compartment had shown that the humidity is low (< 100 ppmV), while in the DS, the humidity is higher but below 1000 ppmV. No PD had been observed before the breakdown. The time to failure is 19 years.

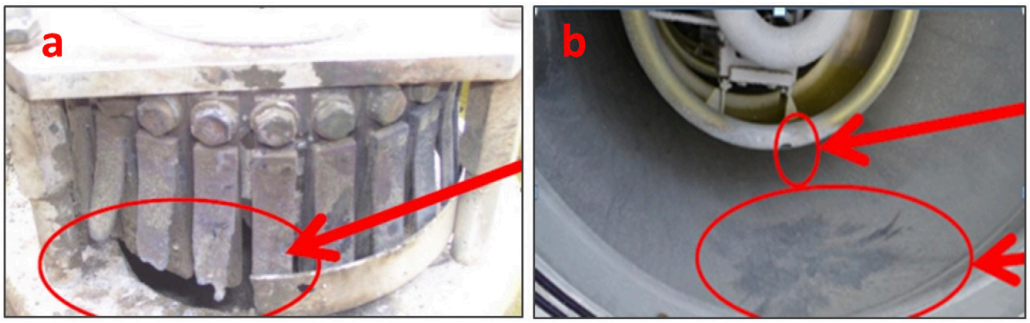

Figure 2.13 Forensic findings from Case #6: a) Melted main contacts of the affected DS. b) A spark trace at the ground of the CB enclosure next to the affected DS.

Potential failure mode:

The failure was due to the incomplete stroke on one phase of the DS during the closing operation. The cause might be due to the kinematic failure of the coupling between the energy storage and the main contacts. The degradation of this part could be due to the accelerated corrosion by the moist environment and the salty pollutants.

Following the kinematic failure, the distance between the main contacts of the failed DS was not sufficient to maintain the dielectric strength at a more extended closing operation. Reflection and refraction of traveling waves in the contact-gap generated the VFTO, and a breakdown occurred at the maximum curvature of the stress shield where the highest electric field is located.

2.5.3 Failures in connection with transients from causes external to the GIS

Two failures in 2 locations occurred in connection with the voltage transients from causes external to the GIS. In the first case, the failure occurred directly after a lightning stroke near a substation, while the other occurred after a cable breakdown in a feeder line connected to GIS. The following paragraphs give the details.

2.5.3.1 Case #7: Spacer flashover on gas-insulated line (GIL) after a lightning stroke

Event description:

A spacer flashover occurred at the outdoor 500 kV GIL, about 5 meters from the SF_6-to-air bushing termination. The record from the Digital Fault Recorder (DFR) had shown that the breakdown took place after a lightning stroke on the connected Overhead Line close to the substation. The surge arrester has been reported as failed to operate.

Forensic finding:

Arcing mark and fissures had been found on the spacer surface, which indicates a high energy discharge during the event. The other finding was the arcing trace on the spacer's connection to the conductor (see Figure 2.14, b).

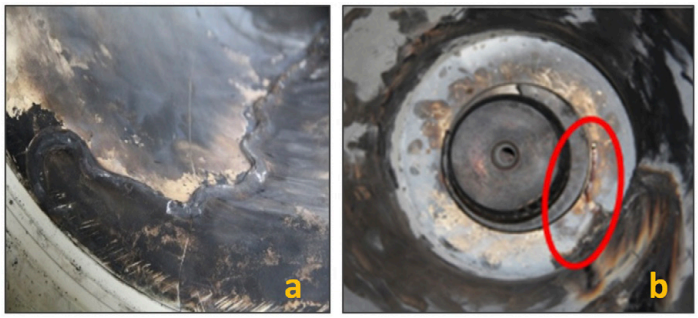

Figure 2.14. Forensic findings from Case #7: a) A carbonized track at the surface of the conic spacer, b) the melted part on the connection between the spacer and the conductor.

Historical data:

The GIS substation location is in a metropolitan area, where pollutants from vehicles are intense. The spacer is located at the outdoor GIL. No gas analysis has been reported. The time to breakdown is 13 years.

Potential failure mode:

From the evidence, the flashover started from the connection between the spacer and the conductor in the direction to the ground. In the early stage, a loose connection between the contacts probably started the partial discharges. This loose connection probably due to vibration during GIS operation, or improper installation.

In the more extended period, PD grew, and decomposed solid by-products might be accumulated at the spacer surface that decreased the withstand of the insulation system, even worse if the gas was humid. The breakdown was then likely to occur under the voltage transient from the lightning.

2.5.3.2 Case #8: Joint conductor failure after a fault in the system

Event description:

A joint-connection of Voltage Transformer (VT) of an indoor 150 kV GIS had a breakdown directly after a dielectric failure on an XLPE cable-line connected to the GIS (see Figure 2.15). The GIS has a three-phase per enclosure configuration. The failure caused the separation of the joint-conductor between the VT and the busbar. A high energy discharge had occurred as indicated by the blasting of the rupture disc.

Forensic finding:

During the investigation, the flashover mark on the enclosure was observed (see Figure 2.15, a). The separated joint-conductor on the three phases have been found, by which the white powders have covered them. The joint-contacts were melted (Figure 2.15, b and c).

Figure 2.15. Forensic findings from Case #8: a) VT enclosure with flashover mark on its external body, b and c) the broken conductors that linked the VT with the busbar below (male and female connections).

Historical data:

The GIS installation is indoor and located in a metropolitan area. The gas analysis before breakdown shows there was no excessive humidity in the affected enclosure. The time to breakdown is 25 years.

Potential failure mode:

It is difficult to draw a failure mode due to limited information about the case. Deterioration probably firstly occurred in the joint-contacts, due to, probably, the PD. Furthermore, by considering that the service time was 25 years, the PD development might be slow and took years, for example, due to vibration during the load cycle or the circuit breaker operation. After years, although the degraded contacts could withstand against the AC voltage stress, they had failed under the higher voltage stress which originated from the cable-line failure.

In this case, the influence of the tropical parameters has not been observed.

2.6 *Failure Mode Effect and Criticality Analysis (FMECA)*

The former sections have explained the failure experiences of GIS operating under tropical conditions as observed in the JABA Case Study. According to the statistical analysis, the high failure rates of the case study were mostly contributed by failures in outdoor GIS and GISs installed before 2000. Failures of both classes GIS were mostly occurring in the switching components, like in CB and DS. While in 150 kV GIS, a significant number of failures on primary conductor and termination has also been observed.

The intense fault-interruptions by the lightning incidence in the JABA Case Study were found to be characteristics for GIS operating under tropical conditions. This fact arises a concern to ensure the readiness of surge arresters in a substation.

On the other cases, hidden failures [3,37] due to faulty relays can be addressed to aging and corrosion of wiring and auxiliary contacts. Therefore, it is essential to keep the relay's cubicle dry.

Our observation also found humidity contents above recommended limits in many non-CB enclosures of 150 kV GIS. The value of humidity can be significantly high if the GIS

has not been equipped with the absorbent. The major source of humidity is the absorbed and adsorbed moisture of internal components in GIS. Care should be taken during GIS handling, particularly in the activity with opening enclosures.

On the other observation, leakage rates above 10% of its original weight per year have been found in several enclosures of the JABA Case Study. The value is higher than the previous report by [26]. Although the leakages provide only a small contribution to the humidity content in gas, it arises environmental concern and the possibility of a major failure at the later stages.

Our forensic investigations provide various failure modes from the JABA Case Study. The investigation found that in many cases the insulation system breakdown is the end-result of the catastrophic failures. In some cases, it has been preceded by failures of the other subsystems in GIS. The tropical parameters could be involved both directly and indirectly in a failure.

Following the findings above, the critical failure modes of GIS operating under tropical conditions will be determined in this section. A method which is known as the Failure Mode Effect and Criticality Analysis (FMECA) [38] is used. The objective is to find which failure modes contribute to the highest company loss, so that actions, like maintenance and predictive tasks, could be prioritized.

2.6.1 GIS Hierarchical Layers

The FMECA is usually performed on a component level, for example, a circuit breaker or a power transformer. The FMECA sees a component as a system which owns at least a single main function. Within a system there are subsystems of each also owns at least a single subfunction. Further division of subsystems into sub-sub-systems is possible depending mainly on the available data.

GIS consists of bays, enclosures, components, and parts. Therefore, when performing FMECA on GIS, its “hierarchical layers” should be taken into consideration. Figure 2.16 shows how a GIS can be seen based on its physical layers (in the horizontal direction), and by its functionality layers (in the vertical direction). In this thesis, a GIS is divided into four layers functionalities, namely (from top to bottom hierarchy), substation, bay, enclosure, and component. The lower layer becomes a subsystem of the higher layer, for example, a GIS substation has subsystems of bays, while a GIS’ bay consists of subsystems of enclosures, and so on.

The component-layer consists of subsystems based on sub-functionalities. For example, a Circuit Breaker (CB) has four subsystems, namely, primary, secondary, driving mechanism, and construction and supports (see Table 2.12). Physically, a component consists of parts.

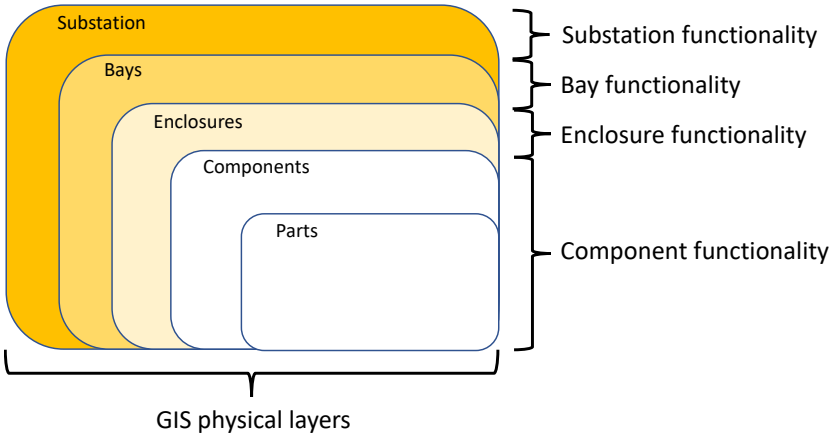

Figure 2.16 The hierarchical layers in GIS. The physical layers see a GIS based on the grouping of components, while the functional-layers see a GIS based on the division of functions.

As a first step in performing FMECA, GIS functionality on each layer should be first determined. This is given in the following paragraphs.

GIS functions as a substation

In the transmission network, the GIS substation role is being a node to distribute the electricity within the network. The GIS should be able to energize (and de-energize) the high voltage apparatus and to isolate fault within the shortest possible time to maintain overall grid stability [6].

Functions of bays in a GIS substation

The typical arrangement of bays in a GIS substation is as follows [5]:

- Single busbar
- Double busbar
- Double busbar with double circuit breaker
- One and a half circuit breaker scheme
- Ring busbar

In the JABA Case Study, the common scheme is the double-busbar configuration for 150 kV GIS, and one and a half circuit breaker scheme for 500 kV GIS. Table 2.12 provides functions of bays in these two typical configurations.

Table 2.12 Functions of different bays in a GIS substation

Bay Type	Function
Busbar	Busbar roles as the primary path for the current transfer in a substation, where all currents from the incoming and the outgoing feeders are passed.
Feeder	This bay links the GIS with the transmission network (i.e., power cables or overhead lines) and the high voltage apparatus, mostly the power transformer. Including in this group: the line-bay and the transformer-bay.
Bus Coupler	A bus couple makes a couple between two busbars in a double-busbar configuration. It provides redundancy in a substation. In one and a half CB scheme, the bus coupler is represented by a tie-CB in the Diameter-bay.
Bus Section	Bus Section splits two busbars of two subsystems in the power network at a similar substation. It provides redundancy and for contingency planning when a fault occurs in the system.

Functions of enclosures in bays of a GIS substation

An enclosure contains components in GIS. The configuration of enclosures differ among GIS makes and designs. Some components have a dedicated enclosure, like in CB, VT(Voltage Transformer), and termination; while others share the same enclosure. It is also possible to say that the enclosure provides dielectric and construction support functions for components in GIS.

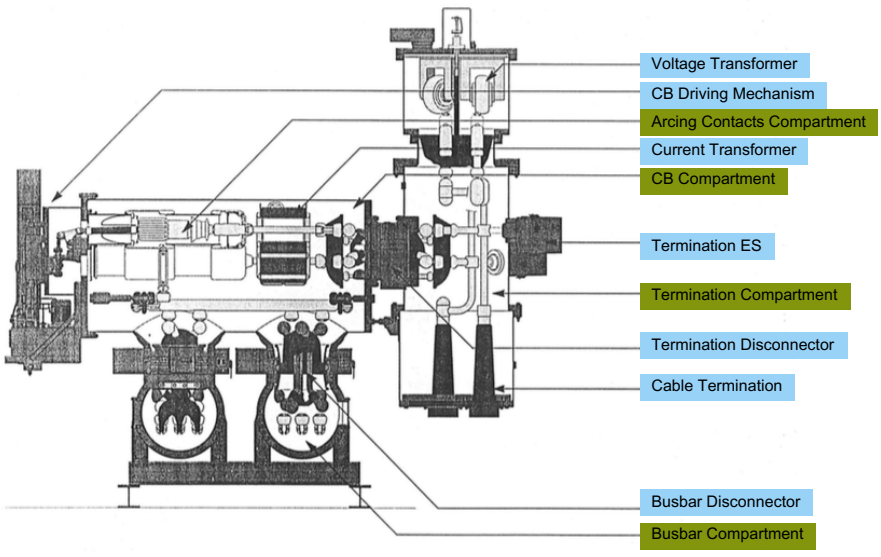

Figure 2.17. An example of a feeder bay in GIS [61]. The components are placed inside different enclosures of GIS.

Functions of components located inside the enclosures.

Based on their functionality, there are six groups of components, namely:

1. Fault- and load-interrupters, i.e., Circuit Breaker (CB).
2. No-load switches including limited-fault interrupter, i.e., Disconnector Switch (DS), Earthing Switch (ES), High-Speed DS (HSDS).
3. The main path for current distributions in GIS and interconnection among GIS feeders, i.e., Busbar, Bus Segment (BS).
4. Link the GIS with the incoming and outgoing feeders, i.e., Terminations (TE).
5. Voltage and current sensing devices, i.e., Instrument Transformers (IT), including the Current Transformer (CT) and the Voltage Transformer (VT).
6. Transient overvoltage limiter, i.e., Surge Arrester (SA).

Each component consists of subsystems. Table 2.13 gives a summary of subsystems in components of GIS.

Table 2.13 GIS components, sub group of components, subsystems, function of subsystems, and key parts

Component	Sub Group of Component	Sub System	Function of Sub System	Key Parts
Circuit Breaker (CB)	CB can be grouped based on its driving mechanism, as follows: Hydraulic CB, Pneumatic CB, Spring CB	Primary	Conduct the current at its rating	Main and arcing contacts, conductor
		Secondary	Sending a command to driving mechanism either from remote control or from local control cubicle.	Wiring, Auxiliary Contacts, Relays
		Driving mechanism	Energy storage to actuate the CB after a command from secondary sub system	Spring, Hydraulic and Pneumatic compressions
			Transform the energy from the energy storage to move the main contacts	Mechanical rod/ link, mechanical joints of CB driving mechanism
		Dielectrics	Extinguish the **arcs** and to insulate HV parts to the ground	SF_6 gas and Spacers
		Construction & Support	• Provide mechanical strength • SF_6 gas containment • Monitor gas pressure /density • Provide overpressure relief	Enclosures body, enclosure's base, sudden pressure relief, gas pressure/ gas density gauge
Switches	Switches can be grouped based on its functionality and driving mechanisms Based on its functionality: DS, ES, HSDS	Primary	Conduct the current at its rating	Main contacts, conductor.
		Secondary	Sending a command to driving mechanism either from remote control or from local control cubicle.	Wiring, Auxiliary Contacts, Relays
		Driving mechanism	Energy storage to actuate the switches	Spring, Hydraulic and Pneumatic compressions

Component	Sub Group of Component	Sub System	Function of Sub System	Key Parts
	Based on its driving mechanism.: Electric DS, Pneumatic DS, Spring DS		Transform the energy from the driving mechanism to move the main contacts	Mechanical rod/ link, mechanical joints of DS driving mechanism
		Dielectrics	Extinguish the **sparks** and to insulate HV parts to the ground. In DS for bus-coupler and HSDS, the dielectric may also distinguish the **arcs** but with limited capacity.	SF_6 gas and Spacers
		Construction & Support	• Provide mechanical strength • SF_6 gas containment • Monitor gas pressure /density • Provide overpressure relief	Enclosure base, enclosure body, Sudden pressure Relief, Gas Pressure/ Density gauge
Busbar, Bus Segment (BS)	-	Primary	Conduct the current at its rating	Primary conductor, including joints of bus conductor
		Dielectrics	To insulate the HV parts to the ground.	SF_6 gas and Spacers
		Construction & Support	• Provide mechanical strength • SF_6 gas containment • Monitor gas pressure /density • Provide overpressure relief	Enclosure base, enclosure body, Sudden pressure Relief, Gas Pressure/ Density gauge
Termination (TE)	Based on types of connection to GIS: 1. SF_6-to-air bushing	Primary	Conduct the current at its rating	Primary conductor of termination
		Dielectrics	To insulate the HV parts to the ground.	SF_6 gas and Spacers

Component	Sub Group of Component	Sub System	Function of Sub System	Key Parts
	2. Cable sealing end 3. GIL with Power Transformer /Reactor Interface	Construction & Support	• Provide mechanical strength • SF_6 gas containment • Monitor gas pressure /density • Provide overpressure relief	Enclosure base, enclosure body, Sudden pressure Relief, Gas Pressure/ Density
Instrument Transformer (IT)	Based on its functionality: Current Transformer (CT), Voltage Transformer (VT)	Active Parts	Transform the current (CT) or the voltage (VT) from a higher value to a lower one. CT and VT are used for monitoring, and part of protection system.	Active parts: primary and secondary windings, dielectrics
Surge Arrester (SA)	-	Active Part	Cutting the peak of transient over voltage accordingly to its V-I characteristics.	Metal Oxide blocks

2.6.2 Failure Modes of GIS Operating under Tropical Conditions

In the next step, failure modes in GIS will be determined. A failure is defined as any deviation of any system or subsystem in fulfilling its function (or subfunction). Since GIS consists of layers, consequently, any failure at the lower hierarchical layer of GIS will fail at the higher layer. Therefore, we start the FMECA by analyzing failure modes at the component-layer, i.e., at the subsystems of components in GIS. The components under analysis were CB, switches, busbar/ bus segment, and termination; where major failures of these components have been reported many from the JABA Case Study.

Apart from the unknown/ other categories, Table 2.3 has provided six kinds (two of them related to insulation system breakdown) of GIS failure modes at the component-layer based on the CIGRE document. Figures 2.18 to 2.22 provides details of failure modes in subsystems of components in GIS based on the forensic investigation from the JABA Case Study. A failure mode which is reported in the CIGRE TB 513 [3] is mentioned in the red box.

Dielectric Subsystem

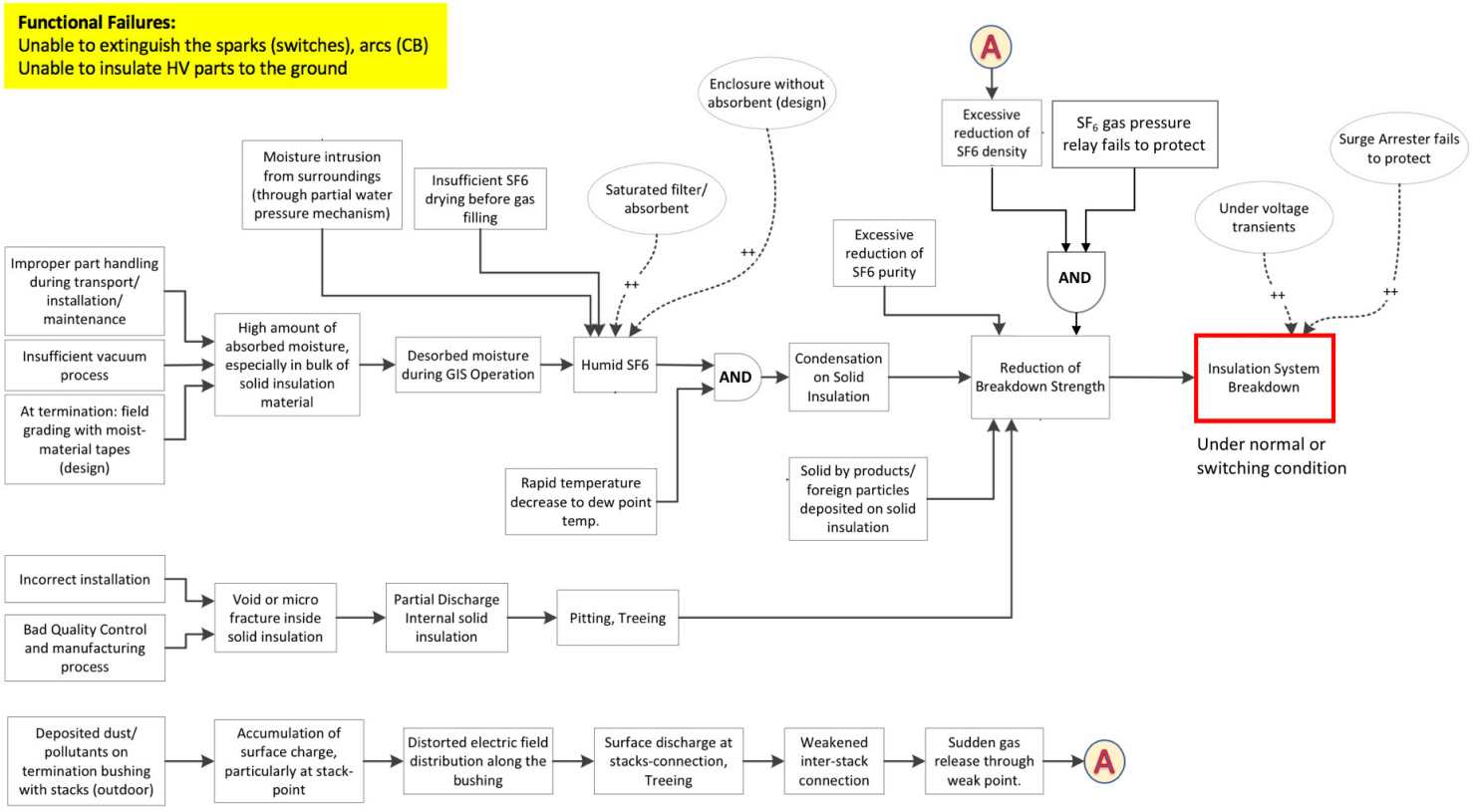

Figure 2.18. Failure modes of the Dielectric Subsystem of GIS operating under tropical conditions as found in the JABA Case Study. A failure mode which is in line with CIGRE TB 513 [3] is shown by the red box. The bubble with dotted lines show the Failure Susceptibility Indicators for circumstances that may increase the likelihood of a failure mode more than usual.

Primary Conductor Subsystem

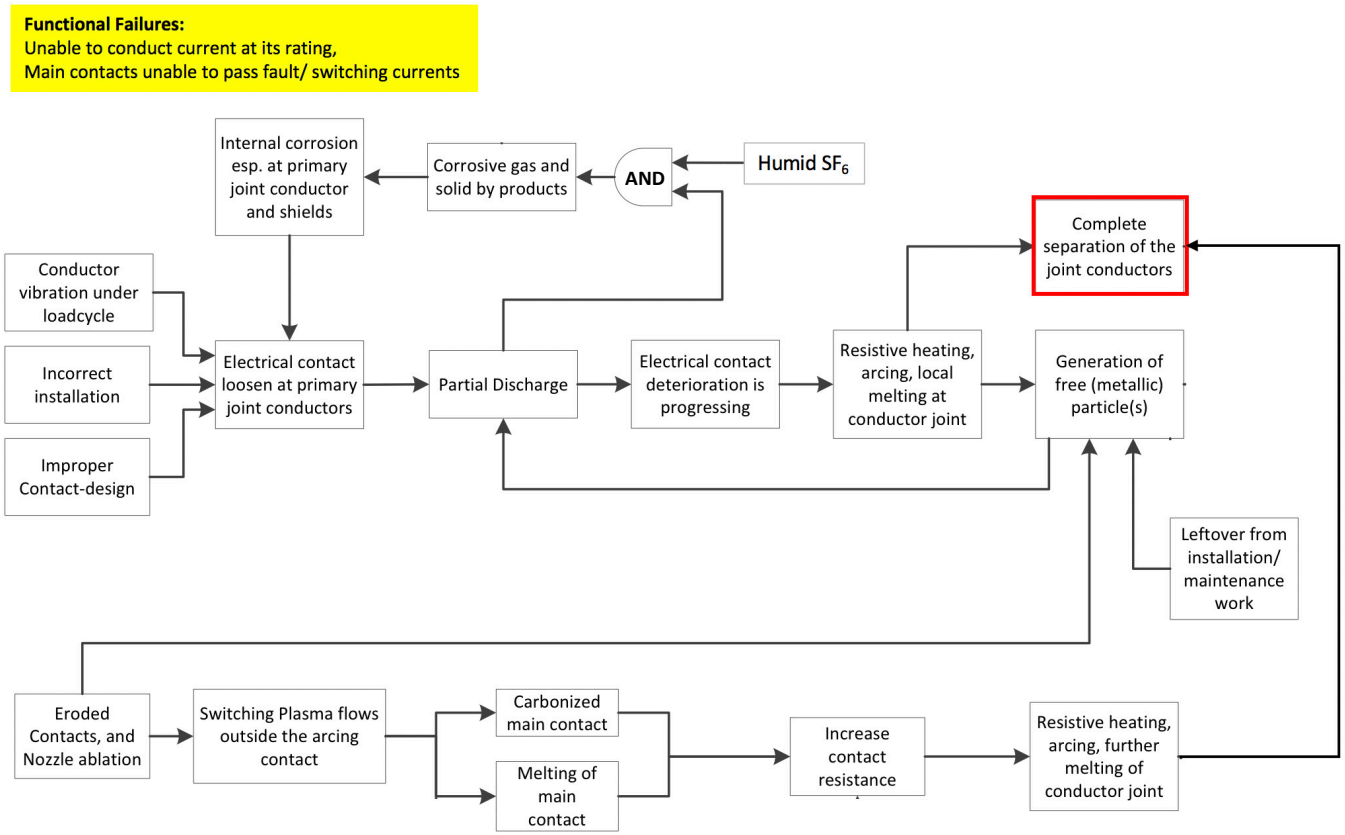

Figure 2.19. Failure modes of the Primary Conductor Subsystem of GIS operating under tropical conditions as found in the JABA Case Study. A failure mode which is in line with CIGRE TB 513 [3] is shown by the red box.

Construction and Support Subsystem

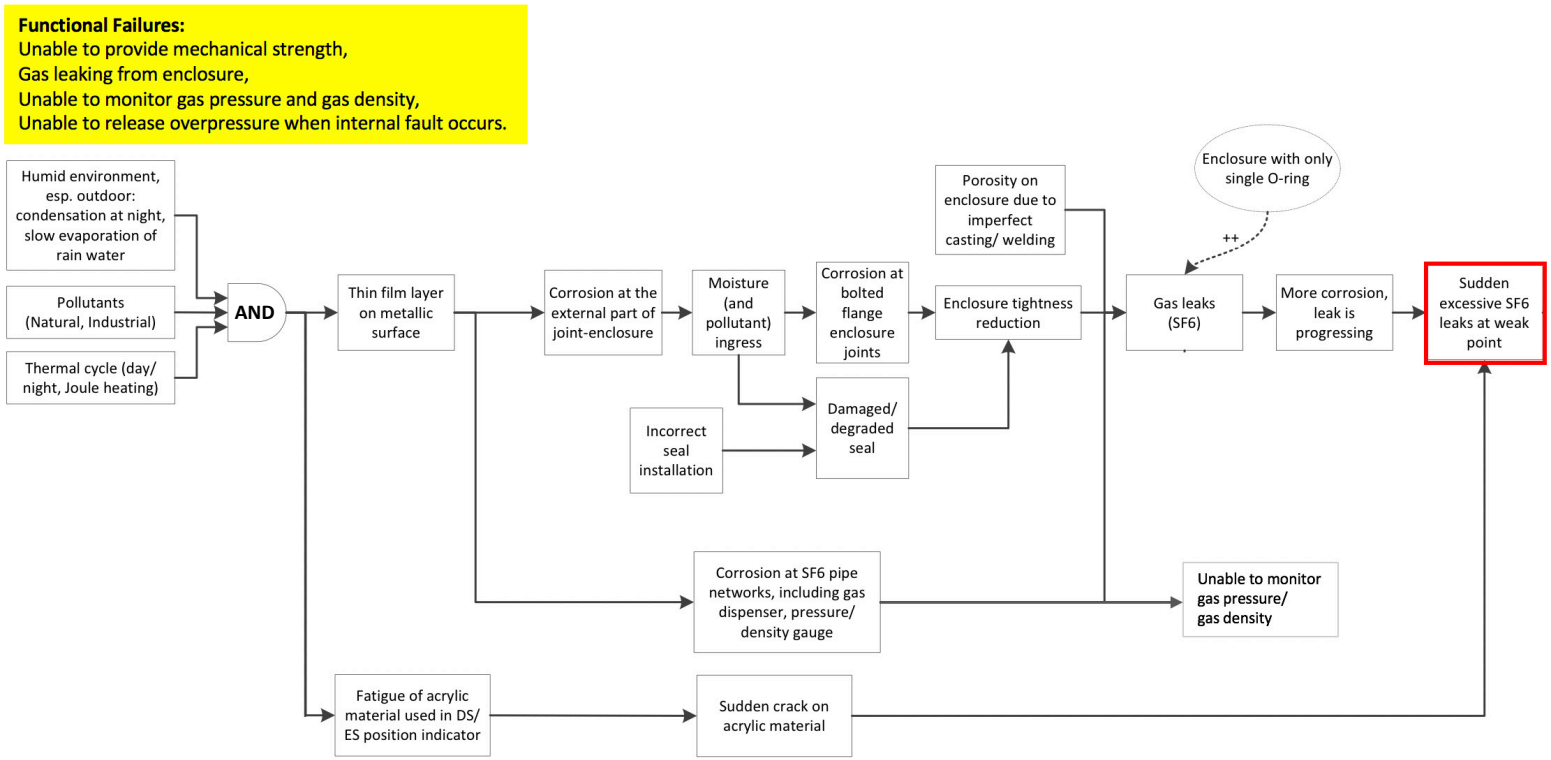

Figure 2.20. Failure modes of the construction and support subsystem of GIS operating under tropical conditions as found in the JABA Case Study. A failure mode which is in line with CIGRE TB 513 [3] is shown by the red box. The bubble with dotted lines show the Failure Susceptibility Indicators for circumstances that may increase the likelihood of a failure mode more than usual.

Driving Mechanism Subsystem

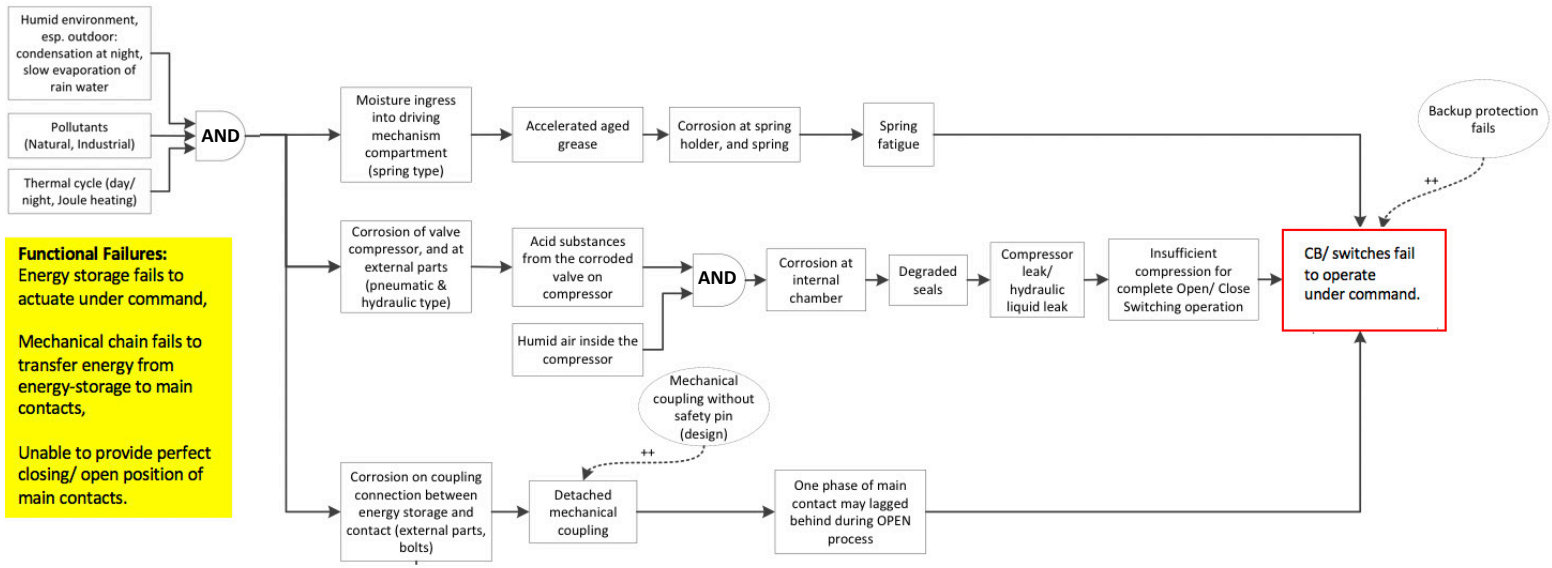

Figure 2.21. Failure modes of the driving mechanism subsystem of GIS operating under tropical conditions as found in the JABA Case Study. A failure mode which is in line with CIGRE TB 513 [3] is shown by the red box. The bubble with dotted lines show the Failure Susceptibility Indicators for circumstances that may increase the likelihood of a failure mode more than usual.

Secondary Subsystem

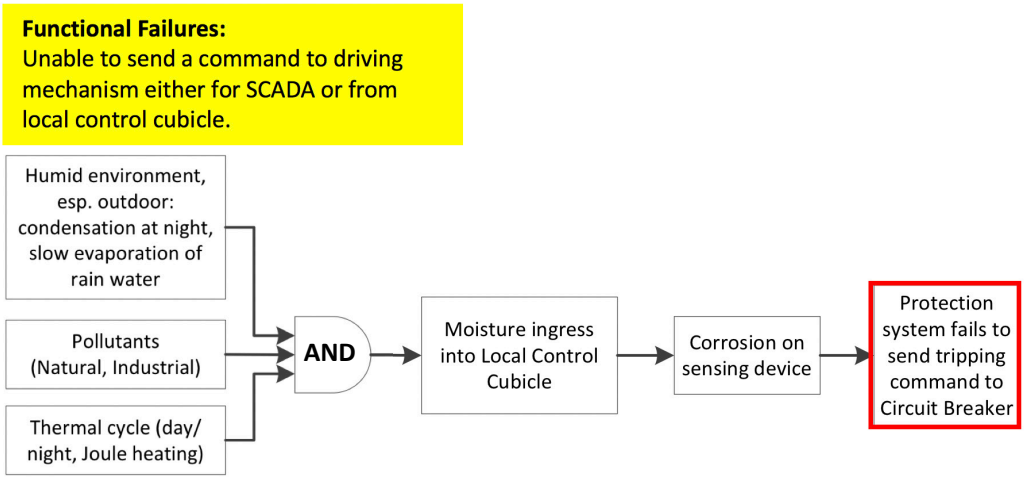

Figure 2.22. Failure modes of the secondary subsystem of GIS operating under tropical conditions as found in the JABA Case Study. A failure mode which is in line with CIGRE TB 513 [3] is shown by the red box.

2.6.3 Failure Modes Effect Analysis

In the following step, the effect of each failure mode is analysed. The effect can be distinguished based on the hierarchical layer, which affected by a failure mode [4]. For example, a failure mode of "insulation breakdown" at a termination (component-layer) of a bay-feeder, give an effect at the component- and enclosure-layers, namely, "the circuit is shorted to ground unintentionally with possible personnel safety and economic issues." The same failure mode contributes to the effect of "unintentionally interruption of the affected bay due to a phase-to-ground fault that exposes to personnel safety, system redundancy, and economic consequences," at the bay layer.

In this thesis, we focused on six failure modes of five subsystems of components, as mentioned in Figures 2.18 to 2.22.

2.6.4 Failure Modes Criticality Analysis (FMECA)

The risk if a failure mode occurs is elaborated in FMECA. A risk is defined as the product of probability (of a failure mode occurs) and its consequences [38]:

Risk = Probability that a failure mode occurs x Consequences … 2.1

When the probability is not available, it can be replaced by the frequency of occurrence and its possibility for detection as follows [14,38]:

Risk = (Frequency of occurrence x Detection) x Consequences … 2.2

A scoring method is used to calculate the risk based on equation 2.2. The score is dimensionless, which shows a relative measure for a ranking purpose. It does not mean that a consequence with a score of 4 has a double impact than the one with a score of 2. Scoring classifications for the frequency of occurrence, detection, and consequences

based on the expert judgments from the JABA Case Study, have been developed. The consequences were taken from the risk matrix of a transmission utility of the JABA Case Study.

The criticality analysis has been conducted on six failure modes, as mentioned in Table 2.3. The criticality analysis of each failure mode will be based on the worst possible scenario that may occur in the JABA Case Study.

2.6.4.1 Occurrence and Detection Criteria

Tables 2.14 and 2.15 provides scoring criteria for occurrence and detection. The values were decided based on expert knowledge, where a linear scoring from 1 to 5 is applied. The higher the score, the more critical the parameter. The score of "detection" represents the possibility to capture a failure mode before a failure occurs.

Table 2.14 Classification of "Frequency of occurrence" and scoring in FMECA

Occurrence (time per year)	Score for calculation
> 1	5
0.6 < f ≤ 1	4
0.3 < f ≤ 0.6	3
0.1 < f ≤ 0.3	2
≤ 0.1	1

Table 2.15 Classification of "Detection" and scoring in FMECA

Detection	Score for calculation
Directly recognized by the available monitoring system (no additional measuring/ diagnostic equipment is needed)	1
Detected by measuring/ diagnostic tools under live condition	2
Detected only with shutdown diagnostic test/ measurement	3
Detected by a small chance with shutdown diagnostic test/ measurement	4
Cannot be detected by the current available monitoring & detection systems	5

2.6.4.2 Consequences Criteria

A risk matrix of a transmission utility [39] of the JABA case study has been adopted to determine the consequences of failure modes. There are six business values, namely, safety, financial due to extra fuel cost (extra cost to run a non-economical power plant

to support the power system), financial due to equipment cost (to replace a damage equipment), energy not served (reliability), customer satisfaction, leadership, and the environment. Each consequence has five severity levels, as mentioned in Tables 2.16 to 2.22. The linear scoring is defined. A failure mode can contribute to different severity levels, depending on many factors, like the location of GIS in the transmission grid, and power flow when a failure occurs.

Table 2.16 Severity level and scoring for Safety business value in FMECA

Consequence of a failure to the Safety	Score for Calculation
Cause death (Fatality)	5
Cause permanent disability	4
Cause temporary disability	3
First aid injury, medical aid injury	2
Near miss	1

Table 2.17 Severity level and scoring for Financial (Extra Fuel Cost) in FMECA

Consequence of a failure to the Extra Fuel Cost	Score for calculation
> 750,000 USD	5
> 75,000 – 750,000 USD	4
> 7,500 – 75,000 USD	3
> 750 – 7500 USD	2
≤ 750 USD	1

Table 2.18 Severity level and scoring for Financial (Equipment Cost) in FMECA

Consequence of a failure to the Equipment Cost	Score for calculation
> 2,000,000 USD	5
> 200,000 – 2,000,000 USD	4
> 20,000 – 200,000 USD	3
> 2,000 – 20,000 USD	2
≤ 2,000 USD	1

Table 2.19 Severity level and Scoring for System Reliability (ENS) in FMECA

Consequence of a failure to the Energy Not Served	Score for calculation
> 4000 MWh	5
> 400 – 4,000 MWh	4
> 40 – 400 MWh	3
> 4 – 40 MWh	2
≤ 4 MWh	1

Table 2.20 Severity level and Scoring for Customer Satisfaction in FMECA

Consequence of a failure to the Customer Satisfaction	Score for calculation
A failure results to Very High Potential Concerns	5
A failure results to High Potential Concerns	4
A failure results to Moderate Potential Concerns	3
A failure results to Low Potential Concerns	2
A failure results to No Potential Concerns	1

Table 2.21 Severity level and Scoring for Leadership in FMECA

Consequence of a failure to the Leadership	Score for calculation
Committed to law/ legal action	5
Top management and government officials are involved	4
Other bodies from local government officials are involved	3
Handled by middle managerial level	2
Handled by local substation supervisor	1

Table 2.22 Severity level and Scoring for Environment in FMECA

Consequence of a failure to the Environment	Score for calculation
Catastrophic contamination, National issue	5
Severe contamination, National/ Regional issue	4
High contamination, Regional/ local issue	3
Medium contamination Local issue	2
Low contamination	1

The total consequence is the summation individual consequence score, as follows

Score of Consequences = Score for Safety + Score for Extra Fuel Cost +Score for Eq. Cost + Score for ENS + Score for Customer Satisfaction + Score for Leadership + Score for Environment … 2.3

2.6.4.3 Result

Table 2.23 provides the risk score of six failure modes and the related subsystems and example of failures from the forensic case in the JABA Case Study. The calculation is based on the equation 2.2. The higher the score indicates the higher the risk of a failure mode. Details of the risk score based on the FMECA are provided in Appendix C.

Table 2.23 Subsystems involved in major failure modes of GIS in tropics

	Failure Mode	Directly involved subsystem	Forensic example in the JABA Case Study	Risk Score	
				150kV	500kV
1	Failing to perform requested operation	Driving mechanism	Case #5, Case #6	**171**	**198**
2	Loss of electrical connections integrity in primary conductor	Primary	Case #1, Case #8	**198**	**81**
3	Loss of electrical connections integrity in secondary	Secondary	-	30	39
4	Dielectric breakdown in normal service	Dielectric	Case #2, Case #3	**176**	**108**
5	Dielectric breakdown in connection with switching, and/or external transients.	Dielectric	Case #7	**198**	**81**
6	Loss of mechanical integrity on enclosures, pressure gauge, including big SF_6 leakage	Const. & Support	Case #4	60	76

From the risk score above, the following interpretations are drawn:

1. In 150 kV GIS (class-2), the order of the top-3 critical failure modes are as follows:
   a. Dielectric breakdown, both under normal service condition and voltage transients.
   b. Loss of electrical integrity in the primary conductor subsystem.
   c. Failing to perform the requested operation (due driving mechanism failure)

2. In 500 kV GIS (class-5), the order of the top-3 critical failure modes are as follows:
   a. Failing to perform the requested operation (due to other than the secondary failure).
   b. Dielectric breakdown, mainly during the normal service operation.
   c. Loss of electrical integrity in the primary conductor subsystem.

3. In both classes, the least critical failure mode is “the loss of electrical connections integrity in secondary.” Although this failure mode contributed to a significant number of interruptions, its consequences are relatively low.

4. The “loss of mechanical integrity on enclosures, pressure gauge, including a sudden SF_6 leakage” also less critical than the three failure modes mentioned in point 1 and 2, but still higher than the failure mode on secondary.

5. From these findings, the three critical subsystems of components of GIS operating under tropical conditions are as follows:
   a. Dielectric subsystem.
   b. Primary conductor (including joints and main-contacts) subsystem.
   c. Driving mechanism subsystem.

2.7 *Conclusion*

From our thorough investigation into GIS operational experiences in tropical conditions in the JABA Case Study, the conclusions are as follows:

1. The influence of tropical conditions on the performance of GIS can be directly and indirectly. In direct connection, the humid environment, the relatively warm temperature, and the long condensation during the night can efficiently produce a thin film layer as a basis for corrosion. The fact that GIS is mostly installed in metropolitan-, industrial-, and next to the sea areas, where pollutants exist; make the corrosion even faster. The corrosion starts at the exposed parts of GIS, especially at the junction between the enclosures, and the driving mechanism subsystems including the energy storage and the mechanical-coupling components. Chain of deteriorations occurs afterward that possibly end up with the insulation system breakdown.

   In indirect connection, the intense lightning in tropical conditions makes the insulation system more susceptible to break down, especially if the surge arrester fails. Therefore, to ensure the condition of the surge arrester in the GIS connected to the Overhead line is essential. It also has been supported by our findings from the analysis of the interruptions.

2. A GIS with outdoor installation is more susceptible to the tropical condition as confirmed by the higher failure rate and the more steep hazard curves in the statistical analyses. The B-lives calculations suggested the sooner interval for major inspection for the outdoor GIS.

3. The humidity content in gas insulation mainly originates from the absorbed moisture inside the component in GIS, especially from the spacer. The amount of humidity in gas typically depends on the enclosure dimension and the volume (and also the material) of the internal component in GIS. Although leakages may introduce the addition of moisture from the ambient, our investigation concluded that the moisture from this mechanism is not significant.

4. All GISs in the tropics should be equipped with sufficient desiccants to avoid high humidity content. The higher humidity in insulating gas was mostly found in the non-CB enclosure of 150 kV GIS, which is caused by insufficient desiccants and/ or improper handling.

5. Through the FMECA, the three critical failure modes for GIS in the tropics are:
   a. The dielectric breakdown.
   b. Loss of electrical integrity in the primary conductor subsystem.
   c. Failing to perform requested operation, mainly due to failure at the driving mechanism subsystem.

   Meanwhile, construction and support- and secondary subsystems are less critical.

6. The performance of GIS operating under tropical conditions depends on internal and external facts (beyond specification), which are indicated as failure susceptibilities in practice. They can be mentioned:

a. Internal factors:
    i. GIS design, including vertical/ horizontal switching assembly, the volume of absorbents, support design, sealing design including its material, and paint materials.
    ii. Wear-out components, including fatigue.

b. External factors:
    i. Environmental stresses, namely, humid ambient, lightning incidence, temperature cycle, and pollutants.
    ii. Workmanship and quality control during manufacturing, erection, and maintenance of GIS (including the major inspection/ overhaul project).
    iii. Power systems where GIS is operated, like, the frequency of system manoeuvre, loading characteristics, system failures, and protection scheme.

These factors we indicate as failure susceptibility indicators [23].

7. Evidence from the forensic finding has shown that the dielectric breakdown preferably took place on the surface of the spacer. On the other hand, we also observed humid SF_6 in many non-CB enclosures of 150 kV GIS; that seems to have an impact on the performance of the insulation system. To verify this finding, we investigated the performance of spacers inside an enclosed humid SF_6. For this purpose, a laboratory setup was constructed in the High Voltage Laboratory in TU Delft. Details of the setup and the test results will be discussed in Chapter 3.

Chapter 3 Experimental Investigation: Spacer Flashover in Humid SF_6 under Different Electrical Stresses

The previous chapter discussed failure modes of GIS operating under tropical conditions. The humid SF_6 has been suspected to be involved in the dielectric failures of GIS in the case study. The concern on the humidity in GIS arises since humid SF_6 has been found in about 20% of the non-Circuit Breaker (CB) enclosures of GIS in the JABA Case Study, although these have been equipped with desiccants [40]. The humidity contents are higher than the recommendation of both the IEEE and IEC standards [24,31].

Following this observation, a series of tests have been conducted in the High Voltage Laboratory of TU Delft to investigate the influence of humidity on the performance of the insulation system in GIS. In principle, there are two regions of the GIS insulation system to be considered separately: 1) the SF_6 gas including its interface to the solid insulating or conducting materials, and 2) the *internal* bulk of the solid insulating material. All dielectric failures observed in the case study are found in the first region [40]. Therefore, the tests focus on this region.

An investigation of the breakdown strength of humid SF_6 had been formerly reported by [26] under the voltage stresses of AC, AC+LI and AC+SI. The conclusion was that both humidity and temperature in the GIS operating under the tropical conditions do not influence the breakdown strength of the gas insulation.

Further investigation of the flashover characteristics of a spacer under humid SF_6 has been conducted in the HV Laboratory of TU Delft. Different researchers have been working on this topic [41-43] but under conditions not representative of the tropical conditions. The tests presented in this chapter have been carried out in conditions similar to the ones in the tropics. The controlled parameters in the tests were the humidity and the gas pressure, while the temperature was kept constant at 20°C. This temperature was considered sufficient to represent the lower limiting temperature in the tropics. The gas pressure has been adjusted to represent the real operating condition. The tests were conducted under-voltage stresses of AC, Switching Impulse (SI), positive Lightning Impulse (LI+), and negative Lightning Impulse (LI-).

This chapter consists of two main parts, the experimental setup, and the test results. Firstly, section 3.1 explains the hypothetical insulation condition in GIS when humid SF_6 exists. Following that, section 3.2 explains the test setups covering the electrode configurations, sample material, gas pressure, and humidity manipulation. Section 3.3 provides voltage generation in the tests. Test results are given in section 3.4, followed by the analysis of test results in section 3.5. Section 3.6 provides a conclusion.

3.1 *Spacer with humid SF_6 in GIS*

In GIS, a spacer has two functions, i.e., 1) to provide mechanical support for the conductor and 2) to isolate different sections in GIS. However, the spacer constitutes the weakest part of the insulation system. The efficiency factor of a spacer, which is the breakdown strength ratio of the insulation system with and without the spacer, is lower at the higher gas pressure [44].

In humid insulating gas, a high amount of water molecules (H_2O) dilutes into the gas system (see the illustration in Figure 3.1). The presence of water molecules influences the withstand voltage of the insulating gas by two opposite mechanisms, i.e., the presence of humidity will reduce the withstand strength by lowering the density of the gas system [26], but on the other hand, since water is also an electronegative gas [45], the presence of a water molecule can improve the withstand strength of the gas system.

However, the interest of the current research is on the influence of humid SF_6 to the withstand of the gas-solid interface. The presence of humidity (i.e., the moisture in the form of gas) hypothetically will not influence on the breakdown of the gas-solid interface, as long it does not perturb the surface condition of the solid insulation. However, in particular condition, the moisture may turn into water or ice. It is worth noting that the water has a dielectric constant of 80, while ice is 2. The presence of water droplets on the insulator surface will raise the electric field in many locations of the solid insulation surface that decrease the withstand strength. Laboratory tests have been carried out to confirm this characteristic.

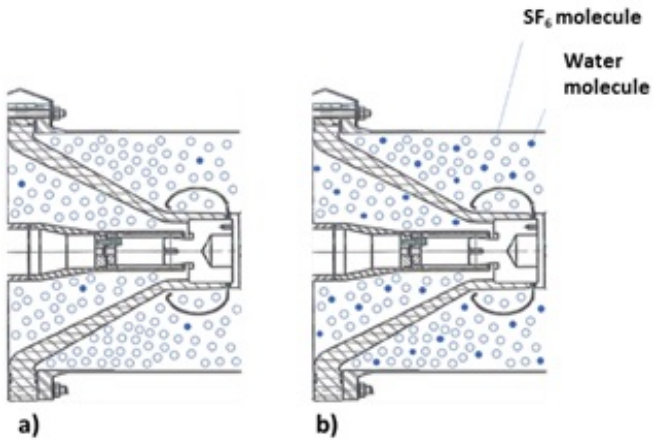

Figure 3.1 Illustration between dry (a) and humid (b) gas inside GIS.

3.2 *Experiment setup*

The setup mainly consists of three parts, i.e., a chamber with the sample and the electrodes, a vessel for mixing the SF_6 with humidity, and a setup for voltage generation. The sample consists of a cast epoxy-resin sample and SF_6 resembling the insulation system of a GIS. The next subsections give the setup details, including the electrode configurations, material specification, and dimension of the sample, gas pressure in the test, and humidity manipulation in the test chamber.

3.2.1 Electrode configurations

For testing purposes, a miniature of “spacer-and-gas” model has been developed. A cylindrical sample made of epoxy resin is placed between two electrodes inside a small chamber and filled with an SF_6 and H_20 mixture. The volume of the gas in such a vessel is 60 ml. Figure 3.2 shows the test-vessel.

Two electrode configurations were used to simulate three electric field distributions on the surface of the epoxy sample, namely:

1. *Homogeneous field configuration*, where the electric field parallel to the sample’s cylindrical surface is constant at any location.
2. *Quasi-homogeneous field configuration*, where the electric field parallel to the sample has a declining slope from the maximum to the minimum (which is representing the coaxial configuration of GIS).
3. *Inhomogeneous field configuration*, where a particle is attached on the epoxy close to the electrode so that a very high electric field appears at both tips of the particle.

The field-factor [46] has been introduced to measure the degree of homogeneity of each configuration above. The field-factor is the ratio between the maximum and the average electric field along the surface of the sample. The homogeneous configuration has a field factor of 1, the quasi-homogeneous configuration has a field factor in between 1 and 5, while the inhomogeneous configuration has a field factor beyond 5. Simulations with COMSOL® have been made to calculate the field factor of each configuration used in the tests as will be given in the next subsections.

The electrodes are made of stainless steel and to ensure good repetitive results, the electrodes were carefully re-polished to remove the craters before a new series of tests.

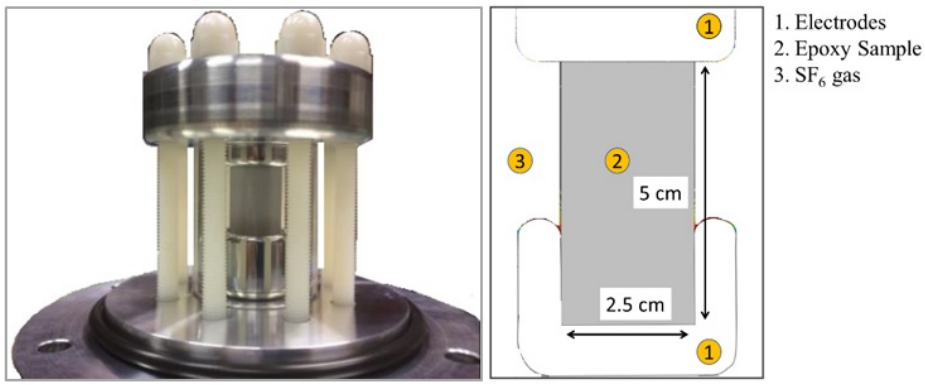

Figure 3.2 The test-vessel with an epoxy sample placed in the middle of the quasi-homogeneous configuration. The right picture shows the schematic diagram. During the experiment, the test-vessel is mounted into the GIS for the voltage application.

3.2.1.1 Electric field distribution on the surface of a conical spacer in GIS

In the JABA Case Study, the flashovers frequently took place on a conic spacer in GIS with single-phase configuration. Therefore, a simulation of the electric field distribution on a conic spacer based on a 420-kV spacer in the HV Laboratory of TU Delft has been made, as seen in Figure 3.3 below.

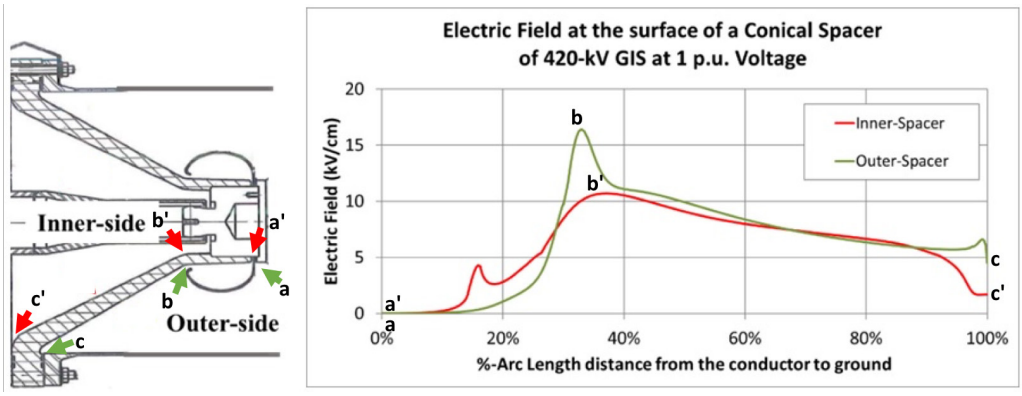

Figure 3.3 A schematic diagram of a 420-kV conical spacer in GIS in the HV Laboratory of TU Delft. The right figure shows the electric field distribution. Due to the corona ring, the high electric field region is placed at the region close to the tip of the corona ring. The maximum electric field at 1 p.u. is 16.4 kV/cm with an average of 8.2 kV/cm, while the field factor (E_{max}/E_{avg}) is 2.

It can be seen from the figure that the maximum electric field strength on the spacer at one p.u. is 16.4 kV/cm. This value is located near the tip of the corona ring. The GIS itself has the radii of the conductor and the internal enclosure of 65 and 270 mm, respectively. With this coaxial configuration, the maximum electric field without the spacer is 26.2 kV_{RMS} /cm. The insertion of a corona ring reduces the field concentration effectively in the connection between the spacer and the conductor.

3.2.1.2 Homogeneous configuration

The schematic diagram and the electrostatic simulation of the homogeneous configuration are presented in Figure 3.4. Point “a” and point “b” represents the electric field along the surface of the epoxy sample. A 38 mm-length epoxy sample is placed in between the two identical electrodes with a curvature radius of 4 mm. From the simulation, the field factor is 1.2, which is considered homogeneous.

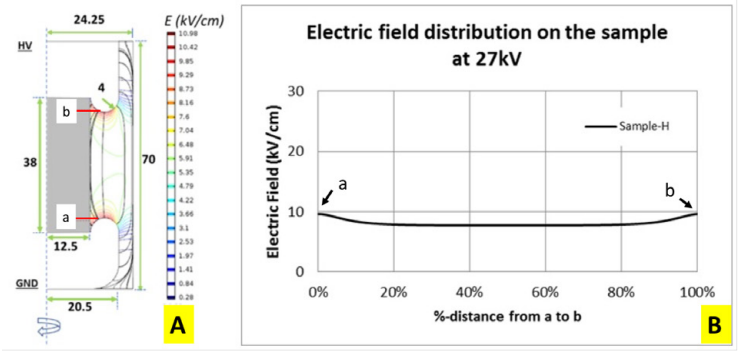

Figure 3.4 *(A)* A one-half of axis-symmetrical electric field distribution on an epoxy sample with the homogeneous configuration at 27 kV_{RMS}. The voltage has been chosen to obtain the similar electric field as in real operating conditions. The values shown in the figure are in mm. *(B)* The electric field distribution on the sample surface from a to b at 27 kV.

3.2.1.3 Quasi-homogeneous configuration

The schematic diagram and the electrostatic simulation of the quasi-homogeneous configuration are presented in Figure 3.5. A 50 mm-length epoxy sample is placed in between two non-identical electrodes. One electrode is planar, while the other has an insertion of 20 mm. Both electrodes have curvature radii of 4 mm. The field-factor for this configuration is 1.9. The electric field comparison between a conic spacer, as presented in 3.2.1.1, and the sample is shown in Figure 3.5.

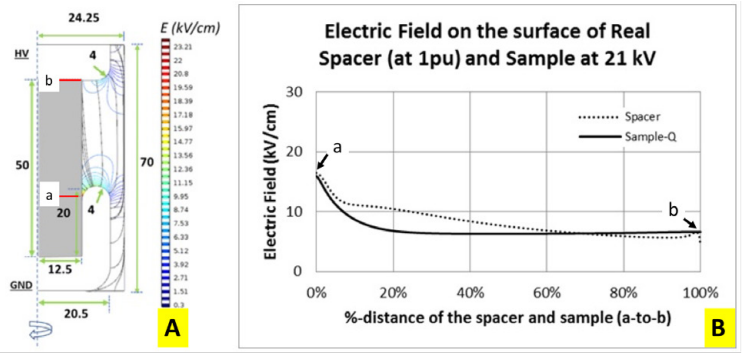

Figure 3.5 *(A)* A one-half of axis-symmetrical electric field distribution on an epoxy sample with the quasi-homogeneous configuration at 21 kV_{RMS}. The voltage has been chosen to obtain the similar electric field as in real conditions. The values shown in the figure are in mm. *(B)* The electric field distribution on the sample from a to b at 21 kV_{RMS} (bold line) and the electric field distribution on a 420-kV conical spacer at one p.u. (dotted line).

3.2.1.4 Inhomogeneous configuration with a particle attached on the sample

In GIS, a local field enhancement in the insulation system may occur due to a free-floating particle and a protrusion. Even after a good quality control during the GIS assembly, some particles may appear due to, for example, the mechanical abrasions of the switching contacts or the vibration on conductors under load operation. These defects are particular cases detectable by the Partial Discharge (PD) measurements in the case study [47]. A wire-like conducting particle is the most dangerous to the insulation. The author in [48] has discussed the dynamic behaviour of a free-particle. The VHF/ UHF PD system can detect a particle as small as 2 mm.

The influence of humidity on the flashover voltage in such inhomogeneous conditions is also investigated. To that purpose, a wire-like particle made of aluminum 0.25 mm in diameter and 2 mm long, is carefully attached to the epoxy sample, close to the maximum curvature of the HV homogeneous electrode configuration, to simulate the worst possible case in GIS (see Figure 3.6). The microscopic dimension of the particle's tip may vary among different particles. In this configuration, only one flashover is allowed per series of test.

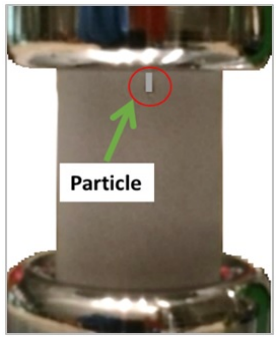

Figure 3.6 A wire-like particle 2 mm (±10%) long and 0.25 (±10%) mm radius attached on the surface epoxy sample, close to the maximum curvature of the HV homogeneous electrode configuration.

3.2.2 Material specification and dimension of the sample

A GIS spacer is usually made of epoxy resin with different kinds of fillers such as alumina and silica. Spacers of alumina fillers are known to have better withstand against surface tracking [42]. The laboratory test used epoxy with silica fillers with a purpose to observe the flashover traces and to be representative with existing GIS materials. All samples have a cylindrical shape with a diameter of 25 mm, with two kinds of height, i.e., 50 mm (for the test with quasi-homogeneous configuration) and 38 mm (for the test with homogeneous configuration).

All epoxy samples were provided by the company who produces spacers to a GIS manufacturer. The population of this GIS in the JABA Case Study is about 18% of the total. Table 3.1 gives the specification of the epoxy.

Table 3.1 *Material specification of the epoxy sample used in the tests*

Specification			
Resin Type	Solid epoxy resin based on Bisphenol A		
Hardener	Phthalic anhydride PSA		
Filler	Quartz LM-10		
Parameter	**Unit**	**Value**	**Measurement Standard**
Loss Factor (Tan δ)	%	2.2	IEC 60250, 50 Hz, 20°C
Dielectric Constant (ε_r)	-	4.1	IEC 60250, 50 Hz, 20°C

Before a test, the sample was cleaned by using Isopropanol Alcohol (IPA).

3.2.3 Gas pressures in the test

From the observation in the case study, humid insulating gas was mostly found in the non-CB enclosures with single-phase enclosure configuration. Therefore, the gas pressures in the test have been adjusted to represent such a condition. Table 3.2 gives operating gas pressures of GIS of 4 major manufacturers in the case study. In this thesis, except mentioned differently, all values of gas pressures are in bar-absolute.

Table 3.2 *Gas Pressures of GIS from various Manufacturers in the Case Study*

Manufacturer	**Phase Configuration**	**Rated kV**	**CB**	**Other than CB**
			Operational Pressure (**bar$_a$**, 20°C)	Operational Pressure (**bar$_a$**, 20°C)
A	1-ph	525	7.5	5.3
	1-ph	170	7	3.3
	3-ph	170	7.9	7.1
B	3-ph	170	9.6	9.6
C	1-ph	170	7.2	4.8
D	3-ph	170	5.9	5.9

As seen in Table 3.2, the non-CB enclosures in GIS with a single-phase configuration have pressures between 3.3 - 5.3 bars (at 20°C). Therefore, the investigated gas pressures were within 1 to 6 bars. However, the value was also limited by the capability of the setup; for example, the test with AC was only up to 3 bars due to the capacity limit of the power transformer.

3.2.4 Humidity manipulation in the test chamber

Four kinds of humidity levels have been simulated in the tests, namely (the humidity content is within the brackets), dry (100-1000 ppmV), humid (2000-6000 ppmV), saturated, and condensation. The gas manipulation was done inside a “mixing vessel,” as seen in Figure 3.7. The procedure was as follows:

The creation of humid gas:

The air inside the mixing vessel was firstly evacuated to 0.2 millibars. Afterward, a prescribed amount of demineralized water (with a volume of 0.05-0.2 ml) was injected into the mixing vessel. At 0.2 millibars, the water evaporates at 20 ^{o}C. Following this step, the SF_6 was slowly injected into the mixing vessel up to the investigated gas pressure. The amount of humidity was monitored by the built-in dew point sensor inside the mixing-vessel. The conversion from dew point (T_d, in ^{o}C) into ppmV was based on the Magnus Formula [31-33] After 15-30 minutes of stabilisation time, the humid SF_6 was slowly transferred into the test chamber through a connection point.

The creation of saturating gas:

The procedure was similar to the creation of humid gas, but the prescribed water injected into the mixing vessel was raised to 0.5-1 ml. The saturation was indicated when the dew-point temperature, T_d, equals the room temperature (T_a).

The creation of condensation:

Firstly, the air inside the mixing vessel and test chamber was evacuated down to 0.2 millibars. Afterward, a high amount of demineralized water (1-3 ml of volume) was injected into both chambers. This step was to ensure both chambers have a very humid condition inside of them. The next step was slowly letting the SF_6 coming into the mixing-vessel up to the investigated pressure. After stabilisation time, the humid gas was transferred into the test chamber.

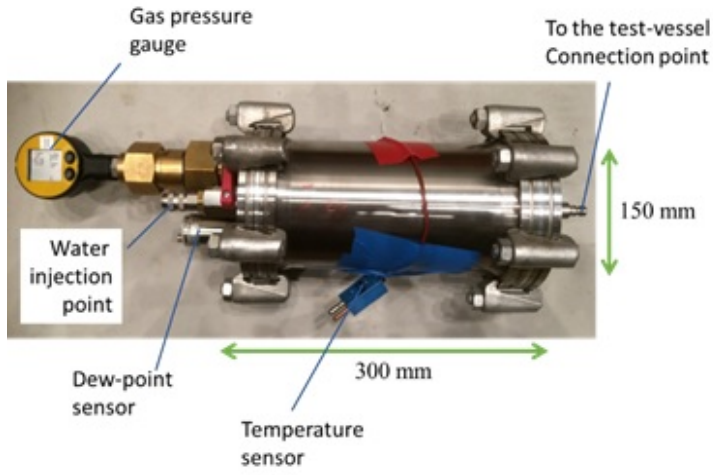

Figure 3.7 The “mixing vessel." In this vessel, the SF_6 and the water vapor were mixed.

3.3 *Voltage generation*

During the test, the test chamber was mounted into a GIS setup, as seen in Figure 3.8. The complete voltage generation setups are presented in Figure 3.9 (for AC) and 3.10 (for LI and SI). Once a breakdown was observed, relaxation time of 10-15 minutes was taken before the next voltage application.

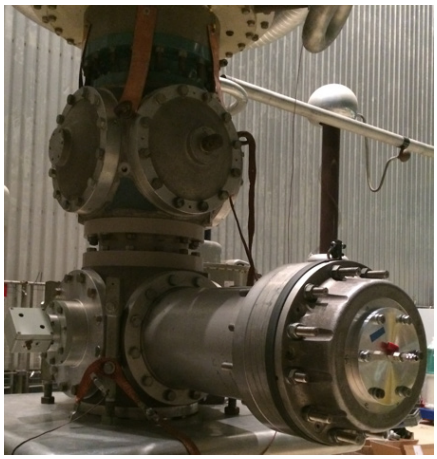

Figure 3.8 GIS Setup for Voltage Application. During the test, the test chamber was installed inside the GIS.

3.3.1 AC voltage generation

A single-phase power transformer provided the AC voltage with a maximum capacity of 200 kVA (point 4 in Figure 3.9). The high voltage side of the power transformer was connected to the GIS, while a voltage regulator (point 2 in Figure 3.9) was attached at the low voltage side to regulate the voltage output. A high-speed tripping circuit was installed to limit the flashover current. That allows several breakdowns on one sample since it limits the damage. The voltage raised from zero in steps of 20 kV and 1 kV/s rate.

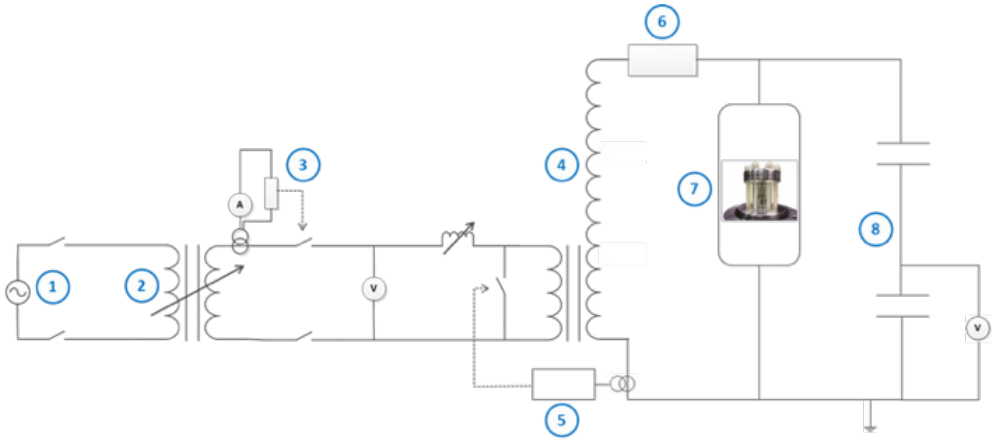

Figure 3.9 AC Voltage Generation Setup. 1. 220V-AC grid; 2. Voltage regulator; 3. Current limiter; 4. Power transformer; 5. High-speed tripping circuit; 6. Damping resistor; 7. Test chamber; 8. Capacitive voltage divider.

3.3.2 LI and SI voltage generation

Ten stages of the Marx Generator in the HV Laboratory in TU Delft had been used to generate the Lightning Impulse (+/-) and the Switching Impulse with shapes following the IEC 60060-1:2010 standard [49]. Each impulse started from about 50% of the estimated breakdown voltage and then increased in 20 kV steps.

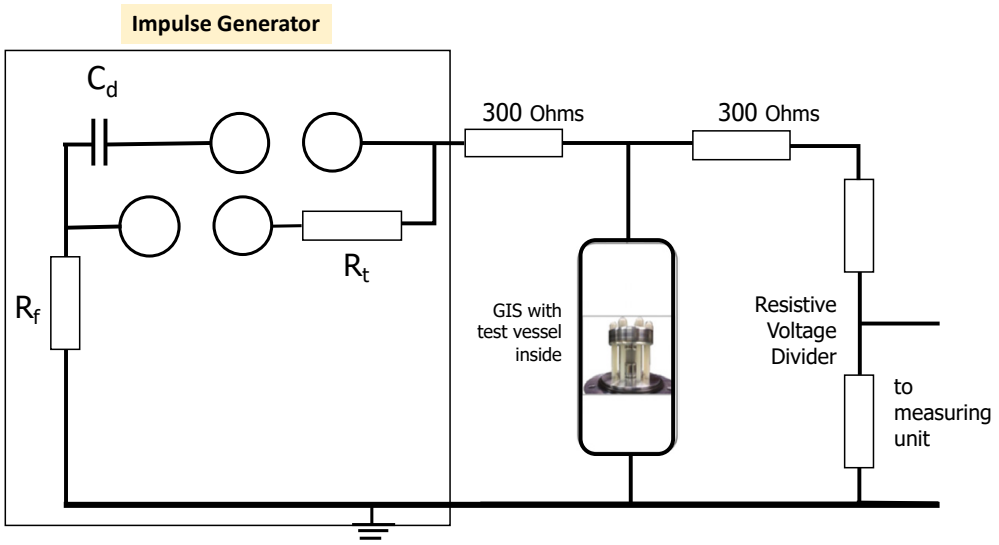

Figure 3.10 Setup for Impulse Generation. C_d is the discharge capacitance, R_f is the front resistance which determines the front time, R_t is the tail resistance which determines the time to half-value.

3.4 *Experimental results*

Most of the tests were done with the quasi-homogeneous field configuration. Table 3.3 gives a summary of the tests in a matrix with the voltage stress and the electrode configuration. The test with the homogeneous setup was only under LI+ and SI, while tests with a particle-attached on the spacer were done under LI+ and LI-.

Section 3.4.1 to 3.4.3 presents the test results. A minimum of three flashovers was applied to each experiment, except during the test with a particle attached on the epoxy sample.

Table 3.3 Overview of the humidity content in the flashover experiments. The columns give the electrode configuration, while the rows show the voltage stresses.

		Electrode Configuration					
		Homogeneous		Quasi-homogeneous		Inhomogeneous (w/ particle attached on spacer)	
		Humidity (ppmV)	Gas Pressure (bar_a)	Humidity (ppmV)	Gas Pressure (bar_a)	Humidity (ppmV)	Gas Pressure (bar_a)
Voltage Stress	AC	None		1000	1-3	None	
				2000	1-3		
				4000	1-3		
				6000	1-3		
				Sat.	1-3		
				Cond.	2 and 2.5		
	LI+	100	2-3	1000	1-4	100	3.5 and 4.3
		2000	2-3.5	4000	1-4	3000	3.5 and 4
		Cond.	3.5 & 4.5	6000	1-4	6000	3.2 and 3.8
				Sat.	1-3		
				Cond.	2 and 2.5		
	LI-	None		1000	1-4	100	3.5 and 4.4
				Sat.	1-4		
	SI	100	2.5-6	1000	2.5-6	None	
		2000	2.5-5.2	3000	2.5-6		
		4000	3.5-4.5	4000	2.5-6		
		Sat.	3.2-5	6000	2.5-5		

**Sat.= saturation, Cond.= condensation*

3.4.1 Flashover voltage in quasi-homogeneous configuration

The test with the quasi-homogeneous configuration has been conducted under AC, LI+, LI-, and SI stresses. The test with saturated gas was simulated only under AC, LI +, and LI-; while the test with condensation was done only under AC and LI+. The investigated gas pressures for each type of voltage stress are as follow:

1. Under AC Voltage: 1-3 bars.
2. Under LI+/-: 1-4 bars.
3. Under SI: 2-6 bars.

The flashover voltage under AC was recorded in kV-peak/√2, while the results from LI and SI were in kV-peak. Figure 3.11 presents the flashover voltage from the test with the quasi-homogeneous setup with all kinds of voltage stress. Meanwhile, Figure 3.12 to 3.14 sequentially give the flashover of the same setup under AC, LI, and SI. The last number in the legend in each graph identifies the humidity content in ppmV.

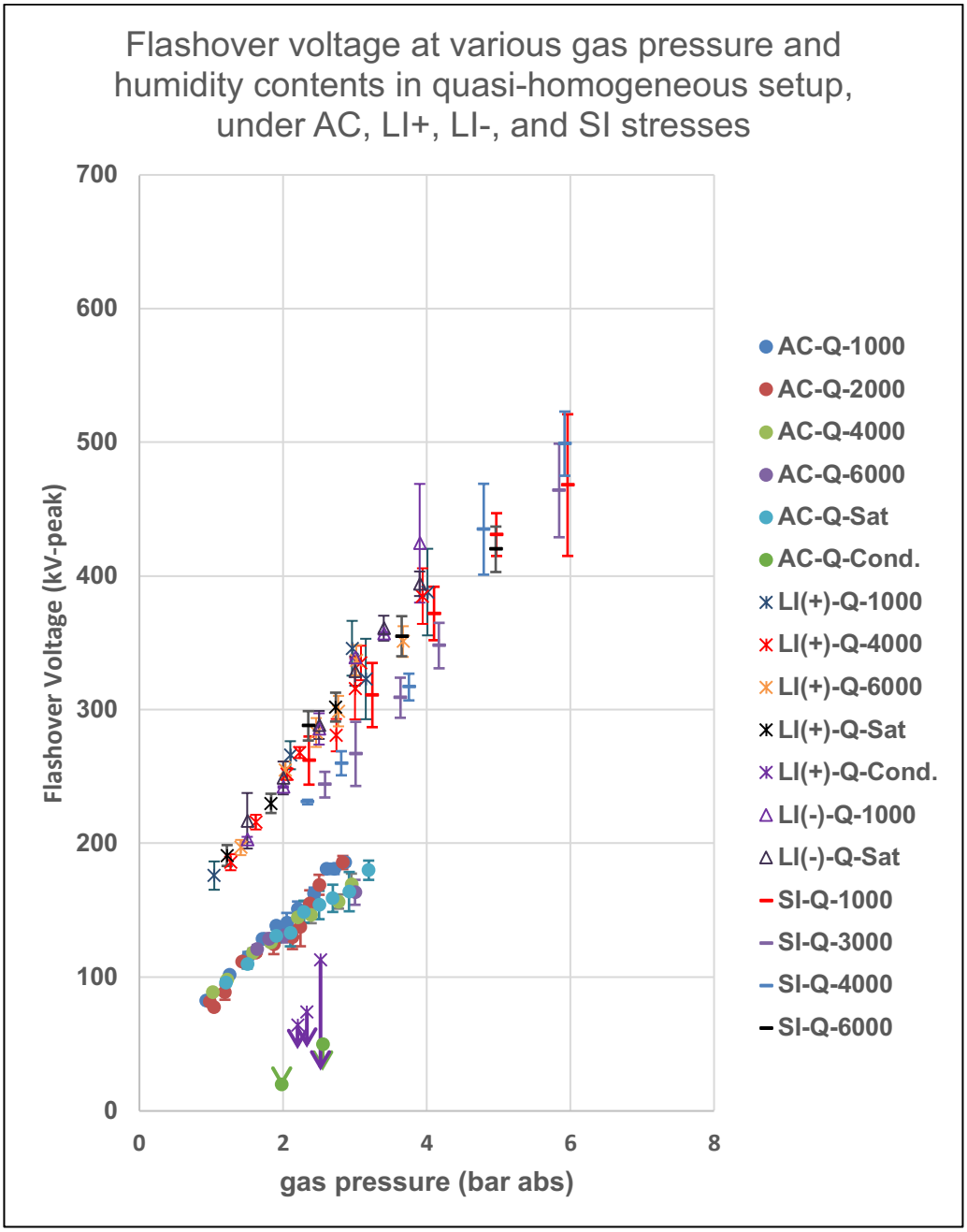

Figure 3.11 The flashover voltage as a function of gas pressure at various humidity contents in the quasi-homogeneous setup under AC, LI+/-, and SI Voltage Stresses. For AC, the value is in kV-peak/√2, while LI and SI are in kV-peak. The result from the tests with condensation, under AC and LI+, are shown by points with an arrow pointing down because the flashover voltage was decreasing gradually.

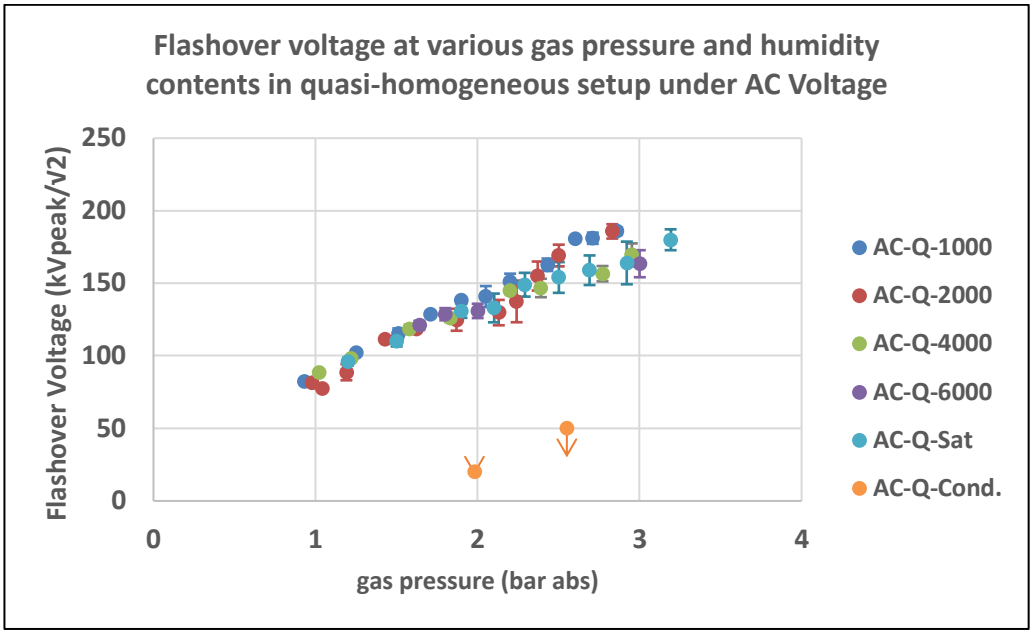

Figure 3.12 The flashover voltage as a function of gas pressure at various humidity contents in the quasi-homogeneous setup under AC Voltage Stress. The value is in kV-peak/√2.

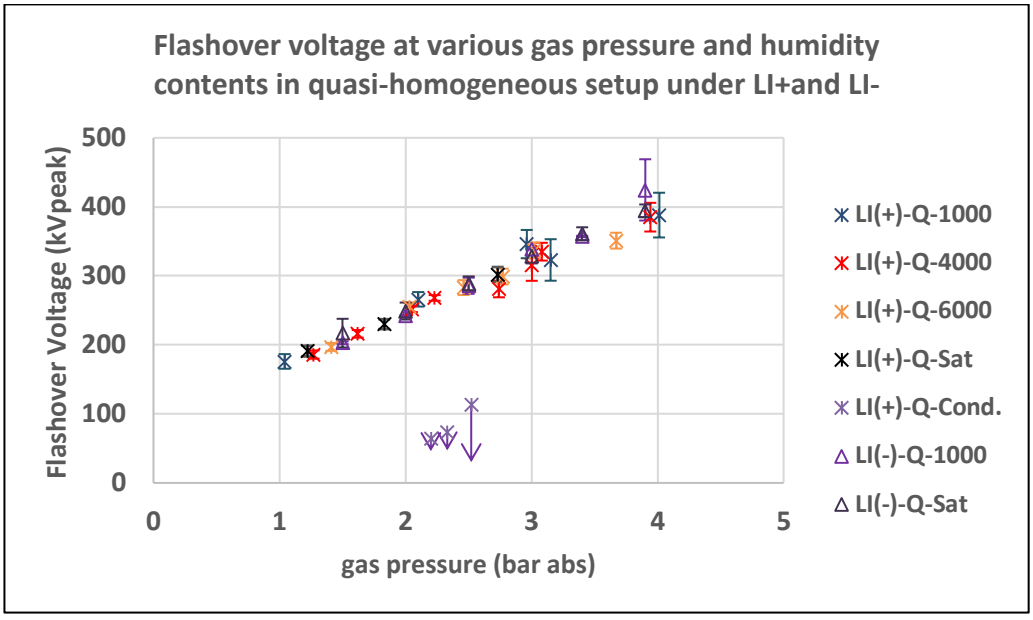

Figure 3.13 The flashover voltage as a function of gas pressure at various humidity contents in the quasi-homogeneous setup under LI+ and LI- voltage stresses. The value is in kV-peak.

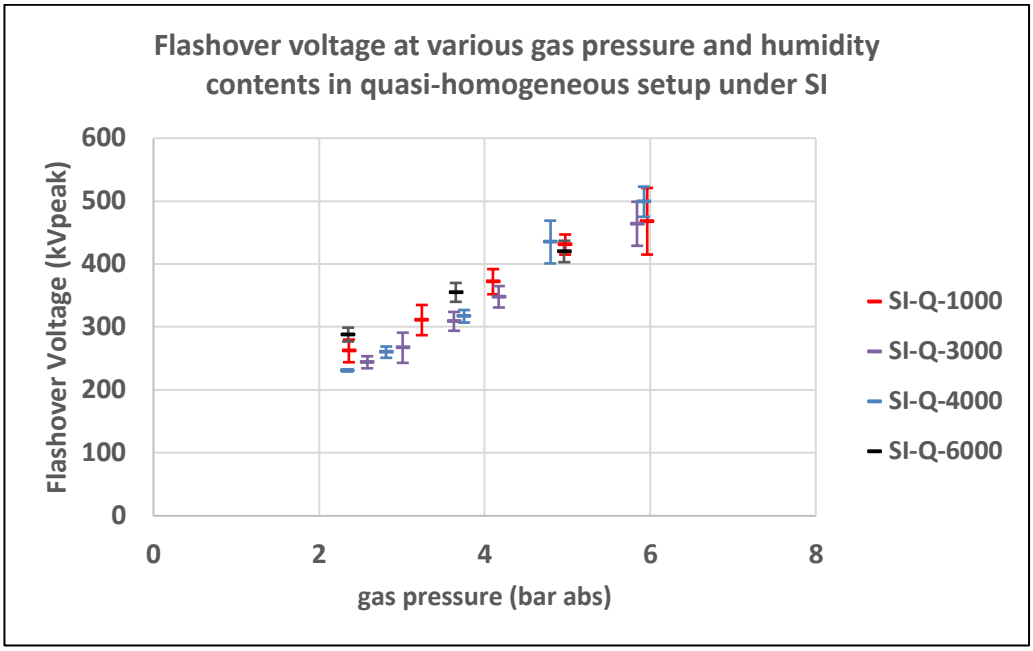

Figure 3.14 The flashover voltage as a function of gas pressure at various humidity contents in the quasi-homogeneous setup under SI. The value is in kV-peak.

According to Figure 3.11, the flashover voltage under LI is higher than SI and AC. A standard deviation above 10% has been observed under all voltage stresses. The value is higher at higher gas pressure. The latter is probably due to the stabilisation factor of the test setup, where at the higher flashover voltage, higher discharge energy occurred that causing more prominent craters on the electrode.

For each type of voltage stress, as shown in Figures 3.12 to 3.14, the flashover voltage is increasing as a function of pressure. There is no tendency that the increased humidity content in gas decreases the flashover voltage, except in case of condensation. Our tests under AC and LI+ confirmed that the flashover would be significantly decreased when condensation occurs.

Figure 3.13 shows the setup after a series of tests under LI+. It is seen that the flashovers took place on the epoxy surface. The craters were found on both electrodes at the “triple-junction” location. The maximum roughness of 10 µm is necessary to ensure the craters do not influence the breakdown strength of SF_6 [46]. The higher the energy discharge, the more significant the crater on the electrodes. Therefore, the electrodes were carefully re-polished after a series of test, and the number of flashover in the tests limited to gas pressure levels above 4 bars.

White powders have been discovered at the surface of the electrodes and the sample. These powders probably the Aluminium Fluorides [32] produced after a flashover. More powders were observed from the test under AC rather than the tests with the impulses. The reason is probably due to the longer period of partial discharge under AC before a complete breakdown. The more humidity in gas, the more Aluminium Fluorides observed.

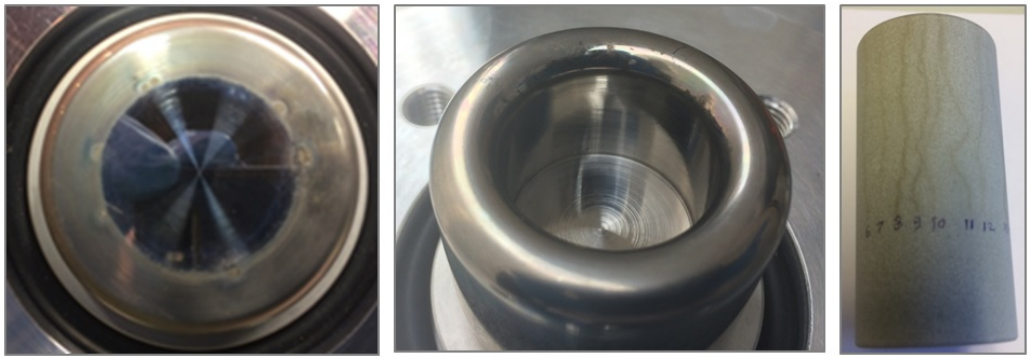

Figure 3.15 The setup after a series of tests under LI+ stress: (2 figures from the left) HV and LV electrodes of quasi-homogeneous setup, (the most right figure) an epoxy sample with flashover traces. The solid by-products, possibly the aluminium fluorides, and craters were observed in the setup after the test.

3.4.2 Flashover voltage inhomogeneous configuration

The test with the homogeneous configuration has been conducted under LI+ and SI voltage stresses. The saturating-gas has been tested under SI, while the condensation has been tested under LI+. The gas pressures are as follows:

1. Under LI+ : 2-4.5 bars.
2. Under SI : 2-6 bars.

The flashover voltage was recorded in kV-peak. Figure 3.16 presents the flashover voltage from the test with the homogeneous setup with LI+ and SI, while details are provided in Figures 3.17 and 3.18. Figure 3.19 shows the setup after a series of tests.

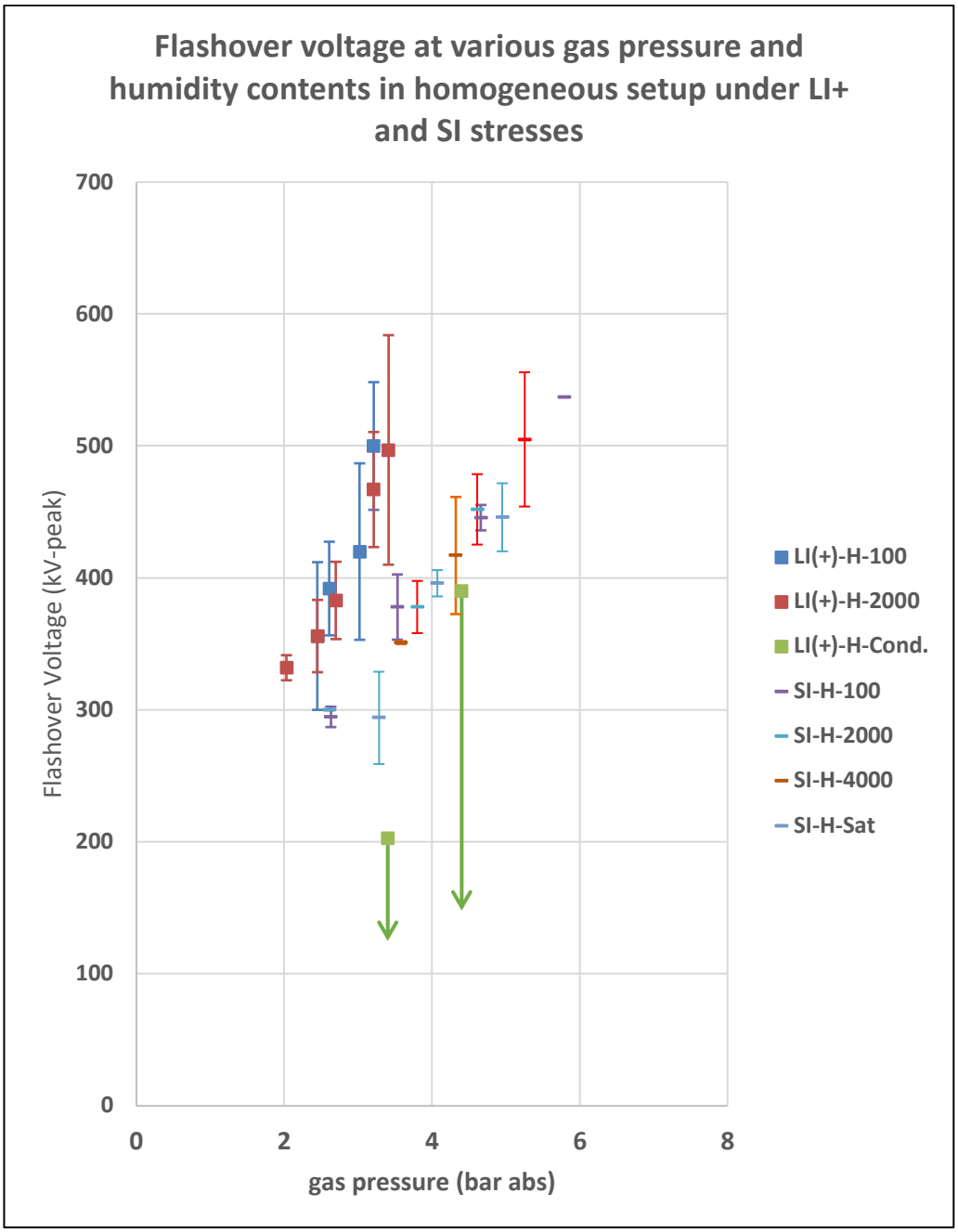

Figure 3.16 The flashover voltage as a function of gas pressure at various humidity contents in the homogeneous setup under LI+ and SI Voltage Stresses. The value is in kV-peak. The result from the tests with condensation, under LI+, are shown by points with an arrow pointing down as the flashover voltage was decreasing gradually.

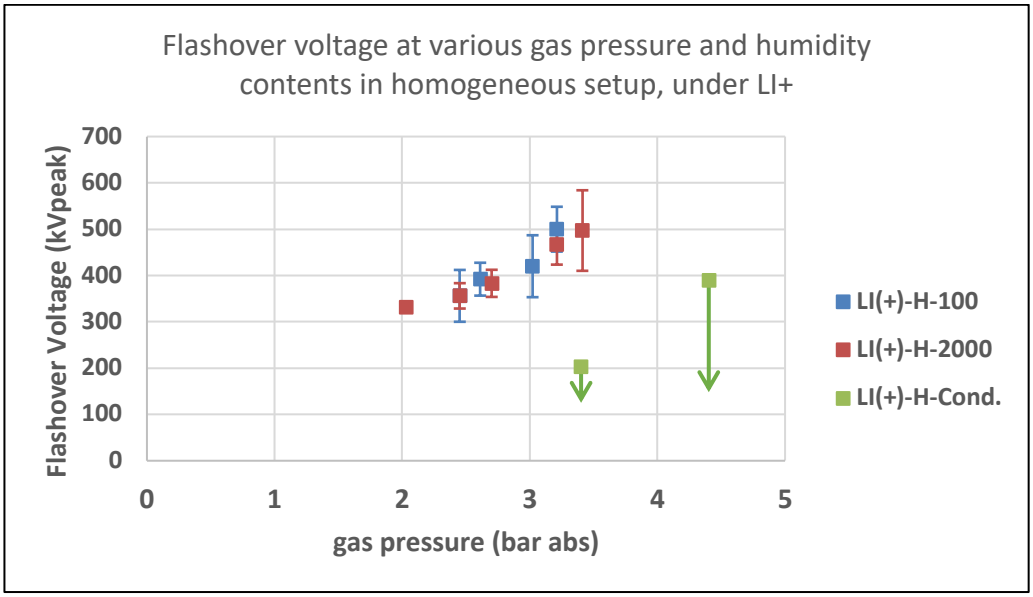

Figure 3.17 The flashover voltage as a function of gas pressure at various humidity contents in the homogeneous setup under LI+ Voltage Stresses. The value is in kV-peak.

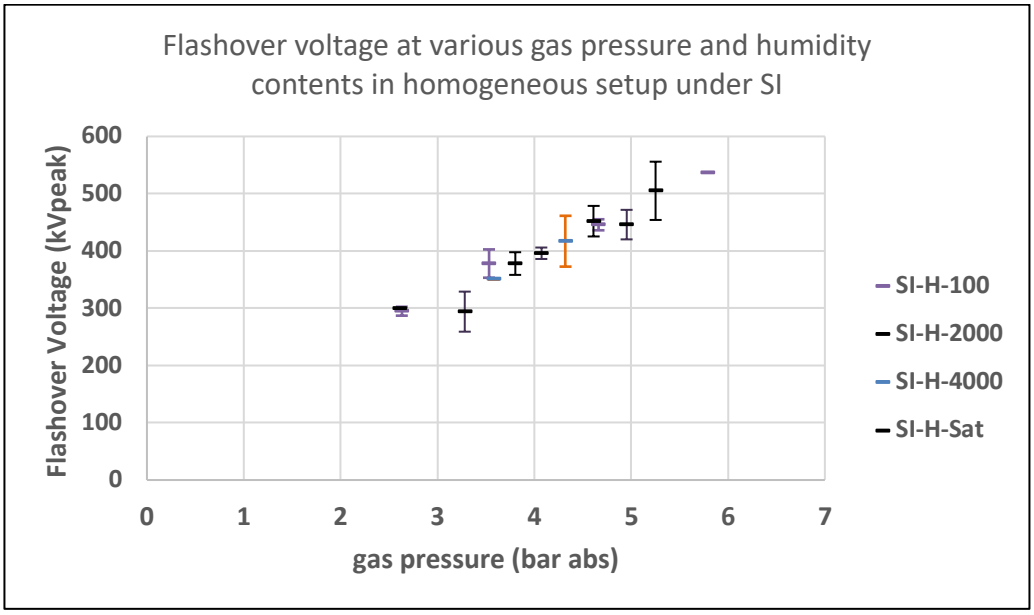

Figure 3.18 The flashover voltage as a function of gas pressure at various humidity contents in the homogeneous setup under SI Voltage Stresses. The value is in kV-peak.

Figure 3.19 (2 pictures in the left) HV and LV electrodes of homogeneous configuration after a test with the LI+. (2 pictures in the right) Two samples after a series of tests with the homogeneous setup under LI and SI sequentially.

By comparing the results in Figures 3.11 and 3.16, in general, the flashover voltage is higher in the test with a homogeneous setup rather than in the quasi-homogeneous setup at a similar gas pressure and humidity content. This finding is in line with our expectations since a breakdown is a function of the electric field, and a higher voltage is needed in the homogeneous configuration to develop a similar electric field as in non-homogeneous configuration.

Figures 3.17 and 3.18 show a similar tendency as in the test with the quasi-homogeneous setup, where the humidity content does not influence the flashover voltage, as long there is no condensation.

From Figure 3.19, compared with the test with the quasi-homogeneous setup, the flashover traces on the sample surface are lesser in the test with the homogeneous setup. Most of the breakdown probably took place inside the gas, especially in the experiment with the LI. Punctured craters were observed at the maximum curvature of both electrodes. This finding agrees with our simulation in COMSOL®, as shown in Figure 3.4. The high field regions are equally distributed at both electrodes, and then the field runs parallel to the surface of the sample. The highest electric field region is located at the tip of the electrode. As long as there is no irregularity on the surface, the breakdown voltage at the interface between epoxy and SF_6 should be equal to that in a free gas [50].

It has been observed that the standard deviation is more significant from the tests with a homogeneous setup, especially in the tests with gas pressure above 3 bars. The standard deviation of 18% has been observed from the test with LI+. The latter was probably due to higher energy discharge occurred in the flashover at the higher pressure, which resulted in big craters on electrodes that contributed to the variation of flashover voltages.

3.4.3 Flashover voltage in the setup with a particle attached on the sample

The tests with this configuration have been conducted only under the LI+ and LI- stresses, which represents the highest electrical stress during the GIS operation.

Only the first breakdown was recorded, and two samples were used to determine the maximum and the minimum flashover voltages as a function of gas pressure. Figure 3.20 shows the results.

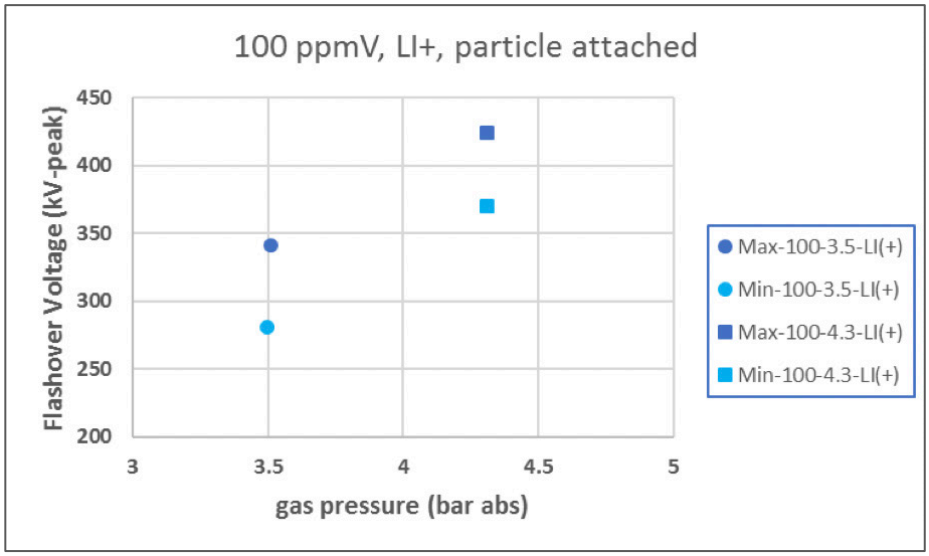
100 ppmV, LI+, particle attached
Flashover Voltage (kV-peak)
450
400
350
300
250
200
3
3.5
4
4.5
5
gas pressure (bar abs)
Max-100-3.5-LI(+)
Min-100-3.5-LI(+)
Max-100-4.3-LI(+)
Min-100-4.3-LI(+)

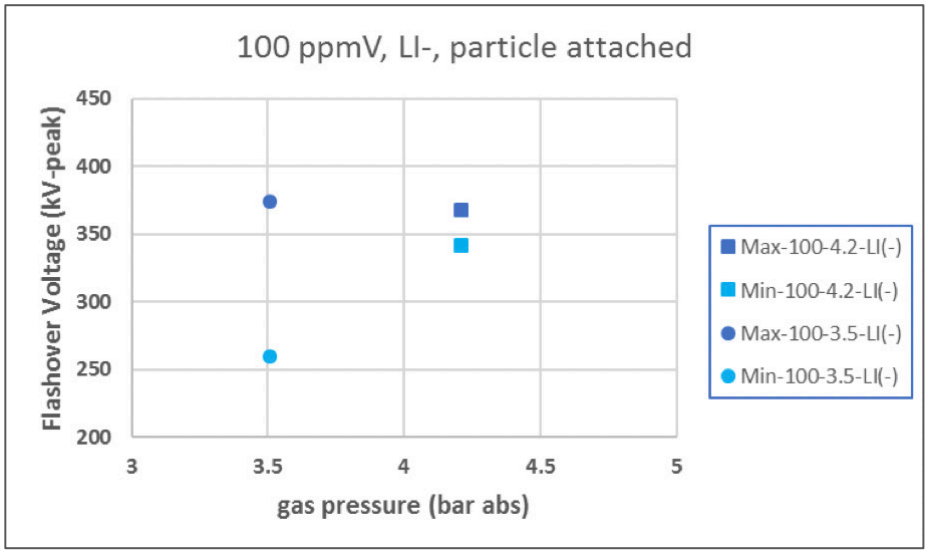
100 ppmV, LI-, particle attached
Flashover Voltage (kV-peak)
450
400
350
300
250
200
3
3.5
4
4.5
5
gas pressure (bar abs)
Max-100-4.2-LI(-)
Min-100-4.2-LI(-)
Max-100-3.5-LI(-)
Min-100-3.5-LI(-)

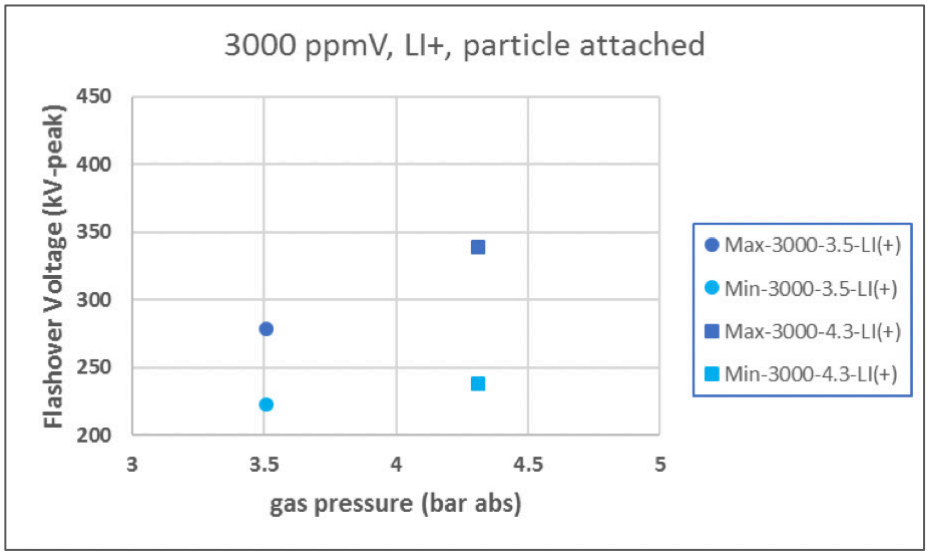

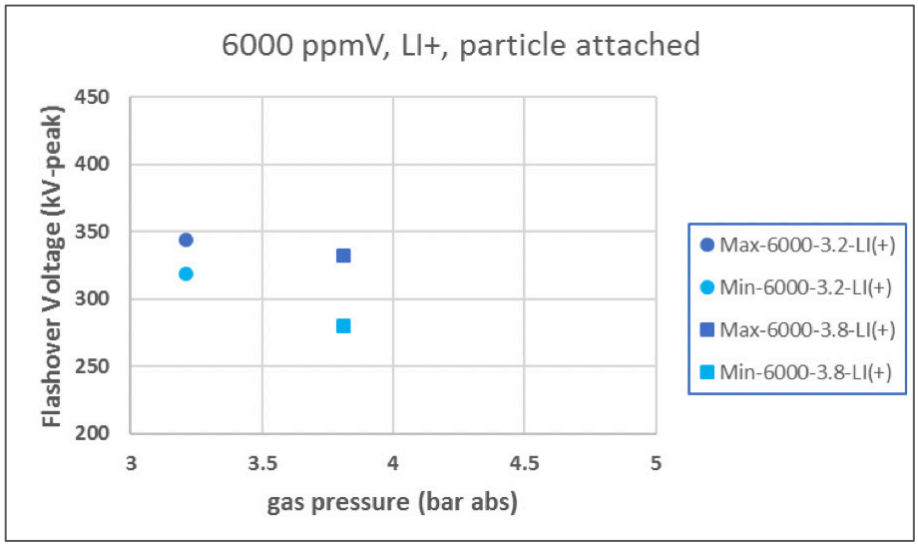

Figure 3.20 The flashover voltage as a function of gas pressure at various humidity contents in the experiment with a particle attached on the epoxy sample, under LI+ and LI- (only with 100 ppmV). The value is in kV-peak.

The investigated pressures were from 3.2 to 4.3 bars. As seen from the graphs, the flashover is increasing as the gas pressure increased, except for the results from the test with 6000 ppmV under LI+. Under the same voltage stress, the tendency of decreasing flashover voltage has been observed, when the humidity increases from 100 to 6000 ppmV. Probably corona stabilisation [48] was occurring at 6000 ppmV of humidity content, but it is arguably since the number of data is limited.

Figure 3.21 shows the setup after a flashover under LI+. On both electrodes, there was a punctured-point, which was the location of flashover. Both electrodes and sample were clean because there was only single flashover.

The flashover track was evident in the sample, as seen in the figure. The track was originated from the particle towards the other electrode. This track can be a straight line, or with branches, dependent on the stochastic condition (i.e., the availability of free electrons) when the flashover occurs.

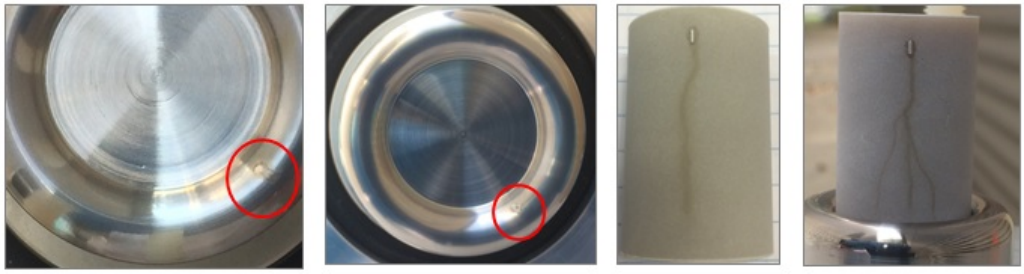

Figure 3.21 (2 pictures on the left): 2-identical electrodes after the experiment with the particle attached on the epoxy sample under LI+. (2 pictures on the right) two epoxy-samples after a single flashover. The track can be a straight-line or with branches.

3.5 *Analysis of test results*

The following analysis will be presented in the following subsections:

1. The influence of humidity content to the flashover voltage of spacer under various electrode configurations, gas pressures, and kinds of voltage stresses.
2. The influence of gas pressure decreases to the spacer flashover under various electrode configurations, humidity contents, and voltage stresses.
3. The polarity effect on the flashover under LI+ and LI- stresses.
4. The Influence of the electric field distribution on the spacer flashover voltage.

3.5.1 Analysis-01: The influence of humidity on the flashover voltage

An analysis using best-fitting regression is used to estimate the mean value of the flashover voltage as a function of the gas pressure at a particular humidity content. The factor R^2 defines the curve fitness, where a value close to 1 means a good fit. Afterward, the ratio of the flashover voltage between humid and dry, or between higher and lower humidity content, is calculated.

Table 3.4 provides the regression functions of all tests which are valid only within the gas pressures in the tests, whilst Table 3.5 provides the flashover voltage ratio of all tests. Details of each regression are provided in Appendix D.

Table 3.4 *Regression functions of the flashover voltage as a function of gas pressure at various humidity contents of all tests.*

ppmV	Best Fit Regression	R^2 (%)	Regression Function (kV: Flashover Voltage, p: pressure in bar-abs)
Configuration: AC, Quasi homogeneous			
1000	Power	99.4	$kV = 86.112\ p^{0.7339}$
2000	Power	96.5	$kV = 79.096\ p^{0.772}$
4000	Power	99.3	$kV = 88.255\ p^{0.5941}$
6000	Linear	99.2	$kV = 30.65\ p + 71.348$
Sat.	Power	99.1	$kV = 85.776\ p^{0.6295}$
Cond.	-	-	-
Configuration: LI+, Quasi homogeneous			
1000	Power	98.5	$kV = 172.57\ p^{0.5872}$
4000	Power	98.4	$kV = 159.07\ p^{0.6324}$
6000	Power	98.1	$kV = 161.5\ p^{0.622}$
Sat.	Power	98.7	$kV = 168.07\ p^{0.5686}$
Cond.	-	-	-
Configuration: LI+, Homogeneous			
100	Exponential	90	$kV = 139.39\ e^{0.3855p}$
2000	Exponential	97.6	$kV = 172.5\ e^{0.3066p}$
Configuration: LI+, Particle Attached			
100	Linear	100	$kV = 109.38p - 71.312$
3000	Linear	100	$kV = 76p - 13.5$
Configuration: LI-, Quasi homogeneous			
1000	Polynomial	99.3	$kV = 6.1681p^2 + 56.977p + 104.17$
Saturation	Polynomial	99.9	$kV = 0.485\ p^2 + 72.954p + 104.38$
Configuration: SI, Quasi homogeneous			
1000	Polynomial	99.4	$kV = -3.6387p^2 + 89.702p + 66.442$
3000	Power	98.8	$kV = 116.54\ p^{0.762}$
4000	Polynomial	98.6	$kV = 0.6081\ p^2 + 73.157\ p + 51.087$
6000	Polynomial	100	$kV = -0.7357\ p^2 + 55.953\ p + 160.57$
Configuration: SI, Homogeneous			
100	Power	99.5	$kV = 145.04\ p^{0.742}$
2000	Linear	98.4	$kV = 78.182\ p + 90.746$
4000	Linear	100	$kV = 371.1\ \ln(p) - 139.74$
Saturation	Logarithmic	97.2	$kV = 89.189\ p + 31.703$

Table 3.5 *The flashover voltage ratio of all tests.*

Gas Pressure (bars)	Humidity Content to compare (in ppmV)		Flashover Voltage (FO) Ratio (in %) = $FO_{at\ Higher\text{-}content}$ / $FO_{at\ Reference}$
	Reference	Higher content	
Configuration: AC, Quasi homogeneous			
3	1000	2000	96%
	1000	4000	88%
	1000	6000	84%
	1000	Saturation	89%
2.6	1000	Condensation	≤ 72%
2	1000	Condensation	≤ 86%
Configuration: LI+, Quasi homogeneous			
3	1000	4000	97%
	1000	6000	97%
	1000	Saturation	95%
2.5	1000	Condensation	≤ 62%
Configuration: LI+, Homogeneous			
3	100	2000	**102%**
3.4	100	Condensation	≤ 33%
Configuration: LI+, Particle Attached			
4	100	3000	79%
Configuration: LI-, Quasi homogeneous			
4	1000	Saturation	94%
Configuration: SI, Quasi homogeneous			
3	1000	3000	89%
	1000	4000	91%
	1000	6000	**106%**
4	1000	3000	91%
	1000	4000	96%
	1000	6000	**102%**
Configuration: SI, Homogeneous			
4	100	2000	99%
	100	4000	96%
	100	Saturation	92%
	2000	4000	96%
	4000	Saturation	96%

From Table 3.5, in general, at 3 and 4 bars gas pressures, in comparison to the dry condition, the addition of humidity slightly decreases the flashover voltage, but there is no consistent tendency that the higher humidity will decrease the flashover voltage [41]. Only a small fraction of the result shows the higher flashover voltage at the higher humidity content.

In the test with the quasi-homogeneous setup under SI, the FO-ratio is peculiarly increasing as the humidity raised from 3000 to 6000 ppmV, at 3 and 4 bars.

The flashover voltage dropped by 21% when the humidity increases from 100 to 3000 ppmV, in the test with a particle attached on the epoxy. The inhomogeneity at the tip of the particle probably has more influence on the reduction of the flashover voltage, rather than due to the addition of humidity.

The flashover voltage in a homogeneous setup with and without a particle is compared under LI+ at a gas pressure of 3.3 bars and humidity content of 100 ppmV. As a result, the presence of an attached particle in the setup has decreased the flashover voltage by 42%. This value is still below the reduction due to the condensation, which was 67% in a similar setup.

However, the calculation in this section is based on the mean flashover voltage, where a standard deviation above 10% has been found in the test. The deviation due to the addition of humidity content is still within the standard deviation, except when the condensation occurs, or when a particle is attached to the epoxy sample.

3.5.2 Analysis-02: The influence of gas pressure decrease on the flashover voltage in dry condition

Leakages are the common minor failures found in the JABA Case Study. Therefore, we also analyzed the influence of gas pressure decrease to the flashover voltage. The similar regression method, as formerly used in subsection 3.5.1, was applied. The mean value of the flashover voltage was estimated as a function of gas pressure based on the test results under dry condition. The influence of gas pressure reduction to the decrease of flashover voltage is shown by the Flashover ratio, as shown in Table 3.6.

Table 3.6 *The reduction of flashover voltage with a decrease of pressure under different voltage stresses at "dry" condition*

		Flashover Voltage (FO) Ratio (in %) = $FO_{at\text{-}LOWER\ Pressure}$/ $FO_{at\text{-}HIGHER\ Pressure}$				
Configuration	ppmV (dry)	From 6 to 5 bars gas pressure	From 5 to 4 bars gas pressure	From 4 to 3 bars gas pressure	From 3 to 2 bars gas pressure	From 2 to 1 bar gas pressure
AC, Quasi	1000	n/a	n/a	n/a	74%	60%
LI(+), Quasi	1000	n/a	n/a	85%	79%	67%
LI(-), Quasi	1000	n/a	n/a	77%	n/a	n/a
LI(+), Homo	100	n/a	n/a	n/a	95%	n/a
LI(+), Particle	100	n/a	n/a	70%	n/a	n/a
LI(-), Particle	100	n/a	n/a	84%	n/a	n/a
SI, Quasi	1000	89%	87%	83%	76%	n/a
SI, Homo	100	87%	85%	81%	n/a	n/a

The following interpretations were drawn from the table above:

1. In general, the flashover ratio tends to become lower at the lower gas pressure. For example, in AC with quasi-homogeneous setup, the gas pressure reduction from 3 to 2 bars resulted to an FO ratio of 74%, while further reduction from 2 to 1 bar dropped the FO ratio to 60%.

2. The influence of the setup configuration is analysed from the Flashover Voltage (FO) ratios at a gas pressure reduction from 4 to 3 bars because the data are available for almost all setup configurations. As seen in the column "from 4 to bars gas pressure," the FO ratios are within 70% to 85%. The lowest ratio has been found in the setup with the LI(+) with particle. The particle on spacer reduced the flashover voltage more significantly in the test with LI+ rather than under LI-.

3. By comparing the results in Tables 3.5 and 3.6, in general, the influence of humidity addition from "dry" to "saturating" condition to the flashover voltage is less than due to the gas pressure decrease of 1 bar.

3.5.3 Analysis-03: The effect of lightning polarity on the flashover voltage

About 92% of lightning strokes in the JABA Case Study had a negative polarity. Therefore, the polarity effect has been investigated by using the test results under LI+ and LI- with quasi-homogeneous configuration and humidity content of 1000 ppmV. Figure 3.22 shows the flashover voltage as a function of gas pressure of both tests, including their line regressions. The legend presents the regression-function and the humidity content in ppmV. The regression formulas were already presented in Table 3.4.

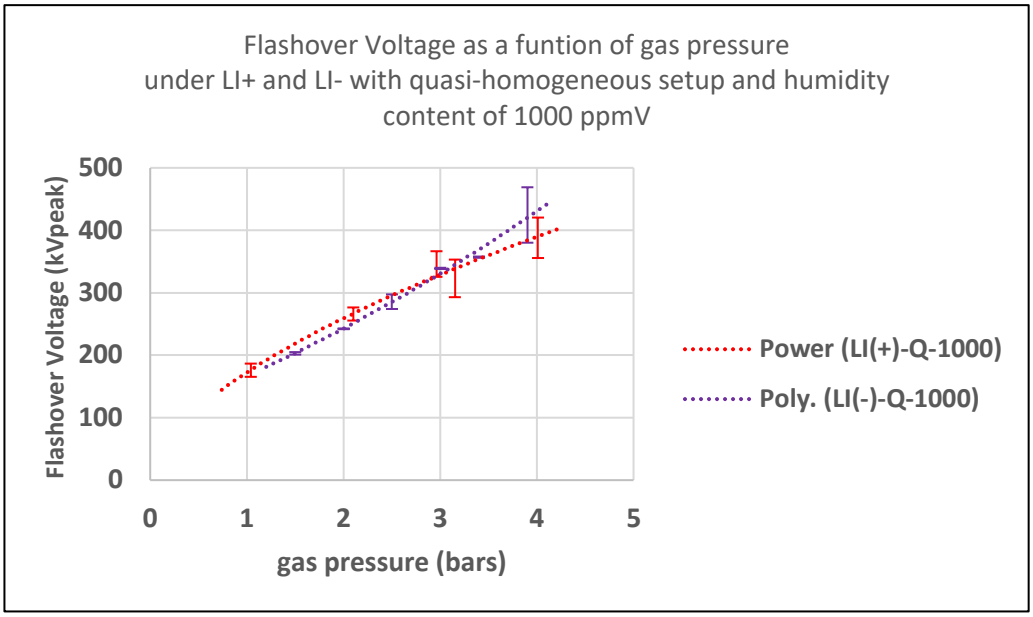

Figure 3.22 Flashover Voltage as a function of gas pressure under LI+ and LI- from the test with the quasi-homogeneous setup with a humidity content of 1000 ppmV. The regression functions are shown with dotted lines.

In gas breakdown, the influence of voltage polarity was contributed by the much greater mobility of electrons than the positive ion and by the fairly long lifetime of the electrons in the free state [51]. Usually, breakdown under LI+ is lower than under LI-, especially if the degree of non-uniformity is high [50]. However, as seen in Figure 3.22, the flashover voltages from the tests with both polarity were closely similar. The regression lines show that up to 3 bars, the flashover voltage are higher under LI+. However, from 3 to 4 bars, the LI- is higher.

In an insulation system that consists of a spacer and SF_6 gas, the influence of polarity also depends on the surface charge accumulation between the two electrodes. The amount of surface charge depends on the following factors, namely, the gas composition and density, the parameters of the voltage stress (like the rise and tail times), and the geometry between the discharge gap [51]. In our test, however, the effect of polarity on the flashover voltage could not be observed.

3.5.4 Analysis-04: The influence of electric field distribution on the spacer flashover

Three kinds of electric field distributions have been simulated in the tests. In this subsection, the electric field when a flashover occurred on each of setup configurations is estimated using the following steps:

1. The flashover voltage at a particular gas pressure and humidity content was calculated from the regression functions mentioned in Table 3.4.
2. Afterward, the flashover voltage is converted into the electric field strength (in kV/mm) by a calculation in COMSOL ®. The electric field is presented by the average and maximum values along the surface of the epoxy sample.
3. For the analysis, the following comparisons of flashover electric field were applied:
   a. Between homogeneous and quasi-homogeneous configurations, under LI+, at a gas pressure of 3.3 bars, with a dry condition.
   b. Between homogeneous and quasi-homogeneous configurations, under SI, at a gas pressure of 4 bars, with a humidity content of 4000 ppmV.
   c. The flashover electric field from the test with AC, at 3 bars, with a dry condition, is also provided.

The results are presented in Table 3.7.

Table 3.7 *Comparison of the estimated electric field (maximum and average) of flashover between quasi-homogeneous and homogeneous setups under LI+, SI, and AC stress at particular gas pressure and humidity content*

Setup	Bars	kV	E (kV/mm)		Std. Dev. (kV/mm)		Ratio of E: Quasi-H./ Homogeneous	
			Max.	Avg.	Max.	Avg.	Max.	Avg.
LI(+)_Homogenous, dry	3.3	497	17.9	15.3	2.9	2.5	1.5	0.9
LI(+)_Quasi-homogeneous, dry		348	26.3	13.7	2.3	1.2		
SI_Homogeneous., 4000 ppmV	4	388	13.9	11.9	2.5	2.2	1.9	1.2
SI_Quasi-homogeneous, 4000 ppmV		353	26.7	13.9	8	4		
AC_Quasi-homegeneous, dry	3	273	20.6	10.7	0.17	0.33	n/a	n/a

From the table, the following interpretations are drawn:

1. According to the test results from LI(+) and SI, the flashover voltage is always higher in homogeneous rather than in quasi-homogeneous setups. However, the maximum flashover electric field strength is lower under homogeneous rather than in quasi-homogeneous setups. On the other hand, the average flashover electric

fields in both setups are closely similar. This is shown by the ratio of the average electric field strengths of 0.9 (for LI+) and 1.2 (for SI), which are close to 1.

2. The maximum flashover electric field under AC with the quasi-homogeneous setup in the dry condition is 20.6 kV/mm. The latter value is about nine times higher than the estimated maximum electric field in a 420 kV spacer at 1 p.u. AC, as formerly shown in Figure 3.3. This finding indicated that as long there is no field distortion, by, e.g., particles, the operating voltage stresses in GIS are significantly lower than the withstand strength of the spacer.

3.6 *Conclusion*

1. The humidity does not influence the flashover voltage of the spacer if there is no condensation. It has been proven through the tests under AC, LI+, LI-, and SI with quasi-homogeneous and homogeneous setups. The flashover up to the saturation is within the standard deviation of the flashovers in a dry condition, under various gas pressures investigated in the tests. The findings agree with [31], and these show similar behaviour as in the humid SF_6 that we formerly investigated in [26].
2. From the tests with LI+, at 3.4 bars gas pressure, and 100 ppmV of humidity content, the flashover under condensation is lower than when a 2-mm particle is attached in the setup.
3. In our tests, the effect of polarity of a lightning impulse on the flashover voltage in the quasi-homogeneous setup, could not be observed.
4. From the analysis of the electric field distribution during a flashover, we found that the average electric field along the spacer is closely similar for both quasi-homogeneous and homogeneous setups.
5. From our tests, the highest parameter that contributes to the reduction of flashover voltage is the field distortion on the surface of the spacer. This can be due to particle, condensation, or accumulated solid by-products on the surface of the spacer. The next significant parameter is the gas pressure, while the least significant parameter is the humidity content.

Chapter 4 Asset Health Index Model for GIS Operating under Tropical Conditions

A breakdown in GIS is undesirable because it is costly, and it causes an extensive outage time. Therefore, such a failure should be avoided by firstly identifying the condition of GIS, accurately, followed by the correct mitigating actions.

In the asset management framework [52], this kind of asset's decision and performance-analysis is critical to success. Asset management tools have been developed, which serves several purposes [16-22,27,53-54]:

1. To assess the condition of the asset.
2. Defining the asset's health index that expresses the likelihood of failure modes.
3. To quantify the risk if the asset fails (i.e., risk assessment) in relation to KPI's/ business drivers.
4. To decide a correct mitigating action based on health index and risk assessment.

In this chapter, a health index model for GIS operating under tropical conditions is proposed. The purpose of the model is to give the health status of a GIS with its likelihood to a failure. The base for this Asset Health Index, or AHI, is the condition assessment of subsystems of components in GIS. The condition indicators were obtained from the diagnostic measurements (DM) and the routine visual inspections (RVI). The output of the model is an index. The condition scaling on the condition indicators is based on norms that were obtained from our investigations as presented in Chapter 2 and 3, in combination with GIS manuals, standards, publications, and discussion with the experts from the JABA Case Study.

This chapter starts with the objectives of the AHI model in section 4.1, including the concept and objectives, methodology, and boundary of the AHI. After that, section 4.2 discusses the selection of condition indicators used in the model. Section 4.3 discusses the approaches to generate norms. A norm is a boundary or a set of criteria that translates measured values for condition indicators into condition scale codes. Section 4.4 provides asset health indexing. Next, Failure Susceptibility Indicator (FSI) is given in section 4.5. These are the factors that could initiate an onset of a failure mode earlier. We determine the FSI based on the findings from the JABA Case Study. Section 4.6 discusses on how to deal with data uncertainty. Section 4.7 gives an example of how applying the model to operating GIS, and finally, a conclusion is provided in section 4.8.

4.1 *GIS AHI Model*

The AHI represents the deterioration level of an asset in general, or its critical subsystems by incorporating operating observations, field inspections, and the tests from both onsite and in the laboratory [16-17]. The AHI indicates an asset's likelihood of failure.

The current asset health of GIS is influenced by its life experiences, from the pre-operating period up to the moment when the health status is assessed. The last-mentioned factors are the failure susceptibility indicators (FSI). They are not failure modes, but they could be responsible for an earlier on-set of failure mode than usual. In this thesis, the FSI has been grouped into 3 categories: the inherent factors, the operation and maintenance factors, and the environmental factors. Section 4.5 gives a discussion about the FSI.

Figure 4.1 gives an illustration of how the AHI is processed and its relation with the phase life of a GIS. The figure assumes the AHI has been measured for three times, i.e., at c1, c2, and c3. The condition status at c3 is affected by the GIS experiences during the period a-to-b, and from b to c3. The AHI also gives a prediction of the likelihood of failure, in this case, from c3 to d.

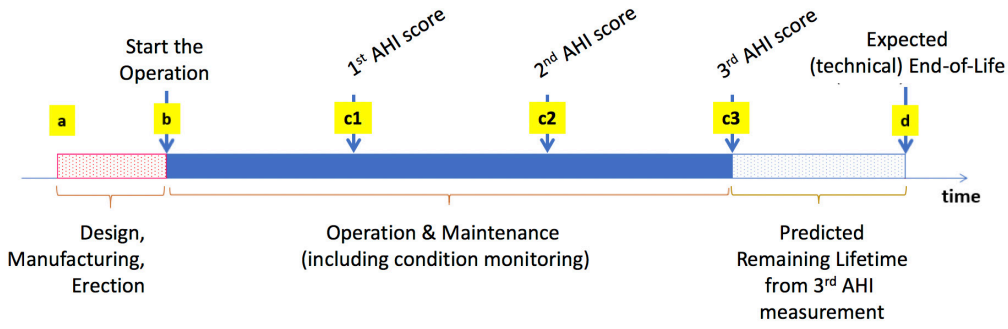

Figure 4.1 A schematic diagram showing how an AHI is processed within the lifecycle of an asset, in this case, a GIS. Points c1, c2, and c3 are showing the regular monitoring of GIS. By taking c3 as a reference, the condition status of GIS at this point is affected by the GIS experiences from a to b, and from b to c3. It is expected that the AHI can give a predicted remaining lifetime, which is shown by the area within c3 and d.

The AHI focuses on the technical condition of GIS. Consequently, the predicted remaining lifetime (i.e., the likelihood of failure) is only based on a technical point of view. Documents in [15,55-56] stated that the end of life of an asset could be due to the non-technical reasons, like cost, but this is not discussed in the current AHI. From a technical point of view, the end of life of an asset is when it can no longer perform the function as required by its user, under the current operating conditions, due to aging or deterioration that is reducing its reliability.

The other important factor in building an AHI system is to clarify which condition indicators to include in the model, that is sometimes mixed up with the failure susceptibility indicators. Within the asset management activities, the work of assessing the AHI is in parallel with the day-to-day activities of keeping the asset in operation. The

routine maintenance management can handle defects and minor failures, but not the catastrophic failures, like a breakdown of GIS. Therefore, the AHI captures the asset degradations that cannot be fixed through routine maintenance management.

The failure susceptibility indicators, such as the number of voltage transients due to switching per year, pollutant level, and lightning density indicate an individual asset to be vulnerable to earlier onset of a failure mode than other comparable assets.

In this thesis, the AHI gives an index representing the health status of GIS operating in a tropical environment. The AHI is based on condition indicators that have been selected as proper diagnostics for selected failure modes as found in the FMECA of the JABA Case Study.

4.1.1 Methodology

The measured values of a condition indicator (of a subsystem) are converted into a condition code (can also be called as "score") during the AHI assessment. Code is being assigned to each condition indicator that quantifies the health status of subsystems of a component based on a set of norms. There are several methods to aggregate the condition codes of subsystems into a single condition code representing the overall condition of an asset, as presented in [18] for power transformer HI.

In the current work, we use a "hybrid" coding system that combines the "worst score approach" and the "summation" of individual subsystem condition code. We employ the first approach at the subsystem-, component-, enclosure- and substation layers; while the "summation" is applied only at the "bay-layer." The reasons are as follow:

1. The approach is simple, yet they provide transparency during the aggregating process. So, the link between the final index with the failure mode of a subsystem could easily be traced back.
2. Remedial action on GIS (e.g., refurbish, replace, repair) is usually taking place at the bay-layer. Although it is possible to do the action only on a specific part/ component, it requires the outage of the affected bay. Therefore, the "overall" condition of a bay is necessary for deciding the optimal mitigating action. This is the reason why we apply a "summation" process only at the bay layer. Providing a (sub) health index of every bay should be handy for the asset manager, yet it is still possible to show an index of a complete GIS substation.

Logarithmic base-3 scale codes, i.e., 1, 3, 10, 30, and 100, are used to represent the condition status of subsystems in GIS. The higher the score, the more likely a failure mode to occur accordingly to the measured condition indicators. The logarithmic scale-code has benefited during the summation process, as it allows the poor indicators to stand out rather than the linear scoring system [18,22].

The model also takes into account the failure susceptibility indicators (FSI). We grouped the FSI into 3 categories, namely, high, moderate, and low. High susceptibility factor means the high likelihood of an on-set of a failure mode could start earlier than formerly predicted. However, the FSI is only an expectation. It differs from condition indicators where evidence (e.g., resulting from inspections) is involved. We present the FSI-index, in colours, as follows, red to represent HIGH-FSI, yellow to represent MODERATE-FSI, and green to represent LOW-FSI.

The final result contains both (sub) AH index and FSIs which are applicable at the bay- and substation layers. The final AH index, in principle, is an aggregation of indicators codes of subsystems in GIS. We grouped the health index into 5 categories that coded by a linear scaling score of 1 to 5. The higher the score, the worse the health status. The linear scaling code for the AH Index is easier for the user.

The AHI for GIS is unique because not like in the other HV components, a GIS basically consists of more than one component within hierarchical-layers as presented in subsection 2.6.1. Besides, the varying configurations among GIS makes should be taken into consideration in the development of GIS HI model.

The steps of health indexing in this thesis is shown in Figure 4.2 and can be explained as follow:

1. The process starts at the lowest layer, where the worst code of condition indicators defines the condition code of a subsystem.
2. At the next layer, a component will have subcodes of subsystems within it. No aggregating process at this layer.
3. The process continues to the enclosure layer, but now, only the worst condition code of subsystems among components passed the process.
4. The similar process as in point-3 continues to the bay layer. Now, the worst condition code of subsystems among enclosures passed the process.
5. We generate a (sub) health index at the bay layer in 2 steps as follows:
   a. All condition codes of a bay (i.e., worst-codes of subsystems that have passed step 1 to 4) were added into a single condition code.
   b. The code found in point a is then translated into an index.
6. The worst (sub) health index of bays in the same substation defines the total GIS's health index. It is possible to give additional information about the number of bays with a similar index in GIS. For example, an index of 5(2) means there are 2 bays in GIS that own index of 5.

Section 4.4 discusses more details about the health indexing.

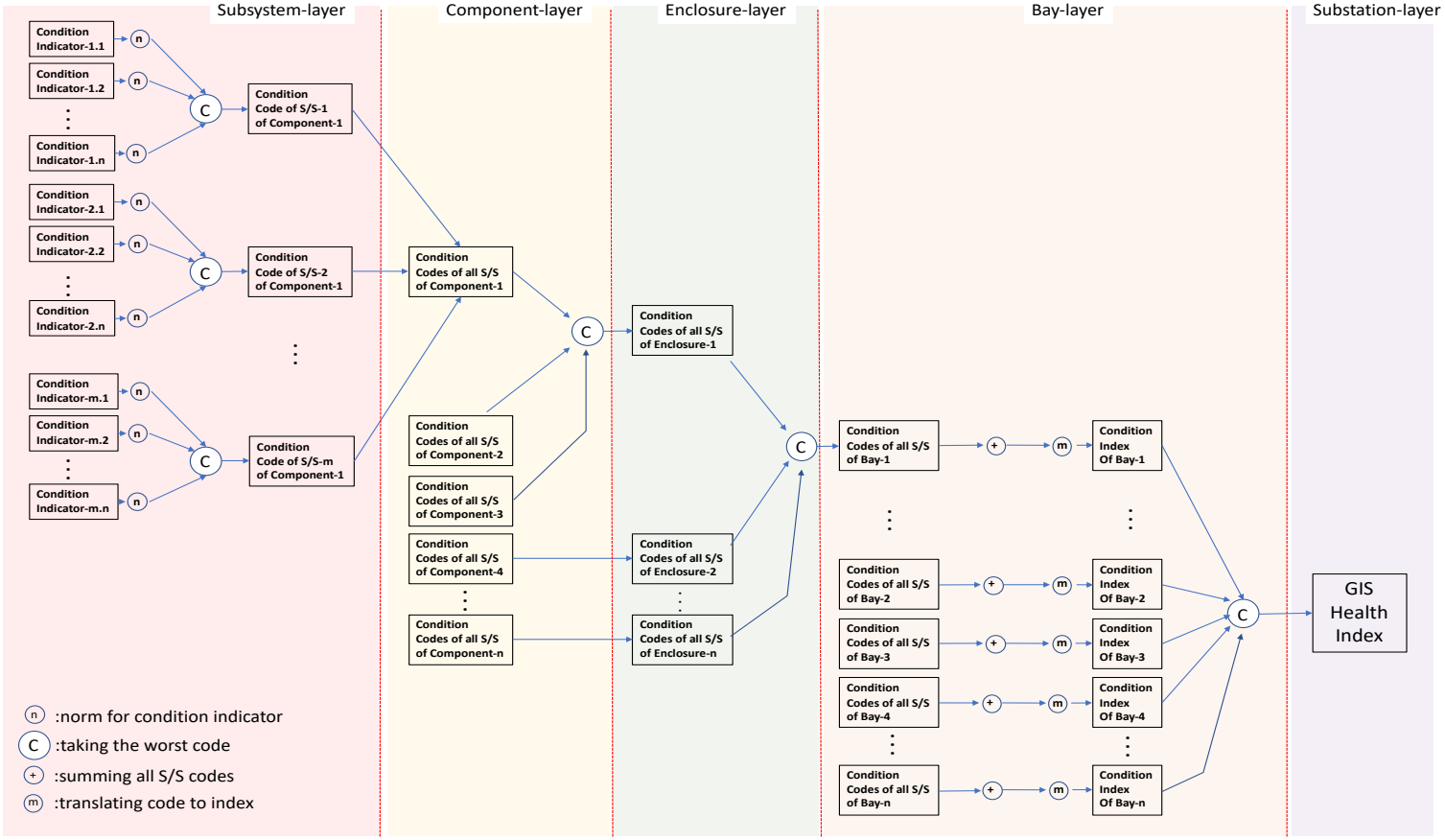

Figure 4.2 The hierarchy of health indexing of GIS in this thesis. Fundamentally, the likelihood of failure of subsystems defines the GIS health index as a whole. The current work uses a hybrid coding method that combines the worst-code and the summation approaches.

4.1.2 Boundary of the GIS HI Model

The AHI gives condition status and the likelihood of failure of an individual GIS in the system. In this thesis, the model focuses on the six failure modes of GIS, as presented in Table 2.23. Although the criticality of these failure modes has been evaluated through the FMECA, the model should not only focus on the critical ones.

The likelihood of failure presented by the AHI does not reflect an exact numerical remaining lifetime of the GIS. It can only give an estimation as to be shown in Table 4.5.

4.2 *Selecting condition indicators*

Condition indicators are the gathered indicators from inspections (e.g., visual inspection, measurement, and diagnostics) that indicate the condition status of subsystems in GIS. Selecting condition indicators is critical in developing the Asset Health Index model. Understanding the aging and deterioration in subsystems of GIS can be a good starting point as presented in the following subsection.

4.2.1 Aging and Deterioration in GIS

During its service lifetime, GIS is exposed to failure modes with different forms of failure susceptibility indicators, including mechanical stress, electrical stress, thermal stress, and chemical stress that come through both internal and external circumstances of a GIS. These factors lower the GIS performance after some period/ cycle of works. The following terminologies define this performance change or reduction:

1. Deterioration [37]
   Any physical asset that fulfils a function which brings it into contact with the real world, and so it is subject to a variety of stresses. These stresses cause the asset to deteriorate by lowering its capability, or more accurately, its resistance to stress. The deterioration covers all forms of “wear and tear” (including fatigue, corrosion, abrasion, erosion, evaporation, insulation deterioration).
2. Aging [25]
   Aging is an intrinsic physical or chemical phenomenon that involves irreversible changes, in characteristics of the materials with time, in some circumstances in interaction with its environment.

In GIS, the deterioration occurs such as in the main contacts of a CB after the arcing, and in gears and mechanical-coupling of the driving parts. On the other hand, the aging occurs, for instance, in seals, and in a solid spacer with void [55,57]. The condition indicators should capture both deterioration and aging in GIS. Table 4.1 summarizes various deteriorations and aging in subsystems of a Circuit Breaker [54,58-62]. As the other components might have the same subsystems, similar degradations might apply.

Table 4.1 Functional decomposition of a Circuit Breaker (CB) in GIS including its deterioration and aging mechanism

Compo-nent	Sub-system	Key Parts	Deterioration or Aging Mechanism	
Circuit Breaker	Primary Conductor	Main contacts and conductor	Deterioration	Electrical wear because of the contact erosion and nozzle ablation after the interruption
				Electrical contact deterioration in conductor due to, for example: loosening of a bolt connection
	Secondary	Auxiliary Contacts, Relays, and Wiring	Deterioration	Loosen wiring connection in the Local Control Cubicle (LCC)
				Internal Corrosion at Auxiliary Relay
			Aging	The insulation of the old wiring becomes brittle that lower its insulation level to the ground
	Dielectrics	Insulating Gas (SF_6)	• The gas itself is not subject to either aging or deterioration • The gas quality may be an indicator of other irregularities (like PD due to the particulate contamination, or the loosen primary conductor) • The gas leakages can be an indication of deterioration of the metallic housings, or aging of seals	
		Solid Insulation (Spacer)	Aging	In the presence of void or metallic inclusion, due to, e.g. the bad manufacturing process, the "electrical treeing" and PD may grow over time
			Deterioration	Deposited solid by-products on the surface of the spacer can decrease the insulation level of the solid spacer
				When condensation occurs, the withstand voltage will significantly decreased.

Compo-nent	Sub-system	Key Parts	Deterioration or Aging Mechanism	
	Driving mechanism	Energy Storage element (e.g. spring, hydraulic compression, pneumatic) and the mechanical chain between the energy storage element and the contacts	Deterioration	Mechanical fatigue at the highest stressed parts, i.e. the energy storage sub system, and the mechanical sub-system.
				Corrosion at parts that exposed to the ambient
	Construction and Supports	Metallic Enclosures	Deterioration	Flanges deterioration due to moisture ingress (and deposited pollutants), especially in outdoor GIS (with consequential impact on the gas tightness)
		Seals	Aging	Seals aging depends on many factors, including: temperature, exposure to O_2, Ultraviolet, and their combination. Dynamic seals also vulnerable to corrosion and mechanical wear.
		Pressure relief device	Deterioration	Corrosion by the moisture and the deposited pollutants.
				Fatigue caused by the cyclic temperature (and pressure) either due to the loading current and solar radiation. Outdoor GIS is more affected by this phenomenon.
		Gas monitoring, sensors, gas piping, valves		Corrosion at the mechanical parts due to the moisture ingress.

4.2.2 Methodology to capture condition indicators

Capturing condition indicators can be performed through a simple visual inspection up to complex diagnostic tests and measurements. Ideally, selecting an inspection method should be based on the three factors, namely, detectability (i.e., how good an inspection could detect a deterioration that could lead to a failure mode), cost of diagnostic, and risk of related failure mode. An inspection that is able to detect critical failure modes, in an easy way, with an economic cost; is preferable. In this thesis, however, the model uses the available condition indicators found in the JABA Case Study. There are three activities to capture the condition indicators in GIS, as follows:

1. *Routine visual inspection (RVI)*

   The RVI is a general visual inspection without shutting down the GIS. In the case study, this activity has a daily interval. The output from this activity can be qualitative information like good or bad wiring connection, corrosion state on the enclosure. On the other hand, numerical data is also possible; for example, the number of CB operations, the gas pressure, and the ambient temperature.

2. *Diagnostic test and measurement (DM)*

   Diagnostic test and measurement are used to compare the characteristic condition indicator(s) of an asset to verify that it performs its function correctly [24]. This activity is conducted online or offline without opening the GIS enclosure. Examples of DM are the measurements of gas purity and humidity content in gas, Partial Discharges (PD) and contact-travel time of CB. In the JABA Case Study, the DM has intervals from 6 months up to 2 years or more, depending on the GIS condition.

3. *Thorough inspection (TI)*

   This activity needs the opening of the GIS enclosure. An expert of the OEM (Original Equipment Manufacturer) is usually involved in this activity. Therefore, it is costly and time-consuming. In the JABA Case Study, the TI is typically conducted after 20 years of service time. Figure 4.3 shows an example of a thorough inspection of a Circuit Breaker in a GIS from the JABA case study.

In the current work, the HI model uses the output from the RVI and the DM. The results from TI so far are limited and cannot be used in the model. Table 4.2 summarizes the condition indicators along with the methods to capture them.

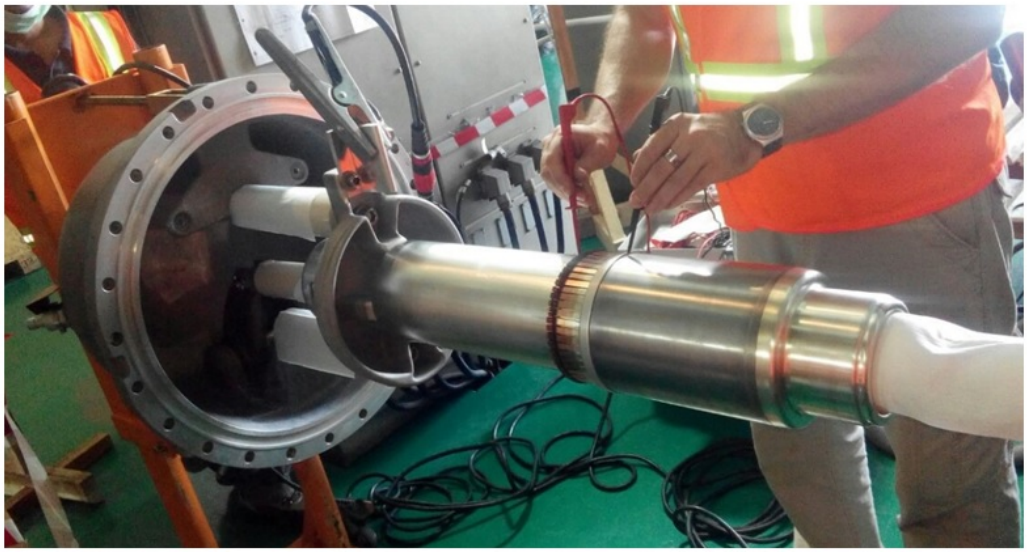

Figure 4.3 An example of a thorough inspection by opening the Circuit Breaker enclosure in one of the GIS of the JABA Case Study. In this figure, the static contact resistance of the CB main contacts was being measured by an OEM expert. In the case study, this major inspection is conducted after the GIS reached the operational life of 20 years.

Table 4.2 *The condition indicators in subsystems GIS as obtained from the Routine Visual Inspection (RVI) and the Diagnostic test and Measurement (DM)*

Condition Indicator's Code & Component		What to Check	Method	Condition Indicator	Unit
Primary Conductor Subsystem					
P1.1	CB	Deterioration of main contacts in CB and switches	RVI	Cumulative short circuit current	kA^2
P1.2	CB		RVI	Number of short circuit interruption	times
P2.1	CB & Switches		DM	Static contact resistance	μΩ
P2.2	CB, Switches, and Primary Conductor	Contact resistance of primary joint conductor	DM	Hot spot on the enclosure	^oC and pattern
Dielectric Subsystem					
D1.1	All Components	Density of SF_6	RVI	Gas Pressure (Leakage Rate)	Bar, MPa
D1.2			RVI	Gas Density (Density reduction)	kg/m^3
D2.1		Quality of SF_6	DM	SF_6 Purity	%-SF_6
D2.2		Partial Discharge Activity	DM	SO_2 content	ppmV
D2.3			DM	SF_6 by-products other than SO_2	ppmV
D2.4			DM	PD Pattern & PD Growth	*"Multiple Indicator"*
D2.5		Possibility to have condensation on the surface of solid insulation	DM	Humidity content in SF_6	ppmV
D2.6			DM	Dew point in SF_6 at gas pressure	^oC

Condition Indicator's Code & Component		What to Check	Method	Condition Indicator	Unit
Driving Mechanism Subsystem					
E1.1	CB DE	Mechanical wear	RVI	Number of mechanical works	times
E1.2	Hydraulic/ Pneumatic CB	(Compression) energy storage readiness	RVI	Number of gas pressure replenishing unintendedly (if any)	times/ period
E2.1	CB	Mechanical integrity	DM	Contact timing Open & Close	ms
E2.2	CB		DM	Contact travel record	Contact position vs. time
E2.3	Electric Switches	Electric motor readiness	DM	Motor Current	A
Secondary Subsystem					
S1.1	CB and Switches	Any corrosion or dust deposited in wiring connections	RVI	Corrosion of wiring and aux relays	-
S1.2			RVI	Deposited dust in wiring and aux relays	-
S2.1			DM	Hot Spot in wiring in LCC	^{o}C and pattern
S2.2		Functionality of relays & remote controls	DM	Relay & control function; Indicators check	OK/ Not OK
Construction and Support Subsystem					
C1.1	All	Corrosion on enclosures	RVI	Corrosion level	-
C1.2			RVI	Deposited Pollutants	-
C1.3		Foundation integrity	RVI	Foundation integrity	-

4.3 *Generating norms*

The result from the RVI and DM needs to be interpreted to justify the health status of the subsystems in GIS components. It is achieved by setting the limit, or the boundary values, known as the "norm." In this thesis, the norm justifies whether the measured values of the condition Indicators fall in one of the five health indexed states, i.e., Very good, Good, Deteriorate, Bad, and Very Bad, which is further translated into a condition scale code as given in Table 4.5.

Seven approaches are possible to develop a norm, as follows:

1. By using statistical analysis on the condition indicators taken from field inspections.
2. By using recommendations from literature, like, GIS manuals, international standards, publications.
3. By trending analysis of the condition indicators.
4. By comparing condition indicators among sister components.
5. By deterministic analysis, like, from failure modes observed during a forensic investigation, or by a laboratory test.
6. By expert's judgement (can be through discussion with the maintenance expert group or by a Delphi test [63]).
7. By a combination of two or more approaches above.

Table 4.3 provides a summary of the different approaches above on the norm generation of various condition indicators from the JABA Case Study.

Table 4.3 *Approach for Norm Generation for condition indicators of all subsystems in GIS as obtained from the RVI and the DM*

Code	Condition indicator	Approach for Norm Generation						
		Statistics of field data	*Guides, Standards*	*Trending Analysis*	*vs. Sister Component*	*Laboratory tests*	*Expert Judgement*	*Combination*
		A1	*A2*	*A3*	*A4*	*A5*	*A6*	*A7*
Primary Conductor Subsystem								
P1.1	Cumulative Short Circuit Current	-	Maximum limit based on the manufacturer recommendation	-	-	-	Judgement on the intermediate health status	-
P1.2	Number of Short Circuit Interruption	-	Maximum limit based on the manufacturer recommendation	-	-	-	Judgement on the intermediate health status	-
P2.1	Static contact resistance	Maximum limit based on the statistics of the identical components	Maximum limit based on the manufacturer recommendation	The maximum increase from the last measurement	The maximum difference from the mean value of sister components	-	-	Statistics and Trending analysis, to obtain statistics of gradient increase
P2.2	Hot spot on the enclosure	-	-	The maximum increase from the last measurement	Yes/ No Hotspot in comparison adjacent sister component	-	-	-

Code	Condition indicator	Approach for Norm Generation						
		Statistics of field data	*Guides, Standards*	*Trending Analysis*	*vs. Sister Component*	*Laboratory tests*	*Expert Judgement*	*Combination*
		A1	*A2*	*A3*	*A4*	*A5*	*A6*	*A7*
Dielectric Subsystem								
D1.1	Gas Pressure (Leakage rate)	Maximum leakage rate based on the statistics of population	Maximum leakage rate based on standard/ guide	-	-	-	-	-
D1.2	Gas Density (Density decrease)	Maximum density reduction based on the statistics of population	Maximum density reduction based on standard/ guide	-	-	-	-	-
D2.1	SF_6 Purity	Minimum SF_6 purity based on the statistics of population	Minimum SF_6 purity for operational GIS based on standard/ guides	-	-	-	-	-

Code	Condition indicator	Approach for Norm Generation						
		Statistics of field data	*Guides, Standards*	*Trending Analysis*	*vs. Sister Component*	*Laboratory tests*	*Expert Judgement*	*Combination*
		A1	*A2*	*A3*	*A4*	*A5*	*A6*	*A7*
D2.2	SO_2 content	Maximum SO_2 content based on the statistics of population	Maximum SO_2 content based on the manufacturer recommendation and guide	YES/ NO of increase of SO_2 content in the non-switching enclosure	-	-	-	-
D2.3	SF_6 by-products other than SO_2	Maximum by-products limit based on the statistics of population	Maximum by-products limit based on manufacturer recommendation and guide	YES/ NO of increase of Key Gasses content in the non-switching enclosure	-	Maximum content based on the laboratory test (e.g. breakdown strength)	-	Limit based on statistics and laboratory test
D2.4	PD Pattern & PD Growth	-	-	YES/ NO PD Growth (based on amplitude or pattern)	-	Provide Norm on PD pattern, limit of PD inception voltage	Maximum PD limit based on field experiences	Combination of lab test, expert judgement and trending analysis

Code	Condition indicator	Approach for Norm Generation						
		Statistics of field data	*Guides, Standards*	*Trending Analysis*	*vs. Sister Component*	*Laboratory tests*	*Expert Judgement*	*Combination*
		A1	*A2*	*A3*	*A4*	*A5*	*A6*	*A7*
D2.5	Humidity content in SF_6	Maximum humidity limit based on statistics in the population	Maximum humidity limit based on manufacturer recommendation and guide	The maximum increase from the previous value	-	Maximum humidity content based on laboratory test (breakdown strength)	Judgement on the maximum limit to avoid corrosion in internal GIS	Combination of lab test and expert judgement.
D2.6	Dew point in SF_6 at gas pressure	Maximum dew point based on statistics in the population	Maximum dew point based on manufacturer recommendation and guide	The maximum increase from the last measurement	-	Maximum dew point based on laboratory test (breakdown strength)	Judgement on the maximum limit to avoid corrosion in internal GIS	Combination of lab test and expert judgement.
Driving Mechanism Subsystem								
E1.1	Number of mechanical operations	-	Maximum number of operation based on manufacturer guide, or standard	-	-	-	Judgement on the intermediate health status	Combination between limit from guide, &judgement for the intermediate health status

Code	Condition indicator	Approach for Norm Generation						
		Statistics of field data	*Guides, Standards*	*Trending Analysis*	*vs. Sister Component*	*Laboratory tests*	*Expert Judgement*	*Combination*
		A1	*A2*	*A3*	*A4*	*A5*	*A6*	*A7*
E1.2	Unintended compressor operation	-	-	The maximum increase on the number of unintended work as a function of time	-	-	Judgement on the intermediate health status	-
E2.1	Contact timing Open & Close	The maximum deviation based on statistics in the population	Maximum timing and error based on the manufacturer recommendation	The maximum deviation from the last measurement	The maximum deviation from the mean value of sister components	-	-	Combination of Statistics and trending analysis
E2.2	Contact travel record	-	Provides a good travel pattern based on the guides	-	Provides good pattern based on the common pattern in the most sister components	-	Judgement on travel pattern based on field experience	Combination between expert judgement and guides, and sister components

Code	Condition indicator	Approach for Norm Generation						
		Statistics of field data	*Guides, Standards*	*Trending Analysis*	*vs. Sister Component*	*Laboratory tests*	*Expert Judgement*	*Combination*
		A1	*A2*	*A3*	*A4*	*A5*	*A6*	*A7*
E2.3	Motor Current	-	Maximum current and error based on manufacturer recommendation	The maximum deviation from the last measurement	The maximum deviation from the mean value of sister components	-	-	-
Secondary Subsystem								
S1.1	Corrosion of wiring and aux relays	-	-	-	-	-	Provide qualitative judgment on corrosion limit	-
S1.2	Deposited dust in wiring and aux relays	-	-	-	-	-	Provide qualitative judgement on pollutants limit	-

Code	Condition indicator	Approach for Norm Generation						
		Statistics of field data	*Guides, Standards*	*Trending Analysis*	*vs. Sister Component*	*Laboratory tests*	*Expert Judgement*	*Combination*
		A1	*A2*	*A3*	*A4*	*A5*	*A6*	*A7*
S2.1	Hot Spot in wiring in LCC	-	-	-	Yes/ No Hotspot in comparison adjacent sister component	-	-	-
S2.2	Relay & control function; Indicators check	-	Guides to do the checklist	-	-	-	-	-
Construction & Support Subsystem								
C1.1	Corrosion level	-	-	-	-	-	Provide qualitative judgment on corrosion limit	-
C1.2	Deposited Pollutants	-	-	-	-	-	Provide qualitative judgment on pollutants limit	-

Code	Condition indicator	Approach for Norm Generation						
		Statistics of field data	*Guides, Standards*	*Trending Analysis*	*vs. Sister Component*	*Laboratory tests*	*Expert Judgement*	*Combination*
		A1	*A2*	*A3*	*A4*	*A5*	*A6*	*A7*
C1.3	Foundation integrity	-	-	-	-	-	Provide qualitative judgment on pollutants limit	-

4.3.1 Example of Norm Generation

In the following paragraphs, an example of norm generation for the humidity content for a GIS operating under the tropical conditions will be demonstrated by using three different approaches, which refer to row D2.5 in Table 4.3.

Approach-01: *The deterministic approach by calculation of the maximum humidity content in GIS, with a correction factor.*

The flashover test with the "spacer and gas" model, as discussed in Chapter 3, has shown that the humidity does not influence the flashover voltage as long as there is no condensation. Therefore, the maximum humidity content (i.e., before condensation) in GIS insulation system can be estimated from the calculation using the Magnus formula [31-33], with a correction factor.

The partial pressure of the water vapor in the gas necessary to a condensation, at temperatures above 0°C, can be calculated through the Magnus formula, as follows:

$$e = 611.2 \cdot exp\left(\frac{17.62 \cdot T}{243.12 + T}\right) \quad \ldots 4.1$$

where:

e is the water vapor partial pressure in Pascal (in Pascals, Pa),
T is the temperature in °C (valid for T = 0°C up to 50°C)

It is assumed that the condensation occurs when the temperature of the gas reaches the ambient temperature, and the effect of desorption of water molecules into the spacer or compartment surface is negligible. The partial pressure of the water vapor at ambient conditions can be calculated by putting the ambient temperature into equation 4.1. Following that, the humidity content to obtain a condensation can be calculated from the following equation:

$$\mathrm{ppmV_{max}} = \frac{e_{max}}{p - e_{max}} \cdot 10^6 \quad \ldots 4.2$$

where:

$\mathrm{ppmV_{max}}$ is the humidity content in SF_6 to obtain condensation at the ambient temperature. The "max" terminology is used to define the allowable humidity content in GIS (ppmV)
e_{max} is the maximum water vapor partial pressure to have condensation at the ambient temperature (in Pascals, Pa)
p is the total pressure at which e_{max} is measured (in Pascals, Pa)

In tropical conditions, the lowest ambient temperature is reached during the night or at the early morning, with the temperature within the range of 18 up to 25°C. Then the condensation might start in the gas close to the enclosure. The minimum humidity contents to create condensation, as a function of gas pressure, at the lowest possible temperatures in the tropics are presented in Figure 4.4.

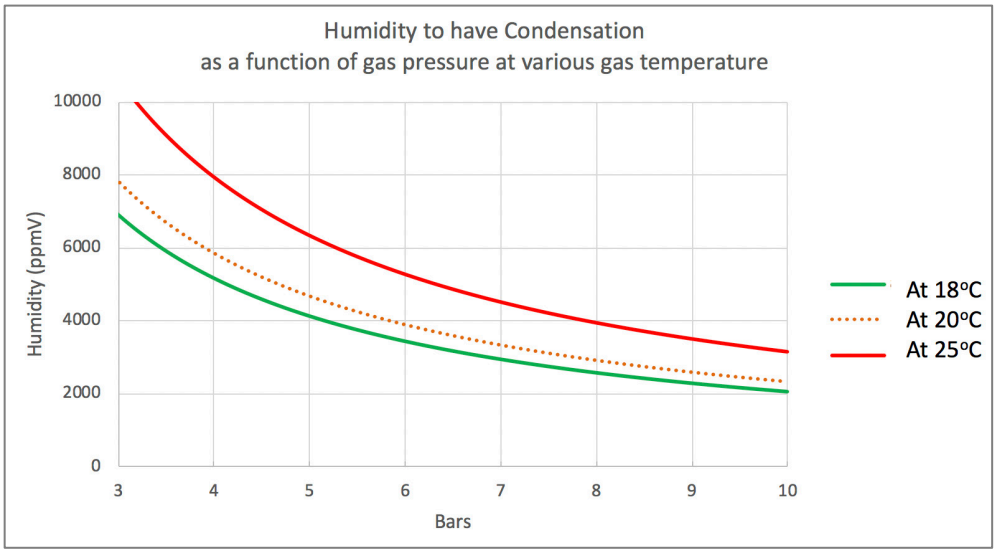

Figure 4.4 Humidity content to have condensation as a function of gas pressure at various temperatures as calculated with the Magnus formula. It is assumed that the gas temperature is similar to the ambient temperature.

The result from the calculation above gives an optimistic result. Although the humidity does not influence the flashover of the insulation system, when a partial discharge occurs, the chain reaction between the SF_6 and the water molecules produces the corrosive by-products which are detrimental to the GIS insulation system. The deposited solid by-products on the spacer are responsible for the reduction of the breakdown strength. These mechanisms are possible to occur in GIS, and they should also be taken into consideration when justifying the norm.

Therefore, we introduce a "correction factor," C_h, based on the expert's judgement. So, the maximum humidity content becomes:

$$ppmV_{max\text{-}operation} = C_h \,.\, ppmV_{max} \qquad \ldots 4.3$$

where:

$ppmV_{max\text{-}operation}$	is the humidity content maximum in SF_6 during operation of GIS (in ppmV).
C_h	correction factor, dimensionless, in this thesis the value is 0.1
$ppmV_{max}$	is the humidity content in SF_6 to obtain condensation at the ambient temperature as calculated from 4.2. (in ppmV)

If the humidity content is up to the value from the calculation in 4.3, the condition status is "Very Good." Now, another expert judgment is used to justify the limit for the other four possibilities of condition statutes, as follows:

1. Very Good, if *humidity-content* ≤ $ppmV_{max\text{-}operation}$
2. Good, if $ppmV_{max\text{-}operation}$ < *humidity-content* ≤ $1.5.ppmV_{max\text{-}operation}$
3. Deteriorate, if $1.5.ppmV_{max\text{-}operation}$ < *humidity-content* ≤ $2.5.ppmV_{max\text{-}operation}$
4. Bad, if $2.5.ppmV_{max\text{-}operation}$ < *humidity-content* ≤ $4.ppmV_{max\text{-}operation}$
5. Very Bad, if *humidity-content* > $4.ppmV_{max\text{-}operation}$

This approach can be an alternative when the limit of humidity content from the manufacturer is absent. However, the result from this approach tends to give a higher value than the other approaches; therefore, we suggest its application only for the non-switching enclosure and when the PD does not occur in GIS.

The following calculation is given for the non-CB enclosure of 150 kV GIS from Manufacturer A. The lowest ambient temperature is assumed at 20°C, with the operating gas pressure at 4.8 bars. Calculation by using equation 4.1 and 4.2 gives the minimum humidity to have condensation of 4883 ppmV so that the maximum humidity content during operation is 488 ppmV. The boundaries for condition status become as follows:

1. Very Good : *humidity-content* ≤ 488 ppmV
2. Good : 488 < *humidity-content* ≤ 732 ppmV
3. Deteriorate : 732 < *humidity-content* ≤ 1221 ppmV
4. Bad : 1221 < *humidity-content* ≤ 1953 ppmV
5. Very Bad : > 1953 ppmV

Approach-02: By using the statistics of humidity content from field data

The investigation of the humidity contents in Chapter 2 reveals that the amount of humidity is characteristic for GIS from different manufacturers and dependent on the enclosure's design. The enclosures without the absorbents have higher humidity content.

The statistics using the distribution fitting method can be used for the definition of the boundary values as proposed in [27]. An estimated probability density function (PDF) is derived, then we define the boundary of "Very Good," "Deteriorate," and "Bad" based the boundaries of 1-σ (68.3%) and 2-σ (95.4%) values. It means that, if the humidity content in the enclosure is higher than 68.3% of the estimated PDF, the condition status is "Deteriorate." Meanwhile, when the value is above, 95.4% of PDF is defined as the "Bad" condition. Confidence bounds of 95% are typically added at the boundary of 95.4% [27]. In this thesis, the Upper and the Lower boundaries are also used as another limit between "Bad" and "Very Bad" conditions.

The following demonstration is based on the humidity content in 150 kV GIS from Manufacturer A with service time over ten years. None of the gas replacement has been conducted up to the moment of the gas measurement. The fitted distribution is the Gamma distribution for humidity content in the CB enclosure and the Lognormal distribution for the non-CB enclosure. The PDF of the humidity contents in both type of enclosures, including the boundary limits, are presented in Figures 4.5 and 4.6.

As seen in the figures, the boundary values for the three-condition status are as follow:

1. For CB enclosure:
    a. Very Good : *humidity-content* ≤ 135 ppmV
    b. Deteriorate : 135 < *humidity-content* ≤ 277 ppmV
    c. Bad : 277 < *humidity-content* ≤ 336 ppmV
    d. Very Bad : > 336 ppmV

2. For Non-CB enclosure:
   a. Very Good : *humidity-content* ≤ 209 ppmV
   b. Deteriorate : 209 < *humidity-content* ≤ 660 ppmV
   c. Bad : 660 < *humidity-content* ≤ 804 ppmV
   d. Very Bad : > 804 ppmV

This approach is easy to use, and it is applicable for GIS that has sufficient data.

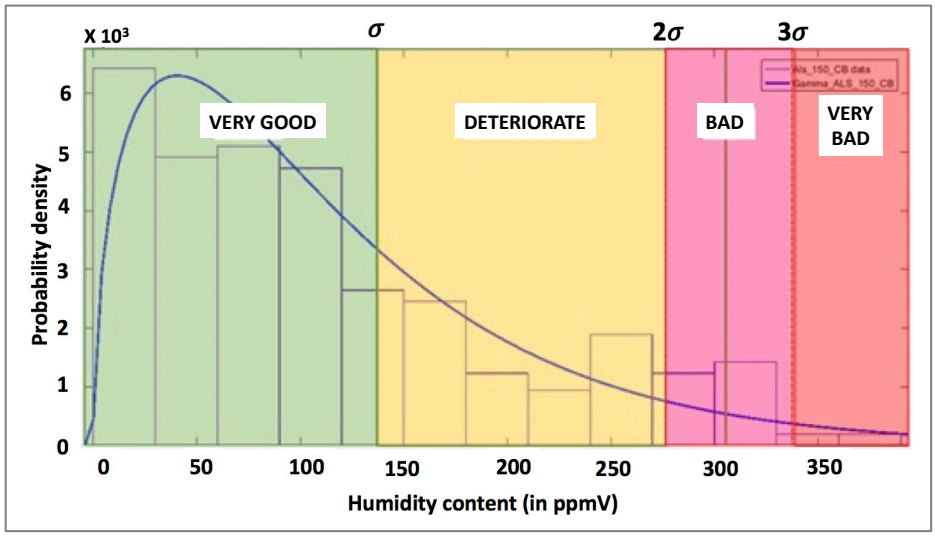

Figure 4.5 Boundary values for humidity content in the CB enclosure for GIS from Manufacturer A. The fitted distribution is the Gamma distribution.

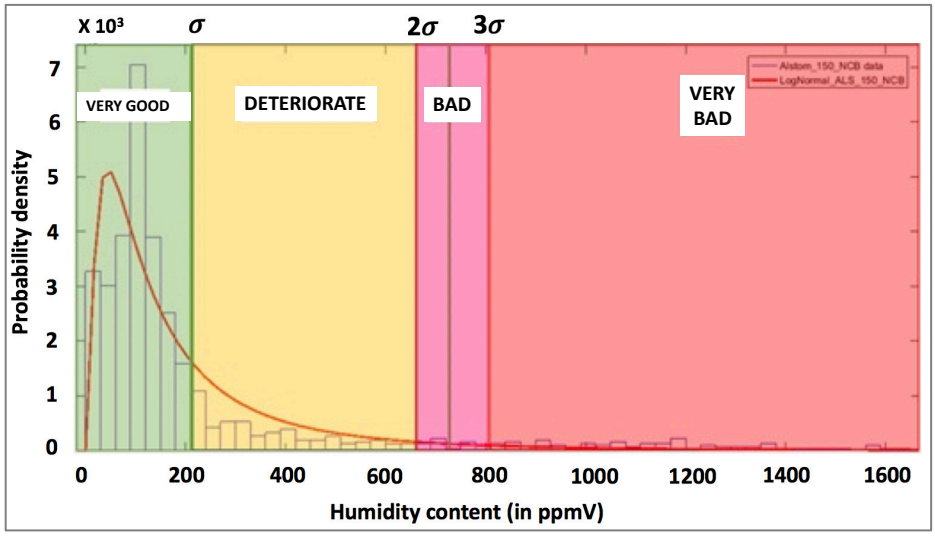

Figure 4.6 Boundary values for humidity content in the Non-CB enclosures for GIS from Manufacturer A. The fitted distribution is the Lognormal distribution.

Approach-03: Recommendation limit from standards and manual from the manufacturer

The maximum humidity limit from the literature usually can only be interpreted as "Good," if the measured value is below the recommended limit, and "Bad" if the measured value is above the limit. These recommendations are as follow:

1. Maximum humidity content from the Manufacturer A's Guide:
   a. CB enclosure : 350 ppmV
   b. Non-CB enclosure : 840 ppmV
2. Limit from the IEC Standard [24] : at pressure = 5 bars, 804 ppmV
3. Limit from the CIGRE [32,34] : at pressure < 8.5 bars, 200 ppmV

Summary *of Different Approaches:*

The norm for the humidity content in GIS from Manufacturer A as derived from different approaches have been summarized in Table 4.4.

Table 4.4 *Summary of Norm for Humidity Content for 150kV GIS from Manufacturer A. which has been generated from different approaches*

No.	Approach	Humidity Content (in ppmV), h, per Health Status									
		Very Good		Good		Deteriorate		Bad		Very Bad	
		CB	Non CB	CB	Non CB	CB	Non CB	CB	Non CB	CB	Non CB
1	Deterministic	N/A	≤ 488	N/A	488 - 732	N/A	732-1221	N/A	1221-1953	N/A	> 1953
2	Statistics	≤135	≤ 209	-	-	135 - 277	209 – 660	277-336	660 - 804	> 336	> 804
3	Manf. (A)	N/A		≤ 350	≤ 840	N/A		> 350	> 840	N/A	
	IEC [24]	N/A		≤ 804		N/A		> 804		N/A	
	CIGRE [32,34]	N/A		≤200		N/A		> 200		N/A	

The results in the table indicate that the boundary for the non-CB enclosure from the manufacturer's guide is higher than the other values from the different approaches, although this is not always the case.

The second approach of using the statistics of field data is applicable for both CB and non-CB enclosures. The first and the third approaches, or the combination of both are suggested for a new type of GIS int the population, or when the recommended limit from the manufacturer is not available.

4.4 *Health Index Coding*

It is easier for the asset managers to see the health status of all GISs in his network in an index number. Therefore, we design the final output of the AHI by a linear scaling number of 1 to 5, which the higher the score is indicating, the worse condition and the higher likelihood of a failure mode to occur (see later in Table 4.11).

However, before obtaining the final result, there is an aggregating process on condition indicators as formerly provided in Figure 4.2. During this process, a logarithmic base-3 scaling condition codes have been chosen to represent the condition status of subsystems in GIS. Table 4.5 defines each condition code used in this thesis.

Table 4.5 *Definition of condition scale codes used in this thesis*

Code	Qualitative meaning	Description	Likelihood of a failure mode to occur
1	Very Good Condition	As good as new, no evidence of ageing or deterioration.	Very Low GIS can continue working properly.
3	Good Condition	Slight deterioration/ ageing process is observed, but it is considered at normal stage. Minor defect may be observed, but it does not influence the GIS performance both in short and longer terms.	Low GIS can continue working properly. It's running at normal deterioration/aging process.
10	Moderate Condition	Deterioration/ aging process has been observed beyond the normal stage. Intervention is required as deterioration/ aging may interfere the GIS performance in long-term.	Moderate GIS can continue working but remedial action is advised, otherwise it may contribute to GIS performance in longer term
30	Bad Condition	Severe deterioration/ aging has been observed. Intervention is required in short-term	High The GIS performance is possibly reduced in short-term.
100	Very Bad Condition	Very severe deterioration/ aging (i.e. at a final stage) has been observed. Emergency action is required.	Very High GIS shutdown is required for further action to fix GIS performance.

The following subsections will explain the condition coding of condition indicators at each layer of GIS.

4.4.1 Condition Coding of Subsystems in GIS

The boundaries for the health status of subsystems in GIS were determined by the various approaches as formerly presented in Table 4.3.

4.4.1.1 Condition coding of primary conductor subsystem in GIS

At the primary conductor subsystem, the observed failure mode is the “loss of electrical connections integrity in the primary.” The key parts in the primary conductor subsystem consist of the main contacts (in the CB and disconnector switches), and the conductor, including the joint-conductor and the shields. The health scoring for the primary conductor subsystem is shown in Table 4.6. Below the column of “Inspection Code,” the method is mentioned within the bracket.

Table 4.6 *Condition codes of primary conductor subsystem in GIS*

Inspection Code (Method)	Comp.	Condition Indicator	Unit	Condition Code				
				1	3	10	30	100
P1.1 (RVI)	CB	Cumulative Short Circuit Current	I_{CUM-SC}	≤ 20% of limit	20% < limit ≤ 40%	40% < limit ≤ 70%	70% < limit ≤ 100%	> limit
P1.2 (RVI)	CB	Number of Short Circuit Interruption	N_{SC}					
P2.1 (DM)	CB, DE	Static Contact Resistance	$R_{st-contact}$	$\Delta R_{st-contact} \leq 5\%$	-	$5\% < \Delta R_{st-contact} \leq 10\%$	$10\% < \Delta R_{st-contact} \leq 20\%$	$\Delta R_{st-contact} > 20\%$
P2.2 (DM)	All	Hot Spot on the Enclosure	(Pictorial)	No Hot Spot	-			Hot Spot Found

As seen in the table, the RVI for the primary conductor subsystem is only applicable to the Circuit Breaker. The visual inspections give the value of the cumulative circuit current (P1.1, I_{CUM-SC}) and the number of the short-circuit interruptions (P1.2, N_{SC}). In practice, the information is difficult to be obtained, especially from the old version of GIS. The short-circuit information from the past is rare. When the information is not available, a default value can be determined based on the judgment of the expert. However, when it is available, the norm for both indicators have been selected as follows:

1. Code of 1 : if I_{CUM-SC} or $N_{SC} \leq 20\%$ of the design limit.
2. Code of 3 : if $20\% < I_{CUM-SC}$ or $N_{SC} \leq 40\%$ of the design limit.
3. Code of 10 : if $40\% < I_{CUM-SC}$ or $N_{SC} \leq 70\%$ of the design limit.
4. Code of 30 : if $70\% < I_{CUM-SC}$ or $N_{SC} \leq 100\%$ of the design limit.
5. Code of 100 : if, I_{CUM-SC} or $N_{SC} > 100\%$ of the design limit.

The static contact resistance (P2.1, $R_{st-contact}$) is applicable for both CB and switches (disconnectors). The assessment of this indicator depends on the availability of information, i.e., by one of the following approaches:

1. From the deviation with the initial value during the commissioning test (R_{in}).
2. From the deviation with the maximum value recommended by the manufacturer (R_{man}).
3. From the trending analysis from at least 2 measurements at different maintenance inspections (ΔR_1).

4. By comparing the measured value with other results from the sister components (ΔR2).

The norm has been selected as follow:

1. Code of 1:
   if ($R_{st\text{-}contact}$-R_{in}) ≤ 5% of $R_{st\text{-}contact}$
   OR if ($R_{st\text{-}contact}$-R_{man}) ≤ 5% of $R_{st\text{-}contact}$
   OR if ΔR1 ≤ 5% of $R_{st\text{-}contact}$
   OR if ΔR2 ≤ 5% of $R_{st\text{-}contact}$

2. Code of 10:
   if 5% of $R_{st\text{-}contact}$ < ($R_{st\text{-}contact}$-R_{in}) ≤ 10% of $R_{st\text{-}contact}$
   OR if 5% of $R_{st\text{-}contact}$ < ($R_{st\text{-}contact}$-R_{man}) ≤ 10% of $R_{st\text{-}contact}$
   OR if 5% of $R_{st\text{-}contact}$ <ΔR1 ≤ 10% of $R_{st\text{-}contact}$
   OR if 5% of $R_{st\text{-}contact}$ <ΔR2 ≤ 10% of $R_{st\text{-}contact}$

3. Code of 30:
   if 10% of $R_{st\text{-}contact}$ < ($R_{st\text{-}contact}$-R_{in}) ≤ 20% of $R_{st\text{-}contact}$
   OR if 10% of $R_{st\text{-}contact}$ < ($R_{st\text{-}contact}$-R_{man}) ≤ 20% of $R_{st\text{-}contact}$
   OR if 10% of $R_{st\text{-}contact}$ <ΔR1 ≤ 20% of $R_{st\text{-}contact}$
   OR if 10% of $R_{st\text{-}contact}$ <ΔR2 ≤ 20% of $R_{st\text{-}contact}$

4. Code of 100:
   if ($R_{st\text{-}contact}$-R_{in}) > 20% of $R_{st\text{-}contact}$
   OR if ($R_{st\text{-}contact}$-R_{man}) > 20% of $R_{st\text{-}contact}$
   OR if ΔR1 > 20% of $R_{st\text{-}contact}$
   OR if ΔR2 > 20% of $R_{st\text{-}contact}$

Where:
R_{in} : Initial resistance from commissioning test.
R_{man} : Contact resistance, as recommended by the manufacturer.
$R_{st\text{-}contact}$: Static contact resistance from the measurement.

The maximum of 20% limit is determined based on the manufacturer's recommendation in the JABA Case Study [64]. The high contact resistance indicates a deterioration of the contacts; an example is given in Figure 4.7, where a carbonized female-contact has been found in one of the CBs from the JABA Case Study found during a major inspection. The measurement before the opening of the enclosures gave a deviation above 20%.

Figure 4.7 A carbonized female-main contact in one of Circuit Breaker in GIS in the case study. The measurement before opening the enclosure had shown the increase of the static contact resistance above 20% from the last result.

The other condition indicator is the hotspot. It indicates a final stage of deterioration at the primary conductor of any components in GIS. An example of the hot spot from the JABA Case Study is given in Figure 4.8. The norm is decided only to contain two boundaries, i.e., Code of 1 if the hotspot is not found, and the code of 100, if the hotspot is observed.

To highlight the likelihood of a failure mode to occur, the worst condition indicators define the condition code of the primary conductor subsystem as follows:

For primary conductor subsystem of CB:

$CC_{Primary\text{-}CB}$ = MAX (P1.1, P1.2, P2.1, P2.2) … *4.4*

For primary conductor subsystem of Switches (DS, ES):

$CC_{Primary\text{-}DE}$ = MAX (P2.1, P2.2) … *4.5*

For primary conductor subsystem of non-switching components:

$CC_{Primary\text{-}NonSwitching}$ = P2.2 … *4.6*

Figure 4.8 An example of a hotspot in one phase of sealing end compartment in a GIS in the case study. The thermal image camera captured the picture. The highest temperature point is indicated by the "plus" symbol in the picture. Further investigation reveals the degraded jointing of the primary conductor at that point.

4.4.1.2 Condition coding of the dielectric subsystem in GIS

The failure mode at the dielectric subsystem is a dielectric breakdown, either in normal service or in connection with switching and/ or external transients. The critical parts of the dielectric subsystem in GIS consist of two, i.e., 1) the insulating gas (SF_6) and 2) the spacer, including its interface with the gas insulation. This subsystem is critical in GIS operating under tropical conditions [26,40].

The condition indicators, including their norms, have been summarized in Table 4.7. The output from the RVI consists of Gas Pressure (D1.1), and Gas Density (D1.2). In most of the cases, only the gas pressure is available. The gas pressure is temperature-dependent; consequently, the measured pressure should be first converted into the gas pressure at 20°C, following the ideal gas formulation:

$$\frac{P_{at\ 20^oC}}{293} = \frac{P_{measured}}{(273+t)} \quad \ldots 4.7$$

where:

P_{at20^oC} = Gas pressure at 20°C (in bar)
$P_{measured}$ = Gas pressure at t°C (in bar)
t = temperature at measurement (in °C)

The norm is generated based on the leakage rate per year. This can be estimated from the following equation [26]:

$$\Delta P = \left(1 - \frac{P_2}{P_1}\right) \cdot t_{cf} \cdot 100\% \qquad \dots 4.8$$

$$t_{cf} = \frac{365}{\Delta t} \qquad \dots 4.9$$

where:

ΔP = Leakage rate per year
P_1 = SF_6 gas pressure from the last measurement (in bar)
P_2 = SF_6 gas pressure from the current measurement (in bar)
t_{cf} = time correction factor
Δt = time between two respective measurements of gas filling in days (i.e. time between P_1 and P_2).

The boundary values are following the previous research in [26] in combination with the maximum recommendation from [24], as follow:

1. Code of 1 : if $\Delta P \leq 0.5\%$ [24].
2. Code of 3 : if $0.5\% < \Delta P \leq 1\%$.
3. Code of 10 : -
4. Code of 30 : if $1\% < \Delta P \leq 7\%$.
5. Code of 100 : if $\Delta P > 7\%$.

The calculation and norm for the gas density follow the approach as above.

The measurements in the dielectric subsystem give the following condition indicators: 1) The SF_6 purity, 2) The SO_2 content, 3) the by-products other than the SO_2, 4) the PD-pattern, and the PD growth, 5) the humidity content, and 6) the dew point. The norms for each condition indicator are discussed in the next paragraphs.

The best-fitting statistical approach is used for setting the norms for the SF_6 gas purity (D2.1) and the SO_2 content (D2.2), based on the data in the case study. The fitted distributions are the Weibull distribution for the SF_6 purity, and the Lognormal distribution for the SO_2 content. The 10% of PDF is determined as the boundary between the “Very Good” and “Moderate,” and 50% at the boundary between the “Moderate” and “Bad.” The Very Bad condition is defined when the value is above the limit from CIGRE [32,34]. The latter norms are as follows:

For the Purity of SF_6 (G_{pur})
1. Code of 1 : if $G_{pur} > 98.7\%$
2. Code of 3 : -
3. Code of 10 : if $98.7\% \geq G_{pur} > 97.8\%$
4. Code of 30 : if $97.8\% \geq G_{pur} > 97\%$
5. Code of 100 : if $G_{pur} < 97\%$ [55]

For the Content of SO_2 (G_{SO2})

1. Code of 1 : if $G_{SO2} \leq 1$ ppmV
2. Code of 3 : -
3. Code of 10 : if $1 < G_{SO2} \leq 4.6$ ppmV
4. Code of 30 : if $4.6 < G_{SO2} \leq 10$ ppmV
5. Code of 100 : if $G_{SO2} > 10$ ppmV [32,34]

The presence of SO_2 in the switching enclosure, especially in the CB, may indicate a normal switching operation. Therefore, it is suggested that the measurement of this gas should be conducted at least three days after the last switching operation.

The gas laboratory analysis (D2.3) may detect the by-products other than the SO_2. The common system is the GCMS (Gas Chromatography and Mass Spectrometer). Some gases that need to be considered in the insulating system are:

1. Air. The presence of air can reduce the arc extinguishing capability of the gas system. The maximum limit in the gas insulation is 1% of volume [26].
2. CO_2 and CO. They indicate the presence of air and the oxidation process at the O-ring or Spacer.
3. CF_4 (Carbon Tetrafluoride). One of the by-products gas can reduce the insulation performance. The maximum limit in the gas insulation is 1% of volume [26].
4. SOF_4, SO_2F_2, SOF_2, and HF. These gases indicate the partial discharges and the follow-up reactions after the PD. These gases are the agent of corrosions, and the maximum recommended content in total is 50 ppmV [34].
5. WF_6 (Tungsten Hexafluoride). This gas indicates contact erosion in CB.

In the JABA Case Study, the gas laboratory analysis is not part of the regular maintenance. The data for the statistical analysis is not available in the case study. Consequently, the presented norm is limited to the gasses that are mentioned in the documents like [34] and the manufacturer's guides (see the value in Table 4.7). For the other gases, a further study by observing the data trending is suggested.

The non-conventional PD detections have conducted the PD measurements (D.2.4) by using the acoustic measurement and the UHF/ VHF sensors. The applicability of this measurement depends on GIS design. Some GIS is equipped with the internal UHF/ VHF sensors, while in some old GIS, only the acoustic measurement is applicable. The norm for the PD measurement is determined by two factors, namely, PD pattern, and PD growth, as follows:

1. Code of 1 : if both PD pattern and PD growth are not observed.
2. Code of 3 : -
3. Code of 10 : -
4. Code of 30 : if PD pattern is observed, but PD growth is not existing
5. Code of 100 : if both PD pattern and PD growth are observed.

The humidity content (D2.5) and the dew point (D2.6) are both indicating the number of water molecules in the gas insulation. Some field measurements give the ppmV reading, while others in dew point. They both are interchangeable through the Magnus equation, with an assumption that the gas consists only SF_6 and H_2O. Therefore, the boundary

values for the dew point is derived from the ppmV-limit through the following equation [31-33]:

$$t_d = 272.62 \cdot \frac{ln\left(\frac{e}{611.2}\right)}{22.46 - ln\left(\frac{e}{611.2}\right)}$$ for t_d between -60 °C to 0°C … *4.10*

$$t_d = 243.12 \cdot \frac{ln\left(\frac{e}{611.2}\right)}{17.62 - ln\left(\frac{e}{611.2}\right)}$$ for t_d between 0 °C to 50°C … *4.11*

where:

$$e = \frac{h \cdot p}{h + 10^6}$$ … *4.12*

e = Partial water pressure at pressure p (in Pascal)
p = the total pressure at which the vapor pressure e is measured (in Pascal)
h = limit of humidity content, in ppmV

It is important to notice that some equipment give a dew point at the atmospheric pressure. This value needs to be translated into the dew point at the gas (operating) pressure through the procedure mentioned in the documents [31-33].

To highlight the likelihood of a failure mode to occur, the worst condition indicators define the condition code of the dielectric subsystem as follows:

$CC_{Dielectric}$ = MAX ((D1.1 OR D1.2), D2.1, D2.2, D2.3, D2.4, (D2.5 OR D2.6)) … *4.13*

Table 4.7 *Condition codes of dielectric subsystem in GIS*

Inspection Code (Method)	Comp.	Condition Indicator	Unit	Condition Code				
				1	3	10	30	100
D1.1 (RVI)	All	Gas Pressure	ΔP_{rate} /year	Up to 0.5%	>0.5% up to 1%	-	>4% up to 7%	>7%
D1.2 (RVI)	All	Gas Density	ΔD_{rate} /year	Up to 0.5%	>0.5% up to 1%	-	>4% up to 7%	>7%
D2.1 (DM)	All	SF_6 Purity	G_{pur}	$G_{pur} \geq$ 98.7%	-	97.8% ≤ G_{pur} <98.7%	97% ≤ G_{pur} <97.8%	<97%
D2.2 (DM)	All	SO_2 content	G_{SO2}	G_{SO2} ≤ 1 ppmV	-	1 < G_{SO2} ≤ 4.6 ppmV	4.6 < G_{SO2} ≤ 10 ppmV	>10 ppmV

Inspection Code (Method)	Comp.	Condition Indicator	Unit	Condition Code				
				1	3	10	30	100
D2.3 (DM)	All	SF_6 by-products other than SO_2	$G_{non-SO2}$	Air <1% Vol *OR* CF_4 < 1% Vol *OR* SOF_4+ SO_2F_2 +SOF_2+ HF < 50 ppmV	-	-	-	Air ≥1% Vol OR CF_4 ≥ 1% Vol OR SOF_4+ SO_2F_2 +SOF_2+ HF ≥ 50 ppmV
D2.4 (DM)	All	PD-Pattern & PD-Growth	Multiple	PD Pattern: NO PD Growth: NO	-	-	PD Pattern: YES PD Growth: NO	PD Pattern: YES PD Growth: YES
D2.5 (DM)	All	Humidity content in SF_6 gas	$H_{content}$	Depends on the manufacturer and approach used in developing norm				
D2.6 (DM)	All	Dew point in SF_6 gas at gas pressure	T_d	Follows the limit from Humidity Content (D2.5)				

4.4.1.3 Condition coding of driving mechanism subsystem in GIS

Failure mode at the driving mechanism subsystem is “failing to perform the requested operation” due to failure either at the energy storage or mechanical coupling sub subsystems. Therefore, condition indicators of this subsystem should check the following: 1) the mechanical integrity of the circuit breaker and 2) the energy storage readiness for CB and switches. The condition indicators including their health scores have been summarized in Table 4.8.

The RVI inspections give two condition indicators: 1. the number of mechanical operations of the driving mechanism, and 2. the compression – for CB with hydraulic and pneumatic energy storage. The norms for both indicators are defined by either expert judgment and guides, as follows:

The norm for the number of mechanical operations of the driving mechanism (N_{CB}, E1.1):

1. Code of 1 : if $N_{CB} \leq 5\%$ design limit.
2. Code of 3 : if $5\% < N_{CB} \leq 10\%$ design limit.
3. Code of 10 : if $10\% < N_{CB} \leq 50\%$ design limit.
4. Code of 30 : if $50\% < N_{CB} \leq 100\%$ design limit.
5. Code of 100 : if $N_{CB} > 100\%$ design limit.

Where the design limit is the mechanical endurance class guaranteed by the manufacturer, the classes are grouped into M1 (limit of 2000 times) and M2 (limit of 10000 times) [24].

The norm for the condition of the compressor (E1.2) (for GIS with pneumatic or hydraulic only, based on the expert judgement):

1. Code of 1 : no leakage, compressor working properly.
2. Code of 3 :
3. Code of 10 : compressor unintendedly working (replenish) 1-2 times in a year
4. Code of 30 : compressor unintendedly working (replenish) 3-12 times in a year
5. Code of 100 : compressor unintendedly working (replenish) >12 times in a year

Aged seals at the old pneumatic or hydraulic system of GIS contribute to this failure mode. In the worst case, the compressor may unintendedly work several times a day.

The mechanical integrity of a circuit breaker can be checked through the two condition indicators; namely, 1) The contact timing for the OPEN/ CLOSE position (E2.1), and 2) the contact travel's record (E2.2). The norm-setting for the contact timing is based on the deviation between the measured value, with one of the following possibilities: 1) the value from the commissioning, 2) the technical specification, 3) the value from the previous measurement, and 4) the comparison with the sister components. The norm for the contact timing ($|\Delta t_{contact}|$) is as follows (E2.1):

1. Code of 1 : if $|\Delta t_{contact}| \leq 2\%$.
2. Code of 3 : -
3. Code of 10 : if $2\% < |\Delta t_{contact}| \leq 5\%$.
4. Code of 30 : if $5\% < |\Delta t_{contact}| \leq 10\%$.
5. Code of 100 : if $|\Delta t_{contact}| > 10\%$.

The travel record may reveal the hidden failure in the driving mechanism of a Circuit Breaker, like 1) delay in releasing the energy storage, 2) poor damping, 3) low contacts speed, and 4) too low insulation distance in open position [55]. The norm-setting for this indicator consists of 2 boundaries (E2.2):

1. Code of 1 : Records show no deviation in contact-travel's pattern.
2. Code of 3 : -
3. Code of 10 : -
4. Code of 30 : -
5. Code of 100 : Records indicate one of the hidden failures as mentioned above.

The disconnector- and the earthing-switches are mostly electric motor driven, the investigation on the motor current can reveal not only the readiness of the motor but also the possibility of the mechanical integrity flaws. The increase of the motor current indicates a higher load that might be due to the misalignment of the mechanical coupling

of the main contacts. The norm is determined by the deviation between the measured value and the guide. The boundaries are decided either by the comparison with the manuals and by the expert judgments in the JABA Case Study, as follows (E2.3):

1. Code of 1 : if $|\Delta I_{motor}| \leq 2\%$
2. Code of 3 : -
3. Code of 10 : if $2\% < |\Delta I_{motor}| \leq 5\%$
4. Code of 30 : if $5\% < |\Delta I_{motor}| \leq 15\%$
5. Code of 100 : if $|\Delta I_{motor}| > 15\%$

To highlight the likelihood of a failure mode to occur, the worst condition indicators define the condition code of the driving mechanism subsystem as follows::

For GIS with spring driving mechanism:
$CC_{Driving\text{-}CB\text{-}spring} = MAX\ (E1.1, E2.1, E2.2)$ … 4.14

For GIS with pneumatic/ hydraulic driving mechanism:
$CC_{Driving\text{-}CB\text{-}pneumatic/hydraulic} = MAX\ (E1.1, E1.2, E2.1, E2.2)$ … 4.15

For electrical switches:
$CC_{Driving\text{-}DE} = MAX\ (E1.1, E2.3)$ … 4.16

Table 4.8 *Condition codes of driving mechanism subsystem in GIS*

Inspection Code (Method)	Comp.	Condition Indicator	Unit	Condition Code				
				1	3	10	30	100
E1.1 (RVI)	CB DE	Number (counter) of mechanical works of the driving mechanism	N_{CB}	≤ 5% limit	5% < N_{CB} ≤ 10% limit	10% < N_{CB} ≤ 50% limit	50% < N_{CB} ≤ 100% limit	> 100% limit
E1.2 (RVI)	CB	Compressor tightness	Leak/ No Leak	No Leak	-	Replenishing >1-2x/ year	Replenishing >3-12x/ year	Replenishing >12x/ year
E2.1 (DM)	CB	Contact timing Open & Close	$\lvert\Delta t_{contact}\rvert$	$\lvert\Delta t_{contact}\rvert$ ≤ 2%	-	2% < $\lvert\Delta t_{contact}\rvert$ ≤ 5%	5% < $\lvert\Delta t_{contact}\rvert$ ≤ 10%	$\lvert\Delta t_{contact}\rvert$ > 10%
E2.2 (DM)	CB	Contact travel record	L_{pos} vs. t_{travel}	Good result	-			Problem found
E2.3 (DM)	(Electric) Switches	Motor Current	ΔI_{motor}	$\lvert\Delta I_{motor}\rvert$ ≤ 2%	-	2%< $\lvert\Delta I_{motor}\rvert$ ≤ 5%	5%< $\lvert\Delta I_{motor}\rvert$ ≤ 15%	$\lvert\Delta I_{motor}\rvert$ > 15% OR Motor fails

4.4.1.4 Condition coding of secondary subsystem in GIS

Failure mode at the secondary subsystem is “loss of electrical connections integrity in secondary.” The key elements consist of relays, auxiliary contacts, wirings, and lamp/ status indicators. This subsystem has primary and sub-functions. The primary function is to actuate the driving mechanism to operate the circuit breaker or the switches, while the sub-function is giving the status (close/ open) of the switching component on both Local Control Cubicle (LCC) and control room. The condition assessment of this subsystem consists of checking the physical condition of the wiring and relays, and the functional tests of the relaying system, including controls and indicators.

The discussion with the experts and comparison with the guide from the manufacturer set the norms. Table 4.9 provides the norm for condition coding of the secondary subsystem.

As seen from the table, the output from the RVI is a qualitative measure on the condition of wiring and relays in the LCC (S1.1 and S1.2). The level of corrosion and deposited dust defines the score, as follows:

1. Code of 1 : No Corrosion/ Dust
2. Code of 3 : Slight Corrosion/ Dust
3. Code of 10 : -
4. Code of 30 : Severe Corrosion/ Dust
5. Code of 100 : Massive Corrosion/ Dust

While the norm for hot spot inspection on the loosen wiring connection (S2.1) is similar as in the primary subsystem inspection (P2.2), i.e., 1 if no hotspot, and 100 if the hotspot is found.

The relays’ function check (S2.2) is regularly conducted under offline condition. The purpose is to find the hidden failure. If all tests are passed, the condition code is 1. On the other hand, if only the monitoring/ supporting indicator is failing, the code is 30. Code of 100 is given when at least one of the relay protection fails.

To highlight the likelihood of a failure mode to occur, the worst condition indicators define the condition code of the secondary subsystem as follows:

$CC_{Secondary}$ = MAX (S1.1, S1.2, S2.1, S2.2) *… 4.17*

Table 4.9 *Condition codes of secondary subsystem in GIS*

Inspection Code (Method)	Comp.	Condition Indicator	Unit	Condition Code				
				1	3	10	30	100
S1.1 (RVI)	CB & Switches	Wiring & Relays Conditions in Local Control Cubicle (LCC	-	No corro-sion	Slight Corro-sion	-	Severe Corro-sion	Massive Corro-sion
S1.2 (RVI)			-	No dust	Slight Dust	-	Se-vere Dust	Massive Dust
S2.1 (DM)		Hot Spot in wiring in LCC	°C and Pattern	No Hot Spot	-			With Hot Spot
S2.2 (DM)		Relay & control function; Indicators check	OK/ Not OK	All OK	-	-	Any indica tor fails	Any relay fails

4.4.1.5 Condition coding of the construction and support subsystem

Failure mode at the construction and support subsystem is “loss of mechanical integrity on enclosures, pressure gauge, including big SF_6 leakage”. Corrosion is a common problem in the GIS operating under tropical conditions, especially in the outdoor GIS [26,40]. It is difficult to observe the corrosion at the inter-junction between the enclosures through the RVI and DM, which is actually the critical part for the gas leaking (see Figure 4.9). However, the gas leaks can be an indicator of an advanced stage of corrosion, which is usually involving aged seals. The norm for corrosion, dust, and the foundation are measured qualitatively, which rely on expert judgment.

Figure 4.9 Corrosions at the inner junction between enclosures found in the case study: (left) the corrosion at the junction between the bushing termination with the GIS enclosure after 25 years of service time. The GIS is located outdoor and close to the seashore, (right) the corrosion at the inner junction between enclosures after 30 years of operation, the GIS is located outdoor at the relatively benign environment.

The norms for condition indicator of corrosions (C1.1) and deposited pollutants (C1.2) are as follow:

Condition codes for the corrosion level and deposited pollutants on the enclosures:
1. Code of 1 : as good as new
2. Code of 3 : slight corrosion/ pollution
3. Code of 10 : moderate corrosion/ pollution
4. Code of 30 : severe corrosion with possible leaking, severe pollution
5. Code of 100 : catastrophic corrosion/ pollution, with possible big leaks

Condition codes for the inspection on the foundation (C1.3) are as follows:
1. Code of 1 : as good as new
2. Code of 3 : no crack, normal weathered condition
3. Code of 10 : -
4. Code of 30 : -
5. Code of 100 : crack and/ or enclosure's misalignment is observed

Finally, to highlight the likelihood of a failure mode to occur, the worst condition indicators defines the condition code of the construction and support as follows:

$CC_{Construction\&Support} = MAX\ (C1.1, C1.2, C1.3)$ *… 4.18*

Table 4.10 *Condition codes of construction and support subsystem in GIS*

Inspection Code (Method)	Comp.	Condition Indicator	Unit	Condition Code				
				1	3	10	30	100
C1.1 (RVI)	All	Corrosion level	-	As good as new	Slight Corrosion, No Leaks	Moderate Corrosion, No Leaks	Severe Corrosion, Small Leaks	Catastrophic corrosion; big Leaks
C1.2 (RVI)		Deposited Pollutants	-	As good as new	Slightly Polluted	Moderately Polluted	Severely Polluted	Catastrophic
C1.3 (RVI)		Foundation integrity	-	No crack				With crack, **OR** Misaligned enclosure

4.4.2 Condition coding of components in GIS

A component consists of subsystems. Condition codes of subsystems define the code for a component. There are two groups of components, the switching (e.g., CB, DS, ES) and the non-switching components (e.g., termination, busbar). The switching component has 5 subsystems' condition codes, while the non-switching component has 3 subsystems' condition codes.

Example:

CB-01 consists of 5 subsystems, so the Condition Codes of CB-01 consists of the following: Subcode of primary subsystem ($CC_{primary\text{-}CB01}$), Subcode of dielectric subsystem ($CC_{dielectric\text{-}CB01}$), Subcode of driving mechanism subsystem ($CC_{driving\text{-}CB01}$), Subcode of secondary subsystem ($CC_{secondary\text{-}CB01}$), and Subcode of construction and support subsystem ($CC_{construction\&support\text{-}CB01}$).

4.4.3 Condition coding of enclosures in GIS

An enclosure may contain only a single component, like in CB and VT, but in many cases it contained more components. Condition codes of an enclosure consist of the worst condition codes of subsystems owned by the components within it.

Example:

Enclosure-01 consists of 3 components, namely, DS-bus, CT-bus, and busbar-segment. The three components actually share the same dielectric subsystem and construction and support subsystem since they are enclosed in the similar compartment. On the other hand, only DS-bus who has the driving and secondary subsystems. Each component has their own primary subsystem. The condition codes of enclosure-01 will be the following:

$CC_{primary\text{-}Enclosure01} = MAX\ (CC_{primary\text{-}DSbus}, CC_{primary\text{-}CTbus}, CC_{primary\text{-}bbar})$ …4.19

$CC_{dielectric\text{-}Enclosure01} = CC_{dielectric\text{-}DSbus} = CC_{dielectric\text{-}CTbus} = CC_{dielectric\text{-}bbar}$ …4.20

$CC_{driving\text{-}Enclosure01} = CC_{driving\text{-}DSbus}$ …4.21

$CC_{secondary\text{-}Enclosure01} = CC_{secondary\text{-}DSbus}$ …4.22

$CC_{const\&supp\text{-}Enclosure01} = CC_{const\&supp\text{-}DSbus} = CC_{const\&supp\text{-}CTbus} = CC_{const\&supp\text{-}bbar}$ …4.23

4.4.4 Condition coding and indexing of bays in GIS

The condition code of a bay, CC_{bay}, is determined by the summation of the worst codes of subsystems within it, as follows:

$$CC_{bay} = CC_{worst\text{-}primary} + CC_{worst\text{-}dielectric} + CC_{worst\text{-}driving} + \ldots \\ \ldots + CC_{worst\text{-}secondary} + CC_{worst\text{-}const.\&supp.} \quad \ldots 4.24$$

A (sub) health index of a bay is generated based on a value from equation 4.24 above. There is a possibility that one bay GIS may contain 5 (i.e., if there is a switching component in it) or 3 subsystems. To make both scales comparable, the condition code of a bay with 3 subsystems should be normalized into the range of 5 subsystems before converting into an index. The formula for the conversion is as follows:

$$CC_{bay\text{-}5'} = \frac{5}{3} . CC_{bay-3} \quad \ldots 4.25$$

where:

$CC_{bay\text{-}5'}$ = New condition code of a bay as normalized to 5 subsystems code
$CC_{bay\text{-}3}$ = Condition code of a bay with 3 subsystems

There are 119 possible distinguished (total) condition codes of a bay with the value from 5 to 500. We divide these codes into five intervals to obtain the index as provided in Table 4.11.

Table 4.11 *Classification of bay index based on the conditon codes*

Condition Code (CI_{bay}) Range	Interpretation	Bay Index
5	All subsystems have condition code of 1 (very good)	**1**: Very Good
$7 \leq CI_{bay} < 14$	At least 1 subsystem has a code of 3 (good) but none of them has a code of 10 (moderate)	**2**: Good
$14 \leq CI_{bay} < 34$	At least 1 subsystem has a code of 10 (moderate) but none of them has a code of 30 (bad)	**3**: Moderate
$34 \leq CI_{bay} < 104$	At least 1 subsystem has a code of 30 (bad) but none of them has a code of 100 (very bad)	**4**: Bad
$CI_{bay} \geq 104$	At least 1 subsystem has a code of 100, *OR* At least 3 subsystems have a code of 30 each and the addition with the other 2 codes give the total code ≥ 104	**5**: Very Bad

4.4.5 Condition indexing at the substation layer of GIS

The number of bays among GISs could be different. In the JABA Case Study, a GIS with up to 24 CB-bays has been found, while the minimum number of bays is 3. In this thesis, the condition index of a GIS is determined by the worst index of bays in the same substation. To include the variation of the number of bays in one location, the number of bays with the similar maximum index (i.e., with the similar worst status) is given within the bracket next to the index.

Example:

GIS-A consists of 5 bays, with the sub-health index of each bay is given as follows:

Bay-01 : 2
Bay-02 : 2
Bay-03 : 4
Bay-04 : 4
Bay-05 : 1

The condition index for GIS-A is **4** *(2)*.

4.5 *Failure Susceptibility Indicators (FSI)*

Failure Susceptibility Indicators (FSI) are the factors that may or could initiate an onset of a failure mode in a GIS. The FSI is not a failure mode, it is also not a condition indicator, but it might increase the likelihood of failure. However, since FSI is only an expectation,

so it functions only as a “warning flag” during condition assessment of an asset. It stands as “side notes” of AHI.

According to the extensive investigation of failures from the JABA Case Study (see Chapter 2), the FSI can be grouped into three categories, as follows:

1. Environmental indicators (sub-FSI_E)
    a. Pollutants-level
    The failure rate of GIS outdoor is higher than the indoor. The failure susceptibility indicator is even higher for an outdoor GIS located in the highly polluted area.
    b. Lightning stroke
    GIS connected to an over headline is more prone to a lightning stroke than the one connected with power cable. The likelihood of failure is higher in the area with a high density of lightning, and if surge arrester fails to protect.

2. Operation and maintenance indicators (sub-FSI_{OM})
    a. Voltage transients intensity due to interruptions (switching) in GIS
    Switching activity increases the likelihood of insulation breakdown as has been reported from the forensic investigation, particularly when a defect occurs at the insulation system.
    b. Service time
    As discussed in subsection 2.2 about the statistical lifetime analysis in the JABA Case Study, the likelihood of GIS failure due to the three critical failure modes is increasing with the service time. The B5 value for 500kV-outdoor, 150kV-outdoor, and 150kV-indoor sequentially 18, 15, and 25 years. We decide to use these B5 values to indicate the failure susceptibility indicator due to service time.
    c. Maintenance history
    The likelihood of failure is increased when there is a history of unsolved corrective maintenance in GIS, for example, flaws in the hydraulic compression system, and the loss of mechanical integrity in the driving mechanism.

3. Inherent/ design indicators (sub-FSI_{ID})
    a. Single/ double O-ring design
    A likelihood to leak is higher in GIS with a single O-ring design than double design.
    b. Absorbent availability
    An enclosure that is not equipped with the absorbent will have high humidity content as it was found from one of GIS manufacturer in the JABA Case Study. Humid gas increases the likelihood to have condensation at the insulation system and accelerate corrosion.
    c. GIS makes
    Failure experiences from the case study show that GIS from a particular manufacturer has lesser reliability than the average of the population. An example is given in Table 2.11, where an excessive gas leak was observed only after 3 years of service time. The root cause was unclear, but it can be related to the

material issue, bad quality control during the manufacturing process, and poor workmanship.

Each sub-FSI may fall into one of the following statuses: High, Moderate, and Low; based on the influence of the factors to accelerate the likelihood of failure. The index is presented in colours as **Red** (HIGH), **Yellow** (MODERATE), and Green (LOW). Definition of each status is given in Table 4.12.

Table 4.12 *Classification of sub-FSI index*

Sub-FSI Index	Sub-FSI Index in Colour	Interpretation
LOW	Green	The risk factors have a Low influence to accelerate the onset of a failure mode in GIS
MODERATE	Yellow	The risk factors have Moderate influence to accelerate the onset of a failure mode in GIS
HIGH	Red	The risk factors have High influence to accelerate the onset of a failure mode in GIS

The following sub subsections explain the aggregating process to obtain sub-index of sub failure susceptibility indicators (sub-FSI_E, sub-FSI_{OM}, sub-FSI_{ID}) We apply the FSI analysis at the bay layer, an example is provided in section 4.7.

4.5.1 Sub FSI due to environmental indicators (Sub FSI_E)

There are 2 sub failure susceptibility indicators, namely pollutants-level (Sub FSI_{E1}) and lightning density (Sub FSI_{E2}).

4.5.1.1 Sub FSI due to pollutants (Sub FSI_{E1})

The failure susceptibility indicator due to pollutants is determined based on the GIS installation (indoor/ outdoor) and the pollutants level. The type of GIS' area defines the pollutants susceptibility indicator. Table 4.13 gives the Sub FSI_{E1} index.

Table 4.13 *Sub Failure Susceptibility Indicator due to pollutants*

GIS Installation	Location	FSI_{E1} index
OUTDOOR	Seashore	HIGH
	Industrial Area	HIGH
	Big Cities	HIGH
	City side	MODERATE
INDOOR	Seashore	MODERATE
	Industrial Area	MODERATE
	Big Cities	MODERATE
	City side	LOW

4.5.1.2 Sub FSI due to lightning stroke (Sub FSI_{E2})

The failure susceptibility indicator due to lightning stroke increases in GIS connected to an overhead line. The Sub FSI_{E2} is determined by the lightning density on the area and the condition status (i.e., readiness) of the surge arresters.

In this work, the lightning density has been grouped into three (i.e., High, Moderate, Low) based on the report of the PLN Research Institute [11]. The condition status of surge arrester has also been grouped into three (i.e., Good, Deteriorate, Bad) following the procedure provided in Appendix E. Table 4.14 gives the sub FSI_{E2} index.

Table 4.14 *Sub Failure Susceptibility Indicator due to lightning stroke*

Type of GIS Termination	Lightning Flash Density (strikes/ km^2/ year)		Surge Arrester Status	Sub FSI_{E2} index
None of GIS bays connected to an overhead line	All		-	LOW
At least one bay of GIS connected to an overhead line	> 30	HIGH	GOOD	MODERATE
		HIGH	DETERIORATE	HIGH
		HIGH	BAD	HIGH
	15 - 30	MODERATE	GOOD	MODERATE
		MODERATE	DETERIORATE	MODERATE
		MODERATE	BAD	HIGH
	≤ 15	LOW	GOOD	LOW
		LOW	DETERIORATE	MODERATE
		LOW	BAD	HIGH

4.5.2 Sub FSI due to operation and maintenance indicators (Sub FSI_{OM})

There are 3 sub failure susceptibility indicators regarding the operation and maintenance GIS, namely, the intensity of voltage transients due to switching (Sub FSI_{OM1}), service time (Sub FSI_{OM2}), maintenance history (Sub FSI_{OM3}).

4.5.2.1 Sub FSI due to voltage transients generated during interruption (Sub FSI_{OM1})

Formerly in subsection 2.3, GIS interruption statistics from the JABA Case Study has been presented. 2039 interruptions have been reported from 10 years of data records. A single interruption could generate a high-frequency voltage-transients over the insulation system that increases the likelihood of a breakdown. Therefore, the interruption density is also a failure susceptibility indicator. We classify this FSI into three as given in Table 4.15. The interval has been determined based on the statistics of interruptions from the JABA Case Study.

Table 4.15 *Sub Failure Susceptibility Indicator related to interruption density*

Average Interruption of a CB-bay per year	Sub FSI_{OM1} index
< 1.23	LOW
1.23 - 1.98	MODERATE
> 1.98	HIGH

4.5.2.2 Sub FSI related to service time of GIS (Sub FSI_{OM2})

The service time of GIS is counted from the beginning of the operation, but, when there is an overhaul (i.e., lifetime extension project), the service time is reset to zero. Currently, we use the B5 value from the statistical lifetime analysis in subsection 2.2 to develop the boundary of the status of the index, based on the discussion with our local maintenance experts. The boundary for the 500 kV GIS indoor follows the 150 kV GIS indoor. Table 4.16 classifies the Sub FSI_{OM2}.

Table 4.16 *Sub Failure Susceptibility Indicator related to GIS service time*

GIS Voltage Level & Installation	Service Time	Sub FSI_{OM2} index
GIS 150 kV INDOOR	> 25 years	HIGH
	15 – 25 years	MODERATE
	< 15 years	LOW
GIS 150 kV OUTDOOR	> 15 years	HIGH
	8 – 15 years	MODERATE
	< 8 years	LOW
GIS 500 kV INDOOR	> 25 years	HIGH
	15 – 25 years	MODERATE
	< 15 years	LOW
GIS 500 kV OUTDOOR	> 18 years	HIGH
	10 – 18 years	MODERATE
	< 10 years	LOW

4.5.2.3 Sub FSI related to the maintenance history (Sub FSI_{OM3})

The likelihood of failure is increased if there is a history of unsolved (corrective) maintenance in GIS, for example, the unsolved flaws in the hydraulic compression system although corrective action has been taken for several times. This sub FSI, however, increasing the only onset of specific failure mode related to the issue found during the maintenance. The classification of this sub FSI is provided in Table 4.17.

Table 4.17 *Sub Failure Susceptibility Indicator based on the maintenance history*

Any record of unsolved maintenance in GIS related to a specific failure mode?	Sub FSI_{OM3} index
YES	HIGH
NO	LOW

4.5.3 Sub FSI due to inherent/ design indicators (Sub FSI_{ID})

The inherent and design factors consist of three subfactors, i.e., O-ring design of the GIS enclosure (Sub FSI_{ID1}), availability of absorbent in GIS enclosures (Sub FSI_{ID2}), and GIS makes (Sub FSI_{ID3}).

4.5.3.1 Sub FSI related to the O-ring design of GIS (Sub FSI_{ID1})

Most of the GIS design uses two kinds of O-ring seals, as seen in Figure 4.10. The inner seal has a function to protect the gas from leaking, while the other one is to protect pollutants, including moisture, to passing through into GIS. However, GIS with a single O-ring design has been found in the case study, especially in GIS with the older design. GIS with such design is more prone to a gas leaking. Table 4.18 classifies the sub failure susceptibility indicators related to sealing design.

Table 4.18 *Sub Failure Susceptibility Indicator related to sealing design of GIS*

Number of O-ring	Sub FSI_{ID1} index
Single	HIGH
Double	LOW

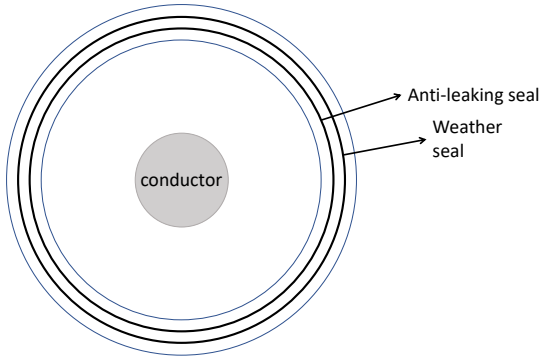

Figure 4.10 O-ring design of most common GIS. There are two seals layer in between two enclosures. The internal one is the anti-leaking seal, while the other one is the weather seal.

4.5.3.2 Sub FSI due to availability of absorbent in GIS (Sub FSI_{ID2})

As formerly discussed in subsection of 2.4.1, the humidity content in an enclosure of GIS will be high in the absence of absorbent. Therefore, the susceptibility factor to have condensation in such enclosure is also high. Table 4.19 classifies the sub failure susceptibility indicator due to the availability of absorbent in enclosures of a bay.

Table 4.19 *Sub Failure Susceptibility Indicator due to availability of absorbent*

All enclosures equipped with absorbent?	**Sub FSI_{ID2} index**
No	HIGH
Yes	LOW

4.5.3.3 Sub FSI related to GIS specific make/ manufacturer (Sub FSI_{ID3})

The JABA Case Study consists of GIS from 12 brands. Failure experiences in the case study have shown that several GIS-makes have lower performance than the others. It has been recorded that major failures in such GIS occurred in less than 5 years of service time. Table 4.20 classifies the sub failure susceptibility indicator related to GIS makes based on its experience to an infant failure. This sub FSI, however, relates only to the failure mode that correlated with the specific issue on GIS makes.

Table 4.20 *Sub Failure Susceptibility Indicator related to GIS makes*

Failure due to specific failure mode < 5 years?	**Sub FSI_{ID3} index**
Yes	HIGH
No	LOW

4.5.4 Relating Failure Susceptibility Indicators with Failure Modes in GIS

The HI model in this thesis focuses on six failure modes of GIS as formerly presented in Table 2.23 of Chapter 2. On the other hand, it should be noted that some Sub FSIs may increase the likelihood of the onset of all failure modes while some others impact only to a specific failure mode of GIS. Therefore, assessing the FSIs should be treated carefully so that the correlation between the AHI and FSIs becomes clear to the user.

An example is given as follows:

Given GIS-A with an AHI of 5 with the very high likelihood of failure at the secondary subsystem. The related failure mode is the "loss of electric connections in secondary." *In such a case, the onset of failure mode at the secondary S/S will not be affected by the fact that GIS-A has a single O-ring design (Sub FSI_{ID1}).*

In the current work, we decided not to process the sub FSIs further; as in making it into a single FSI-index; to give a comprehensive view to the user and to report the susceptibilities separately, as e.g., Table 4.21 gives the relation between the (sub) FSIs, failure modes, and affected subsystems In GIS.

Table 4.21 *Failure Susceptibility Indicators (FSI) in relation with related failure modes and affected subsystems in GIS*

FSIs	**Related Failure Mode**	**Affected Subsystem**
Sub FSI due to pollutants (Sub FSI_{E1})	All failure modes	All subsystems
Sub FSI due to lightning stroke (Sub FSI_{E2})	Dielectric breakdown	Dielectric S/S
Sub FSI related to Voltage transients generated during interruption (Sub FSI_{OM1})	1. Dielectric breakdown	1. Dielectric S/S
	2. Failing to perform requested operation	2. Driving mechanism S/S
	3. Loss of electrical connections integrity in secondary	3. Secondary S/S
Sub FSI related to GIS service time (Sub FSI_{OM2})	All failure modes	All subsystems
Sub FSI related to maintenance (Sub FSI_{OM3})	Specific failure mode related to the unsolved (corrective) maintenance	Depends on what failure mode
Sub FSI related to O-ring design (Sub FSI_{ID1})	Gas leaking	Construction and Support S/S
Sub FSI related to availability absorbent (Sub FSI_{ID2})	Dielectric breakdown (possibility to have condensation)	Dielectric S/S
Sub FSI related to GIS makes (Sub FSI_{ID3})	Specific failure mode related to GIS design	Depends on what failure mode

4.6 *Dealing with Data Uncertainty*

Data uncertainty could influence the confidence degree of the asset health index. This uncertainty might be due to different origins [18], namely, mistakes during data entry, uncertainty on the condition indicator (especially when it is a subjective measure), old data, and incomplete data (e.g., some condition indicators are missing). An extensive discussion about data uncertainty followed by examples on power transformer can be found in [18]. In this subsection, however, the discussion is limited only on a methodology to show data uncertainty in the health index due to missing condition indicators.

Data incompleteness is a common problem in the Asset Health Index assessment. For example, in the current model, it is possible that not all 24 condition indicators are

available for the AHI process. Several indicators may be difficult to find, due to reasons like:

1. No records in the past (e.g., the cumulative short circuit current of the main contacts of old GIS CB).
2. No facility to capture the condition indicators (e.g., no facility to measure the contact travel characteristic of old GIS CB).

Some approaches are available to solve the missing condition indicator, as follows:

1. By setting a default code for the missing condition indicator based on the expert judgment [18].

   This approach is the easiest one, but the judgment should be objective. A method like Delphi [63] can be an option to obtain a consensus.

2. By a transfer function [17,18]

   This approach includes the deduction of condition indicators based on the physical aspects. For example, if the information about the corrosion level is not available, then by default it can be deducted from details like distance from the sea, type of pollutants, indoor/ outdoor installation.

   As another example, this approach is applicable when the PD measurement is not possible. The data about SO_2 content (D2.2) and SF_6 by-products other than SO_2 (D2.3) are maybe sufficient to indicate the PD activity particularly in the non-switching GIS enclosure; although the exact location of PD source cannot be found.

   If the deduction is not possible, the statistical inference is used, for example, by using the statistical result from the sister components, or the mean value of the population. It is applicable, for example, in estimating the number short circuit interruption (P1.2) based on several observations.

However, these approaches lower the "confidence degree" of the health index. Therefore, it is necessary to inform the user whenever any approach is used. In this thesis, the "confidence degree" is stated by the percentage (%) of the condition indicators that is completed.

$$HI_{Confidence-degree} = \frac{n_{completed-data}}{n_{total\ condition\ parameter}} \qquad \dots 4.26$$

For example, if 20 out of 24 of condition indicators are available for the AHI process, then the confidence degree is 83%. The remaining 17% represents the missing condition indicators that are solved through the approaches above.

4.7 *Applying AHI to GIS example*

We test the AHI model, including the FSI, to the real operating GIS to ensure it is applicable and all aspects have been completed. To that purpose, a GIS from the JABA Case Study has been chosen. The example is a 150 kV indoor GIS, with eight bays consisting of 4 transmission feeders, 3 transformer feeders, and a bus coupler (see Figure 4.11). The service time of GIS is 23 years, and it has not been overhauled/ experienced any lifetime extension program. The data is from the company records from 2010 to 2016. The assessment was conducted in 2018.

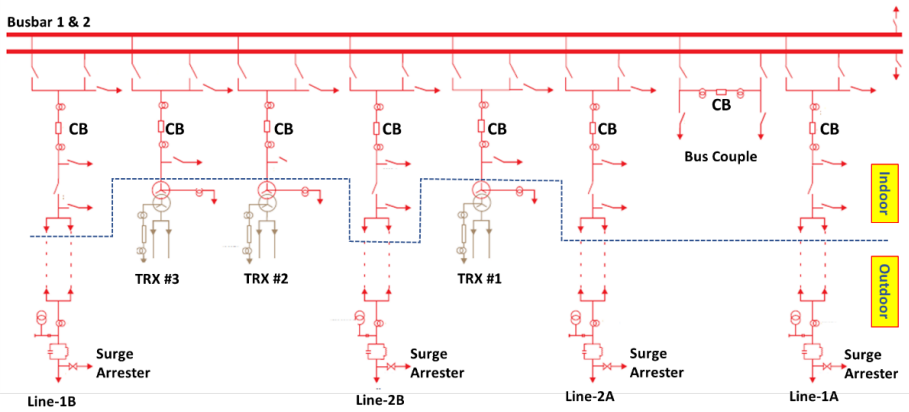

Figure 4.11 The single line diagram of the GIS example from the case study. The GIS consists of 8 bays: 4 transmission feeders, 3 transformer feeders, and 1 bus coupler. The surge arresters are located outdoor connected to an overhead line.

As a first step, the hierarchical configuration of GIS is being studied. In this example, the bays are grouped into three, namely: line-feeder, transformer-feeder, and bus-coupler. Each group contains part of busbars (see Figure 4.12).

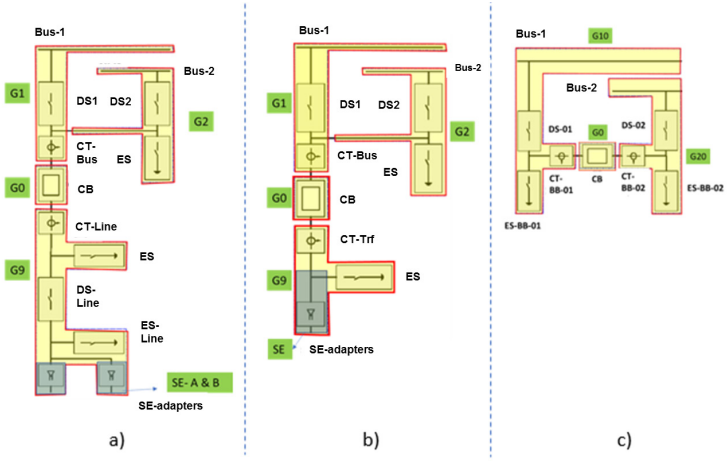

Figure 4.12 The configuration of enclosures in three types of bays in GIS example: a. the line feeder, b. the transformer feeder, and c. the bus-coupler. The busbars are segmented among these configurations.

According to Figure 4.12, the line and transformer-feeder have 5 enclosures in each bay, while the bus-coupler has 3 enclosures. All bays have switching components, so there will be 5 subsystems in each bay. The distribution of components in each enclosure is provided in Table 4.22.

Table 4.22 *Configuration of bays, enclosures, and components of GIS example*

Enclosure Configuration	Enclosure Code	Component
Line/ Transformer Feeder	G0	CB
	G1	BB-1 segment DS-bus1 CT-bus
	G2	BB-2 segment DS-bus2 ES-maintenance
	G9	DS-line ES-maintenance ES-line Sealing End
Bus Coupler	G0	CB
	G10	BB-1 segment DS-bus1 CT-bus ES-maintenance1
	G20	BB-2 segment DS-bus2 ES-maintenance2 CT-bus

4.7.1 Condition Indexing a GIS example

4.7.1.1 Condition Coding of Circuit Breaker

The condition coding starts from the circuit breaker. All CBs in the substation are contained in the enclosure of G0. Since G0 only has a CB inside, then the sub condition codes at the component-layer are similar as in the enclosure-layer. There will be 5 subsystems condition codes, namely, primary, dielectric, driving mechanism, secondary, and construction and support subsystems.

Some condition indicators are not available for the assessment. For example, the P1.1 and P1.2 are missing because there was no record from the site. As discussed in section 4.6, the missing data can be estimated from the other condition indicator that is indicating a similar failure mode. In this case, we use the deviation of static contact resistance (P2.1) as the value for the missing indicators.

The condition codes of all subsystems of CB in all bays of GIS example have been summarized in Tables 4.23 to 4.27. The estimated or default value of condition indicators is written in blue coloured. Only the worst score of the three phases is reported.

Table 4.23 *Condition Codes of Primary Subsystem of CBs in GIS example*

Code	Condition Indicator	Condition Code							
		Line1A	Line1B	Line2A	Line2B	Trx01	Trx02	Trx03	Bus Coupler
P1.1	Cumulative Short Circuit Current	30	30	1	1	1	10	1	1
P1.2	Number of Short Circuit Interruption	30	30	1	1	1	10	1	1
P2.1	Δ Static Contact Resistance Measurement (%)	11.9%	11.2%	-2.1%	-0.6%	4.6%	9.8%	-0.2%	-1.2%
	HI Score	30	30	1	1	1	10	1	1
P2.2	Hot Spot on the Enclosure	None	None	None	None	None	None	None	None
	HI Score	1	1	1	1	1	1	1	1

Table 4.24 *Condition Codes of Dielectric Subsystem of CBs in GIS example*

Code	Condition Indicator	Condition Code							
		Line1A	Line1B	Line2A	Line2B	Trx01	Trx02	Trx03	Bus Coupler
D1.1/ D1.2	Leakage Rate per year	< 0.5%	< 0.5%	< 0.5%	< 0.5%	< 0.5%	< 0.5%	< 0.5%	< 0.5%
	HI Score	1	1	1	1	1	1	1	1
D2.1	SF_6 Purity (%)	99.7%	99.5%	99.7%	99.9%	99.9%	99.9%	99.9%	99.9%
	HI Score	1	1	1	1	1	1	1	1
D2.2	SO_2 Content (in ppmV)	0	0	0	0	0	0	0	0
	HI Score	1	1	1	1	1	1	1	1
D2.3	SF_6 by products other than SO_2 Content	1	1	1	1	1	1	1	1
D2.4	PD Pattern & PD Growth	1	1	1	1	1	1	1	1
D2.5	Humidity content in SF_6 gas (ppmV)	223	363	152	198	162	211	284	102
	HI Score	10	**100**	10	10	10	10	30	1
D2.6	Dew point in SF_6 gas at gas pressure (°C)	-15.3	-9.7	-19	-16.7	-18.3	-15.5	-12.6	-23
	HI Score	10	**100**	10	10	10	10	30	1

Table 4.25 *Condition Codes of Driving Mechanism Subsystem of CBs in GIS example*

Code	Condition Indicator	Condition Code							
		Line1A	Line1B	Line2A	Line2B	Trx01	Trx02	Trx03	Bus Coupler
E1.1	% of Mech. limit	36%	37%	35%	33%	23%	24%	22%	23%
	HI Score	10	10	10	10	10	10	10	10
E1.2	Compressor tightness	N/A (non-compression type)							
E2.1	Δ Contact Timing	0.7%	1.7%	3.3%	5%	0.2%	2.1%	3.2%	2.1%
	HI Score	1	1	10	10	1	10	10	10
E2.2	Contact Travel Record	No Deviation	No Deviation	No Deviation	No Deviation	No Deviation	No Deviation	No Deviation	No Deviation
	HI Score	1	1	1	1	1	1	1	1
E2.3	(Electric Switches)	Not applicable for CB							

Table 4.26 *Condition Codes of Secondary Subsystem of CBs in GIS example*

Code	Condition Indicator	Condition Code							
		Line1A	Line1B	Line2A	Line2B	Trx01	Trx02	Trx03	Bus Coupler
S1.1	Corrosion Level of components in LCC	No Corr.	No Corr.	No Corr.	No Corr.	No Corr.	No Corr.	No Corr.	No Corr.
	HI Score	1	1	1	1	1	1	1	1
S1.2	Dust Level of components in LCC	Slight Dust	Slight Dust	Slight Dust	Slight Dust	Slight Dust	Slight Dust	Slight Dust	Slight Dust
	HI Score	3	3	3	3	3	3	3	3
S2.1	Hot Spot in Wiring in LCC	No Hot Spot	No Hot Spot	No Hot Spot	No Hot Spot	No Hot Spot	No Hot Spot	No Hot Spot	No Hot Spot
	HI Score	1	1	1	1	1	1	1	1
S2.2	LCC functions & Indicator	Func.: OK Ind. NOK	Func.: OK Ind. NOK	Func.: OK Ind. NOK	Func.: OK Ind. NOK	Func.: OK Ind. NOK	Func.: OK Ind. NOK	Func.: OK Ind. NOK	Func.: OK Ind. NOK
	HI Score	30	30	30	30	30	30	30	30

Table 4.27 *Condition Codes of Constr. & Support Subsystem of CBs in GIS example*

Code	Condition Indicator	Condition Code							
		Line1A	Line1B	Line2A	Line2B	Trx01	Trx02	Trx03	Bus Coupler
C1.1	Corrosion Level on Enclosures	No Corr.	No Corr.	No Corr.	No Corr.	No Corr.	No Corr.	No Corr.	No Corr.
	HI Score	1	1	1	1	1	1	1	1
C1.2	Deposited Pollutants on Enclosures	Clean	Clean	Clean	Clean	Clean	Clean	Clean	Clean
	HI Score	1	1	1	1	1	1	1	1
C1.3	Enclosures Foundation	No Crack	No Crack	No Crack	No Crack	No Crack	No Crack	No Crack	No Crack
	HI Score	1	1	1	1	1	1	1	1

Discussions on the results:

1. At the primary subsystem:
    a. Both information about the “cumulative short circuit current” and the “number of short circuit interruptions” are not available. One of the reasons is that the old relays were not equipped with a fault recorder. The historical data is not possible to show the short circuits information back to the beginning of the GIS operation. The value reported is deducted from the deviation of the static contact resistance measurement.
    b. The static contact resistance from the last two periodic measurements indicated the increasing contact resistance in the feeder of Line 1A and 1B (with a score of 30), and in transformer-02 (with a score of 10). It should be noted that the measurement also includes the resistance of main contacts of ESs of G2 and G9 (earthing switch for maintenance facility).
    c. No hot spot has been found in all CB enclosures.
2. At the dielectric subsystem:
    a. There are two condition indicators which are not available during the assessment, namely, 1. the gas analysis from the test with Gas Chromatograph Systems (GCMS), and 2. the PD Pattern and Growth. We decided to estimate the code for these missing indicators from a deducted from the code of SO_2 content (D2.2).
    b. Leakage has not been found in all CBs, and gas purity is also very good. No SO_2 has been found in all CBs.

c. High humidity content has been found in CB of Line 1B (Code of 100), followed by the humidity in CB of Transformer 03 Bay (Code of 30). The majority of Circuit Breakers has the humidity code of 10, except the bus-coupler with the code of 1. The scores indicate that most of Circuit Breakers have a considerable amount of humidity.

d. The analysis for dew point follows the humidity content

3. At the driving mechanism subsystem:

   a. According to the guide from the manufacturer, the mechanical limit of the driving mechanism cycle before the major inspection is 2500 times. In GIS example, the highest operational period is 37% of this threshold, i.e., on the CB of Line 1B. The other Circuit Breakers have been in operation from 22% to 36% of the limit. Consequently, all CB has a code of 10.

   b. The delta (Δ) contact timing is calculated from the difference between the measured Close or Open time, with the average value of the three phases. Only the worst value is reported in Table 4.25. The highest deviation is 5%, with the lowest at 0.2%. Therefore, the code is either 1 or 10.

   c. The contact travel test had shown no deviation.

4. At the secondary subsystem:

   a. In general, the secondary subsystem has no serious problem. All relays are still functioning, although slight dust has been observed in all Local Control Cubicle (LCC) of all bays.

   b. However, almost all lamp indicators on the LCC panels were damaged. The spare is not available in the market; therefore, a modification is suggested. Consequently, the health index score for condition indicator S2.2 is 30.

5. At the construction and support subsystem:

   a. The visual inspection of the enclosures found no corrosion. The GIS is indoor, and the personnel has regularly cleaned the enclosures.

   b. The foundation is still intact and in good condition.

The condition code of each subsystem follows the equations 4.4 to 4.6 and 4.13 to 4.18. Since G0 only contains a CB, the condition codes at the enclosure layer can be represented by the subcodes of subsystems. Table 4.28 provides the result.

Table 4.28 *Condition Codes of G0 (CB) enclosures from all bays in GIS example*

Subsystem	Condition Code							
	Line1A	Line1B	Line2A	Line2B	Trx01	Trx02	Trx03	Bus Coupler
Primary	30	30	1	1	1	10	1	1
Dielectric	10	**100**	10	10	10	10	30	1
Driving mechanism	10	10	10	10	10	10	10	10
Secondary	30	30	30	30	30	30	30	30
Construction & Support	1	1	1	1	1	1	1	1

4.7.1.2 Condition Coding for the other components in the other enclosures

We apply similar steps as in CB to the other components and enclosures. The summary of condition codes from each type enclosure is given in Tables 4.29 to 4.31. Details of the condition coding of each component are provided in Appendix F.

Table 4.29 *Condition Codes of G1/ G10 enclosures from all bays in GIS example*

Subsystem	Condition Code							
	Line1A	Line1B	Line2A	Line2B	Trx01	Trx02	Trx03	Bus Coupler
Primary	1	1	1	1	1	1	1	1
Dielectric	**100**	1	10	10	1	1	1	1
Driving mechanism	10	10	10	10	10	10	10	10
Secondary	30	30	30	30	30	30	30	30
Construction & Support	1	1	1	1	1	1	1	1

Table 4.30 *Condition Codes of G2/ G20 enclosures from all bays in GIS example*

Subsystem	Condition Code							
	Line1A	Line1B	Line2A	Line2B	Trx01	Trx02	Trx03	Bus Coupler
Primary	30	30	1	1	1	10	1	1
Dielectric	10	1	10	10	1	1	1	1
Driving mechanism	10	10	10	10	10	10	10	10
Secondary	30	30	30	30	30	30	30	30
Construction & Support	1	1	1	1	1	1	1	1

Table 4.31 *Condition Codes of G9 enclosures from all bays in GIS example*

Subsystem	Condition Code							
	Line1A	Line1B	Line2A	Line2B	Trx01	Trx02	Trx03	Bus Coupler
Primary	30	30	1	1	1	10	1	No enclosure G9
Dielectric	**100**	**100**	**100**	**100**	**100**	**100**	**100**	
Driving mechanism	10	10	10	10	10	10	10	
Secondary	30	30	30	30	30	30	30	
Construction & Support	1	1	1	1	1	1	1	

Discussions on the results:

1. The worst condition code, i.e., 100, has been contributed by the condition of the dielectric subsystem. G9 enclosure in all bays has condition code of 100, while in G1 enclosure has been reported in one bay (Line 1A). The following condition indicators have been reported:

   a. High humidity, within the range of 2500 – 5000 ppmV has been reported at the termination cone which is part of the G9 enclosure. The cause was probably related to the design, where there is no absorbent in such termination. The origin of humidity has been suspected to the absorbed moisture inside the semiconducting layering tapes.

   b. The SO_2 has been reported from all termination enclosures. The finding indicates the PD activity at the cable joint.

   c. The leakage rate above 7% has been found in G9 enclosure of Line 2B.

2. The condition codes of the driving mechanism-, secondary-, and construction and support subsystems are equally distributed among different enclosures of bays in GIS. This indicates these subsystems have similar condition status, among others.

3. Meanwhile, the condition code of the primary subsystem is varying among enclosure G9 and G2/ 20 of different bays. The highest code of 30 has been found in Line1A and Line1B. The value is representing the similar deterioration of main contacts of CB as formerly presented in Table 4.28.

4.7.1.3 Condition coding and condition indexing of bays

Condition code of a bay is determined by equation 4.24, and a bay index is generated following the classification in Table 4.11. The result for GIS example is given in Table 4.32 below.

Table 4.32 *Condition codes and Sub Health Index of bays in GIS example*

BAY	**Condition Code**	**Sub Health Index**
Line Feeder 1A	171	5
Line Feeder 1B	171	5
Line Feeder 2A	142	5
Line Feeder 2B	142	5
TRX-01	142	5
TRX-02	151	5
TRX-03	142	5
Bus Coupler	43	4

As seen from the table, except the bus coupler, the other bays have a condition index of 5, which means “Very Bad” – condition status. As formerly discussed, the reason for this status was the humid insulating gas and the possible PD activity in a specific enclosure of GIS sample (enclosure G9).

4.7.1.4 Condition indexing of GIS substation

Following a chain philosophy, the condition index of the GIS is **5 (7)**. The number within the bracket is indicating the number of bay with the worst index score at the same location. Following equation 4.26, the confidence degree of the index is **70%**.

4.7.2 Assessing Failure Susceptibility Indicators (FSIs)

Failure susceptibility indicators from each bay in GIS example are assessed following the discussions in sub section 4.5. The sub-AHI of GIS example shows that 7 bays are having an index of 5 which means “Very Bad” conditions. If we traced back the analysis, the condition status was mainly influenced by the status of the insulation system, due to either high humidity or the possible PD inside the G9 enclosure. Therefore, the FSIs assessment focuses on the factors that relate to a failure mode of dielectric breakdown.

Tables 4.33 to 4.35 provide the summaries of sub failure susceptibility indicators due to sequentially, environmental indicators (Sub FSI_E), operation and maintenance indicators (Sub FSI_{OM}), and inherent/ design indicators (Sub FSI_{ID}).

Table 4.33 *Sub FSI due to environmental indicators*

BAY	Sub FSI due to pollutants (Sub FSI_{E1})	Remarks On Sub FSI_{E1}	Sub FSI due to lightning stroke (Sub FSI_{E2})	Remarks On Sub FSI_{E2}
Line Feeder 1A	LOW	GIS is located indoor in a benign area	HIGH	High Lightning Flash density: up to 63-76 Strikes/km2 /year [11] Surge Arrester Condition: BAD (All have > 20 years' service time)
Line Feeder 1B	LOW		HIGH	
Line Feeder 2A	LOW		HIGH	
Line Feeder 2B	LOW		HIGH	
TRX-01	LOW		HIGH	
TRX-02	LOW		HIGH	
TRX-03	LOW		HIGH	
Bus Coupler	LOW		HIGH	

Table 4.34 *Sub FSI due to operation & maintenance indicators*

BAY	Sub FSI due to Voltage transients during switching (Sub FSI_{OM1})	Remarks On Sub FSI_{OM1}	Sub FSI due to service time (Sub FSI_{OM2})	Remarks On Sub FSI_{OM2}	Sub FSI due to maintenance (Sub FSI_{OM3})	Remarks On Sub FSI_{OM3}
Line Feeder 1A	LOW	Based on 10 years records. The avg. interruption per year of bays in GIS example: 1-1.6 times /year	MOD	23 years	LOW	No historical data of repetitive flaws/ defects/ corrective maintenance
Line Feeder 1B	MOD		MOD		LOW	
Line Feeder 2A	LOW		MOD		LOW	
Line Feeder 2B	MOD		MOD		LOW	
TRX-01	MOD		MOD		LOW	
TRX-02	LOW		MOD		LOW	
TRX-03	LOW		MOD		LOW	
Bus Coupler	LOW		MOD		LOW	

Table 4.35 *Sub FSI due to inherent/ design indicators*

BAY	FSI due to O-ring design (Sub FSI_{ID1})	Remarks On Sub FSI_{ID1}	FSI due to absorbent design (Sub FSI_{ID2})	Remarks On Sub FSI_{ID2}	FSI due to GIS makes (Sub FSI_{ID3})	Remarks On Sub FSI_{ID3}
Line Feeder 1A	LOW	This Sub FSI does not relate to FM of "insulation breakdown", given the secondary S/S working properly	LOW	All bays equipped w/ desiccants	LOW	No historical record related to infant failure due to insulation breakdown from this GIS makes
Line Feeder 1B	LOW		LOW		LOW	
Line Feeder 2A	LOW		LOW		LOW	
Line Feeder 2B	LOW		LOW		LOW	
TRX-01	LOW		LOW		LOW	
TRX-02	LOW		LOW		LOW	
TRX-03	LOW		LOW		LOW	
Bus Coupler	LOW		LOW		LOW	

Finally, all sub FSIs and sub HIs of GIS example are summarized in Table 4.36.

Table 4.36 *Comprehensive Failure Susceptibility Indicator index of GIS example*

BAY	Sub HI	Sub FSI_{E1}	Sub FSI_{E2}	Sub FSI_{OM1}	Sub FSI_{OM2}	Sub FSI_{OM3}	Sub FSI_{ID1}	Sub FSI_{ID2}	Sub FSI_{ID3}
Line Feeder 1A	5	LOW	HIGH	LOW	MOD	LOW	LOW	LOW	LOW
Line Feeder 1B	5	LOW	HIGH	MOD	MOD	LOW	LOW	LOW	LOW
Line Feeder 2A	5	LOW	HIGH	LOW	MOD	LOW	LOW	LOW	LOW
Line Feeder 2B	5	LOW	HIGH	MOD	MOD	LOW	LOW	LOW	LOW
TRX-01	5	LOW	HIGH	MOD	MOD	LOW	LOW	LOW	LOW
TRX-02	5	LOW	HIGH	LOW	MOD	LOW	LOW	LOW	LOW
TRX-03	5	LOW	HIGH	LOW	MOD	LOW	LOW	LOW	LOW
Bus Coupler	4	LOW	HIGH	LOW	MOD	LOW	LOW	LOW	LOW

Now, a complete result is given by providing the sub-HI and sub-FSIs in the same table. It can be seen that the GIS example owns 7 bays with sub-HI of 5 (i.e., "Very Bad" condition); moreover, there is a warning flag for every bay with "Red" colour indicating susceptibility due to lightning incidence. Another susceptibility indicator with a "moderate" level comes from the GIS' service time, given the fact that GIS has been in operation for 23 years. Susceptibility indicator due to voltage transients generated during interruption at "Moderate" level has been found in the following bays: Line Feeder 1B, 2B, and Transformer-1.

4.8 *Conclusion*

A health index model for GIS operating under the tropical conditions has been proposed in this chapter. The output of the model is an index of GIS representing its likelihood of failure due to possible failure modes in GIS. The model focuses on the six possible failure modes as has been reported in the CIGRE Technical Brochure 513 [3] and as found in the JABA Case Study. Critical points in the development of asset health index for GIS are as follows:

1. The objective of the model should be clear. Development of a health index can be related to support a specific maintenance action, like for replacement index, or refurbishment index. In this thesis, the purpose of the model is to give an index representing the condition status of an individual GIS and its likelihood to failure.
2. What makes a GIS different than the other HV components is it consists of "hierarchical-layers." A GIS can also be seen as a group of components contained in enclosures. Therefore, development of GIS HI should consider the layers within it. In this model, we divide a GIS into four layers based on their functionality, namely, 1. Component-, 2. Enclosure-, 3. Bay-, and 4. Substation-layer. The health indexing starts from the component-layer by assessing condition indicators of subsystems within it. In principle, the worst status of subsystems of all components in GIS defines the health index of GIS.
3. An FMEC-Analysis can be helpful during the selection of condition indicators used in the health index model. The condition indicators should reflect the failure modes of GIS and be captured by the inspections.
4. Developing norms for assessing the condition indicators can be through different approaches, as presented in section 4.3. Expert judgment in most of the time is needed, a methodology to avoid subjectivity is proposed.
5. The model should provide the transparency that the likelihood of failure (which indicated by the index) can be traced back into related failure mode, at related subsystems, by which related condition indicators.
6. A logarithmic scaling code has been used in the current model. The application of this approach in GIS example has proven that this approach allows the poor condition indicators to stand out (i.e., the humidity and SO_2 contents of GIS' termination); particularly in the assessment at the bay-layer. The similar scaling has also been used in [23].
7. The expectation to have an earlier on-set of failure modes can be identified by the failure susceptibility indicator (FSI). In the current work, the knowledge from failure experiences from the case study defines these indicators. It should be noted that sub-FSIs may only identify specific failure modes in GIS, carefully selection on these factors is necessary during FSI assessment to avoid misinterpretation of the result.
8. Health indexing is a data intensive activity. Therefore, data uncertainty is possible to occur that can reduce the degree of confidence of the HI result. In the current work, approaches are proposed to solve the missing data, namely, by expert judgment, and by a transfer function. The percentage (%) of confidence degree has been introduced to state the number of complete data used during the health indexing. The user should be informed about this %-of confidence degree.

Chapter 5 Risk Assessment Model for GIS Operating under Tropical Conditions

In Chapter 4, an Asset Health Index (AHI) model for GIS operating under the tropical conditions has been presented. The model gives an index representing condition status of a GIS as well as its likelihood of failure. Besides, the Failure Susceptibility Indicator (FSI), which are the indicators that identify expected earlier on-set of failure modes, have also been formulated.

Imagine if there are hundreds of GIS running in the grid, every single location will own a HI code along with its FSIs. Now, we can compare the likelihood of failure among GIS locations. However, it should be noted that the FSIs give only expectation, yet no evidence as in condition indicators. Therefore, we apply FSIs only as a "warning flag" in the current model.

Asset's condition status and a likelihood of failure are not the only parameters in management decisions, but also important to know the risk if an asset fails. In Asset Management, prioritising action among assets should be based on the asset's risk to the business.

This chapter provides a Risk Assessment Model for GIS operating under tropical conditions. The risk to be discussed is the risk of a GIS failure to the business.

The contents of this chapter would be as follows: Section 5.1 describes the risk assessment methodology. After that, section 5.2 discusses the likelihood of failure of GIS. Section 5.3 classifies consequences of GIS failure based on business values of a transmission utility from the JABA Case Study. Section 5.4 gives the risk acceptance matrix. Risk assessment on a GIS example is presented in section 5.5. Following to that, section 5.6 discusses a methodology to compare risk among GISs from different locations. Section 5.7 provides a conclusion.

5.1 *Risk Assessment Methodology*

Risk deals with uncertainty. It is defined as the product of a likelihood of an event and its consequences, as follows:

$$\text{Risk} = \text{Likelihood of an event} \times \text{Consequences} \quad \ldots 5.1$$

General guidelines for risk management, including the risk assessment techniques, have been provided in the ISO 31000 [65] and the ISO 31010 [66] standards. However, in practice, the risk activity is tailored among utilities [15,56,67-68]. The reason is that the

risk is subjective where the utilities are owing to their risk attitudes, approaches, business values, and data.

The risk assessment model discussed in this chapter is the risk of failure of a GIS operating under tropical conditions. The development of the model consists of three steps:

1. The determination of the likelihood of a GIS failure based on the AHI as provided in Chapter 4.
2. The determination of consequences based on the business values of the network utility.
3. The development of the risk acceptance matrix based on the likelihood and the consequences as defined above.

Since a remedial action on GIS mostly takes place at the bay layer, we start the calculation of risk at the GIS bay-layer. A bay with the worst risk determines the risk of GIS at substation-layer.

The model classifies the likelihood of failure of a bay in GIS based on the health index status. Meanwhile, the consequences used in the model are based on the consequence matrix of a transmission utility from the JABA Case Study. The matrix has seven consequences accordingly to the business values of the utility. Each consequence has 5 severity levels, namely, Low, Moderate, Serious, Severe, and Catastrophic. As a result, the output risk has also been classified into 5 levels, i.e., Very Low, Low, Moderate, High, and Very High.

5.2 *Estimating the Likelihood of Failure (LoF)*

The AHI model in Chapter 4 provides a health index at bay- and substation-layer of GIS. A linear scaling code provided the index from 1 to 5, which the higher the number means the worse GIS condition with the higher likelihood of failure.

In the Risk Assessment model, the likelihood of failure (LoF) is defined by the health index. In the current work, the likelihood of failure follows the classification as formerly provided in Table 4.5; i.e., Very low, Low, Moderate, High, and Very High. Table 5.1 provides the LoF classification with a similar interpretation as formerly provided in Table 4.5.

Table 5.1 *Classification of Likelihood of Failure (LoF) of GIS in the current model*

HI Code	LoF	Interpretation
1	Very Low (VL)	GIS can continue working properly.
2	Low (L)	GIS can continue working properly. It's running at normal deterioration/aging process.
3	Moderate (M)	GIS can continue working but remedial action is advised, otherwise it may contribute to GIS performance in longer term
4	High (H)	The GIS performance is possibly reduced in short-term.
5	Very High (VH)	GIS shutdown is required for further action to fix GIS performance.

5.3 *Classifying consequences*

A failure may impact not only on direct cost for corrective maintenance but also the other values in the business. Table 5.2 gives the business values used in the model. These are the same values as formerly presented in Tables 2.16 to 2.22 during FMEC- Analysis. Now, the severity level has been classified qualitatively, namely, Low, Moderate, Serious, Severe, and Catastrophic, based on the definition from the case study. The table also provides the rank of importance rank of each business value.

Developing a consequence-matrix requires people from a varied background within the utility in order to obtain objectivity.

Table 5.2 *The consequences matrix based on the business values of a network utility in the JABA Case Study [39]*

		Severity Level				
Importance Rank	Business Value	Catastrophic	Severe	Serious	Moderate	Low
1	Safety	Cause death (Fatality)	Cause permanent disability	Cause temporary disability	First aid injury, medical aid injury	Near miss
2	Extra Fuel Cost	> 750,000 USD	> 75,000 – 750,000 USD	> 7,500 – 75,000 USD	> 750 – 7500 USD	≤ 750 USD
3	Energy not Served	> 4000 MWh	> 400 – 4,000 MWh	> 40 – 400 MWh	> 4 – 40 MWh	≤ 4 MWh
4	Equipment Cost	> 2,000,000 USD	> 200,000 – 2,000,000 USD	> 20,000 – 200,000 USD	> 2,000 – 20,000 USD	≤ 2,000 USD
5	Customer Satisfaction	Very High Potential Riot	High Potential Riot	Moderate Potential Riot	Low Potential Riot	No Potential Riot
6	Leadership	Committed to law/ legal action. Becomes a national Issue.	Top management and government officials are involved	Other external bodies are involved	Handled by middle managerial level	Handled by local substation supervisor
7	Environment	Catastrophic contamination, National warning	Severe contamination, National/ Regional warning	High contamination, Regional/ local warning	Medium contamination, Local warning	Low contamination

5.4 *Risk Acceptance Matrix*

The risk acceptance matrix is made in two-dimensions of rows and columns, as shown in Table 5.3. The horizontal scale is the severity level of the consequence, while the vertical is the LoF. The risk has been classified into 5 levels, i.e., Catastrophic, Severe, Serious, Moderate, and Low. A limit that a company can accept the risk is known as the "risk acceptance." The acceptable limit of a company depends on the risk attitude, whether it is a risk-taker or a risk avoider. In the current work, the limit for risk is at a moderate level (as shown by the yellow dotted line in Table 5.3).

Table 5.3 *A risk acceptance matrix used in this thesis*

		Severity level of Consequence of each business value				
		LOW	*MOD*	*SERIOUS*	*SEVERE*	*CATASTHROPIC*
Likelihood of Failure (LoF)	*VERY HIGH*	MODERATE	HIGH	HIGH	VERY HIGH	VERY HIGH
	HIGH	LOW	MODERATE	HIGH	HIGH	VERY HIGH
	MOD	LOW	LOW	MODERATE	HIGH	HIGH
	LOW	VERY LOW	LOW	LOW	MODERATE	HIGH
	VERY LOW	VERY LOW	VERY LOW	LOW	LOW	MODERATE

5.5 *Applying the Risk Assessment model to GIS Example*

We apply the Risk Assessment model on the same GIS example as in Chapter 4.

5.5.1 Estimating the Likelihood of Failure (LoF) of GIS example

According to the health indexing process in GIS example in section 4.7, 7 out of 8 bays are having an index of 5. Following the definition in Table 5.1, the likelihood of failure of each bay in GIS is presented in Table 5.4.

Table 5.4 *Likelihood of Failure (LoF) of each bay in GIS example*

BAY	**Sub HI**	**LoF**
Line Feeder 1A	5	Very High
Line Feeder 1B	5	Very High
Line Feeder 2A	5	Very High
Line Feeder 2B	5	Very High
TRX-01	5	Very High
TRX-02	5	Very High
TRX-03	5	Very High
Bus Coupler	4	High

5.5.2 Assessing consequences

We use the following assumptions to estimate the consequences if GIS example fails:

1. The GIS failure mode is an insulation breakdown.
2. Breakdown in a bay will cause an outage of all feeders in GIS.
3. The equipment cost is defined as the cost to replace one bay of GIS.

5.5.2.1 Consequence on Safety

Safety is a priority. It ranks the first among business values. There were no recorded death casualties due to a GIS breakdown in the JABA Case Study. The worst reported case was fainted personnel because of lacking oxygen during a failure investigation. So far, no permanent disability has been reported. It is decided that a GIS breakdown can cause a “SERIOUS” safety consequence.

5.5.2.2 Consequence on Extra Fuel Cost

The extra fuel cost appears when a failure provokes a generation of electricity (i.e., to cover the outage) from a plant with a higher production cost. Like for a black-start operation with a diesel power plant.

In the current case, there is no extra fuel cost consequence (i.e., LOW level).

5.5.2.3 Consequence on Energy Not Served (ENS)

According to the contingency simulation, the outage can cost a total of 120 MW loss. However, load manoeuvre by dispatcher can save a third of this loss. Consequently, the load shedding will be 80 MW. By assuming the recovery time is an hour, the ENS will become 80 MWh, which is classified as a SERIOUS consequence.

5.5.2.4 Consequence on Equipment Cost

The equipment cost is determined by the cost to replace one GIS bay, which is an estimated $ 600,000. Therefore, the consequence of equipment cost is SEVERE.

5.5.2.5 Consequence on Customer Satisfaction

As provided in Table 5.2, the measure of customer satisfaction is by estimating a potential riot due to a failure. The VIP customer usually owns a backup system, so a likelihood of riot is low. On the other hand, a riot may occur if the outage spread out over a significant number of customers in extended hours, which is not the case in the failure of GIS example. It is decided the consequence of Customer Satisfaction is MODERATE.

5.5.2.6 Consequence on Leadership

The leadership value measures how well the management can control the business by ensuring the availability of electricity to the customers.

The GIS example is located in a big city, next to the arsenal owned by the military department. Experiences from former failures in GIS example has shown that external bodies, like from the police department, may involve the failure investigation. Therefore, the consequence of leadership is SERIOUS.

5.5.2.7 Consequence on Environment

As seen in Table 5.2, the environmental consequence is determined by two factors: 1. the penalty and warning from the authority and 2. the contamination level. It has been estimated that the cleaning due to failure may take 1-2 weeks. The local authority will also warn the company. Therefore, the environmental consequence is at a “MODERATE” level.

5.5.3 Summarizing the risk of GIS Example

Table 5.5 summarizes the consequences if a failure occurs in GIS example. The consequences range from LOW to SEVERE. By aggregating these consequences with the LoF, sub risks from each business value can be found in Table 5.6 and Figure 5.1.

Since the acceptance level of the company is at Moderate Risk, then only sub risk from “extra fuel cost” can be accepted. The other sub risks have High and Very High risk-level, which are beyond the criteria of the company. Risk treatment is required to reduce the risk into an acceptable limit of the company.

Table 5.5 *Summary of consequences if GIS example fails*

Business Value	Severity Level
Safety	SERIOUS
Extra Fuel Cost	LOW
ENS	SERIOUS
Equipment Cost	SEVERE
Customer Satisfaction	MODERATE
Leadership	SERIOUS
Environment	MODERATE

Table 5.6 *Risk Matrix of GIS Example*

		Severity level of Consequence of each business value				
		LOW	*MOD*	*SERIOUS*	*SEVERE*	*CATASTHROPIC*
Likelihood of Failure (LoF)	*VERY HIGH*	**MODERATE** *(Extra Fuel Cost)*	**HIGH** *(Customer Sat.) (Environment)*	**HIGH** *(ENS) (Leadership) (Safety)*	**VERY HIGH** *(Eq.Cost)*	**VERY HIGH**
	HIGH	**LOW**	**MODERATE**	**HIGH**	**HIGH**	**VERY HIGH**
	MOD	**LOW**	**LOW**	**MODERATE**	**HIGH**	**HIGH**
	LOW	**VERY LOW**	**LOW**	**LOW**	**MODERATE**	**HIGH**
	VERY LOW	**VERY LOW**	**VERY LOW**	**LOW**	**LOW**	**MODERATE**

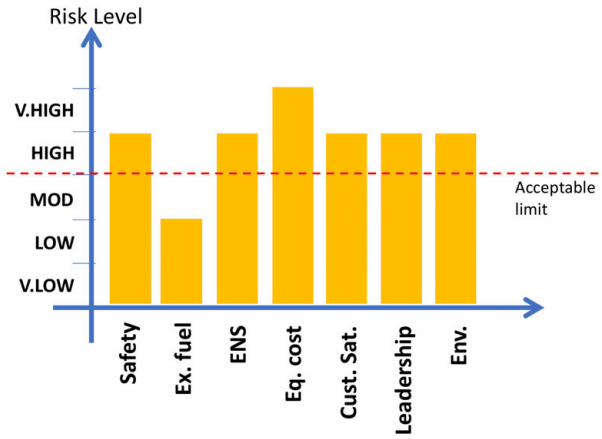

Figure 5.1 Risk level of sub risks from GIS example. The sub risks above the acceptable limit has been observed for business values of safety, ENS, equipment cost, leadership and environment. Risk treatment should be addressed on GIS to reduce sub risks to the acceptable limit.

5.6 *Risk comparison among GISs*

Risk of a GIS failure consists of sub-risks based on the business values of the company. A method to provide a single risk score/ index is needed to compare the risk among GISs, as follows:

1. In case that every business value is equally important to the company, the total risk of a GIS can be calculated by a summation of sub-risk codes, namely the Total Risk Code (TRC). In this approach, every sub-risk is coded by a linear scaling code

from 1 to 5 that sequentially represents the level of risk: Very Low, Low, Moderate, Serious, and Catastrophic. The TRC then follows,

$$TRC = R_1 + R_2 + \ldots + R_n \qquad \ldots 5.2$$

where,

TRC : Total Risk Code of a GIS
$R_1, R_2, \ldots, R_n$: Sub risk codes based on business values of the company

2. The other approach is by using the logic that the highest sub-risk code defines the total risk of a GIS (see equation *5.3*).

$$TRC = MAX (R_1, R_2, \ldots, R_n) \qquad \ldots 5.3$$

3. The second approach above can be combined by looking into the importance degree of business value in the company.

4. Another method is by assigning a weighting factor on each sub-risk code, as follows:

$$TRC = w_1.R_1 + w_2.R_2 + \ldots + w_n.R_n \qquad \ldots 5.4$$

$w_1, w_2, \ldots, w_n$ are the weighting factors for each sub risk code.

5. The other approach is by monetizing all sub risks. This approach requires a statistical (quantitative) probability of failure and a conversion of consequences into a term of money. However, assumptions are mostly used in monetizing intangible values, like, leadership or customer satisfaction, that ended with a doubtable result. This approach is not discussed in this thesis.

5.7 *Conclusion*

A risk assessment model for GIS operating under tropical conditions has been proposed in this chapter. Critical points during the development of the model are as follows:

1. Risk is defined as the product of a likelihood of a failure and its consequences to business values. In the current work, the health index defines the likelihood of failure. Since failure can be due to varying failure modes, it should be clear what failure mode is being investigated during the risk assessment process. The reason is that different failure modes contribute to the different severity level of consequences; which in the end gives different risk result.
2. Prioritizing action on GIS maintenance can be based on the risk. A method to aggregate sub risks into a single value/ index is required to compare risk among GISs from a different location.
3. Risk which is above the acceptable limit of the company should be mitigated, by a risk treatment procedure.

Chapter 6 Risk Treatment

In Chapter 5, a risk assessment model for GIS operating under tropical conditions has been proposed. When the risk is below the acceptable limit of the user, then “do nothing” or possibly “a run to fail” becomes a mitigating option. Otherwise, “do something” should be taken, which is part of a “risk treatment.”

This chapter proposes a method for a decision-making process by using a Multi-Criteria Analysis (MCA) to obtain an optimal mitigating action for GIS. It is assumed that the Time to Failure (TTF) is long enough so that all mitigating options presented in this chapter are possible.

Section 6.1 provides a risk treatment method, followed by a sensitivity analysis in section 6.2. An example of risk treatment on the GIS example is given in section 6.3. Section 6.4 provides a conclusion.

6.1 *Risk treatment method*

Risk treatment is a part of risk management, which involves selecting one or more options for modifying the risks and by implementing those options [65]. Risk treatment can be one or combinational of the following activities:

1. Avoiding the risk.
2. Taking the risk, or even increase the risk to pursue more opportunity.
3. Removing the risk source.
4. Adjusting the likelihood/ probability.
5. Controlling the consequences.
6. Risk sharing
7. Retaining risks by informed decision.

The appropriate action is decided based on the optimisation between benefits and costs. A subsequent risk, which is a new risk that is introduced from taking mitigating action, should be considered in planning a risk treatment.

This thesis proposes a method to select a risk treatment, which consists of three steps, as follows [69]:

1. Step-1: Define the problem or opportunity
   The first step includes:
   a. Evaluating mitigation options for the factors that contribute to the high risk.
   b. Make a shortlist of treatment options.
2. Step-2: Develop cost and benefit parameters
   In the second step, cost and benefit from each mitigation action should be defined either in financial terms (if possible) or using a scoring method (especially for intangible parameters).

3. Step-3: Determine the optimal solution
   In this step, a multi criteria-analysis is used to find the optimal solution. For the economic and financial factors, a Discounted Cash Flow (DCF) analysis is used in combination with the MCA [69].

The following subsections explain the steps above.

6.1.1 Step-1: Defining the problem or opportunity

In the first step, we need to find the problem that was causing the high-risk level (i.e., above the acceptable limit of the user), after that, the opportunity to lower the risk, i.e., by solving the problem, is formulated. A risk consists of likelihood and consequences; therefore, the opportunity is either by reducing one of these two parameters, or even both. The time-to-failure (TTF) of a failure mode, which is pinpointed by the AHI assessment (or any other RCA) should be longer than the time-to-finish the intended treatment indicated in Table 6.3 as assumed in the beginning of Chapter 6. To verify this, further investigation of the remaining lifetime for each relevant failure mode of GIS-components is necessary which is, however, beyond the scope of this work. An example of TTF verification for a GIS leakage rate is provided in [4].

Apart from the possible treatments, there can be a “deal-breaker.” It is a non-negotiable parameter which contradicts on explicitly stated potential objective [69]. A deal-breaker is usually not suitable for long-term implementation; it appears due to a specific reason, like policy or special events. An early screening on potential treatments is done by first assessing the options against the deal-breaker.

6.1.2 Step-2: Developing cost and benefit parameters

In the second step, parameters of cost and benefit from each possible risk treatment are defined. The costs and the direct financial net benefits, such as the cost to refurbish or to replace GIS, are stated in a financial term. There are two known methods to optimise between cost and benefit, namely, the benefit-cost analysis (BCA) and the multi-criteria analysis (MCA). The BCA is used for financial evaluation, which in most cases involves discounted cash flow (DCF) calculation to identify the net-present value (NPV) of future cost and benefit. Meanwhile, the MCA is used for the non-financial parameters.

In this thesis, we use MCA to optimise three parameters, namely, Cost, Residual risk, and Time-to-finish a treatment. A linear scoring code, i.e., from 1 to 5, is used to quantify the what-so-called “criterions” of benefit and cost. Table 6.1 to 6.3 classify criterions for each parameter used in the optimisation process. The ranges have been decided from discussions with an expert from the JABA Case Study.

Table 6.1 *Criteria of Cost (in NPV)*

Cost (PV)	Code for calculation
> 2,000,000 USD	5
> 200,000 – 2,000,000 USD	4
> 20,000 – 200,000 USD	3
> 2,000 – 20,000 USD	2
≤ 2,000 USD	1

Table 6.2 *Criteria of Residual Risk (after a treatment)*

Residual Risk	Code for calculation
Very High	5
High	4
Moderate	3
Low	2
Very Low	1

Table 6.3 *Criteria of Time-to-finish a treatment*

Time to finish a treatment	Code for calculation
> 12 months	5
> 6 – 12 months	4
> 1 – 6 months	3
> 1 week – 1 months	2
< 1 week	1

6.1.3 Step-3: Determining the optimal solution

In the third step, all possible scenarios for a risk treatment will be coded accordingly to the three criteria above. The cost streams over the lifecycle of the asset are firstly treated by the discounted cash flow (DCF) to obtain the NPV. Following this step, the NPV is classified into a code based on the value presented in Table 6.1. The code is then used for the MCA. In this thesis, an option for treatment will be selected if the residual sub-risk of each business value has a maximum level of "Moderate" (i.e., the acceptable limit of the company. We summarize the codes from the three criteria above. The minimum value defines the optimal solution, as follows:

$$\text{Optimal Solution} : f(\text{MIN}(C_{cost} + C_{residual\text{-}risk} + C_{time\text{-}to\text{-}finish})) \quad \ldots 6.1$$

Where,

C_{cost} : Code for Cost criterion
$C_{residual\text{-}risk}$: Code for Residual risk criterion
$C_{time\text{-}to\text{-}finish}$: Code for Time-to-finish criterion

6.2 *Sensitivity Analysis*

During the optimisation process, the cost and benefit may contain some degree of uncertainty. An approach to measuring the uncertainty is through a sensitivity analysis. The objective is to identify the factors that will have the most impact on the feasibility of a treatment option. Adjusting cost on several interest rates is commonly found. The other sensitivity checks are by increasing the investment costs or by decreasing the revenue, while keep evaluating the feasibility of the project. Further discussion about sensitivity analysis can be found in [69], and it is out of the scope of this thesis.

6.3 *Applying risk treatment procedure to GIS example*

The proposed risk treatment method is verified on a similar GIS example used in Chapter 4 and 5. The analysis is conducted at the GIS bay layer.

6.3.1 Step-1: Defining the Problem and Opportunity

As provided in Table 5.5, 6 sub risks are having a level higher than the acceptable limit of the company. The opportunities to reduce these sub risks are as follow:

1. Decreasing the likelihood of failure from “Very high” to “Low,” as this will bring to a maximum sub risk at a “Moderate” level. This can be obtained by improving the health index of the asset from “Very bad condition” (health index of 5) to at least a “Good condition” (health index of 2)
2. Decreasing the severity level of consequences to a “Low” level. Only the “extra fuel cost” that is already at a “Low” severity level.

Evaluating the likelihood of failure:

Except for the “extra fuel cost,” the other consequences have severity level at a minimum of “moderate.” The highest severity level is addressed to the “equipment cost,” followed by the “Energy Not Served,” “Leadership,” and “Safety.” The latest three are having a severity level of “Serious.” “Customer satisfaction” and “environmental” business values are having a “Moderate” severity level.

Question:

With the above descriptions, what are the possible treatment(s) to reduce the likelihood of failure?

Evaluating the consequences:

Except the “extra fuel cost”, the other consequences are having severity level at minimum of “moderate”. The highest severity level is addressed to the “equipment cost” followed by the “Energy Not Served”, “Leadership”, and “Safety”. The latest three are having severity level of “Serious”. “Customer satisfaction” and “environmental” business values are having “Moderate” severity level.

Question:

Except for the “extra fuel cost,” is there any possible treatment to reduce the impacts/ consequences to a “Low” level?

Defining possible risk treatments:

We define the possibilities for treatment are as follow:

1. Overhauling the GIS, with repair/ retrofitting the GIS termination.
2. Replace the surge arresters.
3. Combination of point 1 and 2.
4. Gas reclamation.
5. Gas replacement.

6. Replace the whole GIS (also the surge arresters),
7. Improving safety procedure (i.e., to reduce the impact on safety)

There is no “deal-breaker” in the scenario. First screening on options is by reviewing the likelihood of failure after the treatment:

1. Option-2 will reduce the Sub FSI_{E2} index from HIGH to MODERATE (see Table 4.14), but the health index (i.e., the likelihood of failure) is still at the scale of 5 (i.e., a Very High likelihood of failure). So option 2 should be removed from the list.
2. Options 4 and 5 will reduce the humidity in gas insulation. It will also remove the SO_2, but not the Partial Discharge (PD) at the terminations. If PD still occurs, the health index of GIS will not change. So these options should also be removed from the list.
3. Option-7 will reduce only the impact of Safety. This option will not further be analyzed by using MCA, but its implementation is suggested.

6.3.2 Step-2: Developing Cost and Benefit Parameter

Three indicators will be optimised; i.e., 1. Cost, 2. Residual risk, and 3. Time-to-finish the treatment. The criterions’ coding for each possible treatment and their summary are provided in Tables 6.4 to 6.7.

Table 6.4 Criteria *for Residual Sub-Risks after treatment*

Option	**Residual Risk (after treatment)**							**Maximum Residual Risk Code (after treatment)**
	Safety	Ex. Fuel Cost	ENS	Eq. Cost	Cust. Sat.	Lead	Env.	
Option-1: GIS Overhaul, *(LoF is reduced from 5 to 2, Sub FSI_{E2} is HIGH)*	2	1	2	3	2	2	2	3 (MODERATE)
Option-3: GIS Overhaul + Replace only SA *(LoF is reduced from 5 to 2, Sub FSI_{E2} is MODERATE)*	2	1	2	3	2	2	2	3 (MODERATE)
Option-6: Replace both GIS and SA *(LoF is reduced from 5 to 1, Sub FSI_{E2} is MODERATE)*	2	1	2	2	1	2	1	2 (LOW)

Table 6.5 Criteria *for Time-to-finish a treatment*

	Time-to-finish	Code
Option-1	5-6 months	3
Option-3	5-6 months	3
Option-6	> 12 months	5

The NPV calculation takes a period of 40 years with an interest rate of 11%. In all options, the overhaul is conducted after 25 years of service time. The surge arresters will be replaced after 15 years in service, while the GIS after 40 years of service time (except for Option-6 where the GIS is replaced at year 1). The Net Present Values (NPV) of all scenarios are presented in Table 6.6**,** following their criteria codes.

Table 6.6 *Criteria for Cost (in NPV)*

	Cost* (NPV in mill. USD)	Code
Option-1	3.42	5
Option-3	3.45	5
Option-6	6.30	5

**the analysis period is 40 years with an interest rate of 11%. Overhaul is done at GIS service time of 25 years. Surge arresters are replaced after 15 years.*

Table 6.7 *Summary of criterions from all parameters used for optimisation*

	Code for Residual-risk	Code for Time-to finish	Code for Cost	Total
Option-1	3	3	5	11
Option-3	3	3	5	11
Option-6	2	5	5	12

6.3.3 Step-3: Determining the Optimal Solution

Following equation 6.1, Option-1 and 3 give a similar final condition code. It can be seen that, although option-6 gives a better residual risk than the others, the time-to-finish is longer. Although the code for the cost is equally similar among the options, as seen in Table 6.6, the cost for Option-6 is almost twice than the others.

So now we must choose between Option-1 and 3. Their difference can be seen behind the optimisation codes. Option-3 requires cost 30,000 USD higher than Option-1. The additional cost is about 0.9% of the cost required for Option-1, but on the other hand, the sub FSI_{E2} can be reduced from “HIGH” to “MODERATE.” Since the lightning flash density in the area is High, option-3 is more suggested. Figure 6.1 shows the residual risk of GIS example after the treatment.

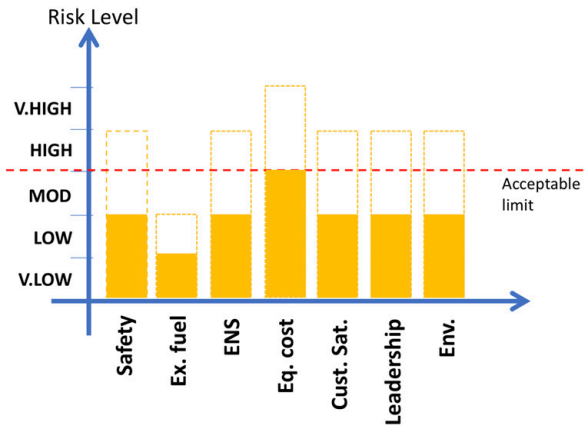

Figure 6.1 Risk level of sub risks from GIS example after the treatment option 3. Now, all sub risks are within the acceptable limit of the company.

6.3.4 Sensitivity Analysis

A sensitivity analysis has been conducted on PV (Present Value) Costs on Option-1 and 3 by adjusting the interest rate from 7 to 13 % and by makes triple the surge arrester cost. As a result, Option-3 is still higher than Option-1, where the additional cost for Option-3 increased to about 3% of Option-1. The sensitivity analysis shows how much the cost may deviate when sensible parameters are changing in the future. Further reading on sensitivity analysis can be found in [69].

6.4 *Conclusion*

An approach for risk treatment has been proposed in this chapter. The discussion has been limited to a risk of GIS failure. Fundamentally, the purpose of risk treatment is to select the optimal solution for mitigating the risk, so the residual risk is within the acceptable limit of the company.

The focus of a risk treatment can be on the likelihood of failure, the consequences, or both. An optimisation process in decision-making is necessary to obtain the optimal treatment. An example of this process by using a Multi-Criteria Analysis (MCA) has been demonstrated in this chapter. In the example, the best option for GIS treatment was decided by the optimal solution of three parameters, namely, 1. Cost, 2. Residual risk after treatment, and 3. Time-to-finish the treatment.

Chapter 7 Conclusions and Recommendations

Based on our findings in the preceding chapters we present our final conclusions in section 7.1. The last section 7.2 we give recommendations for future research and further technical improvement.

7.1 *Conclusions*

In this section we summarize our final conclusions restructured to the three research objectives of section 1.4. After citing the objective we summarize our conclusions accordingly.

Objective-1

To investigate the factors that influence the performance of GISs operating under tropical conditions, which include the internal and external factors that increase the likelihood of failure of a GIS.

1. Influence of the tropical conditions

1.1 The humid environment and the intense sunlight with the constant warm temperature over the year make the corrosion easier at the exposed parts of GIS. The most affected parts include 1. the enclosures and the interface between the enclosures, 2. the mechanical-coupling parts, 3. the energy storage parts, 4. the parts of the secondary subsystem, and 5. the gauge. The outdoor GIS is more suffering to corrosion than indoor GIS.

1.2 The corroded part becomes the path for moisture intrusion. At a later stage, the moisture can be involved in the oxidation between seals. Seals on the hydraulic and pneumatic compressors can be affected by this reaction.

1.3 Once the seal degrades, leakage occurs. The gas inside the GIS is much drier than the ambient air. Consequently, moisture may ingress inside the GIS because the partial water pressure at the outside of GIS is higher than that inside.

1.4 The desorption of moisture from spacer and metallic surfaces contribute even more to the humidity content of the insulating gas than the mechanism at point 3 according to our experimental investigation. The humidity content is characteristic among various enclosures in GIS from different manufacturers, which use desiccants. High humidity content was found in enclosures without desiccants.

1.5 The by-products resulting from the electrochemical reaction between the SF_6, the humidity, and the other GIS materials should be anticipated, as they are

corrosive. The deposited solid by-products on the spacer can reduce the breakdown strength.

1.6 In the tropics, the transients due to frequent lightning increase the GIS' susceptibility to a breakdown. Therefore, it is important to ensure the condition of surge arresters in a substation.

Objective-2

To investigate the condition indicators that constitute the health status of GIS. For the latter, an AHI model should be developed that is well-tuned with today's utility practice, which can categorise the actual health conditions of the components by identifying failure modes and by understanding their deteriorating effects and, finally, can generate an alarm when the expected time to failure falls short. The model has to be based on facts from practical failure experience in the so-called JABA case study and based on an experiment to validate such practical observations.

2 AHI Model

An AHI model of a whole GIS is defined by the health status the subsystems. Condition indicators and norms to assess the status of each subsystem were defined based on practical experience and supported by laboratory tests. In the same order we list below our conclusions on AHI methodology (2.1), condition indicators (2.2), and laboratory testing (2.3):

2.1 AHI methodology

2.1.1 Critical in the development of asset health indexing for GIS is that the objective of the model should be clear, i.e. that the complexity of the model is not more worth than the purpose of the model itself.

2.1.2 What makes a GIS different than the other HV components is that it consists of "hierarchical-layers." A GIS can also be seen as a group of components contained in enclosures. Therefore, development of GIS HI should consider the layers within it.

2.1.3 An FMEC-Analysis can be helpful during the selection of condition indicators used in the health index model. The condition indicators should reflect the failure modes of GIS and can be captured by the inspections.

2.1.4 Developing norms for assessing the condition indicators can be through different approaches, as presented in section 4.3. Expert judgment in most of the time is needed, a way to avoid subjectivity is proposed.

2.1.5 The model should provide the transparency that the likelihood of failure (which indicated by the index) can be traced back into related failure mode, at related subsystems, by which related condition indicators.

2.1.6 A logarithmic scaling code allows the poor condition indicators to stand out, as has been demonstrated in the health-indexing of the bay of GIS in this thesis.

2.1.7 The expectation to have an earlier onset of failure modes can be identified by the failure susceptibility indicator (FSI). The knowledge from failure experiences can be used to determine the indicators. It should be noted that sub-FSIs may only identify specific failure modes in GIS, carefully selection on these factors is necessary during FSI assessment to avoid misinterpretation of the result.

2.1.8 The FSI only gives an expectation that an earlier onset of a failure mode might occur, but, without evidence (from the inspections). Therefore FSI should be separated from the AHI, as well as from the likelihood of failure.

2.1.9 Data uncertainty is possible to occur during the HI assessment that can reduce the degree of confidence of the HI result. The decision-maker should be informed about the confidence degree of the HI result.

2.2 Condition Indicators

2.2.1 The humidity content in GIS should be kept sufficiently low to avoid condensation in GIS.

2.2.2 Monitoring of the insulation system of a GIS is important. Partial Discharge (PD) monitoring can detect the degradation of the insulation system. Practically, a PD can grow, being constant, or even disappear; therefore, despite the PD pattern, the PD growth is also necessary to be monitored.

2.2.3 When PD measurement is not possible, the gas chromatograph analysis is suggested. Norm to justify the limit of by-products content needs to be developed.

2.2.4 The condition of the driving mechanism subsystems is also critical to be monitored, including the main contacts. It can be done by the diagnostic measurement and monitoring the contact timing and the contact travel record.

2.2.5 The other critical subsystem is the primary conductor (including jointing between GIS conductor). The monitoring on this subsystem includes the contact resistance, the hot spot, the PD monitoring, and the gas chromatograph analysis as well.

2.2.6 The statistics indicated that the secondary wirings and auxiliary relays contributed to the unexpected interruption. A failure-finding task is suggested to avoid this kind of failure.

2.3 Laboratory Testing

2.3.1 The humidity does not influence the flashover voltage of a spacer if there is no condensation. The finding is similar to our investigation with the SF6 gas-gap model.

2.3.2 In the experiments under AC and LI+ with quasi-homogeneous setup, it has been observed that the condensation drops the flashover voltage by 14%- 38% from its original value at a dry condition with 2 – 2.6 bars of gas pressure. Under LI+, we observed that the reduction of flashover voltage due to condensation is more significant than the influence of a 2 mm particle-attached on the epoxy sample.

2.3.3 From our tests, the significant parameters that contribute to the reduction of spacer flashover voltage are, from the highest to the lowest: 1. Distortion on the surface of the spacer (due to particle, condensation, accumulated solid by-products), 2. Gas pressure, 3. Humidity content.

Objective-3

After knowing the health index of a GIS, another decision support tool is needed to assess the risk of failure among GIS. For this, an RA method should be proposed for prioritising the maintenance decisions. When several GIS locations have a risk above the acceptance level of the company, a method to mitigate the risk should be provided.

3 RA model

3.1 Risk is defined as the product of a likelihood of a failure and its consequences to business values. Since failure can occur due to varying failure modes, it should be made clear what failure mode is being investigated during the RA process. The reason is that different failure modes contribute to the different severity levels of consequences which, in the end, give different risk results.

3.2 Prioritising the action on GIS maintenance can be based on the risk. A method to aggregate sub risks into a single value/index is required to compare the risk among GISs from different locations.

3.3 A risk that is above the acceptable limit of the company should be mitigated by a risk treatment procedure, as discussed in Chapter 6.

7.2 *Multiple recommendations for future research*

Since some related issues were beyond the scope of our research, we have the following research-oriented recommendations for further investigations in this field:

1. The spacer-and-gas model used in this research only has two controlled parameters: gas pressure and humidity content. Future research can add temperature as another controlled parameter.
2. Further development on norms and knowledge rules, provided that these are based on empirical findings are necessary to replace potentially subjective expert judgement.
3. Further research to combine different diagnostics for indicating a failure mode is advised, for example, PD monitoring with gas analysis.
4. The risk mitigation process and the subsequent risk-based decision can be improved by further research of the time-to-failure (TTF) of GIS components for various failure modes.

Technical recommendations can be found in Appendix G.

References

[1] IEC-Market Strategy Board, "Strategic Asset Management of Power Networks-White Paper," 2015.
[2] BSI Standards Publication, "BS ISO-55000 Series Standard: Asset Management," 2014.
[3] CIGRE TB 513, "Final Report of the 2004-2007, International Enquiry on Reliability of High Voltage Equipment, Part 5: Gas Insulated Switchgear (GIS)," WG A3.06, Paris, 2012.
[4] M.A.G. Al-Suhaily, "Health Indexing for High Voltage Gas-Insulated Switchgear (HVAC GIS)," PhD Thesis, TU Delft, 2018.
[5] CIGRE TB 381, "GIS State of the Art 2008," WG B3.17, Paris, June 2009.
[6] CIGRE Green Books-Substations, SC B3, Springer, Paris, 2018.
[7] WW Travel Organisation, URL: http:// weather-and-climate.com/, last accessed April, 2016.
[8] R. Zoro, R. Mefiardhi, R.R. Aritonang, H. Suhana, "Observation on Improved 20 kV's Overhead Distribution Lines Against Lightning", STEI ITB & PLN Indonesia, 2006.
[9] NASA MSFC, URL: https://lightning.nsstc. nasa.gov, last accessed April, 2016.
[10] An estimation from D.R. Poelman, W.Schulz, G.Diendorfer, M.Bernardi, "European cloud-to-ground lightning characteristics", ICLP, Shanghai, China, 2014.
[11] PLN Research Institute, "Data Petir PLN – Jawa, Madura, Bali, Lampung, Sumatera Selatan, Jambi, Bengkulu, Sumatera Barat, Riau, Bangka Belitung," 2nd edition 2018.
[12] BPLHD DKI Jakarta, URL: http://llhd.jakarta.go. id, Jul - Nov 2016, last accessed April 2017.
[13] Ministerie van Infrastructuur en Milieu, URL: https://www.luchtmeetnet.nl/, Average of 1 year in 2015, last accessed April 12, 2016.
[14] R.P.Y. Mehairjan, "Risk Based Maintenance in Electricity Network Organizations," PhD Thesis, TU Delft, 2016.
[15] CIGRE TB422, "Transmission Asset Risk Management," WG C1.16, Paris, August 2010.
[16] J.H. Jurgensen, A.S. Godin, P. Hilber, "Health Index as condition estimator for power system equipment: a critical discussion and case study," IET Journals, CIRED, 2017.
[17] M. Vermeer, J. Wetzer, "Transformer health and risk indexing, including data quality management," CIGRE session, Paris, 2014.
[18] CIGRE TB 761, "Condition Assessment of Power Transformers," WG A2.49, Paris, March 2019.
[19] Y. Tsimberg et. al., "Determining Transmission Line Conductor Condition and Remaining Life," IEEE PES T&D Conference and Exposition, 2014.
[20] A. N. Jahromi et. al., "An Approach to Power Transformer Asset Management Using Health Index," IEEE Electrical Insulation Magazine Vol. 25, 2009.
[21] M. Al-Suhaily et. al., "Indexing the actual condition of GIS at the component level, bay level, and the GIS level," International Conference on High Voltage Engineering and Application, 2012.
[22] A. McGrail, M. Lawrence, G.M. Kennedy, D. Angell, R. Heywood, "Clarifying the link between data, diagnosis and Asset Health Indices," ISH 19th, Czech Republic, 2015.
[23] CIGRE TB Draft, "Asset Health Indices for Equipment in Existing Substations," WG B3.48, to be published CIGRE Paris 2020.
[24] IEC 62271-1 Ed. 1.0, "High-Voltage Switchgear and Control gear – Part 1: Common Specifications", 2007.

[25] IEC 60050-192, “International electrotechnical vocabulary – Part 192: Dependability”, 2015.
[26] A. Pharmatrisanti, “Long Term Performance of Gas Insulated Switchgear Operating Under Tropical Conditions”, PhD Thesis, TU Delft, the Netherlands, June 2012.
[27] R. A. Jongen, “Statistical Lifetime Management for Energy Network Components,” PhD Thesis, TU Delft, the Netherlands, 2012.
[28] G. Balzer, C. Schorn, “Asset Management for Infrastructure Systems,” Springer, 2015.
[29] K.B. Klaassen, J.C.L. van Peppen, “System Reliability – Concepts and applications,” VSSD, the Netherlands, 2006.
[30] CIGRE TB 176, “Ageing of the System, Impact on Planning,” WG 37.27, Paris, December 2000.
[31] IEEE C37.122.5, “IEEE Guide for Moisture Measurement and Control in SF_6 Gas-Insulated Equipment”, 2013.
[32] CIGRE TB 567, “SF_6 Analysis for AIS, GIS and MTS Condition Assessment”, Paris, February 2014.
[33] CIGRE TB723, “SF_6 Measurement Guide,” WG B3.40, Paris, April 2018.
[34] CIGRE TB 234, “SF_6 Recycling Guide, Revision 2003”, Paris, August 2003.
[35] IEEE Std C37.122-2010, “IEEE Standard for High Voltage Gas-Insulated Substations Rated Above 52 kV,” January 2011
[36] L.Cao et. al., “Accelerated Electrical Ageing of Medium Voltage EPR Cables Energized by Elevated AC Voltage with Switching Impulses Superimposed”, Mississippi State University, USA, 2013.
[37] J. Moubray, “Reliability-Centered Maintenance,” Industrial Press, 1991.
[38] IEC 60812:2006, “Analysis techniques for system reliability – Procedure for failure mode and effects analysis (FMEA)”, 2006.
[39] AM Platform, PLN TJBB, TJBT, TJBTB, “Risk Matrix,” 2017.
[40] A.P. Purnomoadi, “Insulation Performance of GIS Operating under Tropical Conditions,” ISH 20th, Argentina, 2017.
[41] T. Nitta, Y. Shibuya, Y. Fujiwara, Y. Arahata, H. Takahashi and H. Kuwahara, “Factors controlling surface flashover in SF_6 gas insulated systems,” IEEE Transactions on Power Apparatus and Systems, Vol. PAS-97, No. 3, pp. 959-965, 1978.
[42] F. Y. Chu, et al., “A new approach to moisture measurement and control in Gas Insulated Switchgear”, Proceedings of the Canadian Electrical Association, Engineering & Operating Division Meeting, Spring, 1986.
[43] D. H. Peng, Z. Y. Li and J, M. K. Mac Alpine, The Combined Effect of Moisture, Temperature and Conducting Particles on the Discharge Behaviour of Sulphur Hexafluoride, 1999 Conference on Electrical Insulation and Dielectric Phenomena.
[44] M.S. Naidu, “Gas Insulated Substations,” I.K. International Publishing, India, 2008.
[45] L.M. Branscomb and S.J. Smith, "Electron Affinity of Atomic Oxygen," Physical Review," Vol. 98, No. 4, 1955.
[46] N. H. Malik et. al., “Electrical Insulation in Power Systems,” Taylor and Francis Group, USA, 1998.
[47] A. Pharmatrisanti, S. Meijer, “VHF/UHF PD Detection on Aged GIS”, 13th International Symposium on High Voltage Engineering, the Netherlands, pp. 312, 2003.
[48] A.P. Purnomoadi, “Investigation on Free Moving Particles on the Breakdown Voltage in Gas Insulated Switchgears (GIS) under Different Electrical Stresses,” Master Thesis, TU Delft, June 2012.
[49] IEC 60060-1, “High-Voltage Test Techniques – Part 1: General definitions and test requirements”, Edition-3, 2010.

[50] F. H. Kreuger, “Industrial High Voltage, Part-01”, Delft University Press, the Netherlands, 1991
[51] V.Y. Ushakov, “Insulation of High Voltage Equipment,” Springer, 2004
[52] BSI Standards Publication, “BS ISO-55000 Series Standard: Asset Management,” 2014.
[53] T. Hjartarson et. al., “Development of Health Indices for Asset Condition Assessment”, IEEE PES Transmission and Distribution Conference and Exposition, 2003.
[54] B. Quak, “Information Strategy for Decision Support in Maintaining High Voltage Infrastructure”, PhD Thesis, TU Delft, the Netherlands, 2007.
[55] CIGRE TB 499, “Residual Life Concepts Applied to HV GIS,” WG B3.17, Paris, June 2012.
[56] CIGRE TB597, “Transmission Asset Risk Management – Progress in Application,” WG C1.25, Paris, 2014.
[57] M.Mattoso et. al., “Accelerated Aging of SO_2 Switchgear Seals,” DEIS Feature Article, Vol. 32, 2016.
[58] Manual Book, Alstom B95, 1990.
[59] Manual Book, Hitachi CFPT series, 1990.
[60] Manual Book, Siemens 8DQ1, 1991.
[61] Manual Book, EHH TRISEP, 1997.
[62] H. KOCH, “GIS Gas Insulated Substations, “IEEE Press, Wiley, 2014.
[63] H.A. Linstone, M. Turoff, “The Delphi Method: techniques and applications,” 1975.
[64] APP Surabaya, PLN, “Pre-Assessment Report of GIS Waru 150kV Recondition”, 2015.
[65] ISO 31000:2009, “Risk Management – Principles and Guidelines,” 2009.
[66] ISO 31010:2009, “Risk Management - Risk Assessment Techniques,” 2009.
[67] CIGRE TB 541, “Asset Management Decision Making using Different Risk Assessment Methodologies,” WG C1.25, Paris, June 2013.
[68] CIGRE TB309, “Asset Management of Transmission Systems and Associated CIGRE Activities,” WG C1.1, Paris, December 2006.
[69] New Zealand Asset Management Support (NAMS), “Optimized Decision Making Guidelines – A Sustainable Approach to managing infrastructure,” New Zealand, 2004.
[70] A.P. Purnomoadi, “Study on the Resistive Leakage Current Monitoring of Metal Oxide Surge Arresters”, ACED XIV, Bandung, 2008.

List of Abbreviations and Symbols

Abbreviations

AC	:	Alternating Current
AHI	:	Asset Health Index(ing)
AM	:	Asset Management
BCA	:	Benefit Cost Analysis
BS	:	Busbar Segment
CB	:	Circuit Breaker (of GIS)
CDF	:	Cumulative Distribution Functions
CIGRE	:	*Conseil International des Grands Reseaux Electriques* (International Council on Large Electric Systems)
CT	:	Current Transformer
DCF	:	Discounted Cash Flow
DE	:	Disconnector/ Earthing Switches
DM	:	Diagnostic test and measurements
DS	:	Disconnector Switch
ENS	:	Energy Not Served
ES	:	Earthing Switch (of GIS)
FMECA	:	Failure Mode Effect and Criticality Analysis
FSI	:	Failure Susceptibility Indicator
GCMS	:	Gas Chromatography and Mass Spectrometer
GI	:	General Instruments (of GIS)
GIL	:	Gas-Insulated Line
GIS	:	Gas Insulated Switchgear
GWP	:	Global Warming Potential
HI	:	Health Index
HSDS	:	High-Speed Disconnector Switch
HV	:	High Voltage
IEC	:	International Electrotechnical Commission

IEEE	:	Institute of Electrical and Electronics Engineers
ISO	:	International Organization for Standardization
IT	:	Instrument Transformer (of GIS)
JABA case study	:	Jawa Bali Case Study
KPI	:	Key Performance Indicator (of the company)
LCC	:	Local Control Cubicle
LoF	:	Likelihood of Failure (of an individual asset)
LI	:	Lightning Impulse
MCA	:	Multi-criteria Analysis
MV	:	Medium Voltage
NPV	:	Net Present Value
OEM	:	Original Equipment Manufacturer
PD	:	Partial discharges
PLN	:	Perusahaan Listrik Negara
PM10	:	Particulate Matter with diameter 10 micro meters or less
ppmV	:	parts per million by Volume (of humid SF_6)
RCA	:	Root Cause Analysis
RVI	:	Routine Visual Inspections
SA	:	Surge Arrester
SCADA	:	Supervisory Control and Data Acquisition
SI	:	Switching Impulse
TE	:	Terminations
TRC	:	Total Risk Code
TRI	:	Thorough Inspections
TTF	:	Time to Failure
VFTO	:	Very Fast Transient Overvoltage
VHF/UHF	:	Very High Frequency/ Ultra High Frequency (of PD sensor)
VT	:	Voltage Transformer
XLPE	:	Cross-linked polyethylene

Symbols

bar_a	:	Gas pressure in bar absolute
C_d	:	Discharge capacitance (of circuit for impulse testing)
C_h	:	Correction factor for maximum humidity content defined from the Magnus Formula, dimensionless
$CC_{bay\text{-}5'}$	:	New condition code of a bay as normalised to 5 subsystems code
$CC_{bay\text{-}3}$	:	Condition code of a bay with 3 subsystems
Sub FSI_E	:	Sub Failure Susceptibility Indicator related to environment
Sub FSI_{OM}	:	Sub Failure Susceptibility Indicator related to operation and maintenance
Sub FSI_{ID}	:	Sub Failure Susceptibility Indicator related to inherent/ design
ΔR_1	:	Deviation value of maintenance contacts after 2 sequential measurements (in %)
ΔR_2	:	Deviation value between the measured resistance contacts value with the other sister components (in %)
$\lvert\Delta I_{motor}\rvert$	:	Absolute value of deviation of motor current of motor of disconnector switch in GIS
ΔP	:	Leakage rate per year (in % per year)
$\lvert\Delta t_{contact}\rvert$	:	Deviation of time contact of Circuit Breaker in GIS
Δt	:	Time between two respective measurements of gas filling in days (i.e. time between P_1 and P_2).
e	:	Water partial pressure (in Pascals)
e_{max}	:	Maximum water vapor partial pressure to have condensation at the ambient temperature (in Pascals, Pa)
E_{max}	:	Maximum electric field at the surface of spacer/ sample (kV/mm)
E_{avg}	:	Average electric field at the surface of spacer/ sample (kV/mm)
ε_r	:	Relative dielectric permittivity, dimensionless
FO	:	Flashover Voltage (kV)
$FO_{at\ higher\text{-}content}$	:	Flashover Voltage in test with humidity content above the reference value (kV)
$FO_{at\ reference}$	:	Flashover Voltage in test with humidity content at the reference value (kV)

$HI_{confidence-degree}$	:	Confidence degree of Health Index based on completed data (in%)
I_{CUM-SC}	:	Cumulative short circuit current square (of Circuit Breaker)
LI +	:	Lightning Impulse with positive polarity
LI -	:	Lightning Impulse with negative polarity
N_{SC}	:	Number of short circuit interruption
N_{CB}	:	Number (counter) of mechanical works of the driving mechanism
p	:	Gas pressure (in bar absolute or Pascals)
P_1	:	SF_6 gas pressure from the last measurement (in bar)
P_2	:	SF_6 gas pressure from the current measurement (in bar)
P_{at20^oC}	:	Gas pressure at 20°C (in bar)
$P_{measured}$	:	Gas pressure at t°C (in bar)
$ppmV_{max}$	:	Humidity content in SF_6 to obtain condensation at the ambient temperature. The “max” terminology is used to define the allowable humidity content in GIS (ppmV)
$ppmV_{max-operation}$	:	Humidity content maximum in SF_6 during operation of GIS (in ppmV)
p.u.	:	per unit
R_f	:	Front resistance which determines the front time (of impulse circuit)
R_t	:	Tail resistance which determines the time to half-value (of impulse circuit)
R_{in}	:	Initial resistance of main contacts (of CB, from commissioning), in Ohms
R_{man}	:	Resistance of main contacts as recommended by the manufacturer (of CB), in %, in Ohms
$R_{st-contact}$	:	Static contact resistance, in Ohms
SpO_2 index	:	Index indicating how well a patient is breathing and how well blood is being transported throughout the body.
t	:	Temperature of gas at measurement (in °C)
t_{cf}	:	Time correction factor
T_a	:	Ambient temperature (in °C)
T_d	:	Dew point temperature (in °C)
Tan δ	:	The tangent of the loss angle, an indication for the dielectric losses (in %)

Definitions

Ageing

Aging is an intrinsic physical or chemical phenomenon that involves irreversible changes in characteristics of the materials with time, in some circumstances in interaction with its environment [25].

Asset Health Index (AHI)

An index that is representing condition status of an asset, as a whole. The index also gives an indication a likelihood of failure of an asset. Index can be a numeric number, qualitative status, etc. [23].

Condition Indicator (CI)

Indicator of life condition of an individual asset related to failure mode(s). Condition Indicator can be a result from measurement, or visual inspection, or diagnostic tests, or combination of inspections; of subsystems within an asset.

Condition Code (CC)

Code, usually represented by a member of series of number, that translates the condition indicator to a likelihood of failure. It can also be called as “Condition Score.”

Failure Susceptibility Indicator (FSI)

Indicators that might trigger an earlier on-set of a failure mode. FSI is just an expectation that is not based on evidence (e.g. result from inspections). It is not part of a Health Index and cannot be used to indicate a likelihood of failure of an asset.

Deterioration

The deterioration covers all forms of 'wear and tear' (including fatigue, corrosion, abrasion, erosion, evaporation, insulation deterioration) on asset due to stresses [37].

Inspection

Action to capture condition indicators. Including in this activity, namely, visual inspection, diagnostic tests and measurement. Inspection can be done live- or off-line.

Maintenance

Combination of all technical and administrative actions, including supervision actions, intended to retain an item, or restore it to, a state in which it can perform a required function [24].

Failure mode

A mode that could lead to a failure of an asset.

Humidity

Moisture in form of gas.

B-life factor

Factor of reliability indicating the number of failed components (in-%) in a population within period of time (usually per year).

Appendix A List of GIS and Major Failures in the JABA Case Study

List of GIS

Location Number	Installation	Manufacturer	Number of ph/ encl.	Number of CB-bays (per 2014)	CB-bay years (since the first operation)	CB-bay years (within period 2005-2014)
150 kV GIS						
1	INDOOR	A	1	4	20	20
2	INDOOR	A	1	6	72	60
3	INDOOR	A	1	6	120	60
4	INDOOR	A	1	6	60	60
5	INDOOR	A	1	6	126	60
6	INDOOR	A	1	6	120	60
7	INDOOR	A	1	7	154	70
8	INDOOR	A	1	8	176	80
9	INDOOR	A	1	8	176	80
10	INDOOR	A	1	8	176	80
11	INDOOR	A	1	8	136	80
12	INDOOR	A	1	8	152	80
13	INDOOR	A	1	11	231	110
14	INDOOR	A	1	11	220	110
15	INDOOR	A	1	12	252	120
16	INDOOR	A	1	15	270	150
17	INDOOR	A	1	16	352	160
18	INDOOR	B	1	6	162	60
19	INDOOR	B	1	6	168	60
20	INDOOR	B	1	6	90	60
21	INDOOR	B	1	8	232	80
22	INDOOR	B	1	8	216	80
23	INDOOR	B	3	5	15	15
24	INDOOR	B	3	5	10	10
25	INDOOR	B	3	6	36	36
26	INDOOR	B	3	9	135	90
27	INDOOR	B	3	10	150	100
28	INDOOR	B	3	11	198	110
29	INDOOR	B	3	14	196	140
30	INDOOR	B	3	16	352	160
31	INDOOR	B	3	23	506	230
32	INDOOR	B	3	24	504	240
33	INDOOR	C	3	4	64	40
34	INDOOR	C	3	4	64	40
35	INDOOR	C	3	5	80	50
36	INDOOR	C	3	5	80	50
37	INDOOR	C	3	5	75	50
38	INDOOR	C	3	5	90	50
39	INDOOR	C	3	5	80	50
40	INDOOR	C	3	5	80	50

41	INDOOR	C	3	5	50	50
42	INDOOR	C	3	6	108	60
43	INDOOR	C	3	6	84	60
44	INDOOR	C	3	6	60	60
45	INDOOR	C	3	6	60	60
46	INDOOR	C	3	7	105	70
47	INDOOR	D	1	5	115	50
48	INDOOR	D	1	6	42	42
49	INDOOR	D	1	6	114	60
50	INDOOR	D	1	7	154	70
51	INDOOR	D	1	7	161	70
52	INDOOR	F	1	6	42	42
53	INDOOR	G	3	5	145	50
54	INDOOR	G	3	5	145	50
55	INDOOR	G	3	5	80	50
56	INDOOR	G	3	6	78	60
57	INDOOR	G	3	7	112	70
58	INDOOR	H	3	5	85	50
59	INDOOR	H	3	5	85	50
60	INDOOR	H	3	7	105	70
61	INDOOR	I	1	7	154	70
62	INDOOR	J	3	13	286	130
63	INDOOR	K	1	11	66	66
64	INDOOR	K	1	12	60	60
65	INDOOR	K	1	15	45	45
66	INDOOR	L	3	5	70	50
67	INDOOR	L	3	5	75	50
68	INDOOR	L	3	7	154	70
69	OUTDOOR	A	1	3	21	21
70	OUTDOOR	F	1	10	220	100
71	OUTDOOR	G	3	8	240	80
500 kV GIS						
1	INDOOR	A	1	6	132	60
2	INDOOR	A	1	6	90	60
3	INDOOR	F	1	15	330	150
4	INDOOR	K	1	5	20	20
5	OUTDOOR	A	1	2	52	20
6	OUTDOOR	A	1	8	152	80
7	OUTDOOR	A	1	23	483	230
8	OUTDOOR	E	1	11	319	110

List of Major Failures (2005 – 2014)

Event Number	Installation	Failure Mode Group *(see Table 2.3)*	Manufacturer	Number of ph/ encl.	Tim-to-Fail (Years)
150 kV GIS					
1	INDOOR	1	B	3	19
2	INDOOR	1	C	3	8
3	INDOOR	1	D	1	14
4	INDOOR	1	H	3	1
5	INDOOR	4	A	1	21
6	INDOOR	4	A	1	15
7	INDOOR	4	A	1	15
8	INDOOR	4	B	3	24
9	INDOOR	4	G	3	12
10	INDOOR	5	D	1	12
11	INDOOR	5	D	1	13
12	INDOOR	5	G	3	15
13	INDOOR	5	G	3	15
14	INDOOR	6	H	3	14
15	INDOOR	6	H	3	14
16	INDOOR	6	H	3	10
17	INDOOR	7	B	3	12
18	INDOOR	7	B	3	15
19	OUTDOOR	2	B	3	10
20	OUTDOOR	2	F	1	16
21	OUTDOOR	2	G	3	23
22	OUTDOOR	2	G	3	27
23	OUTDOOR	4	F	1	17
24	OUTDOOR	4	G	3	22
25	OUTDOOR	4	G	3	27
500 kV GIS					
1	INDOOR	6	A	1	17
2	INDOOR	7	A	1	20
3	OUTDOOR	5	A	1	13
4	OUTDOOR	1	A	1	18
5	OUTDOOR	1	A	1	15
6	OUTDOOR	4	A	1	18
7	OUTDOOR	4	A	1	17
8	OUTDOOR	7	A	1	10
9	OUTDOOR	1	A	1	26
10	OUTDOOR	1	E	1	28

Appendix B Statistical Lifetime Analysis

B1. Methodology for the Statistical lifetime assessment [27]

The methods for the statistical lifetime assessment consists of the following steps: (see Figure B1)

1. Data validation
   This step ensures the failure of data complies with the population. Specific information about the source of data, such as: if the data is an estimation or not, should be recorded.
2. Distribution fitting and parameter estimation
   This step fits the failure data (including the suspensions) into a specific parametric distribution. The distribution parameters can be estimated through the Median Ranks, or the Maximum Likelihood Estimation (MLE). The MLE is preferred when dealing with small data sets.
3. The goodness of fit tests
   This step determines how well the selected distribution reflects the data. There are some methods available, including the Correlation Coefficient and the Anderson-Darling, further can be found in [27].
4. Analyzing the statistical functions
   The failure behavior is being examined through the statistical functions as follows: 1) probability density function (pdf), 2) cumulative distribution function (CDF), 3) reliability function, 4) failure rate and 5) Mean time to failure (MTTF). In this work, the CDF is used to derive the B-lives that the management wanted to achieve.

Setting the reliability target and makes estimation the statistical lifetime: based on the reliability target, the expected lifetime is defined.

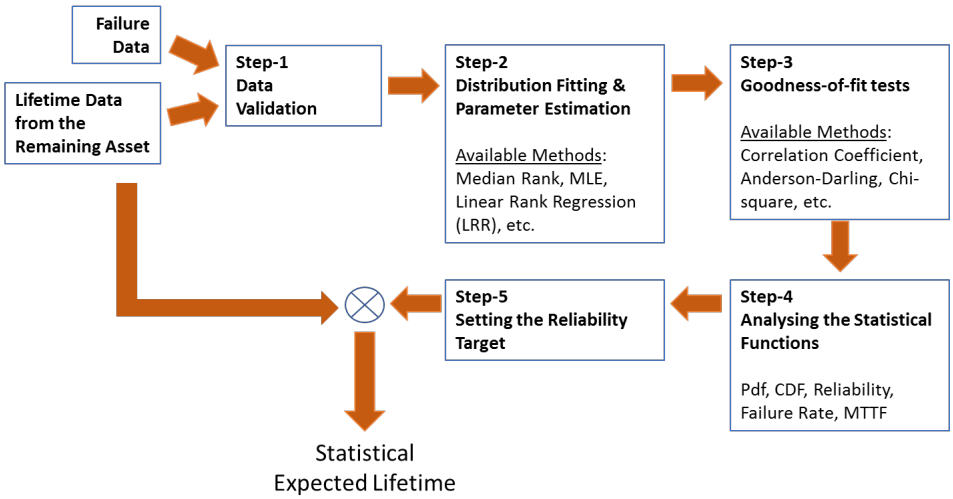

Figure B.1 The steps in performing the statistical lifetime assessment. The input comes from the failure data and the lifetime data from the remaining asset. By setting the reliability target, the statistically expected lifetime can be obtained.

B2. Analytical Statistical Functions [27,29]

1. Random variables

   Failure time data consists of the time-to-failure (e.g., breakdown) of the equipment. The event is assumed to occur randomly, independently, and homogeneously distributed. In the following definition, the random variable is stated by "X". The value of X starts from zero to infinity. The random variable can have a discrete or continuous character.

2. Probability density function (pdf)

   This function describes the probability of occurrence for random variables having a possible value, either for continuous or discrete random variables. If X is the random variable, the probability density function f(x) follows:

$$P(a \leq X \leq b) = \int_a^b f(x)\,dx \quad with\ f(x)dx \geq 0 \quad for\ all\ X \qquad \ldots B1$$

   The probability that X falls within [a, b] is determined by the integral of the graph f(t) between a and b.

3. Cumulative distribution function (CDF)

   This function, F(X), is also known as the unreliability function. It gives the probability of a failure occurring before or at any time, t. For every real number "x", the CDF of "X" follows:

$$F(x) = P(X \leq x) = \int_{-\infty}^{x} f(x')dx' \qquad \ldots B2$$

   F(x) is the probability that a random variable of "X" will have the value ≤ x.

4. Reliability function

   This function is the opponent of unreliability function. The function gives the average between the service-time of a component and the probability that a component survives up to that service-time.

$$R(x) = P(X \geq t) = \int_t^{\infty} f(x')\,dx' = 1 - F(x) \qquad \dots B3$$

5. Failure rate function

   The failure rate is obtained by dividing the probability density function with the reliability function, as follows:

$$\lambda(t) = \frac{f(t)}{R(t)} \qquad \dots B4$$

The failure rate or hazard rate determines the frequency of failures of a component. It usually expressed as the number of failures per unit time.

Appendix C Risk Quantification for FMECA

500 kV GIS

Failure Mode (500 kV GIS)	Likelihood		Consequences							Risk Score
	Occ.	Det.	Safety	Fuel Cost	Eqp. Cost	ENS	Cust. Sat.	Leader ship	Environ ment	
Failing to perform requested operation (due to driving mechanism failure)	3	3	3	3	4	4	2	4	2	198
Loss of electrical connections integrity in primary conductor	1	3	4	4	5	4	3	4	3	81
Loss of electrical connections integrity in secondary	1	3	1	1	3	3	2	2	1	39
Dielectric breakdown in normal service	2	2	4	4	5	4	3	4	3	108
Dielectric breakdown in connection with switching, and/ or, external transients	1	3	4	4	5	4	3	4	3	81
Loss of mechanical integrity on enclosures, pressure gauge, including sudden big SF_6 leakage	1	4	2	1	4	4	2	4	2	76

150 kV GIS

Failure Mode	Likelihood		Consequences							Risk Score
	Occ.	Det.	Safety	Fuel Cost	Eqp. Cost	ENS	Cust. Sat.	Leader ship	Environ ment	
Failing to perform requested operation (due to driving mechanism failure)	3	3	3	2	4	3	2	3	2	171
Loss of electrical connections integrity in primary conductor	3	3	4	3	4	3	2	3	3	198
Loss of electrical connections integrity in secondary	1	3	1	1	2	2	1	2	1	30
Dielectric breakdown in normal service	4	2	4	3	4	3	2	3	3	176
Dielectric breakdown in connection with switching, and/ or, external transients	3	3	4	3	4	3	2	3	3	198
Loss of mechanical integrity on enclosures, pressure gauge, including sudden big SF_6 leakage	2	2	1	1	4	3	1	3	2	60

Appendix D Curves regressions from the laboratory tests

D1. Regression of Flashover Voltages from the test with Quasi-homogeneous setup under AC Voltage Stress

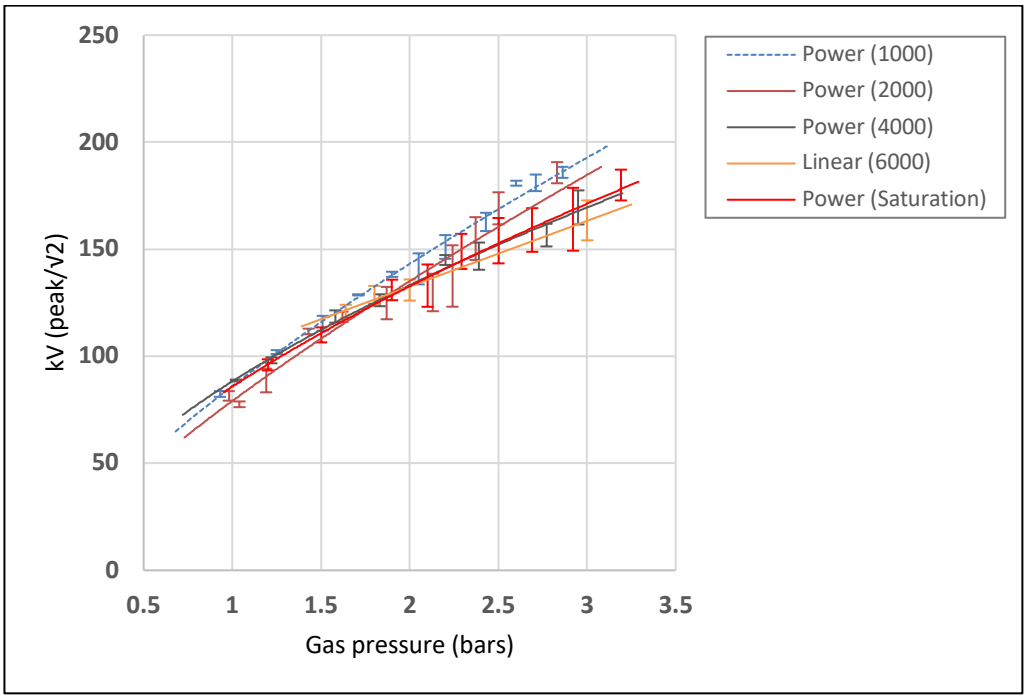

ppmV	Curve Fitting	R^2 (%)	Equation
1000	Power	99.4	$V = 86.112\ p^{0.7339}$
2000	Power	96.5	$V = 79.096\ p^{0.772}$
4000	Power	99.3	$V = 88.255\ p^{0.5941}$
6000	Linear	99.2	$V = 30.65\ p + 71.348$
Sat.	Power	99.1	$V = 85.776\ p^{0.6295}$

D2. Regression of Flashover Voltages from the test with Quasi-homogeneous setup under LI+

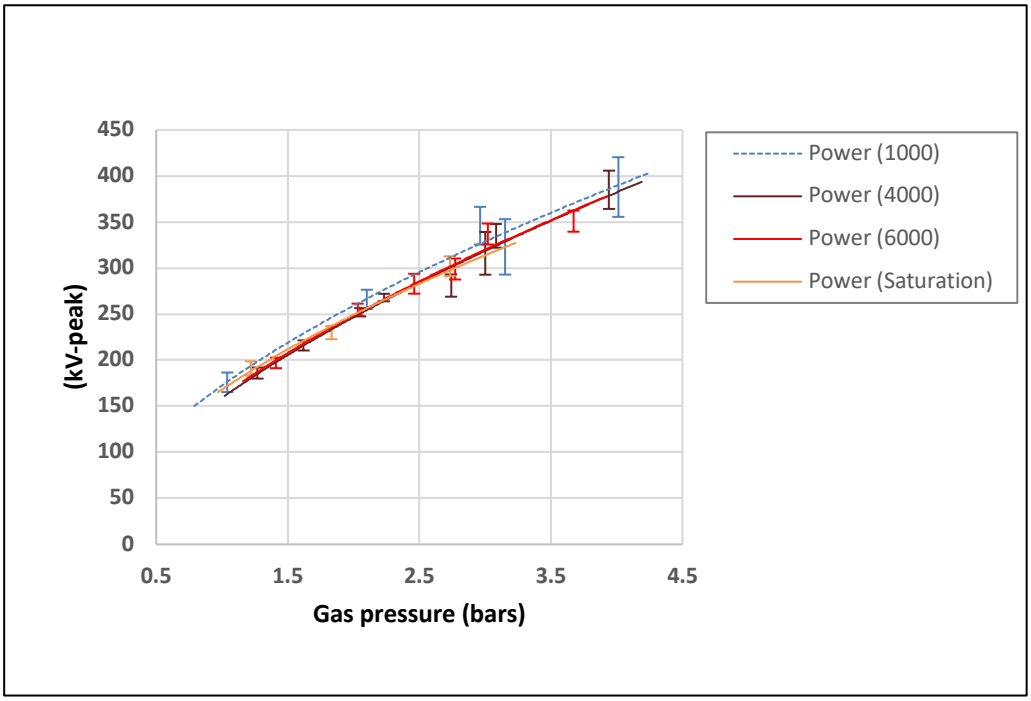

ppmV	Curve Fitting	R^2 (%)	Equation
1000	Power	98.5	$V = 172.57\ p^{0.5872}$
4000	Power	98.4	$V = 159.07\ p^{0.6324}$
6000	Power	98.1	$V = 161.5\ p^{0.622}$
Sat.	Power	98.7	$V = 168.07\ p^{0.5686}$

D3. Regression of Flashover Voltages from the test with Quasi-homogeneous setup under LI-

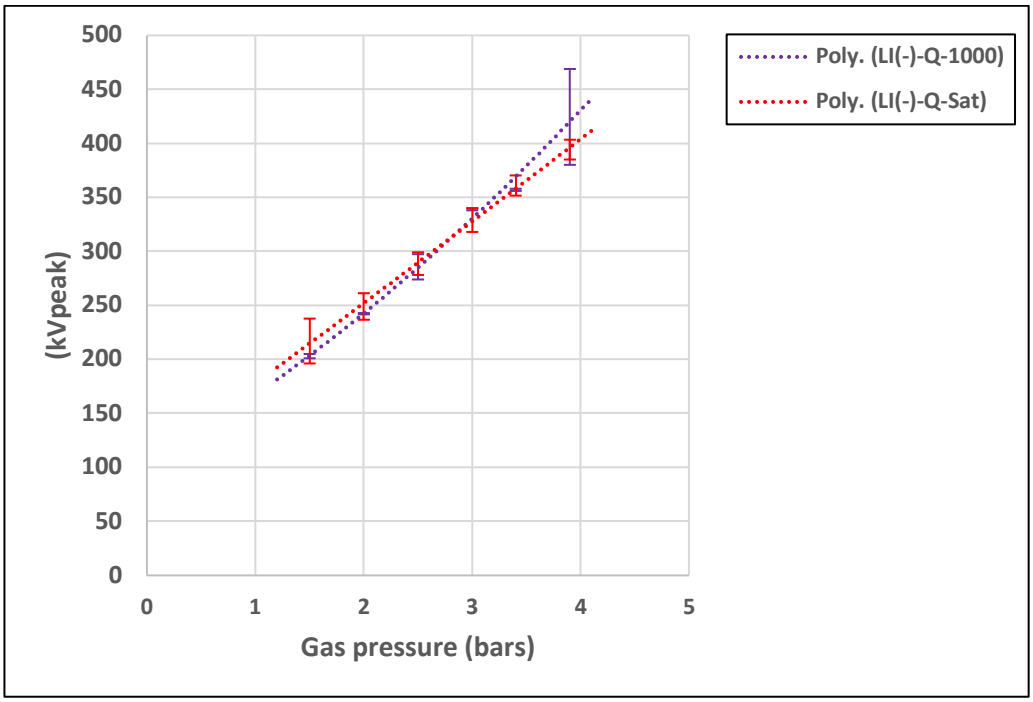

ppmV	Curve Fitting	R^2 (%)	Equation
1000	Polynomial	99.3	$V= 6.1681p^2 + 56.977p + 104.17$
Saturation	Polynomial	99.9	$V= 0.485\ p^2 + 72.954p + 104.38$

D4. Regression of Flashover Voltages from the test with Quasi-homogeneous setup under SI

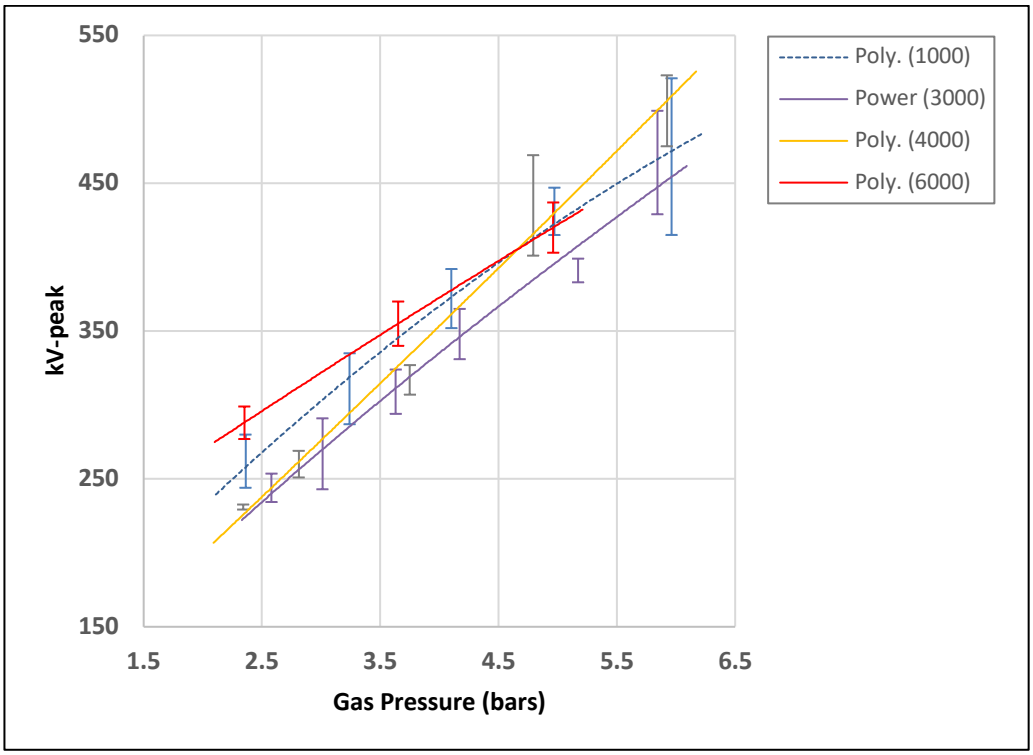

ppmV	Curve Fitting	R^2 (%)	Equation
1000	Polynomial (2nd order)	99.4	$V=-3.6387p^2 + 89.702p + 66.442$
3000	Power	98.8	$V=116.54\ p^{0.762}$
4000	Polynomial (2nd order)	98.6	$V=0.6081\ p^2 + 73.157\ p + 51.087$
6000	Polynomial (2nd order)	100	$V=-0.7357\ p^2 + 55.953\ p + 160.57$

D5. Regression of Flashover Voltages from the test with Homogeneous setup under LI+

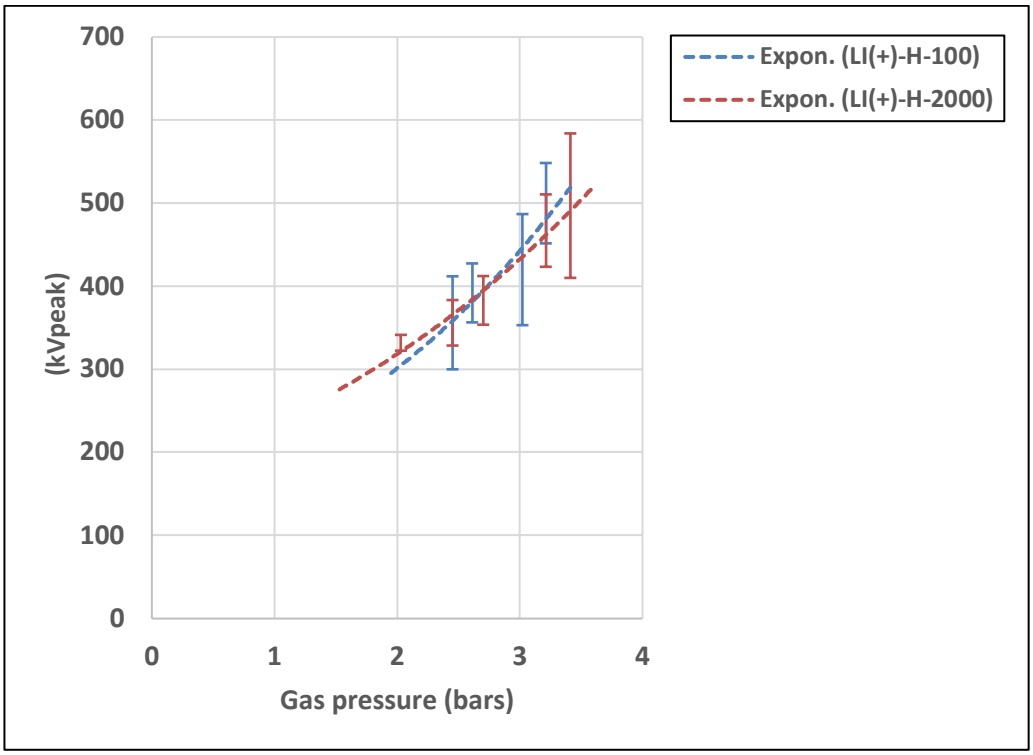

ppmV	Curve Fitting	R^2 (%)	Equation
100	Exponential	90	$V = 139.39\ e^{0.3855p}$
2000	Exponential	97.6	$V = 172.5\ e^{0.3066p}$

D6. Regression of Flashover Voltages from the test with Homogeneous setup under SI

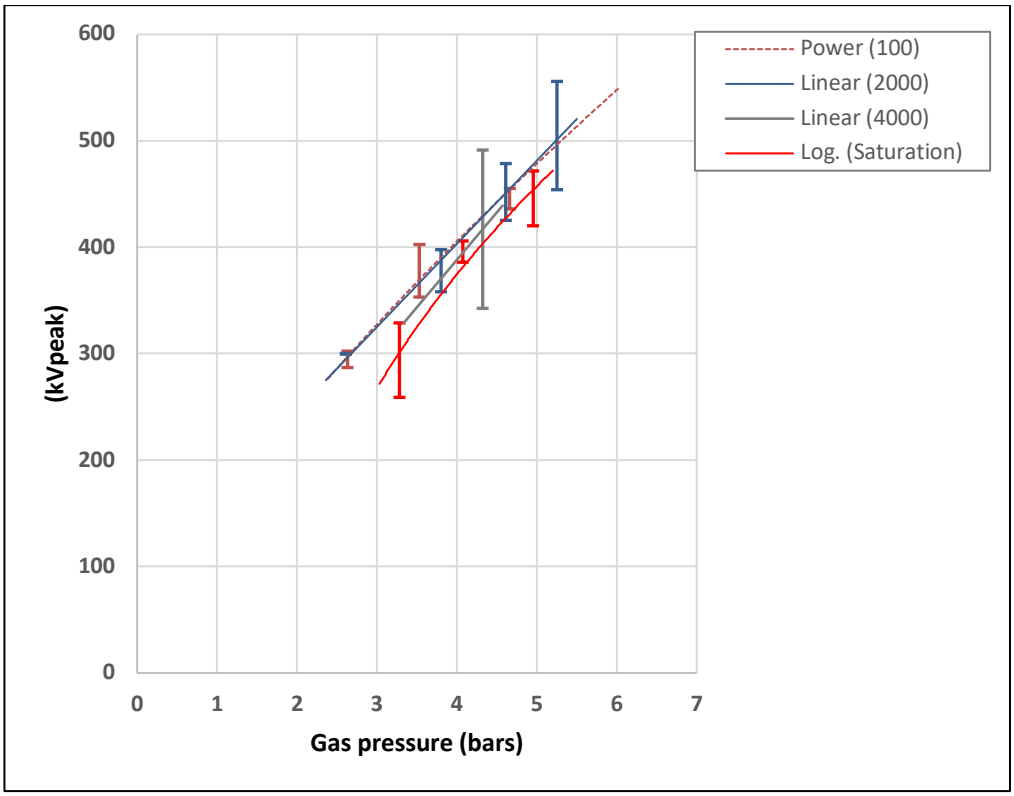

ppmV	Curve Fitting	R^2 (%)	Equation
100	Power	99.5	$V=145.04\ p^{0.742}$
2000	Linear	98.4	$V=78.182\ p + 90.746$
4000	Linear	100	$V=371.1\ \ln(p) – 139.74$
Saturation	Logarithmic	97.2	$V=89.189\ p + 31.703$

D7. Regression of Flashover Voltages from the test with an attached particle on the epoxy under LI+

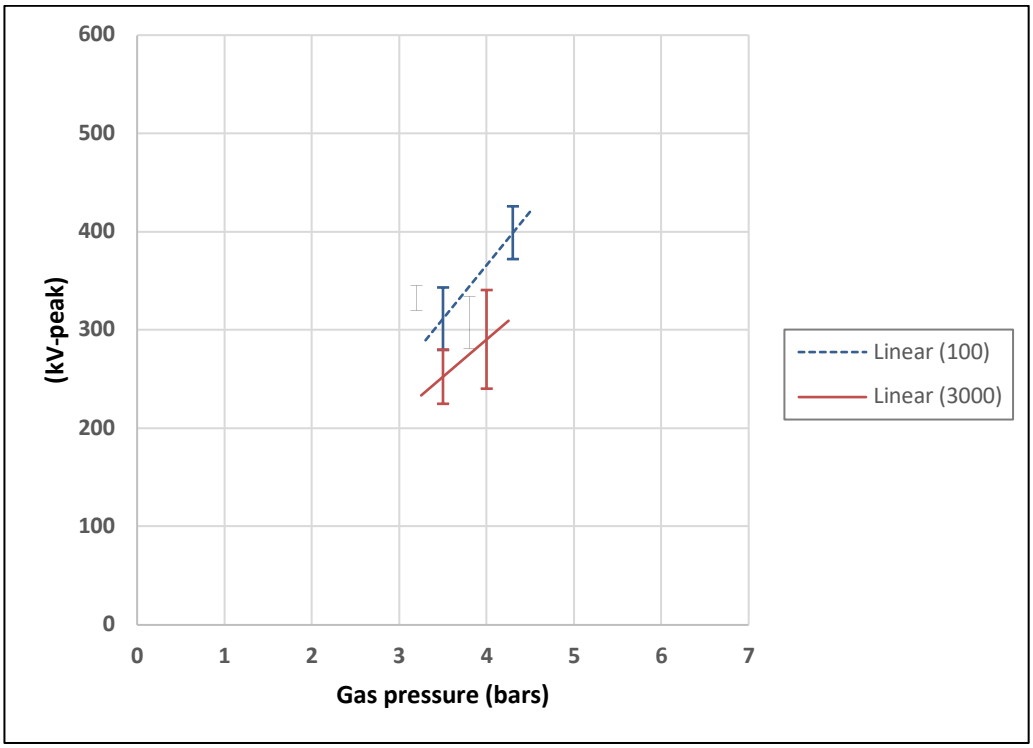

ppmV	Curve Fitting	R^2 (%)	Equation
100	Linear	100	V = 109.38p – 71.312
3000	Linear	100	V = 76p – 13.5

Appendix E Determining condition status of Surge Arrester (SA)

The following methodology is valid only for conventional zinc-oxide surge arresters as installed in almost all locations of GIS in the JABA Case Study.

The critical part of SA consists of the zinc oxide blocks (i.e., the active part). There are two factors determine the life-limiting factor of these blocks: 1. the aging of the metal blocks, mostly due to the influence of the moisture ingress and 2. the cycle, i.e., the number of surge arrester's passing the surge.

The condition status of SA is determined by the following indicators: 1. The number/ times SA's passing the surge (A1), 2. The hotspot at the body of SA (A2), and 3. Service time of SA (A3).

Setting the norm for A1

A former investigation by the author [70] in 2008, on 29 of conventional 150 kV surge arresters, that have the similar make, batch, and service time of 19 years; which were taken from different locations in West Java; had shown that the resistive leakage current was still below the recommended limit after the arrester had been operating up to 50 times. By assuming the discharge energy are equally distributed among arresters, we use this experience to set the boundary to justifying the indicator of A1. By adding a "safety margin" of 50%, the boundary is as follows:

GOOD : $N_{SA} \leq 10$
DETERIORATE : $10 < N_{SA} \leq 25$
BAD : > 25

N_{SA}: times the SA passing the surge.

Setting the norm for A2

According to the experience from the case study, a hotspot on the body of a surge arrester (see Figure E.1) is indicating a final stage of SA's deterioration. The resistive-leakage current during normal operation is high enough to disturb the heat balance of the active parts within the SA. This kind of failure mode in most cases ended with an explosion of the SA. Therefore, we define the following norm:

GOOD : No Hotspot
BAD : Hotspot is found

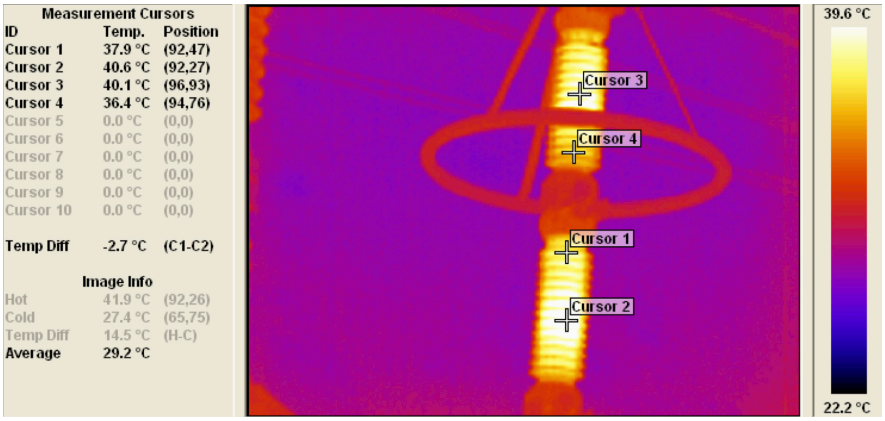

Figure E.1 An example of a thermal image of a degraded Surge Arrester from the case study. The SA consists of three stacks and hot spots have been captured on each of the stacks.

Setting the norm for A3

Statistics from the case study shows that the hazard rate of 70 kV SA is increasing sharply after 15 years. We use this value to set the norm for A3 since there is no available data for the other voltage classes. The norm is as follows:

GOOD : Service time < 10 years
DETERIORATE : 10 < Service time ≤ 15
BAD : Service time > 15 years

Condition status of SA

The final condition status of SA (C_{SA}) is determined by as follows:

C_{SA} = WORST (A1, A2, A3) …D.1

Appendix F Health Index of GIS example

Bay	Encl.	Components	Subsystem	Subsystem Code	Enclosure Code	Bay Codes	Bay Condition Index
Line-1A	G0	Circuit Breaker	Primary	30	30	Primary: 30 Dielectric: **100** Driving Mechanism: 10 Secondary: 30 Const. & Support: 1	Total Condition Codes: 171 Bay Index: **5**
			Dielectric	10	10		
			Driving Mechanism	10	10		
			Secondary	30	30		
			Construction and Support	1	1		
	G1	BB-1 segment,	Primary	1	1		
		DS-bus1		1			
		CT-bus		1			
		DS-bus1	Driving Mechanism	10	10		
		DS-bus1	Secondary	30	30		
		BB-1 segment DS-bus1 CT-bus	Dielectric	100	100		
		BB-1 segment DS-bus1 CT-bus	Construction and Support	1	1		
	G2	BB-2 segment,	Primary	1	30		
		DS-bus2		1			
		ES-maintenance		30			
		DS-bus2	Driving Mechanism	10	10		
		ES-maintenance		10			
		DS-bus2	Secondary	30	30		
		ES-maintenance		30			
		BB-2 segment DS-bus CT-bus	Dielectric	10	10		
			Construction and Support	1	1		
	G9	DS-line	Primary	1	30		
		ES-maintenance		30			
		ES-line		1			
		Termination		1			
		DS-line	Driving Mechanism	10	10		
		ES-maintenance		10			
		ES-line		10			
		DS-line	Secondary	30	30		
		ES-maintenance		30			
		ES-line		30			
		DS-line, ES-line, ES-maintenance,	Dielectric	30	100		
		Termination		100			
		DS-line, ES-line, ES-maintenance, Termination	Construction and Support	1	1		

Bay	Encl.	Components	Subsystem	Subsystem Code	Enclosure Code	Bay Codes	Bay Condition Index
Line-1B	G0	Circuit Breaker	Primary	30	30	Primary: 30 Dielectric: 100 Driving Mechanism: 10 Secondary: 30 Const. & Support: 1	Total Condition Codes: 171 Bay Index: **5**
			Dielectric	100	100		
			Driving Mechanism	10	10		
			Secondary	30	30		
			Construction and Support	1	1		
	G1	BB-1 segment,	Primary	1	1		
		DS-bus1		1			
		CT-bus		1			
		DS-bus1	Driving Mechanism	10	10		
		DS-bus1	Secondary	30	30		
		BB-1 segment DS-bus1 CT-bus	Dielectric	1	1		
		BB-1 segment DS-bus1 CT-bus	Construction and Support	1	1		
	G2	BB-2 segment,	Primary	1	30		
		DS-bus2		1			
		ES-maintenance		30			
		DS-bus2	Driving Mechanism	10	10		
		ES-maintenance		10			
		DS-bus2	Secondary	30	30		
		ES-maintenance		30			
		BB-2 segment DS-bus CT-bus	Dielectric	1	1		
			Construction and Support	1	1		
	G9	DS-line	Primary	1	30		
		ES-maintenance		30			
		ES-line		1			
		Termination		1			
		DS-line	Driving Mechanism	10	10		
		ES-maintenance		10			
		ES-line		10			
		DS-line	Secondary	30	30		
		ES-maintenance		30			
		ES-line		30			
		DS-line, ES-line, ES-maintenance,	Dielectric	100	100		
		Termination		100			
		DS-line, ES-line, ES-maintenance, Termination	Construction and Support	1	1		

Bay	Encl.	Components	Subsystem	Subsystem Code	Enclosure Code	Bay Codes	Bay Condition Index
Line-2A	G0	Circuit Breaker	Primary	1	1	Primary: 1 Dielectric: 100 Driving Mechanism: 10 Secondary: 30 Const. & Support:1	Total Condition Codes: 142 Bay Index: **5**
			Dielectric	10	10		
			Driving Mechanism	10	10		
			Secondary	30	30		
			Construction and Support	1	1		
	G1	BB-1 segment,	Primary	1	1		
		DS-bus1		1			
		CT-bus		1			
		DS-bus1	Driving Mechanism	10	10		
		DS-bus1	Secondary	30	30		
		BB-1 segment DS-bus1 CT-bus	Dielectric	10	10		
		BB-1 segment DS-bus1 CT-bus	Construction and Support	1	1		
	G2	BB-2 segment,	Primary	1	1		
		DS-bus2		1			
		ES-maintenance		1			
		DS-bus2	Driving Mechanism	10	10		
		ES-maintenance		10			
		DS-bus2	Secondary	30	30		
		ES-maintenance		30			
		BB-2 segment DS-bus CT-bus	Dielectric	10	10		
			Construction and Support	1	1		
	G9	DS-line	Primary	1	1		
		ES-maintenance		1			
		ES-line		1			
		Termination		1			
		DS-line	Driving Mechanism	10	10		
		ES-maintenance		10			
		ES-line		10			
		DS-line	Secondary	30	30		
		ES-maintenance		30			
		ES-line		30			
		DS-line, ES-line, ES-maintenance,	Dielectric	30	100		
		Termination		100			
		DS-line, ES-line, ES-maintenance, Termination	Construction and Support	1	1		

Bay	Encl.	Components	Subsystem	Subsystem Code	Enclosure Code	Bay Codes	Bay Condition Index
Line-2B	G0	Circuit Breaker	Primary	1	1	Primary: 1 Dielectric: 100 Driving Mechanism: 10 Secondary: 30 Const. & Support:1	Total Condition Codes: 142 Bay Index: **5**
			Dielectric	10	10		
			Driving Mechanism	10	10		
			Secondary	30	30		
			Construction and Support	1	1		
	G1	BB-1 segment,	Primary	1	1		
		DS-bus1		1			
		CT-bus		1			
		DS-bus1	Driving Mechanism	10	10		
		DS-bus1	Secondary	30	30		
		BB-1 segment DS-bus1 CT-bus	Dielectric	10	10		
		BB-1 segment DS-bus1 CT-bus	Construction and Support	1	1		
	G2	BB-2 segment,	Primary	1	1		
		DS-bus2		1			
		ES-maintenance		1			
		DS-bus2	Driving Mechanism	10	10		
		ES-maintenance		10			
		DS-bus2	Secondary	30	30		
		ES-maintenance		30			
		BB-2 segment DS-bus CT-bus	Dielectric	10	10		
			Construction and Support	1	1		
	G9	DS-line	Primary	1	1		
		ES-maintenance		1			
		ES-line		1			
		Termination		1			
		DS-line	Driving Mechanism	10	10		
		ES-maintenance		10			
		ES-line		10			
		DS-line	Secondary	30	30		
		ES-maintenance		30			
		ES-line		30			
		DS-line, ES-line, ES-maintenance,	Dielectric	30	100		
		Termination		100			
		DS-line, ES-line, ES-maintenance, Termination	Construction and Support	1	1		

Bay	Encl.	Components	Subsystem	Subsystem Code	Enclosure Code	Bay Codes	Bay Condition Index
TRX-01	G0	Circuit Breaker	Primary	1	1	Primary: 1 Dielectric: 100 Driving Mechanism: 10 Secondary: 30 Const. & Support: 1	Total Condition Codes: 142 Bay Index: **5**
			Dielectric	10	10		
			Driving Mechanism	10	10		
			Secondary	30	30		
			Construction and Support	1	1		
	G1	BB-1 segment,	Primary	1	1		
		DS-bus1		1			
		CT-bus		1			
		DS-bus1	Driving Mechanism	10	10		
		DS-bus1	Secondary	30	30		
		BB-1 segment DS-bus1 CT-bus	Dielectric	1	1		
		BB-1 segment DS-bus1 CT-bus	Construction and Support	1	1		
	G2	BB-2 segment,	Primary	1	1		
		DS-bus2		1			
		ES-maintenance		1			
		DS-bus2	Driving Mechanism	10	10		
		ES-maintenance		10			
		DS-bus2	Secondary	30	30		
		ES-maintenance		30			
		BB-2 segment DS-bus CT-bus	Dielectric	1	1		
			Construction and Support	1	1		
	G9	ES-maintenance	Primary	1	1		
		Termination		1			
		ES-maintenance	Driving Mechanism	10	10		
		ES-maintenance	Secondary	30	30		
		ES-maintenance,	Dielectric	10	100		
		Termination		100			
		ES-maintenance, Termination	Construction and Support	1	1		

Bay	Encl.	Components	Subsystem	Subsystem Code	Enclosure Code	Bay Codes	Bay Condition Index
TRX-02	G0	Circuit Breaker	Primary	10	10	Primary: 10 Dielectric: 100 Driving Mechanism: 10 Secondary: 30 Const. & Support: 1	Total Condition Codes: 151 Bay Index: **5**
			Dielectric	10	10		
			Driving Mechanism	10	10		
			Secondary	30	30		
			Construction and Support	1	1		
	G1	BB-1 segment,	Primary	1	1		
		DS-bus1		1			
		CT-bus		1			
		DS-bus1	Driving Mechanism	10	10		
		DS-bus1	Secondary	30	30		
		BB-1 segment DS-bus1 CT-bus	Dielectric	1	1		
		BB-1 segment DS-bus1 CT-bus	Construction and Support	1	1		
	G2	BB-2 segment,	Primary	1	10		
		DS-bus2		1			
		ES-maintenance		10			
		DS-bus2	Driving Mechanism	10	10		
		ES-maintenance		10			
		DS-bus2	Secondary	30	30		
		ES-maintenance		30			
		BB-2 segment DS-bus CT-bus	Dielectric	1	1		
			Construction and Support	1	1		
	G9	ES-maintenance	Primary	10	10		
		Termination		1			
		ES-maintenance	Driving Mechanism	10	10		
		ES-maintenance	Secondary	30	30		
		ES-maintenance,	Dielectric	10	100		
		Termination		100			
		ES-maintenance, Termination	Construction and Support	1	1		

Bay	Encl.	Components	Subsystem	Subsystem Code	Enclosure Code	Bay Codes	Bay Condition Index
TRX-03	G0	Circuit Breaker	Primary	1	1	Primary: 1 Dielectric: 100 Driving Mechanism: 10 Secondary: 30 Const. & Support: 1	Total Condition Codes: 142 Bay Index: **5**
			Dielectric	30	30		
			Driving Mechanism	10	10		
			Secondary	30	30		
			Construction and Support	1	1		
	G1	BB-1 segment,	Primary	1	1		
		DS-bus1		1			
		CT-bus		1			
		DS-bus1	Driving Mechanism	10	10		
		DS-bus1	Secondary	30	30		
		BB-1 segment DS-bus1 CT-bus	Dielectric	1	1		
		BB-1 segment DS-bus1 CT-bus	Construction and Support	1	1		
	G2	BB-2 segment,	Primary	1	1		
		DS-bus2		1			
		ES-maintenance		1			
		DS-bus2	Driving Mechanism	10	10		
		ES-maintenance		10			
		DS-bus2	Secondary	30	30		
		ES-maintenance		30			
		BB-2 segment DS-bus CT-bus	Dielectric	1	1		
			Construction and Support	1	1		
	G9	ES-maintenance	Primary	1	1		
		Termination		1			
		ES-maintenance	Driving Mechanism	10	10		
		ES-maintenance	Secondary	30	30		
		ES-maintenance,	Dielectric	100	100		
		Termination		100			
		ES-maintenance, Termination	Construction and Support	1	1		

Bay	Encl.	Components	Subsystem	Subsystem Code	Enclosure Code	Bay Codes	Bay Condition Index
BUS COUPLE	G0	Circuit Breaker	Primary	1	1	Primary: 1 Dielectric: 1 Driving Mechanism: 10 Secondary: 30 Const. & Support: 1	Total Condition Codes: 43 Bay Index: **4**
			Dielectric	1	1		
			Driving Mechanism	10	10		
			Secondary	30	30		
			Construction and Support	1	1		
	G10	BB-1 segment,	Primary	1	1		
		DS-bus1		1			
		ES-maintenance1		1			
		CT-bus		1			
		DS-bus1	Driving Mechanism	10	10		
		ES-maintenance1		10			
		DS-bus1	Secondary	30	30		
		ES-maintenance1		30			
		BB-1 segment DS-bus1 ES-maintenance1 CT-bus	Dielectric	1	1		
		BB-1 segment DS-bus1 ES-maintenance1 CT-bus	Construction and Support	1	1		
	G20	BB-1 segment,	Primary	1	1		
		DS-bus1		1			
		ES-maintenance1		1			
		CT-bus		1			
		DS-bus1	Driving Mechanism	10	10		
		ES-maintenance1		10			
		DS-bus1	Secondary	30	30		
		ES-maintenance1		30			
		BB-1 segment DS-bus1 ES-maintenance1 CT-bus	Dielectric	1	1		
		BB-1 segment DS-bus1 ES-maintenance1 CT-bus	Construction and Support	1	1		

Appendix G Technical Recommendations

The technical recommendations are as follows:

To improve the technical-performance of GIS operating under tropical conditions:

1. Humidity should be controlled for the whole life of GIS. This can be done through the following activities:
   a. The dryness should be maintained during the erection and maintenance of GIS involving the opening of the enclosures. All GIS spare-parts should be placed in a dry location.
   b. The vacuum time to evacuate moisture from GIS should be sufficient.
   c. In GIS without desiccants, a design modification is suggested to add desiccants inside GIS.
2. Against the corrosion and leakages:
   a. The GIS should be painted with anti-corrosion material and re-painted when the corrosion is observed.
   b. For indoor GIS, the airflow, the temperature, and the humidity inside the GIS building should be maintained. Heating elements in the local control cubicle should be maintained to avoid corrosion on secondary components.
   c. Outdoor GIS experienced higher environmental stress rather than indoor GIS. Special materials, like seals, grease, and painting, are needed.
   d. A GIS with a double-sealing system is more robust to a gas leaking rather than a single-sealing system.
3. Surge Arrester condition has to be regularly monitored by observing operational counter and possible hotspot. When replacing a surge arrester, the counter should also need to be replaced. We suggest replacement of Surge Arrester based on the following: service time (in years), operating time (in the number of passing overvoltage) or existence of hotspot.
4. The statistical lifetime analysis suggests the time-to-major maintenance (or overhauling) for the outdoor GIS is shorter than the indoor GIS. For the JABA Case Study, we propose the time of B5-lives as the interval, as follows:
   a. For 500 kV GIS Outdoor : 18 (13-22) years
   b. For 150 and 500 kV GIS Indoor : 25 (22-30) years
   c. For 150 kV GIS Outdoor : 15 (5-20) years

   The values above were derived from statistical analysis. A regular review on these intervals is suggested.

Acknowledgements

I want to thank God for His grace and provisions during the process of completing this Ph.D. thesis. The last 6 years have been a challenging moment for the author to balance his time as a part-time Ph.D. in TU Delft and as an engineer in PLN that both are separated 7000 miles. The completion of this book could be impossible without engagement and supports from many people around the author. Therefore, I would like to express my gratitude as follows:

To my promotor, Prof. dr. Johan J. Smit, for allowing me to have this part-time Ph.D. project. Thank you for your sincere and constant support during the process. The opportunity to gain knowledge from the running CIGRE's discussion on the asset health index becomes a critical part of this book.

To my co-promotor, Dr. Armando Rodrigo Mor, for his support, discussions, and trust. Thank you for consistently becomes a wakening-alarm for me. Your evaluation on the line-reasoning of the book, particularly in the part of experimental investigations, is so valuable.

To former- and new manager of HV Laboratory of TU Delft, Ir. Paul van Nes, and Ir. Radek Heller, the experiment works could be impossible without supports from you. Thank you also for Wim Termorshuizen and Remko Koornneef for your assistance.

To PT. PLN (Persero), thank you for allowing me to finish this thesis project.

To Dr. ir. Anita Pharmatrisanti of PLN, to share her time for very fruitful and open-discussions about work and life.

To Dr. ir. Muhannad al-Suhaily of DNV-GL, for our brainstorming about GIS and Asset Management. Thank you for representing me in the ISH Conference in Argentina in 2017.

To my colleagues in the (former) High Voltage and Asset Management Group, Jiayang Wu, Luis Carlos, Guillermo, and Fabio Munoz, for their supports. Thank you for the discussions and jokes that made the work more fun.

To Sharmila Rattansingh, for her assistance each time I visit Delft.

To my Delft's mate Yuli Ekowati, Julian Aditya (Jule), Mas Stevie Heru, Mbak Cisca Suxma, Mas Senot Sangadji, and Mbak Pungky Pramesti, for being my family during my stays in the Netherlands.

To my colleagues in PLN whom I could not mention all the names, especially those who are actively involved in the "Belajar GIS yuk" discussion group. Thank you for the insight that adjusts this book with the real operating condition of GISs in the field.

My honor to my guru and fellows who had passed away, Pak Sachri (1953-2015), Pak Ari Muchtar (1964-2018), and Mbak Ninil Ukhita Anggra Wardani (1978-2018). Thank you for the knowledge you have shared. You will always be remembered.

Finally, thank you for the support and love from my parents, my wife Ima, and my sister Putri. And also, for my daughter Daya, who supports her "Bapak Andre" through "a way that she might be not realized at this moment."

Curriculum Vitae

Andreas Putro Purnomoadi was born in Yogyakarta, Indonesia, in 1981. He studied electrical engineering and received a bachelor degree from the Bandung Institute of Technology (ITB) in 2004 and an MSc degree from the Delft University of Technology in 2012. He started his Ph.D. research project in October 2013 at the Department of DCE&S within the (formerly) High Voltage and Asset Management Group.

He has been working in Perusahaan Listrik Negara, PT. PLN (Persero), the Indonesian Government's Electricity Company, since 2005. From 2006 to 2010, he actively involved in the maintenance, power failure investigation, and condition assessment of transmission apparatus in Java and Bali transmission network. After receiving his Master degree in 2012, he has been assigned into the Asset Management Department of Transmission and Load Dispatch Center of Java and Bali (P3B Jawa Bali) until 2015, and then to the Central Java Transmission Service Unit (PLN TJBT) from 2015 to 2018. From August 2018 onward, he is a senior researcher at the PLN Research Institute.

List of publications

Journals

A. P. Purnomoadi, A. Rodrigo Mor, J. J. Smit, "Spacer Flashover in Gas Insulated Switchgear (GIS) with Humid SF_6 under Different Electrical Stresses," International Journal of Electrical Power and Energy Systems, volume 116, available online 29 September 2019.

A. P. Purnomoadi, A. Rodrigo Mor, J. J. Smit, "Health Index and Risk Assessment Models for Gas Insulated Switchgear (GIS) Operating under Tropical Conditions," International Journal of Electrical Power and Energy Systems, volume 117, available online 18 November 2019.

Conference Papers

A. P. Purnomoadi, MAG Al-Suhaily, S. Meijer, J.J. Smit, S. Burow, S. Tenbohlen, "The Influence of Free Moving Particles on the Breakdown Voltage of GIS under Different Electrical Stresses," IEEE Conference, CMD, pp. 383-386, Bali, Indonesia, 2012.

A. P. Purnomoadi, A. Rodrigo Mor, J. J. Smit, "Insulation Performance of GIS Operating under Tropical Conditions," 20th ISH, paper ID 280, Buenos Aires, Argentina, 2017.

A. P. Purnomoadi, A. Rodrigo Mor, J. J. Smit, "Condition Assessment Model for GIS Operating under Tropical Conditions," IEEE Conference, ICHVEPS, pp. 544-549, Bali, Indonesia, 2017.

A. P. Purnomoadi, G. Bonar, A. Rodrigo Mor, J. J. Smit, B. S. Munir, "Health Index Model for GIS Operating under Tropical Conditions," IEEE Conference, ICHVEPS, Bali, Indonesia, 2019.

A. P. Purnomoadi, D. S. Rahmani, A. Rodrigo Mor, J. J. Smit, G. Supriyadi, "Risk Assessment Model for GIS Operating under Tropical Conditions," IEEE Conference, ICHVEPS, Bali, Indonesia, 2019.